ISSN print: 1224-5984
ISSN online: 2248-3942

Rom Biotechnol Lett. 2022; 27(3): 3453-3459
doi: 10.25083/rbl/27.3/3453.3459

Received for publication: June, 16, 2022
Accepted: July 10, 2022

Original paper

Relative leaf expansion rate as an indicator of compensatory growth of defoliated vines of Prokupac (*Vitis vinifera* L.)

DUŠICA ĆIRKOVIĆ[1], SAŠA MATIJAŠEVIĆ[2], BRATISLAV ĆIRKOVIĆ[3], ZORAN BEŠLIĆ[2]*

[1]Academy of Vocational Studies Southern Serbia, Department of Agricultural and Food Studies in Prokuplje, Serbia.
[2]University of Belgrade, Faculty of Agriculture, Nemanjina 6, 11080 Belgrade, Serbia.
[3]University of Pristina – Kosovska Mitrovica, Faculty of Agriculture, Kopaonicka bb, 38219 Lesak, Serbia.

Abstract

Reaction of the grapevine to the early defoliation is to mitigate its effects through compensatory growth by producing more lateral shoots with a greater number of leaves. In this study, we evaluated the usage of non-destructive and continuous measurements of mean and lateral leaf area on the same shoots for the purpose of monitoring the leaf area development and calculating relative leaf expansion rate - RLER during vegetation. This study has shown that the grapevine's ability to recover its leaf area after defoliation depends mainly on the time when the defoliation occurs. Early defoliated vines had time to compensate removed leaves by producing more lateral shoots with a greater number of leaves, which resulted in a larger leaf area. With the decrease in the intensity of shoot growth during vegetation, the recovery ability decreases, therefore, compensatory growth is not enough to restore the reduced leaf area. Based on the value of RLER, if defoliation is performed in the period of intensive growth of shoots, it affects the stagnation of the emergence of new shoots and leaves over several days, followed by a period of re-growth. Very slow or no growth of shoots and leaves occurred after the veraison stage.

Keywords defoliation, leaf area, compensation, relative leaf expansion rate

To cite this article: ĆIRKOVIĆ D, MATIJAŠEVIĆ S, ĆIRKOVIĆ B, BEŠLIĆ Z. Relative leaf expansion rate as an indicator of compensatory growth of defoliated vines of Prokupac (Vitis vinifera L.). *Rom Biotechnol Lett. 2022*; 27(3): 3453-3459 DOI: 10.25083/rbl/27.3/3453.3459

*Corresponding author: Zoran Bešlić, University of Belgrade, Faculty of Agriculture, Nemanjina 6, 11080 Belgrade, Serbia.
Tel.: +381 (63)7036338; E-mail: zbeslic@agrif.bg.ac.rs

Introduction

Leaf removal from the shoots in the fruiting zone is becoming common practice in vineyards with high quality wine cultivars in Serbia. The main aim of defoliation is to improve vine microclimate conditions, especially light conditions, as well as temperature and humidity inside the canopy (SMART [1]; Poni & al. [2]). Improved microclimate conditions prompt accumulation of dry matter in grapes, anthocyanins and polyphenol compounds in berry skins (KLIEWER [3]; HUNTER & al. [4]; SABBATINI & al. [5]; BAIANO & al. [6]). Better aeration of canopy and greater penetration of fungicide reduce the degree of damage caused by disease, especially of grey rot (GUBLER & al. [7]; MOLITOR & al. [8]; GAMBETTA & al. [9]). The effect of defoliation mainly depends on its intensity and the time of application. Early defoliation, carried out within the intensive shoot growing phase, causes the photosynthetic shock due to the removal of the photosynthetically active area and decreases the whole-vine photosynthesis (PETRIE & al. [10]; PALLIOTTI & al. [11]). Total shoot photosynthesis level can be reduced by up to 70%, which causes a halt in the sink organs' development (PONI & al. [12]). These modifications of the source-sink balance can affect the grape and berry structure (COOMBE, [13]; INTRIERI & al. [14]; SABBATINI & al. [5]). The most pronounced changes in the structure of grapes and berries occur when defoliation is performed in the phenological stages of flowering and fruit set, when intensive divisions of berry cells of young berries take place (PONI & al. [15]). During the fruit set, the number of pericarp cell layers is determined and each halt in assimilator inflow results in a decreased cell number. In most studies with defoliation, it is necessary to assess the consequent effect of leaf removal on leaf area change. Leaf area is an important element in the study of plant physiology, particularly when exploring the photosynthetic activity, canopy light conditions and water balance of the plant and when assessing the impact of cultural practices (BESLIC & al. [16]). Furthermore, unfavorable weather conditions, especially hail, diseases and pests can affect the loss of the leaves and reduction of the leaf area. The natural reaction of the grapevine on defoliation is to mitigate its effects through compensatory growth. Compensatory growth is defined as the restoration of morphological and physiological changes that occur in plants following defoliation (COLLIN & al. [17]). Grapevine has a strong capacity of compensation by producing more lateral shoots with a greater number of leaves (CANDOLFI-VASCONCELOS & KOBLET [18]; PETRIE & al. [19]; KURTURAL & al. [20]), which is a response to the disturbed source: sink relation and balancing act of the grapevine canopy upon manipulation (Hunter [21]). The most common method of quantification of the compensation is comparing the performance of defoliated and untouched plants (HILBERT & al. [22]; ANTEN & al. [23]). In this study, compensatory growth is defined as an increase in relative leaf expansion rate – RLER of defoliated vines relative to untouched vines. Non-destructive and continuous measurements of mean and lateral leaf area based on the same shoots enabled the monitoring of the leaf area development and the calculation of the relative leaf expansion rate - RLER during vegetation.

The main aim of this study was to evaluate the changes in RLER caused by different defoliation times and to quantify its role as an indicator of compensation.

Material and methodes

The study was conducted from 2014 to 2016 at a commercial vineyard planted with Prokupac (*Vitis vinifera* L.) variety grafted on Kober 5bb (V. berlandieri × V. riparia) rootstock. Study plots were located at the Toplicki Vinogradi Winery near Prokuplje, Serbia. The location of the trial (lat. 43.12057" N; long. 21.25031" E; alt. 359 m) belongs to the vine-growing region of Toplica, wine district of Prokuplje. It has a temperate continental climate with an annual mean air temperature of 11.4°C and a seasonal mean temperature of 17,0°C. Total annual rainfall averages 556.7 mm, with 347.4 mm of rainfall during the growing season. The vineyard soil type is a lessive cambisol that has favorable physical characteristics. The vineyard was planted in 2009 with a planting space of 2.5 × 0.8 m (5000 plants per ha). The training system is a double Cordon de Royat with a trunk height of 60 cm. At pruning, six 2-node spurs were kept on the permanent cordon corresponding to a bud-load of 12 nodes per vine. The standard vineyard management practices, except main and lateral shoot tipping, were carried out in the study plots. The trials were set in a random complete block design with three blocks and four treatments per block. Defoliation was carried out by hand removal of six basal leaves. The vines were tagged and randomly assigned to the following treatments: (K) non-defoliated (control); (v1) removal of the first six basal leaves at the phenological stage 65 (full flowering: 50% of flowerhoods fallen according to BBCH scale, LORENZ & al. [24]); (v2) removal of the first six basal leaves at the phenological stage 73 (berries groat sized, ovary diameter varying from 3-5 mm); (v3) removal of the first six basal leaves at the stage 81 (ripening begining – veraison, berries begin to color).

The single leaf area, main shoot leaf area and lateral shoot leaf area were estimated according to BESLIC & al. [25]. During the period of 15-31 May of each year, 50 leaves were randomly collected from various vines in all experi-

mental treatments. The leaves were immediately placed in plastic bags and kept and transported in a field refrigerator. Leaf area (LA) and the length of two inferior leaf veins (l) were measured using a computer scanner and Adobe Photoshop 7.0 in laboratory conditions. These data were used to calculate the regression between l and LA. The obtained formula ($LA = -111.3242 + 14.4764 \times l$; $r^2 = 0{,}98$) was used for non-destructive calculation of leaf surface on the basis of leaf vein length data collected in the vineyard. Also, during the period of 15-31 May, 30 shoots were labeled randomly from each treatment and used for calculating the leaf area during vegetation. The main shoot leaf area (MLA) was calculated for all labeled shoots individually. Leaf number (NL), the largest (Lmax) and the smallest leaf area (Lmin) was then determined for each main shoot. Multiple regression analysis was used to obtain the relationship between the dependent variable MLA1 and three independent variables (NL, Lmax and Smin). The obtained formula ($MLA = -1688.43 + 128.36 \times NL + 4.83 \times Lmax + 14.02 \times Lmin$; $r^2 = 0.892$) was used for non-destructive calculation of leaf surface area for main shoots. For the lateral shoots leaf area (LLA), the analogous formula was used: $LLA = -520.212 + 50.462 \times NL1 + 4.806 \times Lmax + 3.739 \times Lmin$; $r^2 = 0.974$). According to the obtained formula, MLA, LLA and total leaf area (TLA = MLA + LLA) were calculated during tree vegetation in the next periods: first measurement was between 70 to 75 days after bud break (DAB); the second was between 85 to 90 DAB; the third was between 100 to 110 DAB and the fourth was between 125 to 130 DAB. Continuous LA measurement in these intervals was used for calculating the relative leaf expansion rate (RLER) that was calculated based on the following formula (DZAMIC & al. [26]):

$$RLER = (\ln LA_2 - \ln LA_1) / (t_2 - t_1)$$

LA_1 – leaf area at the beginning of the observation (t_1), LA_2 – leaf area at the end of the observation (t_2)

Data were processed and analyzed by standard statistical methods using software packages Statistica v.9.0 (StatSoft Inc., Tulsa, OK, USA). Differences between the treatments were tested by F test and Duncan's multiple range test.

Results and discussion

During the period of investigation, defoliation reduced the lateral leaf area in v1 vines by 40% more than the values found in other variants and control plants in the first measurements (DAB 70-75, Table 1). The first measurements of the LA were carried out about 20 days after defoliation of v1 vines. At that moment, the balance between source:sink organs was still not established after the removal of the basal leaves that are the source organs, which caused stagnation in vegetative development and delayed the lateral shoot emergence. Removal of the photosynthetic most active leaves from the fruiting zone during flowering causes a significant decrease in the whole vine photosynthesis and modifies the source:sink relationship (OLLAT & GAUDILLERE [27]; PETRIE & al. [10]; PONI & al. [12]; FRIONI & al. [28]). In a similar investigation of the defoliation effect on Prokupac (*Vitis vinifera* L.), BESLIC & al. [16] emphasized a growth stagnation of up to 30 days after basal leaf removal in stage 65 (BBCH scale). The next measurements were carried out in the second half of July (DAB 85-90), during intensive shoot growth and 20 days after v2 defoliation. This removal of leaves and lateral shoots from six basal nodes was reflected on LLA on v2 vines, in which the LLA was reduced by 50% compared to the control plants. Differences between v1 and v3, and the control plants, respectively, were statistically significant, too. A similar relationship between values of LLA were in the third measurements, which were carried out in a period of decreased growth of main and lateral shoots. Many investigations of grapevine growth in temperate climates, show that the intensity of shoot growth decreases from mid-summer (Mullis & al. [29]). The third measurements were performed before defoliation (v3), so there was no reduction in LLA of v3 vines. The fourth measurements of LLA were carried out after the defoliation at verasion (v3), when the final leaf area was mostly achieved. Defoliation of v3 vines reduced their LLA by 30% in comparison to the control plants. At the end of the observed period, significant differences in LLA were obtained between the control plants and v2, and v3, respectively. V1 vines had a significantly larger LLA with regard to v3. It is evident that the early defoliated vines (v1, v2) had time to compensate removed leaves by producing more lateral shoots with a greater number of leaves, which resulted in larger total LLA. As the intensity of shoot growth decreased during the vegetation, compensation growth was not sufficient to recover the reduction of total leaf area. The growth of new shoots and leaves was induced by lost source organs. Many studies have shown that early defoliation causes an increase in both main and lateral leaf area as a compensatory response (WEAVER [30]; CANDOLFI-VASCONCELOS & KOBLET [31]; HUNTER [21]; KURTURAL & al. [20]). In similar agro-ecological and experimental conditions, STEFANOVIC [32] obtained a significant increase in the lateral leaf area on the early defoliated Cabernet Sauvignon compared to both defoliated vines at veraison and nondefoliated ones. Autor emphasizes that the early defoliated vines were able to re-

Table 1. Average values of lateral leaf area (LLA) (m^2) by measurement terms (2014 – 2016).

Days after budbreak	LLA			
	V 1	V 2	V 3	Control
I (70-75)	0.100^{a}	0.177^{b}	0.194^{b}	0.193^{b}
II (85-90)	0.353^{b}	0.195^{a}	0.414^{c}	0.408^{c}
III (100-105)	0.523^{b}	0.415^{a}	0.615^{c}	0.629^{c}
IV (125-130)	$0.689^{b,c}$	$0.602^{a,b}$	0.532^{a}	0.759^{c}

a,b,c Values were grouped based on Duncan's multiple range test ($\alpha = 0.05$), where different letters within the same row denote significant diferences between treatments. K - control; v1- removal of the first six basal leaves at the phenological stage 65 (BBCH scale); v2 - removal of the first six basal leaves at the phenological stage 73; v3 - removal of the first six basal leaves at the stage 81.

cover their leaf area as a compensatory response to the leaf removal.

Non-destructive and continuous measurements of MLA and LLA area based on the same shoots allowed for the monitoring of LA development and calculation of the RLER during vegetation. After the second measurements of LA, RLER-1 of the main and lateral shoots and all shoots on the vine was the highest on v1 and the lowest on v2 vines (Figure 1).

RLER-1 of lateral shoots on v1 vines was 72% higher than v2 and 41% higher than v3 and the control vines. The reason for the high value at v1 and low at v2, lies in the time of defoliation and the time of LA measurements. The second measurement of LA was performed about 40 days after v1 and 20 days after v2 defoliation. During that period, v1 vines passed through a period of slow growth of the main shoots caused by the carbon assimilation depression (OLLAT & GAUDILLERE, [27]; PETRIE & al. [10]). This was followed by a period of lateral shoot emergence and their intensive growth as compensation for the removed leaves. These results are consistent with the previous experiment on defoliation at flowering stage (CANDOLFI-VASCONCELOS & KOBLET [18]; PASTORE & al. [33]; ACIMOVIC & al. [34]). Unlike the v1 vines, v2 vines were still in the phase of slow growth which was caused by recently performed defoliation. The third measurement of LA and calculation of RLER-2 were 30 days after v2 and 10 days before v3 defoliation. On Figure 1. we can see that v2 vines have the highest RLER values compared to other variants, but the differences are not so pronounced as in the previous measurement. The values of the v2 vine are about 30% higher compared to other variants. As mentioned above, the third measurement was performed during the period of slower growth of the main and lateral shoots, so the level of compensatory growth is lower compared to shoots whose leaves were removed in the phase of intensive growth. The last measurement and RLER-3 calculations were performed about 10 days after v3 defoliation, in the veraison phase, when the growth of shoots is either very slow, or it stops. This result is in accordance with the previous studies (PASTORE & al. [33]; STEFANOVIC [32]). The authors emphasize a significant reduction in the total leaf area in defoliated vines in veraison stage because there was no leaf regrowth after veraison. For the calculated RLER based on the first and last leaf area measurements, a similar situation was obtained. The RLER of the main, lateral and all shoots on the vine were highest on v1 compared to all the variants between which there was no significant difference. This is consistent with the previous condition when the early defoliated vines had time to compensate removed leaves by producing more lateral shoots with more leaves.

Conclusions

Non-destructive and continuous measurements of leaf area based on the same shoots enabled the monitoring of the leaf area development and the calculation of the relative leaf expansion rate. The grapevine's ability to recover the leaf area after defoliation depends mainly on the time when defoliation occurs. This study has shown that early defoliated vines had time to compensate their removed leaves by producing more lateral shoots with a greater number of leaves, which resulted in a larger leaf area. Moreover, the results show that with a decrease in the intensity of shoot growth during vegetation, the recovery ability decreases, so the compensatory growth is not enough to restore the reduced leaf area. Based on the values of the relative leaf expansion rate, it can be concluded that defoliation in the period of intensive growth of shoots affects the stagnation of emergence of new shoots and leaves for several days, followed by a period of regrowth. Very slow or no growth of shoots and leaves occurs after the veraison stage.

Acknowledgments: This research has been supported by the Ministry of Education, Science and Technological Development of the Republic of Serbia (Research grant No 43007).

References

1. R.E. SMART, J.B. ROBINSON, G.R. DUE, C.J. BRIEN, Canopy microclimate modification for the

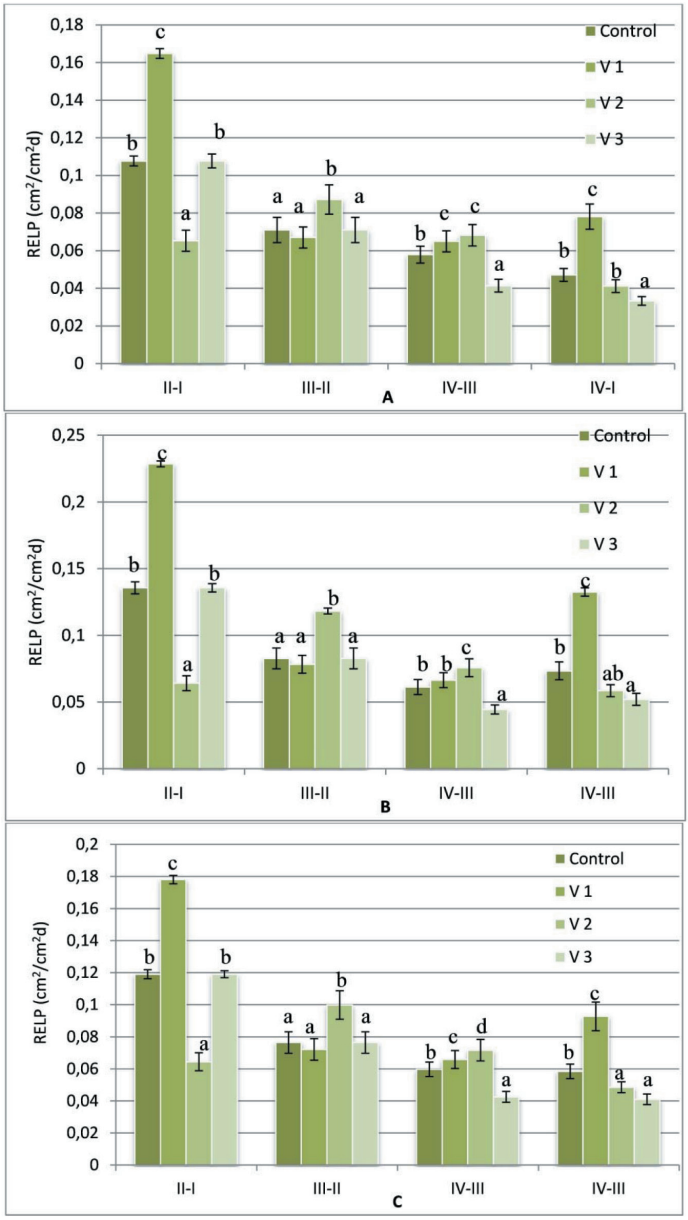

Figure 1. Relative leaf expansion rate (cm^2/cm^2d) of main (A), lateral (B) and total shoots (C). K - control; v1- removal of the first six basal leaves at the phenological stage 65 (BBCH scale); v2 - removal of the first six basal leaves at the phenological stage 73; v3 - removal of the first six basal leaves at the stage 81. (2014-2016).

cultivar Shiraz. II. Effects on must and wine composition. *Vitis.* 24, 119-128 (1985).
2. S. PONI, S. CIVARDI, The effect of early leaf removal on whole-canopy gas exchange and vine performance of *Vitis vinifera* L. 'Sangiovese'. Vitis. 47, 1-6 (2008).
3. W.M. KLIEWER, Effect of time and severity of defoliation on growth and composition of Thomson seedless grapes. Am. J. Enol.Vitic. 21, 37-47 (1970).
4. J.J. HUNTER, O.T. DE VILLIERS, J.E. WATTS, The effect of partial defoliation on quality characteristics of Vitis vinifera L. cv. Cabernet sauvignon Grapes. II. Skin Color, Skin Sugar and Wine Quality. Am. J. Enol.Vitic. 42, 13-18 (1991).
5. P. SABBATINI, G.S. HOWELL, Effects of early defoliation on yield, fruit composition and harvest season cluster rot complex of grapevines. Hort. Sci. 45, 1804-1808 (2010).
6. A. BAIANO, A. DE GIANNI, M.A. PREVITALI, M.A. DEL NOBILE, V. NOVELLO, L. DE PALMA, Effects of defoliation on quality attributes of Nero di Troia (*Vitis vinifera* L.) grape and wine. Food Res. Int. 75, 260-269 (2015).
7. W.D. GUBLER, L.J. BETTIGA, D. HEIL, Comparisons of hand and machine leaf removal for the control of Botrytis bunch rot. Am. J. Enol. Vitic. 42, 233–236 (1991).
8. D. MOLITOR, M. BEHR, S. FISCHER, L. HOFFMANN, D. EVERS, Timing of cluster-zone leaf removal and its impact on canopy morphology, cluster structure and bunch rot susceptibility of grapes. J. Int. Sci. Vigne Vin. 45, 149–159 (2011).
9. G.A. GAMBETTA, J.C. HERRERA, S. DAYER, Q. FENG, U. HOCHBERG, S.D. CASTELLARIN, The physiology of drought stress in grapevine: towards an integrative definition of drought tolerance. J. Exp. Bot. 71, 4658–4676 (2020).
10. P. PETRIE, M. TROUGHT, S. HOWELL, G. BUCHAN, The effect of leaf remuval and canopy height on whole-vine gas exchange and fruit development of Vitis vinifera L. Sauvignon Blanc. Funct. Plant Biology. 30, 711-717 (2003).
11. A. PALLIOTTI, M. GATI, S. PONI, Early leaf removal to improve vineyard efficiency: Gas Exchange, Source-to-Sink Balance, and Reserve Storage Responses. Am. J. Enol. Vitic. 62, 219-228 (2011).
12. S. PONI, L. CASALINI, F. BARNIZZONI, S. CIVARDI, S. INTRIERI, Effects of early defoliation on shoot photosynthesis, yield components and grape composition. Am. J. Enol. Vitic. 57, 397-407 (2006).
13. B.G. COOMBE, Research on development and ripening of the grape berry. Am. J. Enol.Vitic. 43, 101–110 (1992).
14. C. INTRIERI, I. FILIPPETTI, G. ALLEGRO, M. CENTINARI, S. PONI, Early defoliation (hand vs mechanical) for improved crop control and grape composition in Sangiovese (Vitis vinifera L.). Aust. J. Grape Wine Res. 14, 25-32 (2008).
15. S. PONI, F. BERNIZZONI, S. CIVARDI, N. LIBELLI, Effects of pre-bloom leaf removal on growth of berry tissues and must composition in two red Vitis vinifera L. cultivars. Aust. J. Grape Wine Res. 152, 185-193 (2009).
16. Z. BEŠLIĆ, S. TODIĆ, S. MATIJAŠEVIĆ, Effect of timing of basal leaf Removal on yield and grape quality of grapevine (Vitis vinifera L.). Bulg. J. Agri. Sci. 19, 96-102 (2013).
17. P. COLLIN, D. EPRON, B. ALAOUI-SOSSE, P.M. BADOT, Growth Responses of Common Ash Seedlings (Fraxinus excelsior L.) to Total and Partial Defoliation. Annals of Botany 85(3). 317-323 (2000).
18. M.C. CANDOLFI-VASCONCELOS, W. KOBLET, Influence of partial defoliation on gas exchange parameters and chlorophyll content of field-growth grapevines – Mechanisms and limitations of the compensation capacity. Vitis. 30, 129-141 (1991).
19. P.R. PETRIE, M.C.T. TROUGHT, G.S. HOWELL, Fruit composition and ripening of Pinot Noir (Vitis vinifera L.) in relation to leaf Area. Aust. J. Grape Wine Res. 6, 46-51 (2000).
20. K. KURTURAL, F. LYDIA, L.F. WESSNER, G. DERVISHIAN, Vegetative compensation response of a procumbent grapevine (Vitis vinifera cv. Syrah) cultivar under mechanical canopy management. Hort. Sci. 48, 576–583 (2013).
21. J.J. HUNTER, Implications of seasonal canopy management and growth compensation in grapevine. S. Afr. J. Enol.Vitic. 21, 81-91 (2000).
22. D.W. HILBERT, J.K. SWIFT, J.K. DETLING, M.I. DYER, Relative growth rates and the grazing optimization hypothesis. Oecologia. 51, 14-18. (1981).
23. N.P.R. ANTEN, M. MARTINEZ-RAMOS, D.D. ACKERLY, Defoliation and growth in an understory palm: Quantifying the contributions of compensatory responses. Ecology. 84, 2905-2918 (2003).
24. D.H. LORENZ, K.W. EICHHORN, H. BLEIHOLDER, R. KLOSE, U. MEIER, E. WEBER, Growth stages of the grapevine: phenological growth stages of the grapevine (Vitis vinifera L. ssp. Vinifera) - Codes and

descriptions according to the extendended BBCH scale. Aust. J. Grape Wine Res. 1, 100-103 (1995).

25. Z. BESLIC, S. TODIC, D. TESIC, Validation of Non-destructive Methodology of Grapevine Leaf Area Estimation on cv. Blaufränkisch (Vitis vinifera L.). S. Afr. J. Enol.Vitic. 31, 22-25 (2010).
26. R. DZAMIC, M. NIKOLIC, R. STIKIC, Z. JOVANOVIC, Plant Phisiology – Practicum. Naucna knjiga, Beograd, 2001.
27. N. OLLAT, J.P., GAUDILLERE, The effect of limiting leaf area during stage I of berry growth on development and composition of berries of Vitis vinifera L. cv. Cabernet Sauvignon. Am. J. Enol.Vitic. 49, 251-258 (1998).
28. T., FRIONI, D. ACIMOVIC, S. TOMBESI, P. SIVILOTTI, A. PALLIOTTI, S. PONI, P. SABBATINI, , Changes in within-shoot carbon partitioning in Pinot Noir grapevines subjected to early basal leaf removal. Front. Plant. Sci. 9, 1-11 (2018).
29. M.G. MULLINS, A.BOUQUET, L.E. WILLIAMS, Biology of the grapevine. Cambridge University Press, UK. 1992.
30. R.J. WEAVER, Effect of leaf to fruit ratio on fruit quality and shoot development in Carignane and Zinfandel wine grapes. Am. J. Enol.Vitic. 14, 1-12 (1963).
31. M.C. CANDOLFI-VASCONCELOS, W. KOBLET, Yield, fruit quality, bud fertility and starch reserves of the wood as a function of leaf removal in Vitis vinifera – Evidence of compensation and stress recovering. Vitis. 29, 199-221 (1990).
32. D. STEFANOVIĆ, Impact of defoliation timing on biological properties, quality of grapes and wine of Cabernet Sauvignon grapevine variety. Doctoral dissertation. Faculty of Agriculture, University of Belgrade, 2021.
33. C. PASTORE, S. ZENONI, M. FASOLI, M. PEZZOTTI, G.B. TORNIELLI, I. FILIPPETTI, Selective defoliation affects plant growth, fruit transcriptional ripening program and flavonoid metabolism in grapevine. BMC Plant Biology.13-30 (2013).
34. D. ACIMOVIC, L. TOZZINI, A. GREEN, P. SIVILOTTI, P. SABBATINI, Identification of a defoliation severity threshold for changing fruitset, bunch morphology and fruit composition in Pinot Noir. Aust. J. of Grape and Wine Res. 22, 399 - 408 (2016).

ISSN print: 1224-5984
ISSN online: 2248-3942

Rom Biotechnol Lett. 2022; 28(3): 3460-3465
doi: 10.25083/rbl/28.3/3460.3465

Received for publication: June, 10, 2022
Accepted: July 11, 2022

Original paper

Canine eosinophilic bronchopneumopathy: case study

LUCIAN IONIȚĂ[1], ALEXANDRA BRAICA[2], CĂTĂLIN MICȘA[1], NATALIA RĂDULEA[1], ROXANA TURCU[1], ELENA ROMAN[1], ANDREEA NICOLETA MINCĂ[1], CARMEN IONIȚĂ[1]*

[1]University of Agronomic Science and Veterinary Medicine of Bucharest, Romania.
[2]"Vasile Goldiș" Western University of Arad, Romania.

Abstract

Eosinophilic bronchopneumopathy, formerly known as PIE (Pulmonary Infiltration with Eosinophils) syndrome, is defined as an inflammatory pathology characterized by the presence of eosinophilic infiltrate in the lungs and bronchiolary structures. (CECILE CLERCX,2007). Canine eosinophilic bronchopneumopathy has been described similarly to that present in humans, highlighting tropism for the airways and lungs, but also the multitude of factors with the potential to trigger, which is why most of them are ranked with idiopathic factor. (Sol Kim et al,2021). Cases of eosinophilic bronchopneumopathy have been identified in most canine breeds, and according to current studies, the predisposition for large breeds under the age of 6, such as rottweilers, Siberian Husky and Alaskan Malamute, has been reported. (C. Clercx 2017). The present case is represented by a male, canine, of the Husky breed, who showed clinical respiratory signs, these were correlated with complementary examinations such as laboratory examinations, cardiological examination, radiological and endoscopic examination. Based on the haematological results, which present a marked eosinophilia, a differentiated diagnostic protocol was achieved compared to possible parasitosis and reactions of autoimmune type. Differential clinical diagnosis was made against dirofilariosis, angiostrongiliosis, lupus erythematosus, mycotic pneumopathies. PCR technique was used to determine the possible parasites present, sample collection with the help of endoscopy from the pulmonary infiltrate with cytological examination. The diagnosis of certainty was established on the basis of histopathological examination. He underwent treatment with corticosteroids, the evolution being favorable within 14 days of initialization of the treatment, with complete healing.

Keywords Dogs; Husky; Eosinophilic reactions; Immunological response; Repiratory diseases.

To cite this article: IONIȚĂ L, BRAICA A, MICȘA C, RĂDULEA N, TURCU R, ROMAN E, MINCĂ AN, IONIȚĂ C. Canine eosinophilic bronchopneumopathy: case study. *Rom Biotechnol Lett.* 2022; 28(3): 3460-3465 DOI: 10.25083/RBL/28.3/3460.3465

*Corresponding author: Associeted Prof. CARMEN IONIȚĂ, University of Agronomic Science and Veterinary Medicine of Bucharest, Splaiul Independenței nr 105.
E-mail: ionitacarmen63@yahoo.com

Introduction

The acquired immune system, by its excessive action, can produce inflammatory reactions with secondary tissue destruction,autoimmunization or amyloidosis. The reactions were classified into 4 basic types:

- Type I reaction - Immediate hypersensitivity
- Reaction type II - Antibody-mediated cytotoxics
- Reaction type III - Based on antigen-antibody complexes
- Type IV reaction - Cell-mediated immune reactions (Merck Veterinary, page 823)

Eosinophilic bronchopneumopathy is classified as a localized immediate hypersensitivity reaction and is frequently associated with inflammatory infiltrates in the lung, marked eosinophilia at the peripheral blood level and increased changes in serum globulins.

Pulmonary eosinophilia can occur in response to parasitic diseases (for example, Dirofilaria Spp, Dirofilaria immitis, Angiostrongylus vasorum), fungal (for example, Aspergillus), neoplastic (neoplastic formations in the upper or lower respiratory tract) or as an immunological response to external stimuli (foreign body, powders, etc.).

The cited clinical changes include changes in the general condition (apathy, exercise intolerance, breathlessness, decreased body weight) and changes in the respiratory system such as the presence of mucus in the upper respiratory tract, coughing, jetting, "wheezing".

This study focuses on establishing the diagnosis and correlating it with minimally invasive methods (ultrasound, X-ray, endoscopy, and laboratory examinations).

Differentiated clinical diagnosis consists in the exclusion of migratory or stationary parasitosis in the lung, pneumopathies or cardiopathies.

Materials and Methods

Data about the environment and the owner: Urban environment, lives in the apartment, the owner supports the lack of other allergenic factors such as: cigarette smoke, detergents, room perfume, etc.

Figure 1. The patient in the consultation room

Patient data: Canine, Siberian Husky, male aged 6 years, 32 kg at the time of the first consultation, without known allergies.

Anamnesis: Presented in the clinic for general consultation, showing cough with occasional progressive bronchorrhea, progressive dyspnea, respiratory noises, weight loss, intolerance to moderate and low efforts. Appetite present, defecates and urinates normally.

Clinical data:

General clinical examination: good maintenance condition, proper conformation, altered general condition, apparent pink-normal mucous membranes, body temperature 38ºC, no lymphonodal reaction on palpation, no visible lesions in the chest, neck or skull. At the auscultation of the heart does not show pathological breath, at the auscultation of the pulmonary area a breath is perceived, it presents cough with bronchorrhea, without pathological secretions at the level of the nostrils.

Table1. Biochemical examination results:

Test	Results	Reference Interval	LOW / NORMAL / HIGH
Catalyst Dx (April 15, 2022 2:53 PM)			
GLU	96 mg/dL	74 - 143	
CREA	0.9 mg/dL	0.5 - 1.8	
BUN	16 mg/dL	7 - 27	
BUN/CREA	18		
PHOS	4.2 mg/dL	2.5 - 6.8	
CA	9.7 mg/dL	7.9 - 12.0	
TP	7.3 g/dL	5.2 - 8.2	
ALB	3.0 g/dL	2.3 - 4.0	
GLOB	4.3 g/dL	2.5 - 4.5	
ALB/GLOB	0.7		
ALT	73 U/L	10 - 125	
ALKP	197 U/L	23 - 212	
GGT	8 U/L	0 - 11	
TBIL	0.2 mg/dL	0.0 - 0.9	
CHOL	146 mg/dL	110 - 320	
AMYL	419 U/L	500 - 1500	LOW
LIPA	1147 U/L	200 - 1800	

Table 2. Haematological examination results:

Test	Results	Reference Interval	LOW / NORMAL / HIGH
ProCyte Dx (April 15, 2022 2:46 PM)			
RBC	7.27 M/µL	5.65 - 8.87	
HCT	47.7 %	37.3 - 61.7	
HGB	16.3 g/dL	13.1 - 20.5	
MCV	65.6 fL	61.6 - 73.5	
MCH	22.4 pg	21.2 - 25.9	
MCHC	34.2 g/dL	32.0 - 37.9	
RDW	20.1 %	13.6 - 21.7	
%RETIC	1.0 %		
RETIC	69.8 K/µL	10.0 - 110.0	
RETIC-HGB	24.2 pg	22.3 - 29.6	
WBC	25.53 K/µL	5.05 - 16.76	HIGH
%NEU	45.9 %		
%LYM	15.2 %		
%MONO	4.2 %		
%EOS	34.4 %		
%BASO	0.3 %		
NEU	11.75 K/µL	2.95 - 11.64	HIGH
LYM	3.87 K/µL	1.05 - 5.10	
MONO	1.07 K/µL	0.16 - 1.12	
EOS	8.77 K/µL	0.06 - 1.23	HIGH
BASO	0.07 K/µL	0.00 - 0.10	
PLT	159 K/µL	148 - 484	
MPV	13.6 fL	8.7 - 13.2	HIGH
PDW	13.2 fL	9.1 - 19.4	
PCT	0.22 %	0.14 - 0.46	

Results SNAPshot 4Dx and blade/blade:
Immitis Ag - Undetected
Anaplasma spp. AgIgG- Areactiv
B. Burgdorferi AgIgG- Areactiv
Ehrlichia spp. AgIgG- Areactiv
Negative microfilarias - blade/slide test

Table 3. Results SNAPshot 4Dx and blade/blade:

Test	Results
SNAPshot Dx (April 15,	
AP_spp	Negative
EC-EE	Negative
HW	Negative
Lyme	Negative

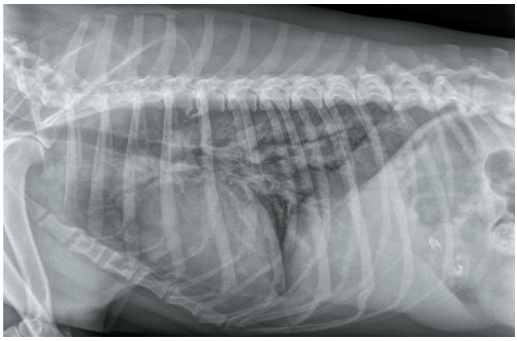

Figure 2. Radiographic image view LL- right

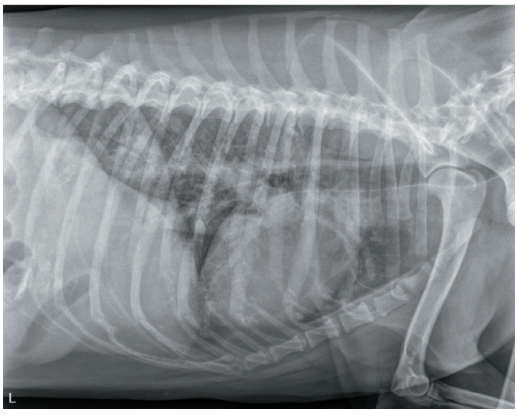

Figure 3. Radiographic image view LL– left

It is recommended complete biochemical and hematological examination, SNAPshot 4Dx, radiography of the skull, neck and chest.

It is observed changes at the level of pancreatic amylase - 419 U / L (reported to 500-1500 U / L), without other biochemical changes, but it is found that the globulins are at the upper limit - 4.3g / dL (reported to 2.5-4.5 g / dL).

During the haematological examination, significant changes were found in the white line, also called the line of defense, represented by WBC = 25.53 K/µL (relative to 5.05-16.76 K/µL), NEU=11.75 K/µL (relative to 2.98-11.64 K/µL), EOS=8.77 K/µL (relative to 0.06-1.23 K/µ L), MPV=13.6 fL (relative to 8.7- 13.2 fL), thus identifying an important increase that marks obvious eosinophilia and mild neutrophilism. Taking into account the present results, I would also like to highlight the values of monocytes and basophils at the upper limit.

Chest radiographic image:

Radiographically, the broncho-alveolar pattern is observed, with highlighting the bronchogram and thickening of the bronchiolary walls.

Following the laboratory results and the radiographic examination, we decided the need to perform a complete cardiological examination from which the following conclusions resulted:

▪ Lack of important morpho-functional changes from the hemodynamic point of view

▪ Low systolic pulmonary arterial hypertension (without a pathology of the left heart present)

▪ Dilation of the pulmonary trunk and lower left and right pulmonary arteries

▪ ECG: sinus rhythm

▪ Average of systolic and diastolic blood pressure values=155/75 mmHg

▪ PCR testing is recommended for D. Immitis and Angiostrongylus vasorum, suspected a pneumopathy.

Table 4. PCR Test Results:

Babesia spp.	Undetected
Dirofilaria immitis	Undetected
Dirofilaria repens	Undetected
Anapiasma spp	Undetected
Ehrlichia spp.	Undetected
Hepatozoon canis	Undetected
Mycoplasma haemocanis	Undetected

Babesia spp. genome identification* by qPCR and melting curve analysis

Genome identification **Dirofilaria immitis*** by qPCR and melting curve analysis

Identification of genome **Dirofilaria repens*** by qPCR and analysis of melting curves

Anaplasma spp. genome identification* by RT-qPCR and melt curve analysis

Identification of **genome Ehrlichia spp.*** by RT-qPCR and analysis of melting curves

Identification of Hepatozoon canis* genome by qPCR and melting curve analysis

Mycoplasma haemocanis* genome identification by qPCR

Results PCR negative for *Babesia* spp., *Hepatozoon canis*, *Anaplasma* spp., *Ehrlichia* spp, *Mycoplasma haemocanis*, *Dirofilaria immitis* si *repens*.

Test result *Angiostrongylus vasorum* - Negative.

Table 5. Result test *Angiostrongylus vasorum*

TEST	RESULT
Angio Detect	Negative

To confirm the diagnosis of canine eosinophilic bronchopneumopathy we recommended performing a Tracheo-Bronchoscopy by examining the upper and lower respiratory segment and then taking tissue and bronchoalveolar fluid from the pulmonary lobes.

Preparation and anesthesia:

Broncho-alveolar lavage is performed under general inhalation anesthesia. Pre-anesthesia clinical examination does not reveal significant changes. The patient is present, with good general condition, restless. It is decided to administer premedication intramuscularly with Dexmedetomidine (2mcg/kg), Butorphanol (0.3 mg/kg) and Ketamine (1 mg/kg). After the administration of the premedication, the patient is left in a quiet and dark room for 15 minutes. After sedation, a peripheral venous catheter is mounted and the induction stage is passed. This stage is performed with Propofol, 2 mg/ kg, followed by orotracheal intubation with endotracheal probe of 10 mm. Maintenance is done with Isoflurane and oxygen. Monitoring during anesthesia includes monitoring of heart rate, heart rate, oxygen saturation and blood pressure measured non-invasively. Fluidotherapy is provided with Ringer, at a rate of 4 ml / kg / h.

Endoscope penetrates through the epiglottis, to the trachea and lungs parallel to the endotracheal probe, taking care that the balloon of the endotracheal probe is not unfluted. After the end of the procedure, the patient is still monitored, until the complete awakening.

Broncho-alveolar lavage:

She tried to take a tissue sample with the help of the biopsy brush but it was revealed the presence of a yellowish secretion and the semi-hard / ceruminous consistency. Sampling was carried out using the cytology brush and then taking bronchoalveolar fluid. An amount of 3ml/kg of sterile saline was introduced into the bronchi and then tried to extract it. The samples were collected from the resulting liquid and scraped.

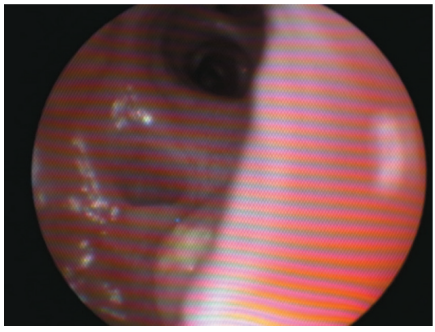

Image 1. Appearance of endoscopic

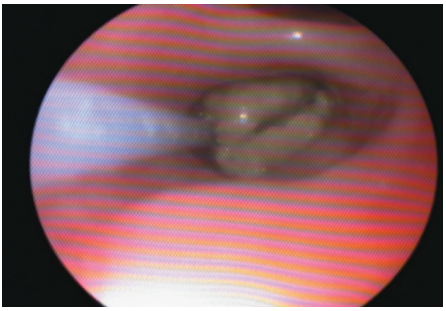

Image 2. Appearance of pulmonary infiltrate

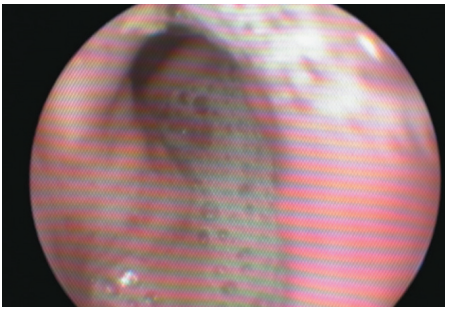

Image 3. Appearance after broncho-alveolar lavage

Result cytological preparation examination:

Cell-rich smear with mucus in moderate quantity, against the background of the numerous inflammatory cells present, the dominant being eosinophilia, neutrophils and macrophages are additionally identified. Normal-looking broncho-alveolar epithelial cells.

Cytological appearance indicates an acute inflammatory process.

Treatment:

I instituted treatment with corticoids (methylprednisolone) per os for two weeks. After a week, significant improvements in general condition are noted, with increased exercise tolerance and a decrease in the presence and intensity of cough.

The final diagnosis being idiopathic canine eosinophilic bronchopneumopathy.

Conclusions

It is found hematological changes of importance at the level of the defense line, the presence of significant eosinophilia (7 times higher relative to the maximum value) cited in such pathologies, WBC about twice as high as the maximum value, mild neutrophilia, which orient the diagnosis to pathologies of an inflammatory or parasitic order.

The lack of changes in serum proteins is emphasized, but the presence of values close to the upper limit indicated by the apparatus is mentioned.

The possibility of the presence or absence of radiological signs indicating a pneumopathy is recognized and the importance of endoscopy with sampling and CT performance is emphasized.

It supports the multitude of triggers of pulmonary localized inflammatory reactions.

It is supported to make a differentiated diagnosis against parasites with pulmonary tropism.

The presence of cough as a characteristic sign is supported, along with dyspnea to varying degrees and intolerance to exertion.

Clinical signs improved significantly within a few days after treatment with an oral corticosteroid.

The possibility of predisposition for the Husky breed, under the age of 6 years, known and noted in the framework of international veterinary studies, is supported.

It is argued the importance of having a general clinical consultation and an annual cardiological specialist consultation.

The importance of blood examinations is supported at least twice a year.

Conflict of interest

The authors declare no conflict of interest.

References

1. CECILE CLERCX 2007. *Canine Eosinophilic Bronchopneumopathy*, Veterinary Clinics of North America, Small Animal Practice; VOLUME 37, ISSUE 5, P917-935, SEPTEMBER 01, 2007
2. Dawn E. E. 2020- *Canine eosinophilic pulmonary granulomatosis*: *case report and literature review,* Abbott and Andrew L. Allen; Journal of Veterinary Diagnostic Investigation 2020, Vol. 32(2) *329–335*
3. Sol Kim and Kyoungwon Seo, Kunho Song 2021.*Successful Management of Eosinophilic Bronchopneumopathy in a Dog; J Vet Clin 2021;38:269-273*
4. Cecile Clercx and Dominique Peeters, Frederic Snaps, Pascale Hansen, Kathleen McEntee, Johann Detilleux,Marc Henroteaux, and Michael J. Day. *Eosinophilic Bronchopneumopathy in Dogs; J Vet Intern Med 2000;14:282–291*
5. Lynelle R. Johnson1 and Eric G. Johnson, Sean E. Hulsebosch1, Jonathan D. Dear1, William

Vernau (2006-2016). *Eosinophilic bronchitis, eosinophilic granuloma, and eosinophilic bronchopneumopathy in 75 dogs;* J Vet Intern Med. 2019;33:2217–2226.

6. Carlos Fernando Agudelo and Ladislav Stehlik, Zita Filipejova,Benicie Koskova, Marie Sterbova, Michal Crha *2022*. *Pulmonary eosinophilic granulomatosis in a dog;* Veterinarni Medicina, 67, (03):150–155.
7. XXX- The Merck Veterinary Manual, 11th Edition.- *IMMUNOLOGIC DISEASES page 825 - Eosinophilic bronchopnewnopathy*
8. The Merck Veterinary Manual, 11th Edition - *EXCESSIVE ADAPTIVE RESPONSES page 823 - Type I Reactions page 823*
9. C. Clercx 2017. *Eosinophilic Bronchopneumopathy in Dogs.* World Small Animal Veterinary Association Congress Proceedings.

ISSN print: 1224-5984
ISSN online: 2248-3942

Rom Biotechnol Lett. 2022; 27(3): 3466-3474
doi: 10.25083/rbl/27.3/3466.3474

Received for publication: June, 01, 2022
Accepted: July 20, 2022

Original paper

Use of Stabilized rice bran for preparing Beef Burger

HAGER IBRAHIM EL-DAKARANY[1], ABDEL MOATY EL-ABD[1], MOHAMED AHMED EL-BANA[2], MOHAMED ABDELBASET SALAMA[2], SAHAR RAMADAN ABDELHADY[3], ADEL GHAZI[3]

[1]Rice Research Section, Field Crops Research Institute, Agric. Res. Center, Giza, Egypt
[2]Food Technology Research Institute, Agricultural Research Center, Giza, 12611, Egypt
[3]Food Technology Department, Faculty of Agriculture, Kafrelsheikh University, Kafrelsheikh, 33511, Egypt

Abstract

This study was performed to investigate the effect of thermal processing (microwave oven, roasting by dry heat at 130°, for 10 and 20 min. and steaming by using an autoclave under atmospheric pressure for 10 and 20 min.) on the stability of rice bran and the utilization of microwave stabilized rice bran as fat replacers in preparing a low-fat beef burger. The obtained results revealed that: rice bran contained high levels of carbohydrates and moderate amounts of ether extract and crude protein. No differences were detected in the refractive index of rice bran oil among the stabilization procedures, whereas slight differences were found in the case of specific gravity. When rice bran oil was subjected to stabilized procedures, the acid value, iodine value, peroxide value, saponification value, and unsaponifiable matter were reduced. Moreover, the total saturated fatty acids content of rice bran oil increased as a result of subjecting to stabilization procedures whereas the total unsaturated fatty acid content decreased. The results show that stabilized rice bran is effective in improving the chemical and functional characteristics of a beef burger.

Keywords Stabilized rice bran, low-fat beef burger, fat replacer

To cite this article: EL-DAKARANY HI, EL-ABD AM, EL-BANA MA, SALAMA MA, ABDELHADY SR, GHAZI A. Use of Stabilized rice bran for preparing Beef Burger. *Rom Biotechnol Lett.* 2022; 27(3): 3466-3474 DOI: 10.25083/rbl/27.3/3466.3474

*Corresponding author: walid.metwali@agr.kfs.edu.eg

Introduction

High-fat diets are associated with several types of diseases, such as obesity, hypertension, cerebral apoplexy, myocardial infarction, diabetics, and coronary heart diseases Husak et al. [1], therefore many consumers now, are looking for no fat or low-fat versions of their traditional foods. Modern consumers interested in low-fat diets have led the food industry to develop or modify traditional food products in order to contain less fat. Rice bran has recently been used in ground beef products for both nutritive and antioxidant functionality. In addition, it possesses high levels of monounsaturated fatty acid, oleic acid, and very high levels of antioxidant compounds including tocopherols, tocotrienols, and oryzanols Godber et al. [2]. However, rice bran, a byproduct of rice milling was considered unfit for prolonged storage and consumption, because of the enzyme lipase, rice bran is no longer used as waste material. The stabilized rice bran (SRB) is an allergen-free functional ingredient that can replace some of all of the traditional binders in meat products Lee et al. [3]. Moreover, rice bran is highly nutritious and hence used as a food additive. Its major use as an additive in foods is due to the dietary fibers present in it which confer upon it the characteristics of a good laxative Kim et al. [4]. Rice bran is a low-cost byproduct of rice (*Oryza sativa L.*), which is widely grown in many places of the world Rukmini, and Raghuram [5]. In 2014, the worldwide production of paddy rice exceeded 738 million metric tonnes (MMT), yielding around 70 MMT of bran FAO/UN [6]. Rice bran is a considerable byproduct of the rice milling process, accounting for 5-10% of milled rice. The bran is a good source of protein, fat, crude fiber, carbohydrates, vitamins, minerals, essential unsaturated fatty acids, and phenolics Saenjum et al. [7]. Rice bran oil is usually used as an excellent cooking medium because of its nutritional superiority, abundant micronutrients longer shelf-life stability at high temperatures, and better taste provided to food items.

The amount of rice bran components vary according to rice type, storage, climate conditions, rice bran stabilization, and processing methods Amarasinghe and Gangodavilage [8]. In addition, rice bran contains 88-89 % neutral lipids, 3-4 % waxes, 2-4 % free fatty acids, and approximately 4 % unsaponifiable Kim et al. [9]. However, because of its enzymatic activity following rice dehulling, rice bran oil's use is limited. Rice bran is abundant in lipids, and excessive lipase activity in the presence of endogenous lipoxygenase induces rancidification of these lipids Paucar-Menacho et al. [10]. Because of the lipid deterioration susceptibility of the rice bran. To avoid fatty acid release, increase shelf life, and allow commercialization for human consumption, it must be enzymatically inactivated immediately after bran extraction Herfel et al. [11]. Rice bran cannot be used as a food component because of the instability that occurs during storage. This instability refers to the lipase enzyme activity present in the outer layers of the rice kernel which is responsible for the hydrolysis of triglycerides yielding glycerol and free fatty acids. Lipoxygenase and peroxidase are also key enzymes responsible for the instability of rice bran Orthoefer [12]. Rice bran oil stands out among the healthiest and most nutritious edible oils. Rice bran oil has a fatty acid composition that is around 19% saturated (palmitic acid), 42% monounsaturated (oleic acid), and 39% polyunsaturated (linoleic acid) Mezouari et al. [13]. When compared to other vegetable oils, crude rice bran oil is noted for its relevant untraditional matter. Refined rice bran oil and crude rice bran oil may contain 1.5-2.6% and 5% unsaponifiable matter, respectively, while the unsaponifiable content of many commonly used oilseed oils is normally 0.4- 0.6% Krishna et al. [14]. Currently, there is an increased interest in the use of dietary antioxidants, including vitamins C and E, to prevent cardiovascular diseases. However, numerous natural antioxidants may be added to meat products to enhance their health advantages. Malekian et al. [15] This work was undertaken to study the possibility of using stabilized rice bran as a food additive for preparing healthy beef burgers.

Materials and methods

Materials

Rice bran samples have been collected as a byproduct of milling of a combination of three Egyptian rice (Oryza sativa L.) cultivars, namely Sakha 101, 105, and 106, which are popular short-grain japonica varieties consumed in Egypt. Rice bran samples were collected at the Rice Research and Training Center (RRTC) in Sakha, Kafrelsheikh Governorate, Egypt, during the 2020 growing season. The red muscle beef, kidney fat, and other components necessary to make beef burgers were obtained from a local market in Kafrelsheikh. The analytical grade chemicals used in the study were obtained from El-Gomhouria for Trading Chemicals and Medical Appliances in Tanta City, Egypt.

Methods

Rice bran conditioning

The full-fat raw bran was cleaned by removing the husk, and the samples collected were free of impurities.

Stabilization of rice bran

Rice bran samples were subjected to different stabilization methods as follows: the control was unstabilized rice bran (Un-RB); the first sample was stabilized by MW

treatment at 900W, for 2 min. and manually mixed every minute according to Faria et al. [16]. The second and third samples were separately roasted in a hot-air oven at 130ºC for l0 min. (HAO1) and 20 min. (HAO2), respectively Bagchi et al. [17]. The fourth and fifth samples were steamed in the autoclave under atmospheric pressure for 10 min. (Autoclave 1) and 20 min. (Autoclave 2), respectively Rosniyana et al. [18]. Finally, the bran samples were stored in the dark at -10°C in water-tight containers until further analyses.

For the clearer presentation of the samples, I suggest you to insert a table and present the final notation and main parameters for each sample. These notations should be the same in all article.

Preparation of beef burger with different percentage of stabilized rice bran

Beef meat and kidney fat were grounded separately grounded in a meat grinder. The beef burger was formulated to contain: 80% grounded red beef meat, 20% grounded kidney fat, 18% (w/w) water, 1.5% salt, 0.3% black pepper (powder), 0.2% red pepper (powder) and 0.2% cumin (powder) as outlined by Aleson-Carbonell et al. [19]. Other burger formulations were added by substitution of fat at levels of 5%, 10%, 15%, and 20%) of microwave stabilized rice bran.

Gross chemical composition of the samples

Moisture, protein, ether extract, and ash contents were analyzed according to A.O.A.C. [20]. Total carbohydrates were calculated by differences.

Rice bran oil extraction

Rice bran oil was extracted from all bran samples by slurring with four volumes of food grade hexane at room temperature for 1 hr. Hexane was evaporated in a rotary evaporator at 40oC Kahlon et al. [21] .

Physical and chemical parameters of extracted oils

Rice bran oils' refractive index, specific gravity, acid value, peroxide value, iodine value, saponification value, and unsaponifiable matter were determined using the procedures described in A.O.A.C. [20].

The fatty acid profile of rice bran oil samples was determined

The methyl ester of fatty acids in rice bran oil samples was evaluated using gas chromatography (GC) in accordance with the A.O.A.C. method [20].

Beef burger cooking parameters

The beef burger studied samples were cooked using an electrical grill (Arcelik Mini Firin, Turkey) at 300 °C (the distance between heat source and the sample was 4 cm) for a total of 10 min, 6 min one side and 4 min in the other side Sorour et al. [22].

Beef burger organoleptic properties

The Sensory characteristics of the cooked burger samples were carried out by well-trained 20 panelists of Food Technology Research Institute (FTRI). Panelists were asked to evaluate color, taste, odor, texture, tenderness, and overall acceptability, of cooked samples according to the method described by Badr, and El-Waseif [23].

Statistical analysis

The data were statistically analyzed by paired samples T test analysis of variance (ANOVA) procedure with SPSS software (Version 16.0, SPSS Inc., Chicago, IL) software as described by Steel, R.G. and Torrie [24].

Results and discussion

Chemical composition of rice bran samples

Many factors influence the chemical composition of rice bran, including rice type, variance in organic compounds in the soil, fertilizer used, climatic and environmental conditions, milling degree, and treatments El-Bana et al. [25]. As a result, chemical compositions were obtained in order to investigate the previously indicated treatments and their influence on the quality of the various samples. The results presented in Table 1, shows the chemical composition of Un-RB and rice bran after the various stabilizing processes MW, HAO1, HAO2, and Autoclave 1 and 2. The moisture content values of rice bran samples were significantly different at ($P<0.05$). The moisture content of HAO2 rice bran was lower than that of Un-RB and rice bran subjected to the other stabilization procedures, this procedure may be effective for samples with a longer shelf life, less microbial contamination, and some nutrient preservation. The obtained results are in accordance with those of Abd El-Hady [26], who reported that the moisture content of stabilized oils depended on the processing temperature and duration of heating. Furthermore, moisture content plays a key role during storage Amorim et al 2004 [27]. Also shown in Table (1) the autoclaved rice bran samples (Autoclave 1 and 2) contained the highest content of crude protein contents 16.94 and 17.04 %, respectively, followed by HAO2 (16.65%) while the lowest crude protein content (15.34%) was found in the control (Un-RB). These results are in line with those obtained by Bagchi et al. [17].

Based on ether extract, Un-RB and stabilized rice bran contained 18.52 to 20.32% crude fat (Table, 1). Furthermore, stabilization by either dry or moist heat helped to in-

Table 1. Gross chemical composition (%) of rice bran after different stabilization procedures.

Treatment	Moisture	Crude Protein	Ether Extract	Ash	Carbohydrates*
Un-stabilized	8.56a+	15.34d	18.52d	8.7b	57.44a
Microwave	6.65c+	16.04c	20.32a	9.31a	54.33b
Hot Air Oven1	6.60c+	16.16c	19.42c	9.20a	55.22b
Hot Air Oven2	6.10d+	16.65b	19.82b	9.40a	54.13b
Autoclave 1	7.30b+	16.94a	19.32c	9.27a	54.47b
Autoclave 2	7.50b+	17.04a	20.02a	9.40a	53.54d

+ Means with the same small superscript letters in a column are not significantly different at p≤ 0.05.

* Total carbohydrates were calculated by the difference.

(1) Un-stabilized (Un-RB). (2) Microwave (MW) 900 W for 2min .

(3) Hot Air Oven1 (HAO1) 130°C for 10 min. (4) Hot Air Oven2 (HAO2) 130°C for 20 min.

(5) Autoclave 1: Steaming for 10 min. (6) Autoclave 2: Steaming for 20 min.

crease the ether extract levels in rice bran. The augmentation of oil extractability could be related to the ability of heat to cause the fat in the cells to coalesce into oil droplets and break down cell structure, thereby improving the speed and extent of oil extraction, or causing degradation of lipoproteins. These results are in agreement with those reported by Vissers et al. [28]. As previously reported by other authors, different stabilization techniques play an active role in reducing enzymatic activity to a greater or lesser degree, hence, increasing or decreasing oil extraction Lakkakula et al. [29]. As shown in Table (1) the ash content of Un-RB and stabilized rice bran ranged from 8.70 to 9.0%, and the total carbohydrate content ranged from 54.13 to 57.44 %. The present findings are similar to those reported by Abd El-Hady and Bagchi et al. [26 and 17].

Physical and chemical characteristics of oils obtained from rice bran after various stabilizing processes

Physical characteristics

The physical characteristics of rice bran oil were determined, and the findings are shown in Table (2). One of the most significant physical factors used in the identification of fats and oils is the refractive index; it may be used to measure the degree of saturation of oils. There were no significant changes in the refractive index of Un-RB (1.4603) or stabilized rice bran oils (1.4671-1.5703) at (p 0.05) (Table, 2). These findings are consistent with those of Kawase et al. [30].

At 25°C, the specific gravity of oils extracted from untreated rice bran was 0.9152. These findings are consistent with those of Iskander et al. [31]. The heat treatments, specifically the MW treatment, increased the specific gravity of rice bran oil to 0.9281. Furthermore, the heat treatments had a slight effect on specific gravity. However, there is a non-linear relationship between temperature and the specific gravity of oils as found by Davies [32]. The obtained results are in agreement with those of Rizk et al. [33].

Chemical characteristics

The chemical properties of rice bran oil were determined and the results are presented in Table (2). The acid and peroxide values of oil extracted from un-stabilized (Un-RB) rice bran were (1.34% and 0.901 meq O2/kg oil), respectively. These results are comparable to those reported by Sanghi and Tiwle [34].

The heat treatments especially MW led to a decline in both acid and peroxide values. Such results may be due to the inhibition of lipase activity in rice bran by heat. Acid and peroxide values reflect oil quality degradation as a function

Table 2. Physical and chemical properties of rice bran oil after different stabilization procedures.

Parameters	Stabilization Treatments					
	Control	MW	HAO1	HAO2	Autoclave 1	Autoclave 2
Refractive index (25ºC)	1.4603a+	1.4671a	1.4603a	1.4602a	1.4602a	1.4703a
Specific gravity (25ºC)	0.9152b+	0.9281a	0.9144b	0.9162b	0.9252a	0.9201ab
Acid value (%)	1.34a+	1.11d	1.29b	1.21c	1.15d	1.13d
Peroxide value (meq/kg oil)	0.901a+	0.655e	0.838b	0.805c	0.751d	0.731d
Iodine value (gI/100g oil)	107.20a+	100.61f	106.10b	105.22c	102.10d	101.41e
Saponification value (mg KOH/g oil)	196.12a+	195.41b	195.55b	194.77c	194.10d	194.30d
Unsaponifiable matter (%)	4.52a+	4.37b	4.31b	4.19c	4.16c	4.11c

+ Means with the same small superscript letters in rows are not significantly different at p≤ 0.05.

(1) Un-stabilized (Un-RB). (2) Microwave (MW) 900 W for 2 min.

(3) Hot Air Oven1 (HAO1) 130°C for 10 min. (4) Hot Air Oven2 (HAO2) 130°C for 20 min.

(5) Autoclave 1: Steaming for 10 min. (6) Autoclave 2: Steaming for 20 min.

Table 3. Fatty acids (%) profile of o rice bran oil after different stabilization procedures.

Fatty acid	Control*	MW oil	HAO1 oil	HAO2 oil	Auto1 oil	Auto2 oil
Myristic, C14:0	0.55	0.57	0.75	0.77	0.69	0.72
Palmitic, C16:0	17.40	17.80	19.65	19.96	19.0	19.30
Palmitoleic, C16:1	0.13	0.14	0.23	0.23	0.16	0.20
Stearic, C18:0	1.72	1.76	2.3	2.34	1.79	2.09
Oleic, C18:1	42.40	42.10	41.17	41.06	41.72	41.42
Linoleic, C18:2	36.40	36.30	34.75	34.55	35.30	35.0
Linolenic, C18:3	0.80	0.76	0.67	0.63	0.76	0.73
Eicosenoic, C20:1	0.60	0.57	0.48	0.46	0.58	0.54
TSFA** (%)	19.67	20.13	22.70	23.07	21.48	22.11
TUSFA** (%)	80.33	79.87	77.30	76.93	78.52	77.89

*- Control = oil extracted from Un-RB.

**TSFA = Total saturated fatty acids, **TUSFA = Total unsaturated fatty acids

of triacylglycerol hydrolysis and the further breakdown of hydroperoxides Nagassapa et al. [35]. Furthermore, Autoclave 2 had a stronger effect on the acid and peroxide values than Autoclave 1. In addition, autoclaving process was more effective than the use of a hot-air oven treatment. Abdel-Aal and Sosulski [36], stated that steam treating of some grains for 5 min. led to a reduction in the acid value of their oils and that steaming oat for one minute reduced the peroxidase activity to 40-60% of that in the control, moreover, the reduction reached 95% of the original activity after steaming for 3 min. Additionally, El-Sayed [37], stated that, heat treatments especially steaming, led to the decline of both acid and peroxide values, in addition to heat treatments for 20 min. were more effective than those for 10 min. The iodine value also indicates the stability of oil against oxidation, since it represents the degree of unsaturation of oils and measures their vulnerability to oxidation Nagassapa et al. [35]. The iodine values of the rice bran samples varied from 107.20 to 100.61 g /100g (Table 2). These results are comparable to those reported by Iskander et al. and Abdel-Aal, and Sosulski [31 and 36]. Furthermore, heat treatment had an obvious effect on the iodine value of rice bran oil and played an active role in decreasing the iodine value. This result could be related to the destruction of double bonds in the unsaturated fatty acids of oils as a function of heating as found by Nagassapa et al [35]. The results in Table (2) showed that the saponification values of rice bran oils ranged from 194.10 to 196.12 mg KOH/g. Crude rice bran oil contains about 96% saponifiable matter and approximately 4% un-saponifiable matter. These results are in agreement with those of Orthoefer [12]. The stabilization process especially in MW had a slight effect on the saponification value. These results are comparable to those found by El-Sayed [37], who reported that heat treatment had a small effect on saponifiable matter. In addition, the reduction of saponification value of oils as a result of heating could be attributed to the chemical reactions that led to the degeneration of products other than free fatty acids Nagassapa et al. [35]. In addition, unsaponifiable matter including hydrocarbons, sterols, vitamins, and pigments, usually play an important role in oil stability. Table (2) shows that the unsaponifiable matter of rice bran oil extracted from the Un-RB and stabilized rice bran oil samples ranged from 4.11 to 4.52%. These results confirmed that, rice bran oil has a large amount of unsaponifiable matter. The results of unsaponifiable matter content were in accordance with those reported by Kahlon et al. and El-Sayed [21 and 37].

Fatty acids composition

The results presented in Table (3) show the fatty acid composition of rice bran oil extracted from Un-RB and stabilized (MW, HAO1, HAO2, Autoclave 1 and 2) rice bran. Oleic acid (C18:1), linoleic acid (C18:2), and palmitic acid (C 16:0) are the dominant fatty acids in Un-RB, and stabilized rice bran oil were in the ranges of 41.06- 42.40; 34.55- 36.40 and 17.40- 19.96%, respectively.

The concentrations of the major fatty acids, namely C18:2, C18:1and C16:0 of the investigated rice bran oils generally agreed with those of Kahlon et al. and Amarasinghe and Gangodavilage [21 and 8], who studied the fatty acid composition of 204 rice varieties and found that the main fatty acids in rice bran oil were palmitic, oleic, and linoleic acids, which were in the ranges of 13.9–22.1, 35.9–49.2, and 27.3– 41.0%, respectively. The level of these fatty acids depends on the variety and cultivation location of the rice Gupta and Awad-Allah [38 and 39]. The reduction in oleic and linoleic acids represents a decrease in the yielded free fatty acids that might be expected during storage. Conditions especially conditions that promoting oxidation reactions. The results of the present study agree with those obtained by Krishna [40]. Concerning thermal processing, the results presented in Table (3) revealed that thermal processing of rice bran caused a decrease in unsaturated fatty

Table 4. Chemical (%) and cooking properties of beef burger supplemented with different levels of microwave stabilized rice bran.

Chemical Characteristics	Moisture	Ash	Crude Protein	Crude Fat	Carbohydrates*
Control	**57.97e	1.88e	52.70 e	23.50 a	21.92 e
5% rice bran	58.55d	2.40 d	54.80 d	18.21 b	24.59 d
10% rice bran	59.35c	2.90 c	56.95 c	14.61 c	25.54 c
15% rice bran	60.40b	3.50 b	58.10 b	11.95 d	26.45 b
20% rice bran	61.20a	4.01 a	59.29 a	9.70 e	27.00 a
cooking properties	Control	5% rice bran	10% rice bran	15% rice bran	20% rice bran
Cooking Yield%	+67.54 e	72.08 d	77.82 c	82.30 b	86.30 a
Cooking Loss%	32.46 a	27.92 b	22.18 c	17.70 d	13.70 e
Shrinkage %	25.15 a	20.86 b	16.89 c	13.89 d	11.69 e

*- carbohydrates were calculated by difference.

**Value in column with the same letters are not significantly different at $p \leq 0.5$.

+- Values in rows with the same letter are not significantly different at $p \leq 0.5$.

acids especially after (HAO2), while saturated fatty acids increased. In contrast, MW processing caused a slight decrease in unsaturated fatty acids. The results of the present study were in agreement with those obtained by Abd El-Hady and El-Sayed [26 and 37].

Chemical and cooking properties of beef burger supplemented with different levels of microwave stabilized rice bran

Microwave stabilized rice bran with levels 5.0, 10.0, 15.0, and 20.0 % was used in the beef burger formula, and the resultant beef burger was subjected to chemical characterization and cooking properties determination. It should be noted from the results shown in Table (4) that, the moisture content of all-beef burgers containing stabilized rice bran with levels (5.0, 10.0, 15.0 %, and 20.0 %) as fat replacer, increased significantly ($p \leq 0.05$) with increasing of replacement level of rice bran. The increment of moisture content may be due to the capability of microwave stabilized rice bran rich with fiber to hold more water via the preparation and cooking process. These results are in agreement with Ibrahium et al. and Sorour et al. [41 and 22], who stated that dietary fiber source has the capacity to hold three or four times the weight of water. For fat content of the control, the beef burger had a high amount of fat with significant difference from that of other treatments. Furthermore, the fat content of all-beef burgers containing stabilized rice bran with levels (5.0, 10.0, 15.0, and 20.0 %) decreased significantly ($p \leq 0.05$) with increasing of replacement level of stabilized rice bran. These results agree with Ibrahium et al. [41]. On the other hand, the protein content of the beef burger was increased as the replacement level increased. Furthermore, protein content percentages of beef burger samples were 52.70,54.80 56.95,59.10, and 61.30 % for the control sample and those formulated by replacing fat with levels (5.0, 10.0,15.5, and 20.0 %). These results agree with, Ibrahium et al. and Sorour et al. [41 and 22].

From analysis of data presented in the same Table (4) it could be noticed that, the ratios of replacement levels increased the total carbohydrates of samples were increased with a significant difference in comparison with the control beef burger. Meanwhile, the ash content in the beef burger formula was significant differences at $p>0.05$. Data of the present study are in agreement with those found by Mahmoud and Badr [42]. According to the data in Table (4), there were significant differences ($P<0.05$) between beef burger control and all low-fat beef burger formulas prepared with microwave stabilized rice bran for cooking properties. Apparent also from the same Table that, cooking loss of beef burgers enriched with stabilized rice bran decreased with increasing the addition levels since beef burgers enriched with stabilized rice bran had cooking loss values lower than that of control. The highest value of the cooking loss was observed with beef burger control (32.46%) while, the lowest value was observed with a low beef burger containing 20.0% microwave stabilized rice bran (13.70%). This may be related to the protein and fiber content of microwave stabilized rice bran which could influence the cooking loss of the beef burger since protein and fibers could reduce the water loss during cooking by forming gels as reported these results are in agreement with those of Choi et al. and Gibis et al. [43 and 44]. From the results presented in this Table, it could be noticed that cooking the yield of beef burgers enriched with different levels of microwave stabilized rice bran is increased with increasing the addition levels, since beef burgers enriched with microwave stabilized rice bran had cooking yield values higher than that of control. Burgers containing 20.0 % stabilized rice bran had the highest cooking yield values while the control had the lowest value. This may be related to the protein and fibers content of stabilized rice bran which could influence the cooking yield of the beef burger since protein and fibers could reduce the water loss during cooking by forming gels

as reported by Choi, et al., Ibrahium et al. and Han, et al. [45 and41 and 46].

The beef burger control had the highest values of shrinkage and cooking loss (25.15 and 32.46 %). On the other hand, using microwave stabilized rice bran at different levels improved the shrinkage and cooking loss of low-fat beef burgers in compare with those of high-fat beef burger control. These results are in harmony with those of Choi et al. and Ibrahium et al. [43 and 41].

Sensory evaluation of beef burgers fortified by different levels of microwave stabilized rice bran

Fortifying meat with other non-meat ingredients has been done in the processed meat industry. This replacement is done for many reasons, such as health or economic purposes, and quality. The replacement of constituents from animal sources with those from plants has been applied in food manufacturing Egbert and Payne [47]. Data presented in figure (1) showed the sensory properties of cooked beef burger samples prepared with different levels of microwave stabilized rice bran compared with control burger samples. Results showed that there were no significant differences in the score values of taste, odor, texture, tenderness, and overall acceptability between control burgers and burgers fortified by 5, 10, or 15% of microwave stabilized rice bran. Therefore, a fortifying burger with microwave stabilized rice bran till 15 % could be suggested to be made as a burger with good quality and suitable sensorial quality . These findings are in agreement with the results of Ibrahium et al. [41] who showed that formulations of beef burgers with partial replacement of beef fat with flaxseed oil and rice bran produced acceptable samples compared to the control burger sample with a consistent texture, adequate juiciness, and good flavor. Rice fiber is neutral in taste and helps to retain moisture and fat leading to producing of a more succulent and juicy meat product Choi et al. [43] But the burgers fortified with 20% microwave stabilized rice bran were significantly different ($P < 0.05$) as compared with the other samples. With regard to the color, taste, odor, texture, tenderness, and overall acceptability, the burgers fortified with 20% of microwave stabilized rice bran had the lowest values.

Conclusions

Data obtained from this experiment indicated that un-stabilized rice bran has higher free fatty acids and can be stopped by stabilization treatment and improve oil extraction yield. In addition, microwave stabilization of rice bran has advantages over other stabilization methods. Furthermore, the beef burger that is prepared from rice bran stabilized by microwave improves chemical, cooking, and sensory properties.

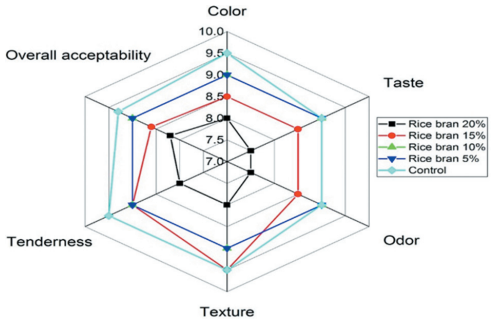

Figure 1. Organoleptic properties of beef burger supplemented with different levels of microwave stabilized rice bran.

Conflict of Interest

The authors declare that they have no conflict of interest.

References

1. Husak, R., Prabhu, G., and Smith, R. (2018). Use of Stabilized Rice Bran as a Replacer of Modified Food Starch or Meat in Smoked Sausage. Meat and Muscle Biology, 1(2).
2. Godber, J. S., Qiao, D., Windhauser, M., and Hegsted, M. (1993). Combining rice bran and beef for improved food quality through complimentary nutritional properties. Louisiana agriculture (USA).
3. Lee, H. C., and Chin, K. B. (2010). Application of microbial transglutaminase and functional ingredients for the healthier low-fat/salt meat products: A review. Food Science of Animal Resources, 30(6), 886-895.
4. Kim, J. S., Godber, J. S., and Prinaywiwatkul, W. (2000). Restructured beef roasts containing rice bran oil and fiber influences cholesterol oxidation and nutritional profile 1. Journal of Muscle Foods, 11(2), 111-127.
5. Rukmini, C., and Raghuram, T. C. (1991). Nutritional and biochemical aspects of the hypolipidemic action of rice bran oil: a review. Journal of the American College of Nutrition, 10(6), 593-601.
6. FAO/UN (2016). FAOSTAT database: http://faostat3.fao.org/home/index.html.
7. Saenjum, C., Chaiyasut, C., Chansakaow, S., Suttajit, M., and Sirithunyalug, B. (2012). Antioxidant and anti-inflammatory activities of gamma-oryzanol rich extracts from Thai purple rice bran. Journal of Medicinal Plants Research, 6(6), 1070-1077.
8. Amarasinghe, B. M. W. P. K., and Gangodavilage, N. C. (2004). Rice bran oil extraction in Sri Lanka: Data for process equipment design. Food and bioproducts processing, 82(1), 54-59.

9. Kim, H. J., Lee, S. B., Park, K. A., and Hong, I. K. (1999). Characterization of extraction and separation of rice bran oil rich in EFA using SFE process. Separation and Purification Technology, 15(1), 1-8.
10. Paucar-Menacho, L. M., Silva, L. H. D., Sant'ana, A. D. S., and Gonçalves, L. A. G. (2007). Refining of rice bran oil (Oryza sativa L.) to preserve γ-orizanol. Food Science and Technology, 27, 45-53.
11. Herfel, T., Jacobi, S., Lin, X., Van Heugten, E., Fellner, V., and Odle, J. (2013). Stabilized rice bran improves weaning pig performance via a prebiotic mechanism. Journal of animal science, 91(2), 907-913.
12. Orthoefer, F.T., (2005). Rice bran oil. In: Shahidi, F. (Ed.), Bailey's Industrial Oil and Fat Products. John Wiley and Sons Inc., Hoboken, NY., USA.,465-489.
13. Mezouari, S., Eichner, K., Kochhar, S. P., Brühl, L., and Schwarz, K. (2006). Effect of the full refining process on rice bran oil composition and its heat stability. European Journal of Lipid Science and Technology, 108(3), 193-199.
14. Krishna, A.G.G., Khatoon, S. and Babylatha, R. (2005). Frying performance of processed rice bran oils. J. Food Lipids., 12:1–11.
15. Malekian, F., Khachaturyan, M., Gebrelul, S., and Henson, J. F. (2014). Composition and fatty acid profile of goat meat sausages with added rice bran. International journal of food science, 1-8.
16. Faria, S. A. D. S. C., Bassinello, P. Z., and Penteado, M. D. V. C. (2012). Nutritional composition of rice bran submitted to different stabilization procedures. Brazilian Journal of Pharmaceutical Sciences, 48(2), 650–657.
17. Bagchi, T. B., Adak, T., and Chattopadhyay, K. (2014). Process standardization for rice bran stabilization and its' nutritive value. Journal of Crop and Weed, 10 (2):303-307.
18. Rosniyana, A., Hashifah, M. A., and Shariffah Norin, S. A. (2009). Nutritional content and storage stability of stabilized rice bran–MR 220. Journal of Tropical Agriculture and Food Science, 37(2), 163-170.
19. Aleson-Carbonell, L., Fernández-López, J., Pérez-Alvarez, J. A., and Kuri, V. (2005). Characteristics of beef burger as influenced by various types of lemon albedo. Innovative Food Science & Emerging Technologies, 6(2), 247-255.
20. A.O.A.C. (2005). Association of Official Analytical Chemists. Official Methods of Analysis of the Association of Official Analytical Chemists.; 18thEd. Washington, DC, USA.
21. Kahlon, T. S., Chow, F. I., Sayre, R. N., and Betschart, A. A. (1992). Cholesterol-lowering in hamsters fed rice bran at various levels, defatted rice bran and rice bran oil. The Journal of nutrition, 122(3), 513-519.
22. Sorour, A. M., Salem, M. A., Arafa, S.G. and El-Bana, M.A. Chemical, physical and Sensory evaluation of low-fat beef burger with Carboxymethyl cellulose produced from rice and wheat bran. International Journal of Environment, 10 (1), 33-46.
23. Badr, S., and El-Waseif, M. (2017). Influence of Caper (Capparis spinosa L) Seeds Powder Addition as Source of Bioactive Phytochemicals on Quality Attributes and Shelf Life Extension of Beef Burger Patties. Middle East J, 6(4), 1243-1258.
24. Steel, R. G., & Torrie, J. H. (1980). Principles and procedures of statistics: a biometrical approach (Vol. 2, pp. 137-139). New York: McGraw-Hill.
25. El-Bana, M. E., Goma, R. A., and Sattar, A. S. (2020). Effect of parboiling process on milling quality, physical and chemical properties of two rice varieties. Menoufia Journal of Food and Dairy Sciences, 5(4), 35-51.
26. Abd El-Hady, S. R. (2013). Effect of some thermal processing on stability of rice bran during storage at room temperature. J. Agric. Res. Kafr El-Sheikh Univ, 39(1): 92-106.
27. Amorim, J., Eliziário, S., Gouveia, D. S. D. S., Simões, A., Santos, J., Conceição, M., and Trindade, M. (2004). Thermal analysis of the rice and by-products. Journal of thermal analysis and calorimetry, 75(2), 393-399.
28. Vissers, M. N., Zock, P. L., Meijer, G. W., and Katan, M. B. (2000). Effect of plant sterols from rice bran oil and triterpene alcohols from shea nut oil on serum lipoprotein concentrations in humans. The American journal of clinical nutrition, 72(6), 1510-1515.
29. Lakkakula, N. R., Lima, M., and Walker, T. (2004). Rice bran stabilization and rice bran oil extraction using ohmic heating. Bioresource Technology, 92(2), 157-161.
30. Kawase, R.; Azami, S. and Maed, A. Y. (2010) Rice bran like composition and food. PCT international patent application publication. 5:1-9.
31. Iskander, M. H.; Awad, A. H. and Hamam, A. M. (1990). Effect of storage condition on the stability of fatty acid composition of corn. 1st Alex. Conf. Food Sci.Tech.,21-36.
32. Davies, R. M. (2016). Effect of the temperature on dynamic viscosity, density, and flow rate of some vegetable oils. Journal of Scientific Research in Engineering & Technology, 1(1), 14-24.
33. Rizk, L. F., Doas, H. A., and Elsakr, A. S. (1994). Chemical composition and mineral content of rice bran of two egyptian rice varieties heated by microwave. Food/Nahrung, 38(3), 273-277.

34. Sanghi, D. K., and Tiwle, R. (2015). A review of comparative study of rice bran oil and rice bran wax. International Journal of Pharmacy Review & Research, 5(4), 403-410.
35. Ngassapa, F. N., Nyandoro, S. S., and Mwaisaka, T. R. (2012). Effects of temperature on the physicochemical properties of traditionally processed vegetable oils and their blends. Tanzania Journal of science, 38(3), 166-176.
36. Abdel-Aal, E. S.M. and Sosulski, F. W. (1993). Rapid tests for residual lipase and peroxidase activities in a steam-heated cereals. Alex. Agric. Res.,38(2):161-179.
37. El-Sayed, M.E.A. (2015). Effect of some heat treatments on canola seed and rice bran characteristics. journal agricultural research kafrelsheikh university, 41(1) 246-265.
38. Gupta, H. P. (1989). Rice bran offers India an oil source. Journal of the American Oil Chemists' Society. 66(5):620-623.
39. Awad-Allah, M. M., Mohamed, A. H., El-Bana, M. A., El-Okkiah, S. A., Abdelkader, M. F., Mahmoud, M. H. and Abdein, M. A. (2022). Assessment of Genetic Variability and Bran Oil Characters of New Developed Restorer Lines of Rice (Oryza sativa L.). Genes, 13(3), 509.
40. Krishna, A.G.G. (2002). Nutritional components of rice bran oil in relation to processing. Lipid Technology, 14(4), 80-84.
41. Ibrahium, M. I., Hegazy, A. I., and El-Waseif, M. A. (2015). Effect of replacing beef fat with flaxseed oil and rice bran on nutritional quality criteria of beef burger patties. Sciences, 5(03), 645-655.
42. Mahmoud, K. A. and Badr, H. M. (2011). Quality Characteristics of gamma-irradiated beef burger formulated with partial replacement of beef fat with olive oil and wheat bran fibers, Food and Nutrition Sciences, 2: 655-666.
43. Choi, Y.S. ; Cho,i J.H. ; Han, D.J. ;Kim, H.Y. ; Lee, M.A.; Kim, H.W. ; Lee, J.W. ; Chung, H.J. and Kim, C.J. (2010). Optimization of replacing pork back fat with grape seed oil and rice bran fiber for reduced-fat meat emulsion systems. Meat Science. 84(1): 212 - 218.
44. Gibis, M., Schuh, V. and Weiss, J. (2015). Effects of carboxymethyl cellulose (CMC) and microcrystalline cellulose (MCC) as fat replacers on the microstructure and sensory characteristics of fried beef patties. Food Hydrocolloids, 45, 236-246.
45. Choi, Y. S., Choi, J. H., Han, D. J., Kim, H. Y., Lee, M. A., Kim, H. W. and Kim, C. J. (2011). Effects of rice bran fiber on heat-induced gel prepared with pork salt-soluble meat proteins in model system. Meat Science, 88 (1), 59-66.
46. Han, M., Clausen, M. P., Christensen, M., Vossen, E., Van Hecke, T., and Bertram, H. C. (2018). Enhancing the health potential of processed meat: the effect of chitosan or carboxymethyl cellulose enrichment on inherent microstructure, water mobility and oxidation in a meat-based food matrix. Food and function, 9(7), 4017-4027.
47. Egbert, W. and Payne, C. (2009). Plant proteins in ingredients in meat products: Properties, functionality and applications. Tarte, R., ed., pp. 111-129. Springer New York.

ISSN print: 1224-5984
ISSN online: 2248-3942

Rom Biotechnol Lett. 2022; 27(3): 3475-3486
doi: 10.25083/rbl/27.3/3475.3486

Received for publication: June, 10, 2022
Accepted: July 26, 2022

Original paper

Effect of Partially Substitution of Rice bran and Soybean Protein Concentrates on Chemical, Nutritional and Organoleptic Properties of Kapreeta tuna-like fish (*Scombromorous* Spp.) Surimi

FATMA N. EBRAHYM, BADIAA A. BESAAR, SAMIR Y. ELSANAT, BADAWY* W.Z.

Department of Food Technology, Faculty of Agriculture, Kafrelshiekh University, Egypt

Abstract

The objective of this research is to study the possibility of utilizing kapreeta fish (like tuna) that has low nutritional value because of its bloody dark flesh and presence of many blood vessels and susceptibility to rapid spoilage, therefore. Kapreeta fish was used to prepare a high nutritional value of Surimi blends prepared from fish flesh supplemented with 15% level of soybean and rice bran protein concentrates to suggest its protein as a new protein source. Various compositional and functional properties were assessed to determine the effect of this substitution treatment on the final product characteristics. The obtained results revealed that: rice bran protein concentrate is considered a good source of protein (72.90% on dry matter), more than 48.10 and 35.60% for soybean protein concentrate, whereas ash content of soybean protein (5.83%) are higher than that its value of rice bran protein concentrate (4.47%). The two protein sources showed to be rich in essential amino acids and met human requirements for all the essential amino acids since they have higher values than that recommended by FAO/WHO (1991) pattern for children of 10-12 years.

Keywords Rice bran protein concentrates, soybean protein concentrate, Kapreeta tuna-like fish, Surimi.

To cite this article: FATMA N. EBRAHYM. Effect of Partially Substitution of Rice bran and Soybean Protein Concentrates on Chemical, Nutritional and Organoleptic Properties of Kapreeta tuna-like fish (*Scombromorous* Spp.) Surimi. *Rom Biotechnol Lett.* 2022; 27(3): 3475-3486
DOI: 10.25083/rbl/27.3/3475.3486

*Corresponding author: walid.metwali@agr.kfs.edu.eg

Introduction

Agriculture byproducts like rice bran store solar energy in their chemical connections, making them a renewable resource. According to **FAOSTAT (2012),** the world's rice output in 2010 was 696,324,394 metric tons (t), whereas Egypt's production was 5,724,103 metric tons (t) each year **(A.S.G.A., 2013)**. When paddy is milled, it generates 70% rice (endosperm) as the main product, along with 20% husk, 8% bran and 2% germ. Approximately 90 percent of the world's rice bran is thrown away or used as a low-cost animal feed component, with the remainder being used to extract rice bran oil **(Schramm et al., 2007; Zullaikah et al., 2009 and Gul et al, 2015).** During the milling process to create white rice, a combination of rice bran (brown layer) and germ is produced as a byproduct. Die Rice Bran Composition varies depending on the Rice Type and Variety as well as the Rice Processing Methods and Climate Conditions **(Saikia and Deka, 2011)**. As a by-product of the rice milling process, defatted rice bran is seen as a waste product. Bioactive substances such as phenolics give it a significant antioxidative effect **(Devi and Arumughan, 2007; Mariod et al, 2010)**. There are vital nutrients such as high-quality proteins with distinct nutritional value **(Gul et al, 2015)**. As a result of protein-energy malnutrition, which is a worldwide concern, especially in poorer nations, proteins are considered the most important macronutrient for humans. Recent years have seen a rise in interest regarding the possible use of protein from under-utilized biomass sources, such as oil meal and legumes **(Otten et al., 2006)**. Because of the limited use of chemical analysis, which is cheap and rapid, but does not always match in vivo results, the assessment of protein quality has depended on indirect methods such as chemical analysis. Nutritionists use protein quality as a measure of bioavailability to determine how well dietary proteins and diets can meet metabolic needs for amino acids and nitrogen, respectively **(Gilani, 2012)**. In the food business, rice bran protein concentrate (RBPC) has gained attention for its unique nutritional value and nutraceutical characteristics. Even though rice bran protein has the potential to be a novel kind of protein, very little research has been done on its nutritional value **(Han et al., 2015)**.

Soy protein is derived from soybeans. It is produced from dehulled and defatted soybean meal. Only soybean protein includes all of the necessary amino acids for human nutrition and is a complete protein **(Dudek, 2001)**.

As an important source of high-quality protein in the human diet, fish has been known for a long time. *Scombromorous* spp. (Kapreeta tuna-like fish) accounts for around 8-10% of Egypt's total marine fish harvest **(Abu-Tor, 2002)**. Egyptians dislike this type of fish because of its crimson black flesh and many blood veins. This means that significant quantities of raw materials are lost every year because of their susceptibility to fast deterioration. As a result, this fish must be used to produce commercial fish products **(Venugopal, 2003)**. Recently, fish processing technology has been evolving in a way that focuses on technological up-grading, diversity, and quality assurance. Due to this, there is an increased demand for seafood/seafood-based convenience foods that may be eaten or cooked right away (**Ammar and Korish *et al,* 2009**).

Fish flesh that has been mechanically deboned and cryoprotectant-treated to extend its shelf life is known as surimi. Wringing out the gel raises the concentration of myofibril protein which increases the gel's strength and flexibility. It also eliminates fat and other unwanted things such as blood, pigment and odoriferous materials. For example, shellfish analogues can be created using this feature **(Maqsood et al., 2013)**. This work carried out to study the effect of partially substitution of rice bran and soybean protein concentrates on chemical, nutritional and organoleptic properties of Kapreeta tuna-like fish (*Scombromorous Spp.)* surimi.

Materials and Methods

Materials

Freshly mixtures of generated rice bran were collected from Desouk rice milling Co., Desouk city, Kafr Elshiekh Governorate, Egypt, then were stored at 4°C in polyethylene bags before use. While soybean protein concentrate was obtained from Food Technology Research Institute, Agricultural Research Center, Giza, Egypt during the winter season of 2019. Kapreeta fish (***Scombromorous Sp***.) like tuna was purchased from the local market of Alexandria City, Egypt during the summer season of 2019. Samples were transported directly in icebox (at 5-10°C) to the laboratory of food technology department, faculty of Agriculture, Kafrelsheikh University. Rice, vegetables (green coriander and parsley), spices (black pepper), salt and sunflower oil were bought from the local market of Kafrelsheikh city. El-Gomhoria Company for Chemicals and Drugs in Egypt supplied the chemicals utilized in this investigation.

Methods

Defatting and rice bran protein concentrating

According to **Kaewka *et al.* (2009)**, defatted rice bran (DRB) was produced using RB that had been newly milled by defatting twice with hexane (1:3, w/v), followed by air drying overnight in the fume-hood, grinding in sample mill, and sieving through a 0.5-mm screen. Distilled

water was added to the defatted bran (1:10). By adding 4 ml of NaOH solution and stirring for 1 hour, the pH of the slurry was adjusted to 9.0. (12,600g, 15 min). With HCl (4 M) acid, we adjusted the pH of the supernatant protein solution to 4.5, agitated it for 30 minutes, and then left it undisturbed for cold precipitation overnight (4°C). Protein precipitates were rinsed three to four times with deionized water after carefully removing the supernatant from the solution. It was then lyophilized and pH adjusted to 7.0. Rice bran protein concentrate was the name given to the final product (RBPC).

Preparation of kapreeta fish

The samples were removed from the icebox and washed by running tap water to remove the adhering sand and silt. Then, treated by whiteness treatments by immersed in 5% H_2O_2 solutions in glass jars for 1 min to remove the blood in fish flesh after removed the head, skin and viscera. The flesh of kapreeta fish isolated from the bones, where it was minced using meat mincer (molunix mincer HV، France) (**Fadl, 2014).** The minced fish flesh used for preparing Surimi blends, as follows in Table (1). The samples of Surimi blends were packed in polyethylene bags and stored in a deep freezer (at -20 °C for 6 months) until analysis.

Frying of Surimi

Frozen Surimi blends were thawed at room temperature to studied chemical, microbiological and organoleptic properties after frying with sunflower oil (at 230-250°C) for 5-10 min compared with unfired Surimi.

Proximate chemical composition of rice bran (RB), defatted rice bran (DRB), rice bran protein concentrate (RBPC) and soybean protein concentrates.

Moisture was assessed by drying it in air oven at 105˚± 5°C until it had a uniform weight; Micro-Kjeldahl method was used to determine crude protein content using nitrogen-to protein conversion factors of 5.75 for rice bran and 5.71 soybean protein concentrate, the ether extract was carried out in a Soxhlet apparatus using petroleum ether (40 - 60°C) as the solvent. The ash content was determined by ashing a known weight of a fat-free sample in refluxing 1.25 percent (w/v) sulfuric acid and 1.25 percent (w/v) sodium hydroxide in an electric muffle at 550°C until complete ashing, and the crude fiber content was determined by digesting a known weight of a fat-free sample in refluxing 1.25 percent (w/v) sulfuric acid and 1.25 percent (w/v) sodium hydroxide. Total and available carbohydrates were calculated by difference. The procedures provided in **A.O.A.C. (2000)**. were used to determine all of the previously listed compounds. All measurements were performed in triplicate.

Determination of minerals content

Minerals were measured using a 6N HCL after wet ashing, and zinc, copper, iron, and manganese were assessed using an atomic absorption spectrophotometer (Zeiss FMD3). Potas-

Table 1 Ingredients and mixtures of Surimi blends (%).

Ingredients (gm)	No1	No2	No3	No4
Whitened kapreeta fish flesh (with 5%H_2O_2)	100	85	85	85
Rice bran protein concentrate	0	15	0	0
Soybean protein concentrate	0	0	15	-
Rice	10	10	10	10
Vegetables (green coriander and parsley)	3	3	3	3
Black pepper	1	1	1	1
Salt	1	1	1	1

Figure 1. Kapreeta (Like tuna fish)

Figure 2. Separation of fish flesh from the bone.

Figure 3. Whitening of the flesh using H_2O_2



Figure 4. Fresh and fried Surimi.

sium, sodium, and Calcium were measured using a flame photometer, and phosphorus was calculated photometrically using a phosphorus molybdate complex spectrophotometer at 650 nm and a standard curve, as reported in **A. O. A. C. (2000)**.

Amino acid analysis

Shimadzu HPLC apparatus (Shimadzu, Kyoto, Japan) was used to evaluate amino acid composition, which included Shimadzu SIL RF10Axl fluorescence detectors, a Shimadzu SCL-10Avp controller with a column oven, and a Shimadzu SIL-10ADvp auto-sampler running the CLASS-VP software (version 5.03). The column was Shimpack Amino-Na (6100mm) and flowed at 0.6 ml/min. The excitation wavelength (EX) was 348 nm, while the emission wavelength (Em) was 450 nm. Elution buffers were (A) 0.2M citrate buffer (pH 3.3), (B) 0.6M citrate+ 0.2 M boric buffer (pH10), and (C) 0.2 M NaOH. Briefly, samples were hydrolyzed using 6 N HCl/1% (w/v) phenol vapor at 110°C for 24 h in vacuo. The amino acids were treated with o-phtalaldehyde (OPA) to form OPA-derivates, which were then analysed using the above HPLC.

Determination of tryptophan

The tryptophan content of each sample was calorically measured individually using alkaline hydrolysis and p-dimethyl –amino –benzaldehyde (DMAB) according to the Miller (1967) technique. The tryptophan concentration was determined using a standard curve created under the same circumstances and quantified spectrophotometrically at 590 nm.

Nutritional quality determinations

Nutritional qualities were calculated on the basis of the amino acid profiles.

Chemical score for essential amino acids (AAS)

According to **Pellet and Young, (1980)** amino acid score is defined as milligrams of essential amino acid per gram nitrogen in tested protein divided by milligrams of essential amino acid per gram nitrogen in the reference protein reported by **FAO/WHO (1991).** The results were multiplied by 100, and the amino acid that showed the lowest proportion is called the limiting amino acid and the ratio obtained was the score.

$$\text{Chemical score} = \frac{\text{Essential amino acid/100 g tested protein}}{\text{Essential amino acid/100 g protein in FAO/WHO}}$$

Computed protein efficiency ratio (C-PER):

The computed technique for protein efficiency ratio (C-PER) was determined using the regression equations published by **Alsmeyer et al. (1974)**, which are listed below:

C-PER = -0.468 + 0.454(LEU) – 0.105(TYR).

Where: LEU and TYR: amino acids leucine and tyrosin.

Biological value (BV) of protein:

Farag et al. (1996) estimated the biological value of protein sources using the following equation:

Biological value (B.V.) = 49.9 + 10.53 C-PER**.**

The net protein value (NPV)

Calculating the net protein value was as simple as multiplying the lowest amino acid score by the protein percentage divided by 100.

NPV = (The lowest amino acid score × % protein)/ 100

The Essential Amino Acid Index (EAAI) was calculated using the method of **Labuda *et al.* (1982)** *according to the equation below:*

$$EAAI = \sqrt[n]{\frac{[\text{Lys x Threo x Val x Meth x Isoleu x leu x Phynylal x Histi x Trypt}]a}{[\text{Lys x Threo x Val x Meth x Isoleu x leu x Phynylal x Histi x Trypt}]b}}$$

Where: [lysine, tryptophan, isoleucine, valine, threonine, leucine, phenylalanine, histidine, and methionine]

a. in test sample and [lysine, tryptophan, isoleucine, valine, threonine, leucine, phenylalanine, histidine and the sum of methionine and cystine]

b. content of the same amino acids in standard protein (%), respectively. The nutritional index of the food samples was calculated using the formula below:

$$\text{Nutritional index}[\%] = \frac{\text{EAAI x \%protein}}{100}$$

Measurement of protein quality by in vitro digestibility

In order to determine the digestibility of rice bran, soybean, and whey proteins, the 4-enzyme technique provided by AOAC (1984) was modified somewhat. With the addition of 0.1 N NaOH or HCl, at 37°C, 10 ml of crude protein (6.25 mg/ml) was adjusted to pH 8. One millileter of newly produced enzyme stock solution was added to the protein suspension at 37°C for 10 minutes. As soon as the solution has been incubated for 10 minutes. We added 1.1 mg/ml of protease enzyme in water (Solution B), incubated for 9 minutes at 55°C, then for 1 minute at 37°C, and measured the pH. In order to determine protein digestibility, the following equation was used:

% Digestibility = 234.84 - 22.56 (X)

Where: X = pH after 20 min incubation.

Determination of the antioxidant activity

A modified version of **Fujinami *et al*. (2001)** technique was used to determine the radical-scavenging activity of DPPH. It was dispersed at 0.50mmol/L of DPPH in ethanol. We added diluted bran extract or L-ascorbic acid (VC), which was employed as a standard, to 1mL of DPPH solution, and the results were compared. For 20 minutes, at 25 °C, the mixture was violently shacked and kept in the dark. We used a UV-1200 spectrophotometer (Shimadzu, Kyoto) to evaluate the absorbance of the solution at 516nm in comparison to 4mL of 50 % (v/v) ethanol in 4mL of 1mL of diphenhydramine (DPPH) solution. The radical scavenging activity of the diluting extraction or VC liquid was determined as the quantity of extract required to decrease the original DPPH concentration by 50%:

Radical scavenging activity = (A - B +C) / A×100 (%)

Where: A represents the starting absorbance of the blank, B represents the absorbance of the diluted extract and DPPH solution mixture at 20 minutes, and C represents the diluted extraction absorbance without the DPPH solution. The radical scavenging activity was quantified in mmol-VC/g-bran as VC equivalent antioxidant capacity. For each bran extraction, triple preparations were carried out.

Microbiological tests

Samples were prepared using the recommended methods for the microbiological examination of food published by **A.P.H.A (American Public Health Association) (1971*).*** Fish samples were aseptically taken using sterilized knives and placed in sterile containers. One gram of samples were emulsified in 99 ml sterile distilled water in a sterile mechanical blender cup. Every determination was done in triplicate. Total viable bacterial counts per gram of Surimi were determined using standard techniques on plate count agar (Difco). Incubation was carried out for 48 hours at 32°C according to **Deng *et al*. (1976).** Mold and yeast counts were determine by plating on acidified potato dextrose agar (Difco), and incubating duplicate plates at 25°c for 5 days (**Nottingham,1971**). Coliform bacterial counts were determined by plating on crystal violet neutral red agar. The plates were incubated at 25 °C for 4 – 5 days. The colonies were count and reported as coli forms per gm of flesh **(Nottingham, 1971*).***

Organoleptic properties

Organoleptic properties were evaluated for color, flavor, texture, and overall acceptability during processing steps. A group 10 as described by **Teeny and Miyauchi (1972*).***

Statistical analysis

One-way ANOVA was used to analyse all the data, with Sigma Stat (v.3.5. Systat Software Inc.). Duncan's novel multiple range test found that there was a significant difference between treatment means at the P 0.05 level **(Steel and Torrie, 1980)**.

Results and discussion

Chemical composition of rice bran, soybean, and whey protein concentrate:

The raw rice bran, defatted rice bran (DRB), rice bran protein concentrate (RBPC), soybean protein (SP), and whey protein concentrate (WP) were chemically analyzed for their contents of moisture; protein; ether extract; ash; crude fiber. Total and available carbohydrates were calculated by difference. The obtained data are presented in Table (1). It could be noticed from the results in Table (1) that the moisture content of RBPC and SP were 3.91 and 7.30, respectively. Raw and defatted rice bran had 9.05% moisture content for each one. Concerning the crude protein content, results disclose that the protein content of RBPC had the highest amount of protein, (72.9%). It is also noted that the defatted rice bran had significantly the highest ash content (11.30%). On the other hand, the carbohydrate and crude fiber contents indicated that there were significant differences between the two sources of proteins. The obtained results are in agreement with the results of **(Supathra *et al*., 2008, Gul *et al*., 2015)** they reported that full fat rice bran were contained 8.5-12.6% moisture, 4.2-7.7% ash, 8.0-18.9% ether extract, 8.8-15.2% protein, 22.2-44.8% total carbohydrates and 18.3-30.5% for total dietary fiber (on dry weight basis).

Table (1): Chemical composition of rice bran and soybean protein concentrates (g/100g dry matter).

Soybean protein concentrate	Rice bran			Components
	Protein concentrate	Defatted	Raw	
7.30[b]	3.91[d]	9.05[c]	9.05[a]	Moisture
92.70[b]	96.09[c]	90.95[d]	90.95[c]	Dry Matter
48.10[a]	72.90[a]	17.24[d]	14.29[c]	Crude protein
6.02[b]	0.00	0.22	17.10[a]	Ether extract
5.83[c]	4.47[d]	11.30[b]	9.37[a]	Ash content
11.50[b]	0.02[d]	18.44[a]	15.29[a]	Crude fiber
40.05[c]	22.63[e]	71.24[c]	59.24[b]	Carbohydrate *
28.22[d]	22.61[e]	52.80[a]	43.95[c]	Available carbohydrate **

Values followed by different letter in row are significantly different at $p \leq 0.05$.

Each value is an average of three determinations.

* Total carbohydrate was calculated by subtracting protein, ash, and ether extract (%) from the total mass of 100.

** Available carbohydrate obtained by subtracting crude fiber from total carbohydrate.

Mineral contents of rice bran and soybean protein concentrates

Mineral contents of rice bran, soybean protein, and whey protein concentrate were analysed and the results are present in Table (2). The data in the mentioned table clearly shown that phosphorus (680 mg/100) and potassium (2410 mg/100g) were the predominant minerals of rice bran protein concentrate and soybean protein concentrates, respectively. On the other hand, calcium (38 mg/100g) and sodium (6.8 mg/100g) in rice bran protein concentrate and sodium (123 mg/100g) in soybean protein showed low amounts. The obtained results also revealed that the three different protein sources used in this study may provide a significant amount of minerals to meet the human mineral requirements (Recommended Dietary Allowance). However, only the whey protein concentrate showed a ratio Ca : P more than 1.0, but the other two types of proteins showed avery low Ca : P ratios, (1 : 17.89 and 1 : 197 for rice bran and soy protein concentrates, respectively).

Amino acid composition

The amino acids composition of rice bran protein concentrate (RBPC) is given in Table (3). Besides the amino acid composition of soybean protein concentrate (SPC). Data in Table (3) show the amino acid composition of RBPC and SPC, along with the professional pattern recommended by **FAO/ WHO (1991)** for school children (10-12 Yr). All the three different types of protein, namely, of RBPC, SPC and WPC, as indicated in Table (3) were rich in essential amino acids and met human requirements for all the essential amino acids. Protein of RBPC and SPC contained 51.39 and 53.60g essential amino acid/100g protein respectively. These values are higher than that recommended by FAO/WHO (1991) pattern for children of 10-12 years (24.10 EAA/100g protein. Tryptophan had the lowest concentrations of essential amino acids and valued 1.96, 2.12 and 2.07, followed by sulfur containing amino acids (methionine + cystine) which amounted 3.76, 4.62 and 5.43 g/100g protein), respectively. Data presented in the same table cleary indicate that glutamic acid (8.20 and 15.02 g/100g protein), followed by aspartic acid (6.13 and 9.78 g /100g protein) were the most abundant amino acids and form a major part of amino acids in RBPC and SPC. The ratio of essential amino acids (EAA) to non-essential amino acids (NEAA) ranged between 1.16 for the SPC and 1.33 for the RBPC.

Table (2): Minerals content of rice bran and soybean protein concentrates (mg/100g on dry weight basis).

Mineral content (mg/100g)	Rice bran protein concentrate	Soybean protein concentrate
Macro-minerals		
Calcium (Ca)	38[c]	377[c]
Sodium (Na)	6.8[d]	123[d]
Potassium (K)	430[b]	2410[a]
Phosphorus (p)	680[a]	743[b]
Trace elements		
Zinc (Zn)	3.2[e]	5.5[f]
Copper (Cu)	0.8[f]	4.8[f]
Iron (Fe)	0.7[f]	15.0[e]
Manganese (Mn)	4.4[e]	12.2[e]

*Values followed by the same letter in row are not significantly different at $p \leq 0.05$.

Values followed by different letter in row are significantly different at $p \leq 0.05$.

In conclusion, it could be observed that some differences in the amino acid contents were noted between the three different types of proteins. However, the content of all essential amino acids was higher than those recommended by FAO/ WHO pattern. And, it is the essential amino acid content that counts for the quality of protein and its capacity to satisfy the needs for essential amino acids.

Chemical score of essential amino acid

Chemical score provides an estimate of the nutritive value of a protein by comparing the levels of essential amino acids between the test protein and those of the FAO/WHO pattern for children of 10- 12 years old. The essential amino acid scores of protein from RBPC and SPC are shown in Table (4). The data in Table (4) indicate that all essential amino acids, except the histidine in whey protein concentrate, of the three different proteins are in excessive amounts. It is the young children who suffer from malnutrition, and protein resembling the scoring pattern in composition should provide essential amino acids in excess when they are consumed by the older age group. The results in Table (4) agreed with other findings by **(Bhaskar *et al*. 2008; Ovissipour *et al*. 2009).**

Nutritional quality of protein

Table (5) shows the data related to the protein efficiency ratio (C-PER) and biological values of RBPC and SPC, compared with casein as a reference protein, along with net Protein Value (NPV), essential amino acid index (EAAI), nutritional index (NI) and in vitro protein digestibility.

Methods based on in vitro (chemical and amino acids bioassay) for assessment of protein quality are important. The digestibility is important criterion that determine the availability of physiologically active amino acids and peptides and is affected by processing treatments **Dudek (2001)**. The true digestibility values of the proteins of RBPCs and the standard protein (casein) found are different from each other. The result in Table (5) indicated that

Table 3. Amino acid composition of rice bran and soybean protein concentrates (g amino acid/100g protein) (on dry weight basis).

FAO/WHO/ 1991 (10-12yr)	Soybean protein conc.	Rice bran protein conc.	Amino acids (g/100g protein)
			Essential amino acids (EAA)
2.8	4.26	4.16	Threonine
2.5	6.16	6.15	Valine
2.8	8.16	7.80	Isoleucine
4.4	7.62	7.43	Leucine
4.4	8.77	8.72	Lysine
1.9	3.28	3.90	Histidine
2.2	2.31	1.88	Methionine
	2.31	1.88	Cystine
	4.62	3.76	Total sulfur amino acid
2.2	5.32	4.84	Phenylalanine
	3.29	2.67	Tyrosine
	8.61	7.51	Total aromatic amino acids
0.9	2.12	1.96	Tryptophan*
24.10	53.60	51.39	Σ1=Total EAA
			Non-essential amino acids (NEAA)
	4.45	5.39	Proline
	9.78	6.13	Aspartic
	3.72	2.26	Serine
	15.02	8.20	Glutamic
	3.66	3.26	Glycine
	3.74	6.13	Alanine
	6.03	7.24	Arginine
	46.40	38.61	Σ_2= Total NEAA
	100	90	$\Sigma = \Sigma_1 + \Sigma_2$
	1.16	1.33	Σ_1 / Σ_2
	47.56	49.67	$A = \Sigma_1 \Sigma_1 + \Sigma_2$

Σ1= sum of essential amino acids; Σ_2= sum of non-essential amino acids.

*Methionine + cysteine (SAA); Phenylalanine + tyrosine (AAA).

[1]Amino acid scoring patterns: Theoretical standard of FAO/WHO/ UNU essential amino acids for children between 10 and 12 years old (FAO/WHO/ UNU, 2007).

- Tryptophan was determined colorimetrically.

Table 4. Chemical score (CS)* of essential amino acids of rice bran and soybean protein concentrates with respect to the required pattern recommended by FAO/WHO (1991).

Soybean protein concentrate		Rice bran protein concentrate		FAO/WHO recommended pattern for 10-12 yr children	Essential amino acids
CS	g/100g protein	CS	g/100g protein		
.36	4.26	1.49	4.16	2.8	Threonine
2.46	6.16	2.46	6.15	2.5	Valine
2.91	8.16	2.79	7.80	2.8	Isoleucine
1.73	7.62	1.69	7.43	4.4	Leucine
1.99	8.77	1.98	8.72	4.4	Lysine
1.73	3.28	2.05	3.90	1.9	Histidine
2.1	4.62	1.71	3.76	2.2	Methionine+cystine
3.91	8.61	3.41	7.51	2.2	Phenylalanine+tyrosine
2	2.12	2.18	1.96	0.9	Tryptophan

* Chemical score was calculated as a percentage of FAO/WHO, 1991 essential amino acids.

* * Limiting amino acid

Table 5. Estimation of nutritional quality of rice bran and soybean protein concentrates and casein, based on their amino acid composition.

Casein	Soybean protein concentrate	Rice bran protein concentrate	Parameters
3.35	2.65	2.62	Computed protein efficiency ratio (C-PER)
85.20	77.80	77.49	Biological value (B.V)
0.78	1.02	1.37	Net protein value (NPV)
1.55	1.81	1.75	Essential Amino Acid Index (EAAI)
1.16	0.87	1.27	Nutritional index (NI) (%)
95.30	90.50	85.20	In vitro protein digestibility

Table 6. DPPH radical scavenging (mmol-VC/g) of rice bran and soybean protein concentrates and casein, based on amino acid composition.

DPPH Radical scavenging (mmol of ascorbic acid (VC/g)	Parameters
0.35^{a}	Rice bran protein concentrate
0.34^{b}	Soybean protein concentrate
0.09^{c}	Casein

Values superscripted with dissimilar letters (a, b and c) are significantly different ($p < 0.05$).

the highest digestibility value using trypsin was found for RBPC (85.20%) in comparisons by SBPC (90.50%). Moreover, the digestibility found for casein was 95.30% **Mune *et al.* (2011)**.

DPPH radical-scavenging activity of rice bran protein concentrates (RBPCs)

Some of the chemicals in rice bran have been found to have antioxidant action. Vitamin E (Tocopherols and Tocotrienols), phytosterols, oryzanol, and amino acids, notably arginine, histidine, cystein, and methionine, are examples of these substances **(Sereewatthanawut et al, 2008)**. It is commonly acknowledged that the DPPH free radical is a good model for assessing the antioxidant properties of diverse samples. The ability of antioxidants to scavenge DPPH radicals was linked to their ability to donate hydrogen. It measures the ability of substances to scavenge free radicals or donate hydrogen atoms. In contrast to the extremely reactive peroxyl and hydroxyl radicals that are involved in lipid peroxidation and tissue damage in biological systems, DPPH is a stable synthetic radical (**Intarasirisawat *et al.,*** 2012). Chemicals that can neutralize free radicals would do so by giving them one of their electrons, which would prevent them from spreading. In this work, RBPCs were evaluated for their ability to scavenge stable DPPH radicals. This was followed by SPC (0.34mmol) and then WPC (0.34mmol), with casein having the lowest total antioxidant capacity and RBPC having the highest total antioxidant capacity (Table 6).

Chemical composition of unwhitened and whitened kapreeta fish flesh (Like tuna) (on dry weight basis)

The results in Table (7) indicated that the chemical composition differs between unwhitened and whitened

Table 7. Chemical composition and minerals content of fresh and whitened Kapreeta fish (like tuna) flesh (on dry weight basis).

Characteristics	Kapreeta fish (fresh)	Kapreeta fish (whitened with 5%H2O2)
Moisture %	77.80[a]	67.14[b]
Crude protein %	78.99[b]	82.30[a]
Ether extract %	6.80[b]	8.02[a]
Ash %	6.46[b]	6.77[a]
Carbohydrates	7.75[a]	2.91[b]
PH	6.92[b]	6.98[a]
Minerals content (mg/100g)		
Ca	35.42[a]	35.35[b]
K	11.80[b]	12.60[a]
Na	25.40[a]	20.70[b]
P	18.40[b]	19.90[a]
Zn	28.10[a]	28.02[b]
Fe	109.22[A]	100.01[B]

Means within the same row of different letters are significantly different at ($P < 0.05$).

Table 8. Chemical composition of unfried and fried Surimi blends prepared from whitened Kapreeta fish flesh supplemented with 15% level of soybean, whey and rice bran protein concentrates (On dry weight basis).

Characteristics (%)	Surimi blends					
	No1 (Control)		No 2 (Added 15% rice bran protein concentrate)		No3 (Added 15% soybean protein concentrate)	
	Unfired	Fried	Unfired	Fried	Unfired	Fried
Moisture	65.58	42.35	62.53	43.24	63.85	42.06
Crude protein	65.67	64.31	62.27	60.31	60.51	59.50
Ether extract	5.41	11.38	4.98	10.65	4.60	10.30
Ash	6.20	5.80	6.68	6.23	6.82	5.64
Carbohydrates	22.72	18.51	26.07	22.81	28.07	24.56

kapreeta fish. It could be observed some changes as affected by whiteness treatment. Crude protein, ether extract and ash content were higher in whitened kapreeta fish, but moisture content and carbohydrate contents were low. The results in the same Table indicated that the unwhitened kapreeta fish had some higher minerals Na and Fe than the unwhitened kapreeta fish and these results agreed with those of **(Abu-Tor, 2002a; Chaijan *et al.*, 2004; korish *et al* 2008 and Ammar and korish, 2009)**. Where they reported that fish whiteness causes a decrease of moisture, carbohydrates, and some minerals but increases the concentration of crude protein, ether extract, and ash.

Chemical composition of Surimi blends prepared from whitened kapreeta fish flesh supplemented with 15% level of rice bran and soybean protein concentrate

The results cleared in Table (8) showed that the chemical composition of fried Surimi blends prepared from whitened kapreeta fish flesh with (5% H_2O_2). Frying process had noticeable effects on the chemical composition of fried Surimi blends. The moisture content of unfried Surimi blends were decreased by heat treatments of frying because of evaporated amounts of moisture during frying. The previous results agree with **Ammar (1999).** As for crude protein, there was a little decrease after the frying process, this may be due to the effect of heat treatment which might have caused the loss of some nitrogenous substances with separated fluids as well as volatilization in the form of amines and other volatile nitrogen substances**.** Ether extracts were increased by the frying process however it was notably that fried Surimi blends in sunflower oil. Ash content was decreased in all samples after frying. It was noticed that there is no difference between ash content in fried Surimi blends. The carbohydrate content showed a higher level in unfried Surimi blends than in the fried ones. Finally, from the presented results in Table (8) it could be observed that protein content and ash of prepared samples were in the same trend as control but carbohydrate was higher than control. The previous results are in agreement with those of **(Ammar, 1999 and Fadl, 2014)**.

Table 9. Organoleptic properties of fried Surimi blends prepared from whitened kapreeta fish flesh supplemented with 15% level of rice bran and soybean protein concentrates.

Fried Surimi blends	Organoleptic properties score					
	Appearance	Color	Odor	Texture	Taste	Overall acceptability
No1(Control)	8	8	7	7	8	7.60
No 2 (Added 15% rice bran protein concentrate)	8	9	8	9	8	8.40
No3 (Added 15% soybean protein concentrate)	8	9	8	7	9	7.80

Organoleptic properties of fried Surimi blends prepared from whitened kapreeta fish flesh supplemented with 15% level of rice bran and soybean protein concentrates:

The results showed in Table (9) show that the organoleptic score of fried Surimi blends (No 1) (control) prepped from whitened kapreeta fish flesh (control) were 8, 8, 7, 7, 8, and 7.60 for appearance, color, odor, texture, taste, and overall acceptability. While the organoleptic score of fried Surimi blends prepared from whitened kapreeta fish supplemented with 15% level of rice bran and soybean protein concentrates were higher than control for the same properties and overall acceptability were 8.40 and 7.80 for rice bran and soybean. Our results cleared that, the addition of 15% rice bran protein concentrates to the kapreeta fish during Surimi making improved the organoleptic characters of the Surimi **Ammar and Korish (2009*)***.

Microbiological properties of unfried and fried Surimi blends supplemented with 15% level of rice bran and soybean protein concentrates.

Table (10), cleared the microbiological qualities of unfired Surimi blends (fresh) prepared from whitened kapreeta fish flesh. Total viable bacterial counts, molds & yeast, and coliform were counted. From these results, we can notice that Surimi blends No 2 were the lowest counts after steam blanching as a sequence of heat temperature. The total viable bacterial count showed a higher level in fresh control kapreeta fish Surimi.

Our results agreed with those of **(Kittikun *et al*., 2012*)*** who reported that the tuna-like fish Surimi does not contain any coliforms, especially *E. coli* due to the water in which tuna-like fish bred it is commonly free from *E. coli* but the most bacterial isolates from Surimi includes *Enterobacter* sp., and *Providencia* sp. Table (10) cleared the differences of microbiological counts of fried Surimi blends prepared from whitened kapreeta fish flesh. The total viable bacterial count in fried Surimi blends No 1, No 2, and No 3 were 4.00×10^3, 3.3×10^3 and 4.2×10^3, respectively. While, the molds and yeast counts in these samples were 0.78×10^2, 1.0×10^2 and 0.58×10^2 respectively. The results also cleared that, the coliform group not recorded in these samples. Finally, we can conclude that samples prepared with 15% of two kinds of added protein were less in counted microbiological qualities in both. Our results agreed with those of **Ammar (2004*)*** who reported that frying the fish destroys most bacteria, molds, and yeasts in the fish.

Conclusions

From the previous results, it could be concluded that all three types of protein, the cereal one, the legume, and the animal source are considered important sources of protein, ash content, carbohydrate, and minerals especially potassium phosphorus, iron, and manganese. The content of all essential amino acids was higher than the recommended by FAO/WHO pattern for 10-12 year children. The nutritional quality of the three different sources of protein was highly

Table 10. Microbiological qualities of fresh (unfried surimi blends (prepared from whitened kapreeta fish flesh (with 5 % H_2O_2).

Surimi blends	Process	Microbiological qualities		
		Total viable bacterial counts	Molds and yeast counts	Coliform bacterial counts
No1(Control)	Fresh	7.2×10^3	5.8×10^3	2.1×10^2
	Fried	2.00×10^2	0.78×10^2	Nil
No 2 (Added 15% rice bran protein concentrate)	Fresh	4.8×10^3	1.20×10^2	Nil
	Fried	1.3×10^2	1.0×0^2	Nil
No3 (Added 15% soybean protein concentrate)	Fresh	5.0×10^3	1.30×10^2	Nil
	Fried	1.55×10^2	0.50×10^2	Nil

Value are Means ± Standard Error. Means within the same row of different letters are significantly different at ($P < 0.01$).

comparable to those of antioxidant activities showed closed values and was higher than that of casein, a standard protein source. Accordingly, it could be concluded that rice bran, soybean, and whey protein concentrates can be recommended for preparing some food products. The tuna-like fish is of poor nutritive value and is not appreciated among consumers, so it can be utilized for the production of fish products as the experiment source of protein. Then using it for Surimi making with the addition of 15% of different sources of protein concentrates will improve the feeding and nutritive quality of this fish.

References

1. A.O.A.C. (2012). Association of Official Analytical Chemists. Official Methods of Analysis.; 17th ed. Washington, DC., USA.
2. A.P.H.A (American Public Health association) (1971). Recommended methods for the microbiological examination of food A.P.H.A., New York USA.
3. A.S.G.A. (2013). Agricultural Statistics General Administration -Arab Republic of Egypt, Ministry of Agricultural and Land Reclamation- Economic Affairs Sector- Agricultural Economic Center Administration.
4. Abu-Tor, E. M. (2002). Production of hot smoked fillets/steaks and fish fingers from tuna-like fish (Sconbromoraus Spp.) food quality-quality distribution. 4th International Conference for food industries quality control. 530 – 553. Alex. Univ.
5. Alsmeyer, R. H.; Cunningham, A. E. and Happich, M. L. (1974). Equations predict PER from amino acid analysis. Food Technol., 28: 34-40.
6. Ammar, A. K. (1999). Chemical and technological studies on mono-sex Bolti fish. M. Sc. Thesis, Dept. Food Techn., Fac. Of Agric., Tanta Univ. Kafr El-sheikh, Egypt.
7. Ammar, A. K. (2004). Chemical and technological studies on some foods. Effect of some preparation and technological processes on Bolti fish quality. Ph. D. Thesis. Fac. Of Agric. Kafr El-Sheikh Univ.
8. Ammar, A. K. and Korish, M. A. (2009). Effect of Precooking Process of Tuna-like Fish (Scombromorous Spp.) Cake on chemical, microbiological and sensory properties. J. Agric. Sci. Mansoura Univ. 34 (6): 6455 – 6465.
9. Bhaskar, N.; Benila, T.; Radha, C. and Lalitha, R. G. (2008). Optimization of enzymatic hydrolysis of visceral waste proteins of Catla (Catla catla) for preparing protein hydrolysate using a commercial protease. Biores. Technol. 99 (2): 335–343.
10. 10. Chaijan, M. S.; Benjakul, W.; Visessanguan and Faustman, C. (2004). Characteristics and gel properties of muscles from sardine and mackerel caught in Thailand. Food Research International. 37 (10): 1021 – 103.
11. 11. Deng, J. C.; Toledo, R. T. and Lillard, D. A. (1974). Effect of smoking temperature on acceptability and storage stability of smoked Spanish mackerel. J. Food Sci. 39 (3): 596 – 601.
12. 12. Devi, R. R. and Arumughan, C. (2007). Phytochemical characterization of defatted rice bran and optimization of a process for their extraction and enrichment. Bioresource Technology, 98, 3037–3043.
13. 13. Dudek, S. G. (2001). Nutrition essential for nursing practice (4th edn) Philadelphia: Lippicott.
14. 14. Fadl, Walaa, M. A. (2014). Chemical and Technological Studies on Kapreta Fish (Like Tuna). M. Sc. Thesis, Food Technology Dept. Fac. Agri, Kafrelshiekh Univ.
15. 15. FAO/ WHO/UNU (2007). Protein and amino acid requirements in human nutrition: Report of a joined WHO/FAO/ UNU expert consultation. WHO Technical report series 935. Geneva. WHO/FAO/ UNU, 276.
16. 16. FAO/WHO, Food and Agriculture Organization / World Health Organization. (1991). "Protein Quality Evaluation" Report of joint FAO/WHO Expert consulation. (12) 4:8 Bethesda, Md. USA.
17. 17. FAOSTAT (2012). Database of food and agriculture organization. Rome, Italy. Viewed from http://faostat.fao.org. Assessed 12.01.13.
18. 18. Farag, S. A.; El-Shirbeeny, A. and Ashga, E. N. (1996). Phiscochemical studies for preparing quick-cooking rice by using gamma irradiation. Annal J. of Agriculture Science, Moshtohor. 34:641-652.
19. 19. Fujinami, Y., Tai, A., and Yamamoto, I. (2001). Radical scavenging activity against 1,1-diphenyl-2-picrylhydrazyl of ascorbic acid 2-glucoside (AA-2G) and 6-acyl-AA-2G. Chemical and Pharmaceutical Bulletin, 49(5), 642–644.
20. 20. Gilani, G. S. (2012). Background on international activities on protein quality assessment of foods. The British Journal of Nutrition, 108(Suppl (S2)), S168–82.
21. 21. Gul, K., Yousuf, B., Singh, A. K., Singh, P. and Wani, A. A. (2015). Rice bran: Nutritional values and its emerging potential for development of functional food-A review. Bioactive Carbohydrates and Dietary Fiber 6, 24–30.

22. 22. Han, S., Chee, K. and Cho, S. (2015). Nutritional quality of rice bran protein in comparison to animal and vegetable protein. Food Chemistry 172, 766 –769.
23. 23. Intarasirisawat, R., Benjakul, S., Visessanguan, W. and Wu, J. (2012). Antioxidative and functional properties of protein hydrolysate from defatted skipjack (Katsuwonous pelamis) roe. Food Chem., 135, 3039–3048.
24. 24. Kaewka, K., Therakulkait, C. and Cadwallader, K. R. (2009). Effect of preparation conditions on composition and sensory aroma characteristics of acid hydrolyzed rice bran protein concentrate. Journal of Cereal Science 50, 56–60.
25. 25. Kittikun, H. and Bourneow C, Benjakul S. (2012). Hydrolysis of surimi wastewater for production of transglutaminase by Enterobacter sp. C2361 and Providencia sp. C1112. Food Chem. 2012 Dec 1;135(3):1183-91. doi: 10.1016/j. foodchem.2012.05.044. Epub 2012 May 22.
26. 26. Labuda J., Kacerovský O., Kováč M., Štěrba A., Výživa a krmenie hospodárských zvierat. (1982). Príroda, Bratislava, p. 164. "Cited by Ijarotimi1, O. S. and Keshinro, O. O. (2013). Determination of Nutrient Composition and Protein Quality of Potential Complementary Foods Formulated from the Combination of Fermented Popcorn, African Locust and Bambara Groundnut Seed Flour. Pol. J. Food Nutr. Sci., Vol. 63, No. 3, pp. 155-166
27. 27. Maqsood, S.; Benjakul, S. and Shahidi, F. (2013). Emerging role of phenolic compounds as natural food additives in fish and fish products. Crit Rev Food Sci Nutr. 2013;53(2):162-79.
28. 28. Mariod, A. A., Adamu, H. A., Ismail, M., and Ismail, N. (2010). Antioxidative effects of stabilized and unstabilized defatted rice bran methanolic extracts on the stability of rice bran oil under accelerated conditions. Grasasy Aceites, 61(4), 409–415.
29. 29. Miller, G. L. (1967). Determination of the tryptophan content of feeding stuffs, with particular reference to cereals. J. Sci. food Agric. 18, 381.
30. 30. Mune, M. A.; Minka, S. R. M., bome, I. L. and Etoa, F. X. (2011). Nutrional potential of bambara bean protein concentrate. Pakistan J. of Nutrition. 10:112-119.
31. 31. Nottingham, P.M. (1971). Microbiological quality control in the meat industry. J. Sci. and Food Agric., 11: 436.
32. 32. Otten, J. J., Hellwig, J. P. and Meyers, L. D. (2006). Dietary reference intakes: The essential guide to nutrient requirements. Washington, DC: The National Academics Press.
33. 33. Ovissipour, M., Abedian, A. M., Motamedzadegan, A., Rasco, B., Safari, R. and Shahiri, H. (2009). The effect of enzymatic hydrolysis time and temperature on the properties of protein hydrolysates from the Persian sturgeon (Acipenser persicus) viscera. Food Chem. 115: 238–242.
34. 34. Pellet, P. C. and Young, V. R. (1980). Nutritional Evaluation of protein Foods. The United Nations University Book, New York, USA.
35. 35. Saikia, D., and Deka, S. C. (2011). Cereals: from staple food to nutraceuticals. International Food Research Journal, 18, 21–30.
36. 36. Schramm, R., Alicia, A., Hua, N., Xu, Z., and Lima, M. (2007). Fractionation of the rice bran layer and quantification of vitamin E, oryzanol, protein and rice bran saccharide. Journal of Biological Engineering, 1, 9. http://dx.doi.org/10.1186/ 1754-1611-1-9.
37. 37. Sereewatthanawut, I., Prapintip, S., Watchiraruji, K., Goto, M., Sasaki, M. and Shotipruk, A., (2008). Extraction of protein and amino acids from deoiled rice bran by subcritical water hydrolysis. Bioresour. Technol. 99, 555-561.
38. 38. Shih, F.; King, J.; Daigle, K.; An, H. J. and Ali, R., (2007). Physicochemical properties of rice starch modified by hydrothermal treatments. Cereal Chemistry 84, 527–531.
39. 39. Steel, R. G. D. and Torrie, J. H. (1980). Principles and procedures of statistics: a biomedical approach (2nd ed.). New York, NY: McGraw-Hill International Book Co.
40. 40. Supathra, L.; Cholticha, T.; Kornkanok , A.; Sumalee , K.; Salisa, C. and Kanit, K. (2008). Partial extraction method for therapid analysis of total lipids and ɤ- oryzanol contents in rice bran. Food Chem, 106: 752 -759.
41. 41. Tang, S., Hettiarachchy, N.S., and Shellhammer, T. H. (2002). Protein extraction from heat-stabilized defatted rice bran. 1. Physical processing and enzyme treatments. J. Agric. Food Chem., 50, 7444-7448.
42. 42. Teeny, F. M. and Miyauchi, D. (1972). Prepararion and utilization of frozen block of mincid block fish muscle. J. Milk & Food technology. 35 (7): 414.
43. 43. Venugopal.V. (2003): Value addition to Aquacultured Fishery Products. Fishing Chimes. Vol.23 (1), P-82-84.
44. 44. Zullaikah, S., Melwita, E. and Ju, Y. (2009). Isolation of oryzanol from crude rice bran oil. Food Chemistry, 100, 299–302.

ISSN print: 1224-5984
ISSN online: 2248-3942

Rom Biotechnol Lett. 2022; 27(3): 3487-3497
doi: 10.25083/rbl/27.3/3487.3497

Received for publication: January, 12, 2022
Accepted: July 25, 2022

Original paper

Effect of ascorbic acid and tri-sodium phosphate treatment at different packaging conditions on cold storage Bagrus bayad fish quality

MOHAMMED S. EL-SHENAWY*[1], MAHMOUD S. GOUDA[2], SAMIR Y. ELSANAT[2] AND ATEF S. OSHEBA[3]

[1]Meat and Fish Tech. Res. Institute, Agricultural Research Center, Giza Egypt
[2]Department of Food Technology, Faculty of Agriculture, Kafrelsheikh University, Egypt
[3]Meat and Fish Tech. Res. Institute, Agricultural Research Center, Giza Egypt

Abstract

This research paper aimed at evaluating the influence of ascorbic acid (AA) and tri-sodium phosphate (TSP) under different packaging condition on improving the shelf life and qualities of fillets of *Bagrus bayad* cold fish at 4±1ºC for 12 days. The microbiological analysis performed were the total bacterial count (TBC), proteolytic bacterial count (PBC), lipolytic bacterial count (LBC), Coliform count (CC), *Staphylococcus aureus* (SA), *Salmonella & Shigella* (SS) and yeast & mold (YM). The obtained results indicated that all noticed analysis parameters (TBC, PBC, LBC, CC, SA, SS, YM, AA and TSP).were gradually increased during storage period in different treatments. The increases of these parameters were significantly higher ($p < 0.05$) in control sample than samples treatment with (AA) and (TSP). The obtained results also showed that there was a significant ($p<0.05$) extension of the shelf-life through delaying the microbial growth of the samples treated with (TSP) and (AA), respectively. In addition, the shelf-life and the storage period for these products were found to be less than 3 days for control sample and more than 12 days of samples treated with (TSP) under cold storage (4°C). Therefore, the (TSP) had a high effectiveness for extending the shelf-life and enhancing quality attributes of raw fish fillets during cold storage.

Keywords Bagrus bayad, ascorbic acid, tri-sodium phosphate, cold storage, quality criteria, and shelf-life

To cite this article: EL-SHENAWY MS, GOUDA MS, ELSANAT SY, OSHEBA AS. Effect of ascorbic acid and tri-sodium phosphate treatment at different packaging conditions on cold storage Bagrus bayad fish quality. *Rom Biotechnol Lett.* 2022; 27(3): 3487-3497 DOI: 10.25083/rbl/27.3/3487.3497

*Corresponding author: walid.metwali@agr.kfs.edu.eg

Introduction

Fish is a valuable part of human nutrition because of high content of protein and polyunsaturated fatty acids with long chain (PUFAs) that are very useful due to their role in prevention of human cardiovascular (KYKKIDOU & al,[1]; ÖZOGUL & al, [2]). Fish fillets are considered better than beef and chicken meat because of their high marine protein efficiency rate (PER) and low-fat content containing long chain n-3 fatty acids, beneficial for health (CHURi & al, [3]). The expansion of the fast-food industry and the increased consumption of processed-meat products make it necessary to reevaluate the quality characteristics of fresh fish fillets products and to be available in the Egyptian market. Although fish and fish products have therapeutic and nutritional value, they have a short shelf-life, due to the vast amounts of free amino acids and volatile nitrogen bases and higher final pH that limit the useful life of the product being highly susceptible to oxidation of unsaturated fatty acids and this can affect the flavor, taste, texture, aroma, and shelf-life (MEXIS & al, [4]). The microbial activity is involved 12 million tons of seafood sector by occurring food spoilage (KULAWIK & al, [5]). To prevent and delay the quality changes that are caused by lipid oxidation in foods and seafood, various synthetic antioxidants have been used. However, with growing concerns regarding the safety of synthetic antioxidants, natural antioxidants have been utilized as a promising source of antioxidants that delay oxidative developments to preserve fish quality. This effect is referring to their favorable action to scavenge free radicals and retard the effect of pathogens through its antibacterial effects (SINGH & al, [6]). *Bagrus bayad* is so abundantly represented in the river Nile. These are generally called catfishes, of which 15 genera occur in the Nile system. Almost 36 common genus is Bagrus, which contain two species *Bagrus bayad* and *Bagrus docmac*. They reach a length of about a meter and their flesh is very good. B. bayad are extensively dispersed in river Nile and lakes. Recently, there has been increasing interest in the utilization of chemical preservatives to control microbial, oxidative and autolytic enzymatic spoilage of fish (GHALY & al, [7]). Of these, organic acids are particularly suitable as they found naturally in foods, are 'generally recognized as safe' (GRAS) (REY & al, [8]). Organic acids consider preservatives factors through lowering the pH of food and can penetrate the lipid membrane of bacteria and destabilizing of pH inside the cytoplasm causing disturbing of bacteria metabolic interaction and growth. Trisodium phosphate (TSP) as a preservative agent can reduce the bacterial growth by destructive lipid structure inside the bacterial cell membrane (MEREDIT & al, [9]; SMYTH & al, [10]). Ascorbic acid can be used as an antioxidant agent to increase shelf life of processed food and conserves. This acid is a strong antioxidant and has a direct synergistic relationship with other antioxidants (AUBOURG & al, [11]). Besides the chemical and natural preservatives agents, seafood products are requiring additional care in packaging technique to prolong their shelf life with keeping its quality. The packaging of fishery products and fresh meat inside modified atmosphere is widely exploited to delay microbial activity and enzymatic bad action (ZHANG & al,[12]) or create a satisfied protection from deteriorative effects and environmental effects. Nitrogen (N_2) is an inert, odorless, and tasteless gas. It is used as a filler to prevent package collapse, because of its low solubility in water and fat in gas packaging. The use of N_2 results in the reduction in lipid oxidation and the inhibition in the growth of aerobic spoilage microorganisms (MASNIYOM, [13]). Therefore, this study was performed to detect the effect of (AA) and tri-sodium phosphate under different packaging condition on improve the quality and shelf life of *Bagrus bayad* fish fillets during storage at 4±1ºC by determination of physico-chemical, microbial and sensory quality criteria so, shelf-life periodically during cold storage.

Materials and Methods

Materials

Whole fresh Bayad fish (*Bagrus bayad*), were obtained from river Nile near Motobus city, Kafr Elshiehk Governorate, Egypt during March, 2018. Fish samples were transported to the Laboratory of Food Technology Department, Faculty of Agriculture, Kafrelshiekh University, in insulated cooler boxes directly within 2 h of purchase and stored whole on ice in a polystyrene box in a chill room at 2ºC. The fish obtained within 48 h of landing and were of a similar weight (1500 ± 100g) and long (35± 2cm). Sunflower oil, wheat flour and NaCl obtained from local market in Kafr El-Sheikh city. Ascorbic acid and tri-sodium phosphate (Merck Co., Germany) obtained from El-Gomhoria Com. Tanta city.

Methods

Preparation of Bayad fillet

The fish samples were beheaded, gutted and washed with tap water to remove all viscera, black membranes, swim bladder and blood. Skin and bones were manually removed and aseptically filleted to produce pure fillets (162 fillet particles). The yield of flesh was about 48%. The filleted samples were exposed to cold water for quick washing and the weight of each fillet was adjusted to 200 ± 5 g. After that, three groups of samples were divided as indicated in Ta-

ble (1). The first group was considered as blank control (BC) that were submerged in sterile distilled water and directly packed in high density polyethylene (HDPE) bags. T1 submerged in 0.5% of ascorbic acid aqueous solution (AA treatment 0.5%) and T3 were submerged in 0.5% of Tri-sodium phosphate aqueous (TSP treatment 0.5%) respectively. After 5 minutes dipping time according to **(TAHERI & al, [14]),** fillets were removed from all solutions and packaged in individual HDPE bags. All samples were packaged in three different conditions: air, nitrogen and vacuum. After packaging, first the fillets were stored by refrigerated in 4°±1C for 15 days. For all types of fish fillets, microbiological analysis were carried out after 0, 6 hours and 3, 6, 9, 12 and 15 days and chemical, physico-chemical and microbial analysis were conducted in three replications.

Fish was eviscerated, de-headed, skinned & filleted. The split portions were weighed individually and their percentage of the total fish weight was calculated. The fillet percent was calculated by: Fillet % = Fillet weight × 100 Total weight.

Fish Yield: Fish was eviscerated, beheaded, skinned & filleted. The split portions were weighed individually and their percentage of the total fish weight was calculated. The fillet percent was calculated by:

$$\text{Fillet\%}=\frac{\text{Fillet weight}\times 100}{\text{Total weight}}$$

Chemical analysis

The proximate analysis of raw samples fillets was investigated according to the **AOAC, [15]).** The moisture content was determined by drying the samples in an air oven overnight at 105±2°C to a constant weight, crude protein content by using the Micro-Kjeldahl method to determine the total nitrogen and multiply its value by the factor of 6.25; ether extract, in a Soxhlet apparatus using the petroleum ether (40 -60 ºC) as a solvent; ash content by ashing in an electric muffle at 550°C until constant weight.

Determination of pH

pH values were recorded by pH meter (Jenway, 3510, UK) according to method of (GOULAS & KONTOMINAS, [16]).

Determination of total volatile basic nitrogen (TVB-N)

The (TVB-N) values were calculated by method of (KIRK & SAWYER, [17]). Briefly, the bases were steam distilled into standard acid and the back-titration was performed by standard alkali.

Determination of trimethylamine nitrogen (TMAN)

The TMAN values were calculated using the above stated TVB-N procedure after suitable modification: formaldehyde solution was utilized to slab the primary and secondary amines (**AMC, [18]).**

Determination of 2-Thiobarbituric Acid (TBA)

2-Thiobarbituric acid (TBA) value of fish samples was determined colorimetrically by using the method published by (KIRK & SAWYER, [17]). TBA values was determined as mg of malonaldehyde (MDA)/kg sample.

Water holding capacity (WHC)

(WHC) and plasticity (tenderness) were measured by following the filter press method of SOLOVIEV [19], using Placom Digetal Planimeter (KP-90 N).

Microbiological analysis

The samples of raw fish minced and fish fillets were examined for microbial profile using standard procedures **(APHA, [20])** for total bacterial count (TBC) (30°C, 3 days) and Psychrophilic bacteria (PCB) (7°C, 10 days) on plate count agar, yeast & mold (YM) counts on potato dextrose agar (21°C, 5 days). The results were expressed as log10cfu/g of sample.

Preparation of samples

Samples were prepared using the recommended methods for the microbiological examination of foods published by **(APHA, [20]).** Samples were aseptically taken using sterilized knives and placed in sterile containers. One gram of samples was emulsified in 99 ml of distilled water in a sterile mechanical blender for 1.5 min to give 1/100 dilution. Serial dilutions were prepared to be used for counting several types of bacteria and yeast and mold counts. Samples were done in triplicates.

Table 1. Fish fillets treatments.

Packaging condition	Additives (%)	Treatment
Air	Control (Untreated)	T1
Under vacuum		
Nitrogen		
Air	Ascorbic acid (AA) 0.5%	T2
Under vacuum		
Nitrogen		
Air	Tri-sodium phosphate (TSP) 0.5%	T3

A. Total bacterial counts (TBC)

TBC per one gram of sample were determined using standard techniques on plate count agar medium (Difco). Incubation was carried out at 37ºC for 48 hours, according to **APHA, [20].**

B. Coliform bacterial counts

Coliform bacterial counts were calculated by planting on crystal violet neutral red agar medium (MacConkey agar). The plates were incubated at 25ºC for 4-5 days. The colonies were counted and reported as total coliform per gram of flesh (NOTTINGHAM, [21]).

C. Proteolytic bacterial counts (PBC)

Standard-plate counts procedure were followed, 5% skim milk was added to medium; till medium became opaque. Plates were incubated for 7 days at 30 ºC. During incubation, the plates were examined at intervals for growth and clearing around the colonies. Before recording the results, the plates were flooded with 1% solution of hydrochloric acid to verify positive results. Colonies are rounded with clear zone counting proteolytic bacteria **(SALEH, [22]).**

D. Lipolytic bacterial counts (LBC)

The nutrient agar medium was used for counting the lipolytic bacterial content of the samples. Sterilized butter fat (5%) was added to every plate before pouring the medium, and vigorously hand shaking. The plates were incubated at 25°C for3 days then, the plates were flood with copper sulfate solution (20%) for10 min. Colonies appeared as blue counting lipolytic bacteria (**Manual, [23]**).

E. *Staphylococcus aureus*:

Staphylococci, which are potential pathogens capable of growing in high salt concentrations, were determined using surface planting on Baird-parker agar medium **(ICMSF, [24]).**

F. Detection of Salmonella-Shigella

The detection of *Salmonella* was performed depending on method described by (REFAI, [25]) using buffered peptone as a pre-enrichment; while tetrathionate broth was used as a selective enrichment, broth and S-S agar was used as a selective plating media.

G. Mold and yeast counts

Mold and yeast counts were determinated by plating on acidified potato dextrose agar (Difco), and incubating duplicate plates at 25°C for 5 days (NOTTINGHAM, [21]).

Organoleptic evaluation of fish

Sensory evaluation of fish was performed by twenty experienced panelists on the basis of a 10-point degree of each sample. The panelists were requested to assess the characteristics of fish treatments on a scale from 10 to 0 (GELMAN & al, [26]). The scores were given in the decreasing order scale with 10-9 for excellent, 8-7 for good, 6-5 for fair and acceptable, 4-3 for poor and 2-1 for very poor. The mean of the scores given by the panel represented the overall sensory quality. A score less than 5 indicates that the smoked herring fish is rejected.

Statistical analysis

Data were subjected to Analysis of Variance (ANOVA). The Least Significant Difference (LSD) procedure was used to test for difference between means (significance was defined at ($p<0.05$) as reported by (SNEDECOR & COCHRAN, [27]).

Results and discussions

Proximate composition of raw Bayad fish fillets treated and untreated with ascorbic acid (AA) or tri-sodium poly phosphate (TSP):

Mean values for the chemical analysis of untreated and treated Bayad fish fillets are shown in Table (2). For raw fillets; the moisture, crude protein, fat and ash contents were 79.7, 78.1, 15.3 and 5.9% (on dry basis), respectively. From these results, it could be noticed that the investigated fish is a satisfied source of manufacturing fish fillet because belonged to high protein content and the big size of fish gave high filleting yield (48%) indicating that fish fillets that healthier than traditional meat particularly due to the presence long chain n-3 fatty acids and protein (OLIVEIRA& al, [28]). From the data shown in Table (2) it can be observed that fish fillets treated with TSP and backed with nitrogen have the best chemical properties among of the other treatments. These results are nearly accordance with obtained by (MOHAMED & al, [29]), who found that *Bagrus bayad* contains 76% moisture, 18.48% crude protein, 3.17% crude fat and 2.35% ash (on wet basis) and (MOHAMED & al, [29]) reported that the yield of mince from *Bagrus bayad* was 46.88%. Also, the obtained results are in the same line with found by (EL-SHERIF & ABD ABD EL-GHAFOUR, [30]; HUDAI, [31]). Physico-chemical changes of raw Bayad fish during storage at 4 ±1°C as affected with ascorbic acid (AA 0.5%) or tri-sodium phosphate (TSP 0.5%) at different packaging conditions on chemical composition during storage period pH value: Changes in pH value of different Bayad fish fillets during cold storage at 4 ±1°C are shown in Table (2). The differences in pH means values between different treated and untreated samples were insignificant ($P<0.05$) at zero time of storage, the initial pH values

of the control and samples treated with individually (AA) and (TSP) were 6.15 and 6.18, respectively.

Also, the results indicated a significant (*P<0.05*) increase in pH values in all fillets samples during storage period by different rates, the highest incremental rates (pH value) were detected in control sample reached to value of 6.94 at the end of storage period compared with samples treated with (AA) and (TSP) which reached to 6.30 and 6.42, respectively.

This reduction in pH values of samples treated with (AA) and (TSP) compared with control indicates the effectiveness of these (AA) and (TSP) as an antimicrobial agent so, it can be used as a way of combating the growth of common microorganisms causes of food poisoning (FISHER & PHILLIPS, [32]). The increase in pH values of all samples treated with (0.5%) (AA) and (TSP) and untreated during the storage period due to the protolytic enzymes that hydrolyzed fish protein to simple proteins, polypeptides and amino acids which were nutritious intermediate compounds as reported by (KHALLAF, [33]). The obtained results were in the same trend of those reported by (ÖZPOLAT & al, [34]). Total volatile basic-nitrogen (TVB-N) content: The impact of the individual tested control, ascorbic acid (AA) and tri-sodium poly phosphate (TSP) on TVB-N values of cold stored fish fillets was showed in Table (2), there were significant differences (*p<0.05*) in TVB-N values between treated fish fillets samples (AA) and (TSP) and the control (untreated) at the beginning of storage.

It is clear from the present results that at the beginning of the storage, TVB-N value was 11.60 mg/100g (on wet basis) for control fillets samples while, were 10.0 and 8.3 mg/100g for samples treated with (AA) and tri-sodium poly phosphate, respectively. During cold storage, the significant (p=0.05) increasing pattern in TVB-N values was observed in all investigated fish fillets samples. This may be due to the breakdown of proteins resulted from proteolytic enzymes and microbial activity (EL-SHERIF & ABD EL-GHAFOUR [30]; KHALLAF, [33]). The highest significant (*p<0.05*) incremental of TVB-N value was recorded in control sample. The treatments with (AA) and (TSP) respectively, were more active in deferring the rate of TVB-N increase during the cold storage period.

This may be due to the role of such chemical agents on microbial population and bacterial growth as antimicrobial agents (SACCHETTI & al, [35]). At the end of cold storage period, the TVB-N values for all samples except control did not exceed the acceptable limit stipulated and mentioned by **EOS, [36]** they stated that 20 mg TVB-N/100g raw samples indicates the spoilage of fish and minced meat.

Thus, control sample of investigated fish fillets considered spoiled (22.15mg/100g) at 15 days of storage while, (AA) and (TSP) sample (15.45 mg/100g) were not surpass the favorable limit at the end of storage period (15 days). The formation of TVB-N is generally related with the activity of micro-organisms and the formation tends to be increase at high microbial population (Chytiri & al, [37]). This finding proves the effect of (AA) and (TSP) in reduction of the bacterial growth then, TVB-N. From results; (AA) and (TSP) were the high effective of Bayad fish fillets in retarding the rate of TVB-N increase, as well as in prolonging the shelf-life of fish fillets throughout the subsequent cold storage (at 4 ± 1ºC for 15 days) and treatments with (AA) and (TSP) could be arranged descending according to the reduced levels of TVB-N as follows: fish fillets treated with (AA) and (TSP) respectively. These results are in agreement with reported by (EL-SHERIF & ABD EL-GHAFOUR, [30]; OSHEBA & al, [38]; ÖZPOLAT, & al, [34]). Trimethylamine Nitrogen (TMAN): is responsible for the pleasant fishy odor that produced from partly effect of intrinsic enzymes and through the bacterial activity **(SHAKILA& al, [39]).**

Changes in TMAN of different bayad fillets treatments during cold storage are shown in Table 2. From statistical analysis of these data it could be noticed that, their significant differences (*p>0.05*) were recorded in TMAN values between all treatments immediately after processing.

Meanwhile, TMAN values of all other treatments not exceeded this limit at any time of cold storage. From Table 2, it could be noticed that, TMNA values were significant decreased in TSP treatment especially with nitrogen compared with both control sample and other treatments. TMAN of treatment prepared with TSP reached the value 9.2 mg N/100 g after12 days of cold storage, exceeding the upper acceptability limit set by **(EOS, [36])** for TMNA values of fish products (10 mg N/100 g).

Thiobarbeturic acid (TBA) value

The influence of individually (AA) and (TSP) treatments on the TBA values of Bayad fish fillets during cold storage at 4±1ºC for 15 days was determined. It could be noticed from Table 2 that immediately after preparation (at zero time of storage) there were no significant (*p<0.05*) variances between the control and other treated samples. The highest value of TBA was found in untreated fish fillets sample; control (0.45 mg malonaldehyde (MDA)/kg flesh), while the lowest value was noted in samples treated with (AA) (0.26 mg MDA/kg) followed by samples treated with (TSP) (0.38 mg MDA). These values of TBA were increased (*p<0.05*) to 1.85 and 2.05 mg MDA/kg flesh, respectively at the end of storage period (15 days). Therefore, although the (AA) and (TSP) had significant (*p<0.05*) reduction effect on the TBA values, there was an increasing in

TBA values in all different fish fillets samples throughout the cold storage by different rates affecting by (AA) and (TSP) and cold storage period.

The incremental in TBA values for all fish fillets samples with increasing the cold storage time may be due to the self-oxidation of fats, bacteriological and/or oxidative rancidity. Thus, the control sample considered spoiled at 5 days of storage (2.15 mg MDA) and sample treated with (AA) (2.05 mg MDA) spoiled at 15 days as reported by (SUMAN & al, [40]) who indicate that TBA values of 2 mg MDA/kg flesh or greater in meat such as beef are considered to be rancid and (BONNELL, [41]) mentioned that fish and fish products of good quality will have TBA value less than 2mg MDA/kg flesh, while poorer quality fish will have 3-27mg

Table 2. Effect of treatment Bayad (*Bagrus bayad)* with ascorbic acid (AA 0.5%) or tri-sodium phosphate (TSP 0.5%) at different packaging conditions on chemical composition during storage period (on dry weight basis).

Storage period (Day)				Sale time (hour)		Packaging condition	Treatment	Chemical parameters
12	9	6	3	6	0			
--	--	76.5	77.2	78.0	79.7	Air^{c}		
--	--	77.0	77.5	78.6	79.7	Vacuum^{b}	Control (Untreated)^{B}	
--	--	78.0	78.4	79.3	80.0	Nitrogen^{a}		
--	75.7	76.4	77	77.5	79.1	Air^{c}		
--	76.0	76.7	77.3	78.0	79.3	Vacuum^{b}	Ascorbic acid (0.5 %)^{C}	Moisture (%)
--	76.4	77.2	78.0	79.2	79.9	Nitrogen^{a}		
--	76.2	77.0	78.0	79.2	80.0	Air^{b}		
--	77.4	78.2	79.0	79.5	80.1	Vacuum^{b}	Tri-sodium phosphate (0.5 %)^{A}	
--	78.1	79.3	80.0	80.6	80.1	Nitrogen^{a}		
--	--	76.7	77.2	77.6	78.1	Air^{c}		
--	--	77.2	77.4	77.9	78.2	Vacuum^{b}	Control (Untreated)^{A}	
--	--	77.3	77.7	78.2	78.4	Nitrogen^{a}		
76.5	77.0	77.4	77.7	78.0	78.2	Air^{b}		
76.8	77.2	77.5	77.9	78.1	78.3	Vacuum^{ab}	Ascorbic acid (0.5 %)^{AB}	Crude protein (%)
77.0	77.4	77.6	77.8	78.0	78.2	Nitrogen^{a}		
76.7	77.1	77.3	77.6	77.8	78.0	Air^{c}		
76.9	77.3	77.5	77.7	77.9	78.1	Vacuum^{b}	Tri-sodium phosphate (0.5 %)^{B}	
77.0	77.3	77.7	78.0	78.2	78.4	Nitrogen^{a}		
--	--	14.7	15.0	15.2	15.3	Air^{c}		
--	--	14.9	15.1	15.2	15.3	Vacuum^{b}	Control (Untreated)^{A}	
--	--	15.0	15.2	15.3	15.4	Nitrogen^{a}		
14.7	14.9	15.1	15.2	15.3	15.4	Air^{c}		
14.8	15.0	15.1	15.2	15.3	15.4	Vacuum^{b}	Ascorbic acid (0.5 %)^{A}	Ether extract (%)
14.6	15.0	15.1	15.2	15.3	15.4	Nitrogen^{a}		
14.6	14.8	15.0	15.2	15.3	15.4	Air^{c}		
14.7	14.9	15.1	15.2	15.3	15.4	Vacuum^{b}	Tri-sodium phosphate (0.5 %)^{B}	
14.8	15.1	15.2	15.2	15.3	15.4	Nitrogen^{a}		
--	--	7.5	6.8	6.4	5.9	Air^{a}		
--	--	7.4	6.8	6.2	5.9	Vacuum^{ab}	Control (Untreated)^{C}	
--	--	7.3	6.7	6.3	5.9	Nitrogen^{b}		
7.8	7.6	7.2	6.7	6.3	5.9	Air^{a}		
7.7	7.3	7.0	6.6	6.3	5.9	Vacuum^{ab}	Ascorbic acid (0.5 %)^{B}	Ash content (%)
7.5	7.1	6.7	6.3	6.1	5.7	Nitrogen^{b}		
7.9	7.5	7.3	6.8	6.4	6.0	Air^{a}		
7.8	7.4	7.2	6.8	6.3	6.0	Vacuum^{b}	Tri-sodium phosphate (0.5 %)^{B}	
7.8	7.4	7.2	6.7	6.3	6.0	Nitrogen^{b}		

All values given are means of three determinations.

Values followed by different letter in row are significantly different at $p<0.05$.

(a.b and c) : comparison of means by packaging condition at ($P<0.05$) by Duncan's multiple comparison tests.

A, B and C: Comparison of means by treatment at ($P<0.05$) by Duncan's multiple comparison tests.

MDA/kg. Accordingly, the fillets samples treated with ginger or rosemary in the current study would not deceive consumers up to 15 days of storage. Finally, the obtained results revealed that the treatment of Bayad fish fillets with (AA) and (TSP), respectively led to extension ($p<0.05$) of their shelf-life comparing with the control sample. These results are in agreement with previous studies by (EL-SHERIF & ABD EL-GHAFOUR, [30]; UÇAK & al, [42]).

Physical changes of raw Bayad fish during storage at 4 ±1°C as affected by (AA) or tri-sodium poly phosphate

As shown in Table (3), water holding and Tenderness values were significantly decreased with increasing storage period. Table (3): Effect of treatment Bayad (*Bagrus bayad*) with ascorbic acid (AA) or tri-sodium phosphate (TSP) on Physical parameters during storage period.

Microbiological load changes of raw Bayad fish fillets during storage at 4 ±1 °C as affected by (AA) or tri-sodium poly phosphate

Total bacterial count (TBC)

Table (4) shows the changes of total bacterial count of different fish fillets samples during cold storage as affected by treated by (AA) and (TSP) individually. At zero time of storage, control samples (untreated) recorded the highest mean counts of TBC comparing to other samples treated with (AA) and (TSP), that caused a significantly ($p<0.05$) reduction in microbial count of treated fish fillets immediately after preparation. The TBC of control and treatment samples with (AA) and (TSP) fish fillets were gradually increased significantly ($p<0.05$) during storage at 4±1ºC with a highly increase in control and depending on the kind treatment. The growth of psychrophilic bacteria under this storage condition might cause the noticed increase (OSHEBA & al, [38]). TBC (cfu/g flesh) of control sample were 3.25 at zero time of storage increased to 7.65 cfu/g fillets sample at the end of storage period (15 days), while samples treated with (AA) and (TSP) were 2.60 and 3.02 (cfu/g flesh) at zero time increased to 3.70 and 4.00 (cfu g^{-1}), respectively. This mentioned that (AA) and (TSP) may be responsible for the antibacterial properties. Also, it could be detected that significant differences ($P<0.05$) (TSP) was noticed have strong inhibitory effect against the growth of TBC followed by (AA). In this study the raw fish fillets of control sample was considered accepted until 6th day of storage and were rejected because TBC count was exceeded than the maximum permissible level MPL (10^6 numbers/g) was reported the acceptable limit of TBC for fil-

Table 3. Effect of treatment Bayad (*Bagrus bayad)* with ascorbic acid (AA) or tri-sodium phosphate (TSP) on Physical parameters during storage period.

Storage period (Day)				Sale time (hour)		Packaging condition	Treatment	Physical parameters
12	9	6	3	6	0			
--	--	4.80	4.6	4.5	4.41	Aira	Control (Untreated)A	Water holding capacity (WHC) (g water retained /g protein)
--	--	4.71	4.6	4.53	4.40	Vacuuma		
--	--	4.63	4.55	4.46	4.38	Nitrogenb		
4.79	4.7	4.63	4.45	4.4	4.35	Aira	Ascorbic acid (0.5 %)A	
4.75	4.63	4.60	4.45	4.39	4.33	Vacuumab		
4.72	4.68	4.55	4.43	4.37	4.32	Nitrogenb		
4.57	4.45	4.37	4.3	4.20	4.11	Aira	Tri-sodium phosphate (0.5 %)B	
4.50	4.38	4.28	4.17	4.10	4.00	Vacuumab		
4.44	4.30	4.19	4.11	4.05	3.95	Nitrogenb		
--	--	3.00	3.10	3.15	3.24	Aira	ControlA (Untreated)	Tenderness
--	--	3.30	3.12	3.17	3.20	Vacuuma		
--	--	3.00	3.05	3.12	3.17	Nitrogenb		
2.77	2.83	2.92	3.00	3.08	3.15	Aira	Ascorbic acid (0.5 %)B	
2.65	2.77	2.85	2.96	3.04	3.12	Vacuumb		
2.61	2.75	2.83	2.94	3.02	3.08	Nitrogenb		
257	2.65	2.73	2.85	2.94	3.00	Aira	Tri-sodium phosphate (0.5 %)C	
2.54	2.63	2.70	2.82	2.90	2.97	Vacuumb		
2.50	2.60	2.67	2.75	2.80	2.94	Nitrogenc		

All values given are means of three determinations.
Values followed by different letter in row are significantly different at p<0.05.
(a.b and c) : comparison of means by packaging condition at ($P<0.05$) by Duncan's multiple comparison tests.
A, B and C: Comparison of means by treatment at ($P<0.05$).

lets, also MPL recommended by the International Commission on Microbiological Specifications for TBC in all fillets products is below 7 log10cfu/g sample **(ICMSF, [24]),** while the other fish fillets samples treated with (AA) and (TSP) remained acceptable microbiologically and safe for consumption up to 15 days storage at 4±1ºC because the values were below the MPL. Therefore, this study demonstrated that the use of (0.5%) (TSP) decreased the microbial attendance of cold raw Bayad fish fillets compared to the control. These results are in agreement with found by (ÖZPOLAT & al, [34]) and (BABATUNDE & ADEWUMI, [43])

Yeast & Mold (YM) counts

Results in Table (4) show the changes in the yeast and mold of the different types of Bayad fish fillets during refrigerated storage at 4±1ºC affected by addition individually (AA) and (TSP), at preparation. YM counts were not detected in any of fillets samples at the 0th day until 6thday of storage. YM counts were detected in control samples (1.85 cfu/g) at 5th day. In treated fillets samples with (TSP), it could be noticed that YM counts were appeared at the 10th day in samples treated with (AA) (1.22 cfu/g) and at 15th day in samples treated with (TSP) (1.20 cfu/g). On the other

Table 4. Effect of treatment Bayad (*Bagrus bayad)* with ascorbic acid (AA) or tri-sodium phosphate (TSP) on total viable bacterial, molds & yeast, psychrophilic bacterial, Lipoletic bacteria and Protoletic bacteria counts during storage period.

Storage period (Day)			Sale time (hour)			Packaging condition	Treatment	Microbiological parameters
12	9	6	3	6	0			
-	-	7.2	4.8	3.2	1.8	Air^{a}		
-	-	6.5	3.6	2.5	1.6	Vacuum^{b}	Control (Untreated)^{B}	
-	-	5.9	3.4	2.3	1.5	Nitrogen^{c}		
7.8	6.0	5.2	3.4	2.7	1.7	Air^{a}		Total bacterial counts (CFU/g ×10^{5})
6.9	5.3	4.1	2.8	2.4	1.5	Vacuum^{b}	Ascorbic acid (0.5 %)^{A}	
5.8	4.9	3.8	2.5	2.0	1.5	Nitrogen^{c}		
7.1	5.7	4.5	3.1	2.3	1.6	Air^{a}		
6.4	4.7	3.4	2.9	2.1	1.4	Vacuum^{b}	Tri-sodium phosphate (0.5 %)^{C}	
5.6	4.4	3.2	2.5	1.8	1.4	Nitrogen^{c}		
-	-	7.4	5.7	3.8	2.2	Air^{a}		
-	-	7.0	5.3	3.5	2.0	Vacuum^{b}	Control (Untreated)^{A}	
-	-	6.8	4.7	3.3	2.0	Nitrogen^{c}		
7.4	6.3	5.5	4.1	3.4	2.0	Air^{a}		Molds & yeast counts (CFU/g ×10^{3})
6.9	5.4	4.6	3.7	2.7	1.9	Vacuum^{b}	Ascorbic acid^{C} (0.5 %)	
6.6	4.9	4.1	3.3	2.5	1.8	Nitrogen^{c}		
8.4	6.7	5.9	4.4	3.6	2.1	Air^{a}		
8.1	6.2	5.3	3.9	3.2	1.9	Vacuum^{b}	Tri-sodium phosphate^{B} (0.5 %)	
7.5	5.9	4.4	3.4	2.9	1.9	Nitrogen^{c}		
-	-	7.0	5.3	4.1	3.0	Air^{a}		
-	-	6.6	5.0	3.9	2.8	Vacuum^{b}	Control (Untreated)^{A}	
-	-	6.0	4.5	3.8	2.6	Nitrogen^{c}		
8.1	6.3	4.9	3.8	3.0	2.5	Air^{a}		Lipoletic bacteria count (CFU/g ×10^{2})
7.2	6.8	4.2	3.5	2.9	2.3	Vacuum^{b}	Ascorbic acid (0.5 %)^{B}	
6.7	5.5	4.0	3.5	2.7	2.1	Nitrogen^{a}		
7.5	5.8	4.6	3.7	3.0	2.4	Air^{a}		
6.6	5.4	4.3	3.4	2.7	2.2	Vacuum^{b}	Tri-sodium phosphate (0.5 %)^{A}	
6.3	5.0	4.1	3.2	2.5	2.0	Nitrogen^{c}		
		5.7	4.3	3.1	2.3	Air^{a}		
		5.2	4.0	2.7	1.8	Vacuum^{b}	Control (Untreated)^{C}	
		4.8	3.7	2.5	1.8	Nitrogen^{c}		
7.2	5.6	4.8	3.4	2.6	1.8	Air^{c}		Protoletic bacteria count (CFU/g×10^{3})
6.7	5.1	4.4	3.3	2.4	1.7	Vacuum^{a}	Ascorbic acid (0.5 %)^{B}	
6.4	4.9	4.0	3.2	2.2	1.6	Nitrogen^{b}		
7.0	5.5	4.5	3.3	2.4	1.6	Air^{a}		
6.3	5.0	4.2	3.1	2.3	1.6	Vacuum^{b}	Tri-sodium phosphate (0.5 %)^{C}	
6.0	4.8	4.0	2.8	2.0	1.6	Nitrogen^{c}		

All values given are means of three determinations.

Values followed by different letter in row are significantly different at $p<0.05$.

(a.b and c) : comparison of means by packaging condition at ($P<0.05$) by Duncan's multiple comparison tests.

A, B and C: Comparison of means by treatment at ($P<0.05$).

Table 5. Organoleptic properties of fried Bayad (*Bagrus bayad)* treated with ascorbic acid (AA) or tri-sodium phosphate (TSP) at zero time

Treatment	Organoleptic properties score					
	Appearance	Color	Odor	Texture	Taste	Overall acceptability
ControlC (Untreated)	8.5	7.5	8.3	8.0	8.1	8.08
Ascorbic acidB (0.5%)	8.5	8.2	8.7	8.5	7.8	8.34
Tri-sodium phosphateA (0.5%)	9.0	8.7	8.6	8.6	8.8	8.74
Significance (P <0.05)						

Means of each column followed by the same letter are not significantly different at the 5% level according to Duncan's Multiple Range Test.
a, b, c and d: Comparison of means by salting time.

hand, YM counts were gradually increased for all fish fillets samples during cold storage as noticed in Table (4) and a highly significant differences (*P<0.05*) between the control sample and other samples treated with (AA) and (TSP) were noticed thus, the control sample was highest (*p<0.05*) count until the final of storage period. At the end of storage period, YM counts reached to (4.00 cfu/g) of control fillets samples, while 2.55 and 2.90 of samples treated with (AA) and (TSP), respectively. Therefore, the fillets sample treated with (TSP) was the lowest YM counts followed by samples treated with (AA) compared with control sample, this indicated that (AA) and (TSP) have stronger effects against the growth of yeast and molds than control in reduction of yeast and molds population. So, the additions of (AA) and (TSP) to fish fillets were extended product shelf life (15 day) compared to the control (15 day). These results are in agreement with reported by (EL-SHERIF & ABD EL-GHAFOUR, [30]; IHEAGWARA, [44]; ÖZPOLAT & al, [34]). Finally, all cold storage fish fillets treatments were completely free from colifrom bacteria, *staphylococcus aureus*, *salmonella* and *Shigella* either at a zero-time or along cold-storage periods, indicating good level of hygiene during the handling, processing and storage.

Sensory properties changes of Bayad fish fillets during cold storage at (4±1ºC) as affected by (AA) and (TSP):

The results of sensory analysis are one of the most important quality criteria used for determination of shelf life of seafood. The changes of sensory properties (taste, color, odor, texture and general acceptability) of fried Bayad fish fillets treated individually with (AA) and (TSP) and untreated (control) during cold storage at (4±1ºC) were recorded in Table (5). It could be found that Bayad fish fillets at zero time of storage had excellent scores for color and texture then very good scores for flavor (taste and odor) immediately after preparation. Therefore, a noticeable significant (*p<0.05*) difference could be observed between samples treated with EOs and control in the case of taste and odor characteristics during the storage period. **EOS, [36]** was found to have an added advantage in terms of their synergistic effect against oxidation and in enhancing the taste and odor. The decline in overall acceptability of control samples as a result of this difference in taste and odor was more prominent during 15-20 days of storage and the off flavor formation was occurred. While, there was no marked difference (*p<0.05*) between the EOs treated samples and control in color and texture during zero time till 10 days of storage then, a significant (*p<0.05*) difference was found until the end of storage period. On the other hand, the taste, color, odor, texture and overall acceptability scores of control sample reached to 4.0, 4.5, 4.5, 4.2 and 4.2, respectively by 20 days of storage which was below the acceptable limit of score (5) and was greatly deteriorated being undesired as softening of texture and off odors was appeared then, this product become rejected for consumers.

In the case of the other samples treated with EOs, the scores were above of acceptable limit even after the end of storage period (25 days). Hence, the scores of overall acceptability garlic, ginger and rosemary samples were 5.3, 6.5 and 5.8 respectively at the end of storage period (25 days) and was in the order samples, ginger > rosemary > garlic. Therefore, Bayad fish fillets samples treated with 1.0% ginger showed the significant (p<0.05) highest mean score of overall acceptability followed by samples treated with 1.0% rosemary and treated with 1.0% garlic compared with untreated samples (control) which rejected before 20 days of cold storage.

Even through the added EOs delayed oxidation and extending the shelf-life, their antioxidant activity reduced during storage by increase significantly (*p<0.05*) differences in all individual tested samples during the end of storage periods.

Conclusion

In conclusion, the results obtained in this study showed the tested ascorbic acid and tri-sodium phosphate had / or presented / antimicrobial properties that improved the physico-chemical, microbiological and sensory quality attributes of raw Bayad fish fillets during cold storage thus, extending the

shelf life. This is justified by the low TVB-N, TBA, and pH as well as bacteria, yeast and mold counts of fish fillets related with EOS than untreated control samples. Sensory evaluation revealed that shelf life of fish fillets samples was longest ($P < 0.05$) for samples treated with TSP as compared to the control (12 days) under storage at4±1ºC. Therefore, the present findings recommended that the TSP and AA should be utilized for extending the shelf-life and enhancing quality attributes and sensory properties of fish fillets during cold storage.

Acknowledgments

The study was supported by a project funded by department of Food Science and Technology, Kafrelshiekh University.

Conflict of interest

The authors have declared that there is no conflict of interest.

References

1. AMC. *Analytical Method Committee. Recommended method for the examination of fish and fish products. Anal., 104: 434-439.* Augbourg, S. and M. Ugliano, 2002. Effect of brine pre-treatment on lipid stability of frozen horse mackerel (*Trachurus trachurus*). Eur. Food Res. Tech., 215(3): 91-95 (1979).
2. AOAC. Official Methods of Analysis of the Association of Official Analytical Chemists , 18th Ed., Published by the Association of Official Analytical Chemists ,Arlington ,Virginia, 2220 USA (2010).
3. APHA. American Public Health Association. In M. L. Speck (Ed.) compendium of methods (1992).
4. EOS. Standards No 288, Egyptian Organization for Standardization and Quality Control, Ministry of Industry. Cairo, Arab Republic of Egypt (2005).
5. ICMSF. International Commission on Microbiological Specification for Food: Microorganisms in Foods 2. Sampling for microbiological analysis: Principles and specific applications (2ndEd.).University of Toronto Press, Toronto. Canada(2002).
6. S. P. AUBOURG, Pérez-Alonso, F.PÉREZ-ALONSO, J. M. GALLARDO. Studies on rancidity inhibition in frozen horse mackerel (Trachurus trachurus) by citric and ascorbic acids. *European Journal of Lipid Science and Technology, 106*(4), 232-240 (2004).
7. O. A. BABATUNDE., A. O. ADEWUMI. Effects of ethanolic extract of garlic, roselle and ginger on quality attributes of chicken patties. *African journal of Biotechnology, 14*(8), 688-694 (2015).
8. A. D. BONNELL. *Quality assurance in seafood processing: a practical guide*: Springer Science & Business Media (2012).
9. S. CHYTIRI, I. CHOULIARA, I. SAVVAIDIS, M. KONTOMINAS. Microbiological, chemical and sensory assessment of iced whole and filleted aquacultured rainbow trout. *Food microbiology, 21*(2), 157-165 (2004).
10. S. EL-SHERIF, S. ABD EL-GHAFOUR. Effectiveness of garlic, rosemary and ginger essential oils on improve the quality and shelf life of Bagrus bayad fish sausage preserved by cold storage. *International Journal of Advanced Research, 4*(11), 276-289 (2016).
11. K. FISHER, C. A.PHILLIPS. The effect of lemon, orange and bergamot essential oils and their components on the survival of Campylobacter jejuni, Escherichia coli O157, Listeria monocytogenes, Bacillus cereus and Staphylococcus aureus in vitro and in food systems. *Journal of applied microbiology, 101*(6), 1232-1240 (2006).
12. A. GELMAN, R. PASTEUR, M. RAVE. Quality changes and storage life of common carp (Cyprinus carpio) at various storage temperatures. *Journal of the Science of Food and Agriculture, 52*(2), 231-247 (1990).
13. A. E. GHALY, D. DAVE, S. BUDGE, M. BROOKS. Fish spoilage mechanisms and preservation techniques. *American journal of applied sciences, 7*(7), 859 (2010).
14. A. E. GOULAS, M. G. KONTOMINAS. Effect of salting and smoking-method on the keeping quality of chub mackerel (*Scomber japonicus*): biochemical and sensory attributes. *Food chemistry, 93*(3), 511-520 (2005).
15. N. HUDA, T. ALISTAIR, H. LIM, R. NOPIANTI. Some quality characteristics of Malaysian commercial fish sausage. *Pakistan Journal of Nutrition, 11*(8), 700-705(2012).
16. M. IHEAGWARA. Effect of ginger extract on stability and sensorial quality of smoked mackerel (Scomber scombrus) fish. *J. Nutr. Food Sci, 3*(3), 1-5 (2013).
17. M. KHALLAF. Properties of smoked sausage processed from common carp fish. *J. Agric. Sci. Mansoura Univ, 15*(8), 1288-1299 (1990).
18. S. KIRK, R. SAWYER. *Pearson's composition and analysis of foods*: Longman Group Ltd (1991).
19. P. KULAWIK, F. ÖZOGUL, R. GLEW, Y. ÖZOGUL. Significance of antioxidants for seafood safety and human health. *Journal of agricultural and food chemistry, 61*(3), 475-491(2013).
20. S. KYKKIDOU, V. GIATRAKOU, A. PAPAVERGOU, M. KONTOMINAS, I. SAVVAIDIS. Effect of thyme essential oil and packaging treatments on fresh Mediterranean swordfish fillets during storage at 4 C. *Food chemistry, 115*(1), 169-175(2009).

21. D. MANUAL. Dehydrated culture media and reagents for microbiological and clinical laboratory procedures. *Difco la boratories*, 1(1971).
22. P. MASNIYOM. Deterioration and shelf-life extension of fish and fishery products by modified atmosphere packaging. *Sonklanakarin Journal of Science and Technology, 33*(2), 181(2011).
23. H. MEREDITH, D. MCDOWELL, D. J. BOLTON. An evaluation of trisodium phosphate, citric acid and lactic acid cloacal wash treatments to reduce Campylobacter, total viable counts (TVC) and total enterobacteriaceae counts (TEC) on broiler carcasses during processing. *Food Control, 32*(1), 149-152(2013).
24. S. MEXIS, E. CHOULIARA, M. KONTOMINAS. Combined effect of an oxygen absorber and oregano essential oil on shelf life extension of rainbow trout fillets stored at 4 C. *Food microbiology, 26*(6), 598-605(2009).
25. H. E. MOHAMED, R. AL-MAQBALY, H. M. MANSOUR. Proximate composition, amino acid and mineral contents of five commercial Nile fishes in Sudan. *African Journal of Food Science, 4*(10), 640-654 (2010).
26. P. NOTTINGHAM. Microbiological quality control in the meat industry (1980).
27. A. OLIVEIRA, B. HIMELBLOOM, N. MONTAZERI, M. DAVENPORT, H. BICEROGLU, K. BRENNER, S. THOMAS, C. CRAPO. Development and characterization of fish sausages supplemented with salmon oil. *Journal of Food Processing and Preservation, 38*(4), 1641-1652(2014).
28. A. OSHEBA, E. SHAMS, S. HUSSIEN. Effect of some herbs on the quality of irradiated beef sausages preserved by cold storage. *Isotope and Radiation Research, 42*, 925-947(2010).
29. Y. ÖZOGUL, F. ÖZOGUL, E. KULEY, A. S. ÖZKUTUK, C. GÖKBULUT, S. KÖSE. Biochemical, sensory and microbiological attributes of wild turbot (Scophthalmus maximus), from the Black Sea, during chilled storage. *Food chemistry, 99*(4), 752-758 (2006).
30. E. ÖZPOLAT, B. PATIR, H. GURAN, M. GUL. Effect of vacuum-packing method on the shelf-life of Capoeta umbla sausages(2014).
31. M. REFAI. *Manuals of food quality control. 4: Microbiological analysis*(1979).
32. M. S. REY, B. GARCÍA-SOTO, J. R. FUERTES-GAMUNDI, S. AUBOURG, J. BARROS-VELÁZQUEZ. Effect of a natural organic acid-icing system on the microbiological quality of commercially relevant chilled fish species. *LWT-Food Science and Technology, 46*(1), 217-223 (2012).
33. G. SACCHETTI, S. MAIETTI, M. MUZZOLI, M. SCAGLIANTI, S. MANFREDINI, M. RADICE, R. BRUNI. Comparative evaluation of 11 essential oils of different origin as functional antioxidants, antiradicals and antimicrobials in foods. *Food chemistry, 91*(4), 621-632(2005).
34. G. SINGH, P. MARIMUTHU, H. MURALI, A. BAWA. Antioxidative and antibacterial potentials of essential oils and extracts isolated from various spice materials. *Journal of food safety, 25*(2), 130-145(2005).
35. C. SMYTH, N. P. BRUNTON, C. FOGARTY, D. J. BOLTON. The effect of organic acid, trisodium phosphate and essential oil component immersion treatments on the microbiology of Cod (Gadus morhua) during chilled storage. *Foods, 7*(12), 200 (2018).
36. G. SNEDECOR, W. COCHRAN. Statistical methods, 8th edn. Affiliated East. *West Press, New Delhi, 13*, 1467-1473 (1994).
37. S. SUMAN, R. MANCINI, P. JOSEPH, R. RAMANATHAN, M. KONDA, G. DADY, S. YIN. Packaging-specific influence of chitosan on color stability and lipid oxidation in refrigerated ground beef. *Meat Science, 86*(4), 994-998 (2010).
38. S. TAHERI, A. A. MOTALEBI, A. FAZLARA. Antioxidant effect of ascorbic acid on the quality of Cobia (*Rachycentron canadum*) fillets during frozen storage. Iranian Journal of Fisheries Sciences. 11(3) 666-680 (2012).
39. İ. UÇAK, Y. ÖZOGUL, M. DURMUŞ. The effects of rosemary extract combination with vacuum packing on the quality changes of Atlantic mackerel fish burgers. *International journal of food science & technology, 46*(6), 1157-1163(2011).
40. M. ZHANG, Z. ZHAN, S. WANG, J. TANG. Extending the shelf-life of asparagus spears with a compressed mix of argon and xenon gases. *LWT-Food Science and Technology, 41*(4), 686-691(2008).
41. Y.G. SALEH. Technological and microbiological studies on convenient foods. Ph.D. Thesis, Fac. Agric., Menufiya Univ., Egypt(1983).
42. R.J. SHAKILA, K.VIJAYALAKSHMI, G. JEYASEKARAN. Changes in histamine and volatile amines of six commercially important species of fish of the Thoothukkudi coast of Tamil Nadu, India stored at ambient. Food Chem., 82(3): 347-352 (2003).
43. A. A. Soloviev. Meat Aging. In Food Industry. Pub., (Moscow), pp: 53-81, 82-164, 242-303(1966).

ISSN print: 1224-5984
ISSN online: 2248-3942

Rom Biotechnol Lett. 2022; 27(3): 3498-3506
doi: 10.25083/rbl/27.3/3498.3506

Received for publication: July, 08, 2022
Accepted: August 01, 2022

Original paper

Direct-Contact and Contact-free Treatment of a DBD-like Non-thermal Atmospheric Pressure Plasma Jet on *Pseudomonas aeruginosa*

TAMER AKAN[1,2], AHMET CABUK[3,4], PINAR AYTAR CELIK[4,5], E. SERHAT YAVAS[4], CAGRI DURMUS[4]

[1] Department of Physics, Faculty of Science and Letters, Eskisehir Osmangazi University, TR-26040 Eskisehir, Turkey
[2] Translational Medicine Research and Clinical Center, Eskisehir Osmangazi University, TR- 26040 Eskisehir, Turkey
[3] Department of Biology, Faculty of Science and Letters, Eskisehir Osmangazi University, TR-26040 Eskisehir, Turkey
[4] Graduate School of Natural and Applied Sciences, Eskisehir Osmangazi University, TR-26040 Eskisehir, Turkey
[5] Environmental Protection and Control Program, Eskisehir Osmangazi University, TR-26110 Eskisehir, Turkey

Abstract

In this study, a Dielectric Barrier Discharge (DBD)-like non-thermal atmospheric pressure plasma jet (NTAPPJ) was exposed to the *Pseudomonas aeruginosa* planktonic bacteria. The P. aeruginosa bacteria were treated by the NTAPPJs in both Ar and He at the non-contact distance (contact-free) and the contact distance (direct-contact). The contact of the NTAPPJs with the bacteria has generated spark discharges in both filamentary mode and diffuse mode. The antibacterial efficacy of the Ar and He NTAPPJs for various treatment times (60, 120, 180, and 300 sec) were investigated by treatment on the bacteria without contact and with contact in both filamentary mode and diffuse mode. The NTAPPJs in both Ar and He caused erosion on the agar surface when treated in direct-contact with the bacteria in the filamentary mode, while the NTAPPJs in Ar in the diffuse mode produced the greatest antibacterial efficacy without damage.

Keywords DBD-like jets, Non-thermal Atmospheric Pressure Plasma Jet, Direct and Indirect treatment, Planktonic Bacteria, Pseudomonas aeruginosa.

To cite this article: AKAN T, CABUK A, CELIK AP, YAVAS ES, DURMUS C. Direct-Contact and Contact-free Treatment of a DBD-like Non-thermal Atmospheric Pressure Plasma Jet on *Pseudomonas aeruginosa*. *Rom Biotechnol Lett.* 2022; 27(3): 3498-3506 DOI: 10.25083/rbl/27.3/3498.3506

*Corresponding author: ORCID IDs: Tamer Akan 0000-0003-0907-2724, e-mail:akan@ogu.edu.tr
ORCID IDs: Ahmet Cabuk 0000-0002-4619-6948, e-mail:acabuk@ogu.edu.tr
ORCID IDs: Pınar Aytar Celik 0000-0002-9447-1668, e-mail:paytar@ogu.edu.tr
ORCID IDs: E. Serhat Yavas 0000-0002-9677-1605, e-mail:ethemserhatyavas@gmail.com
ORCID IDs: Cagri Durmus 0000-0003-0174-0580, e-mail:durmuscagri@gmail.com

Introduction

Plasma is a partially or fully ionized gas consisting of various particles, such as electrons, positive/negative ions, neutral atoms/molecules (can be radicals), excited atoms/molecules (can be metastables), and photons (UV, visible, and thermal radiation). Plasmas are generally divided into thermal and non-thermal in terms of comparing the temperatures of the electrons with the temperatures of the other particles in plasma. While the temperatures (i.e. kinetic energy) of the particles in the plasma are equal in thermal plasmas, the temperatures of the electrons in non-thermal plasmas are higher than the temperature of the other particles, and the gas temperature remains as low as room temperature (Raizer, 1991; Grill, 1994). Non-thermal plasmas have many advantages such as the effects of low temperature, low electric field, and the chemical interactions of the active radicals have various applications. In the last decades, non-thermal atmospheric pressure plasma sources, such as corona, streamer, dielectric barrier discharge (DBD), surface dielectric barrier discharge (SDBD), and plasma jet, have attracted significant interest, because they do not require expensive vacuum equipment and can be readily applied (Lu et al., 2016; Domonkos et al., 2021; Ilik et al., 2020).

Non-thermal Atmospheric Pressure Plasma jets (NTAPPJs) also belong to the large family of non-thermal atmospheric pressure plasmas; they are discharged plasma that can extend outside the plasma generation region between electrodes into the surrounding ambient environments. NTAPPJs are playing an increasingly important role in various plasma processing applications. This is because of their practical capability to provide plasmas that are not spatially bound or confined by electrodes (Laroussi and Akan, 2007; Penkov et al., 2015). Moreover, they can be movable and easily applied to samples with inner surfaces. NTAPPJs generated in air consist of different components such as neutral atoms/molecules, radicals, excited atom/molecules, metastables, charged particles (ions and electrons), reactive oxygen species (ROS), reactive nitrogen species (RNS), photons of UV, visible, infrared, and thermal radiation, and electromagnetic field, all of which may contribute to its antibacterial properties (Khlyustova et al., 2019).

Among other applications, the treatment of temperature-sensitive surfaces such as biological material is of interest, in particular in the field of plasma medicine by the interaction of plasma with living cells, tissues, and bacteria, e.g., for inactivation or sterilization of bacteria, fungi, and spores, cancer treatment, wound healing, dentistry, genetics, and skin treatment (Wu et al., 2016; Lin et al. 2016; Mashayekh et al., 2015; Schmidt et al., 2017; Yaopromsiri et al., 2015; Laroussi, 2015). The temperature-sensitive surface treatment of NTAPPJs has also produced amendatory results in the fields of food safety (Pankaj et al., 2018), agriculture (Velichko et al., 2019), and textile (Peran and Ercegović, 2020).

Biological materials can be treated by plasma in two different methods (Akan and Çabuk, 2014; Saadati et al., 2018 ; Malyavko et al., 2020; Dobrynin et al., 2009; Dobrynin et al., 2011; Morris et al., 2009): Direct treatment is when the biological sample to be treated is in direct contact with the plasma. All plasma agents (plasma-generated species and electromagnetic fields) come in contact with the sample. The most important distinguishing feature of the direct plasma treatment is that a significant flux of charges (ions and electrons) reaches the surface of the sample. The second method is the indirect treatment in which the biological sample is placed at a non-contact distance from the plasma. In this treatment, the charged particles do not play a role since they recombine before reaching the sample, and the active agents are blown to the treated sample. In indirect treatment, the active uncharged species are typically delivered to the surface via a flow of gas through a plasma region. Although mostly active uncharged species (e.g., O, O_2, OH, NO, O_3) will be the acting agents , many of the short-lived neutral reactive oxygen or nitrogen species also do not reach the sample. To date, direct and indirect treatment of bacteria using non-thermal atmospheric pressure plasma in the air is compared in terms of bacterial inactivation rates. It is demonstrated that direct treatment, where charged particles contact with bacteria directly , produces inactivation much faster than the indirect treatment, where plasma afterglow (post-discharge) is delivered to the bacteria with a gas flow through the plasma region (Dobrynin et al., 2011; Morris et al., 2009).

NTAPPJs consist of a gas tube equipped with one or two electrodes. The plasma is ignited inside the tube and transported to the outside as well as to the sample to be treated by a gas flow. NTAPPJs can be distinguished between remote plasmas, where the plasma is potential free and consists of recombining active species, and active plasma jets where the expanding plasma contains free and high energetic electrons. In the latter case, the targeted sample forms a second or third electrode. In many cases, the voltage does not need to be directly connected to this sample electrode, but some current may flow through the sample in the form of either a small conduction current, displacement current, or both. NTAPPJs can be classified into four categories, i.e., dielectric-free electrode (DFE) jets, dielectric barrier discharge (DBD) jets, DBD-like jets, and single electrode (SE) jets (Lu et al., 2012). When the plasma jet is not in contact with any sample (cells or whole tissue), the discharge is like a DBD. However, when the plasma jet is in contact with a

sample, the discharge is running between the high voltage electrode and the sample to be treated. In such a case, it no longer operates as a DBD will work as a streamer, spark, or arc discharge. The NTAPPJ used in this study is a DBD-like jet with and without contact with *P. aeruginosa* planktonic bacteria. Although NTAPPJs are accepted as remote or indirect plasma applications on a sample, DBD-like type jets should be classified according to whether they are in contact with the treated sample. DBD-like type jets change the jet format and transit to spark or arc discharge when contacted with the treated sample. In this case, they are separated from the remote application method by transferring charged particles to the sample to be treated. In addition, when a DBD-like type jet is in contact with a sample, it may create an undesirable chemical or physical effect on the sample to be treated. In this study, the effects of a DBD-like type jet exposed to *P. aeruginosa* planktonic bacteria with and without contact were investigated.

Experimental

Non-thermal Atmospheric Pressure Plasma Jet (NTAPPJ) System

For the non-thermal plasma treatment of *P. aeruginosa* planktonic bacteria, a homemade non-thermal atmospheric pressure plasma jet (NTAPPJ) device was used. A schematic of the NTAPPJ device used, including the spectroscopic measurement system, is given in Fig. 1. In this work, the NTAPPJ device was attached to a support with the jet (plume) shooting downward. Petri dishes containing *P. aeruginosa* planktonic bacteria evenly spread over agar were put right under the plasma jet and on a platform the height of which can be adjusted. In this way, the distance between the nozzle (end of the quartz tube) of the NTAPPJ and the Petri dishes containing *P. aeruginosa* planktonic bacteria to be treated, which is called the exposure distance (ED), can be determined.

The NTAPPJ source consists of two concentric electrodes through which a gas flow. By applying kHz power to the inner electrode, the gas discharge is ignited. The ionized gas from the plasma jet exits through a quartz glass tube, where it is directed onto a substrate (in this study *P. aeruginosa* planktonic bacteria) a few centimeters downstream. A device that is very similar to the NTAPPJ device used in this study was investigated in our previous article (Ilik and Akan 2016). The NTAPP jet assembly consisted of a 100 mm-long quartz tube with a gas inlet, and the inner and outer diameters of the quartz tube are 4 and 6 mm, respectively. A coaxial dielectric barrier configuration was used for the electrode geometry. A tungsten needle with a diameter of 0.5 mm and length of 150 mm is inserted into the center of the quartz tube as a high-voltage electrode. The high-voltage electrode is fixed at a distance of 3 mm away from the open end (the nozzle) and it was insulated with rectangular cubical polyethylene material. A 0.70 mm-thick copper foil with a 10 mm-width was used as the ground electrode and was wrapped on the quartz tube with the outer edge of the electrode at the downstream side being 20 mm away from the orifice of the quartz tube.

High-purity He (99.999%) and Ar (99.999%) enter the tube from the top side of the quartz tube, which is controlled by a mass flow meter division in a range of 0–15 L/min.

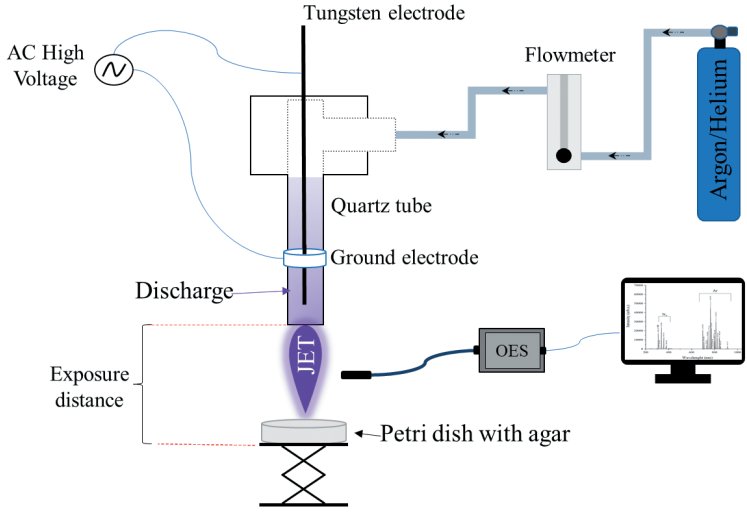

Figure 1. Schematic of the NTAPP jet device used.

A homemade power supply was developed to generate the plasma using a sinusoidal high voltage. For all the inactivation experiments reported in this letter, the peak-to-peak voltage of a 15 kHz sinusoidal waveform was optimized and then fixed at 18 kV.

In the NTAPPJ, the electron collisions excite the plasma species to the higher atomic or molecular levels decaying and emitting a photon at the specific wavelengths. These processes can be detected and analyzed by recording the emission spectrum. Optical Emission Spectroscopy (OES) has been applied to identify the chemical species present in the NTAPP jet (plume) when Ar and He is used as a working gas (Fig. 1). The emission spectrum for the Ar and He NTAPP jets in the air was taken by an Ocean Optics mini-spectrometer USB 2000+XR1-ES equipped with a 2048-element linear silicon charge-coupled device (CCD) array detector. The 300 grooves/mm grating and 10-mm wide slit were used to evaluate spectra in the spectral resolution of the spectrometer 0.1 nm.

Bacterial Strain and Growth Condition

The standard bacterial strain was stored in a deep freezer (Eskisehir Osmangazi University, Biotechnology Laboratory) at -80°C. The bacterial strain was inoculated into Tryptic Soy Broth (TSB) and incubated aerobically at 37°C for 24 hours. The strain was then subcultured on Tryptic Soy Agar (TSA) under the same conditions. To determine the region of growth inhibition, an overnight bacterial culture was diluted (1/1000) in sterile 0.9% saline, 100 µL of the diluted bacterial suspension was then spread evenly on the surface of the TSA plate. It was then immediately treated with the NTAPP jets at specified times. After exposure to the plasma jet, the plates were incubated for 24 hours at 37°C in a static incubator, and photographs of the agar plates showing the bacterial growth inhibition zones were taken using a digital camera. For control experiments, samples are treated by working gas flowing at the same flow rate with the plasma turned off. It should be noted that all experiments reported in this letter were repeated three times and the results were consistent with the same experimental conditions.

Results and Discussion

Non-thermal Atmospheric Pressure Plasma Jet (NTAPPJ) Generation

The origin of non-equilibrium plasmas is based on the development of electron avalanches. The main ionization mechanism in most gases is direct electron impact ionization by free electrons accelerated by the electric voltage applied. At low pressure, the positive ions generated in the ionization process drift to the cathode and lead to secondary electrons emission. This following delivery of free electrons seeds new avalanches, and this is the main characteristic of the Townsend-breakdown mechanism that leads to the generation of a self-sustained gas discharge such as a glow discharge. At higher pressure, the number of ionizing collisions per unit volume increases, and the breakdown mechanism changes significantly. When electron avalanches generate a space charge that locally enhances the electromagnetic field applied, secondary electron avalanches are started in the gas phase. The ionized region and its perturbation of the electromagnetic field grow rapidly and eventually form a separate plasma channel (a streamer-breakdown mechanism) called a streamer. A streamer propagates in the discharge region but does not necessarily connect the two opposite electrodes. Streamer discharges can undergo a transition to more intense spark discharges when it reaches to opposite electrode. An intense spark channel can transit into an arc discharge if the power supply can deliver the necessary current (Bruggeman et al., 2017).

When He is introduced to the NTAPPJ system given in Fig. 1 with a gas flow rate of 5 L/min, the plasma jet is formed in the filamentary mode as seen in Fig. 2a. When the gas flow rate of He is increased to 10 L/min, the length of the plasma jet increases as seen in Fig. 2b, and the plasma jet appears more in diffusive mode. The length, shape, and mode of the plasma jet in He were influenced by the gas flow rate. In filamentary plasmas, in contrast to the mostly diffusive plasmas, the activity of atmospheric pressure plasmas is strictly localized. The formation mechanisms of the diffusive and filamentary of NTAPPJs have been extensively studied (Li et al., 2017). When the NTAPP jet generated in the diffusive mode using He with a flow rate of 10 L/min is exposed to the agar in the petri dish containing *P. aeruginosa* planktonic bacteria, the jet transits to the spark discharge mode as seen in Fig. 2c. For the direct-contact treatment, the bacterial samples on the agar plates are placed right under the plasma jet at an adjustable distance from the nozzle. The bacterial samples are directly contacted with the plasma jet (plume). In this case, many streamers are formed in the area where the plasma jet contacts the agar, and these streamers move around the contact area without causing any visible damage. The agar temperature measured with the standard K-type thermocouple connected to a digital multimeter (Fluke 179) and IR thermometer (Benetech GM320) almost does not change and remains around 25°C during the treatment of 5 min. When the NTAPP jet generated in the filamentary mode using He with a flow rate of 5 L/min is exposed to the agar, the jet is formed in the spark discharge mode as seen in Fig. 2d. In this case, streamers are not formed, and the jet contacts a point on the agar producing a spot (like a small

point). This spot may create a physical or chemical erosion on the agar. After 5 minutes of treatment, the agar temperature increased up to 27°C.

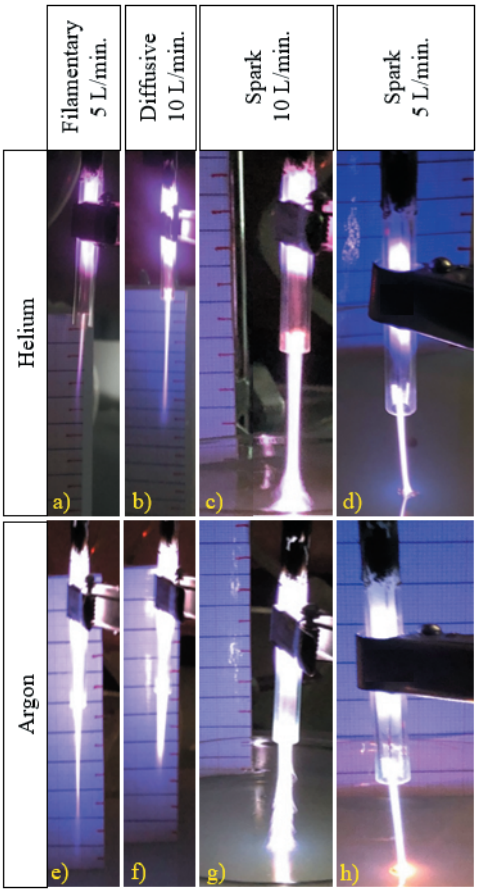

Figure 2. Plasma modes that occur at different gas flow rates and direct-contact treatment on the *P. aeruginosa* planktonic bacteria with the NTAPPJ system.

As can be seen in Fig. 2e and Fig. 2f, the NTAPP jet in Ar with a flow of 5 L/min, which was formed in the filamentary mode, transits to the diffusive mode by shortening when the Ar flow rate was increased to 10 L/min. When the NTAPP jet generated in diffusive mode using Ar with a flow rate of 10 L/min is exposed to the agar, the jet transits to the spark discharge mode as seen in Fig. 2g. When the NTAPP jet generated in the filamentary mode using Ar with a flow rate of 5 L/min is exposed to the agar, the jet is formed in the spark discharge mode as seen in Fig. 2h. No chemical or physical effect was observed on the agar treated by the spark discharge in the diffuse mode of the NTAPP jet in Ar, while a spot was formed when the agar is treated by the filamentary mode. When the agar plates were treated by both modes of the NTAPP jet in Argon, the temperature of the agar has changed between 25-27 °C.

Antibacterial Efficacy of Direct-Contact and Contact-free Treatment of the NTAPPJ on *P. aeruginosa*

The *P. aeruginosa* bacterial samples are treated by the NTAPPJ in two different ways, i.e., direct-contact and contact-free treatments. For the direct-contact treatment, the bacterial samples on the agar plates were placed right under the plasma jet at an adjustable distance from the nozzle. The bacterial samples were directly contacted with the plasma jet to generate a spark discharge. The first group of the experiment is done with Ar in the diffusive mode with a flow rate of 10 L/min and the filamentary mode with a flow rate of 5 L/min, respectively. For the control experiment, the bacterial samples are treated by the Ar at the same flow rate with the plasma off (power off).

Control plates (no plasma and Ar gas exposure, and Ar gas exposure without plasma ignition) exhibited consistent bacterial lawns, whereas the NTAPPJ-treated plates of the *P. aeruginosa* bacterial strains were characterized by the presence of clear zones (killing region) of growth inhibition (Fig. 3). The yellow arrows show the bacteria growth inhibited region after the plasma treatment. The bacteria-containing agar plates were placed under the NTAPPJ in Argon for the following time intervals: 60, 120,180, and 300 seconds. After incubation, photographs of the agar plates, showing bacterial growth inhibition zones, were taken using a digital camera. The Ar-NTAPP jet-exposed plates showed significant bacterial inhibition zones which indicate the extent of bactericidal activity of the plasma jet against *P. aeruginosa*. Although the maximum diameter of the plasma jet (plume) observed in the NTAPPJ in Ar is less than 2-3 mm in the filamentary mode and 4-6 mm in the diffusive mode, inhibition zones of several centimeters are obtained; which indicates that plasma-derived active species are not confined within the visible plasma plume, rather they are present in a larger volume around it. The observable inhibition zone diameter increased with increasing plasma exposure time as can be seen in Fig. 3. The inhibition zone diameter of the filamentary mode-NTAPPJ direct-contact treatment is smaller than that of the diffusive mode-NTAPPJ direct-contact treatment when Ar is used as a working gas. The damage on the agar plates by heating or etching was not observed in the diffusive mode-NTAPPJ direct-contact treatment (Fig. 3d), but spots were observed in the filamentary mode treatment (Fig. 3e). As mentioned earlier, the bacteria are affected by charged particles and reactive species simultaneously in direct-contact treatment.

When all the processes in obtaining the results in Fig. 3, when Ar is used as working gas, were repeated for He, the

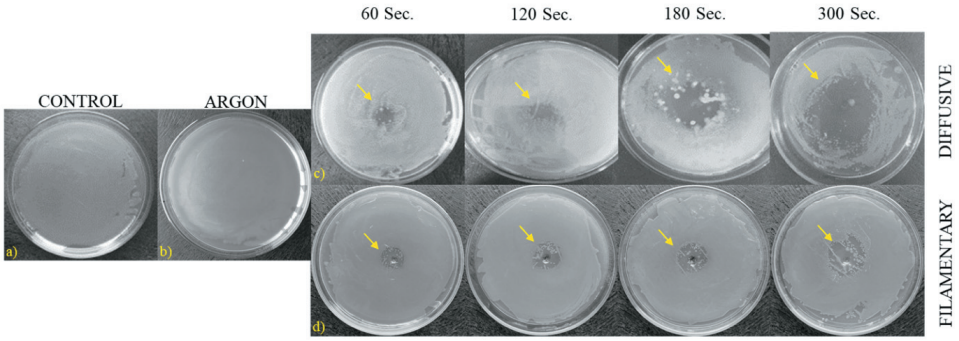

Figure 3. Results of antibacterial direct-contact treatment of *P. aeruginosa* on the agar using the different Ar-NTAPPJ working modes as well as different treatment times. **a.)** Control plate (no gas and plasma exposure), **b.)** Control plate (Argon gas exposure without plasma ignition), **c.)** and **d.)** the variation of observable inhibition zone diameter with the Ar diffusive and filamentary mode-plasma exposure times of 60, 120, 180, and 300 sec., respectively. ED was 20 mm.

results given in Fig. 4 were obtained. When He is used as a working gas, the inhibition zone diameter in the diffusive mode was larger than that of the filamentary mode of the NTAPPJ in direct-contact treatment.

Comparing the antibacterial efficacy of the NTAPP jets in Ar and He after direct-contact with the bacteria, the direct-contact treatment of the Ar-NTAPP jet on the bacteria showed a more effective antibacterial efficacy than that of the He-NTAPPJ.

For the contact-free treatment, the *P. aeruginosa* bacterial samples on the agar plates were placed right under the plasma jet at a distance where they will not contact with the jet, that is, no spark discharge will occur. When the Ar and He NTAPP jets were exposed to the bacteria without contact in the diffuse mode, they produced a zone diameter, while no significant antibacterial effect was observed in the filamentary mode. When the Ar-NTAPPJ in the diffusive mode was exposed to the bacteria without contact, a larger inhibition zone was observed than when the He-NTAPPJ in the diffusive mode was exposed to the bacteria without contact as can be seen in Fig. 5.

When the *P. aeruginosa* are treated by the NTAPP jet in direct-contact using Ar and He, they are exposed simultaneously to charged particles (electrons and ions), UV/visible light, reactive oxygen species (ROS) such as ozone (O_3), atomic oxygen (O), electronically excited oxygen (O_2 ($^1\Delta$)), superoxide (O_2^-), hydrogen peroxide (H_2O_2), hydroxyl radical (OH) and anion (OH^-), reactive nitrogen species (RNS) such as atomic nitrogen (N), electronically excited nitrogen (N_2(A)), nitric oxide (NO), and other excited molecular and atomic species of working gas, all of which may contribute to its antibacterial properties (Nicol et al., 2020; Brun et al., 2018), and thus maximum inactivation effect is obtained in this case. As the plasma jet is launched in the surround-

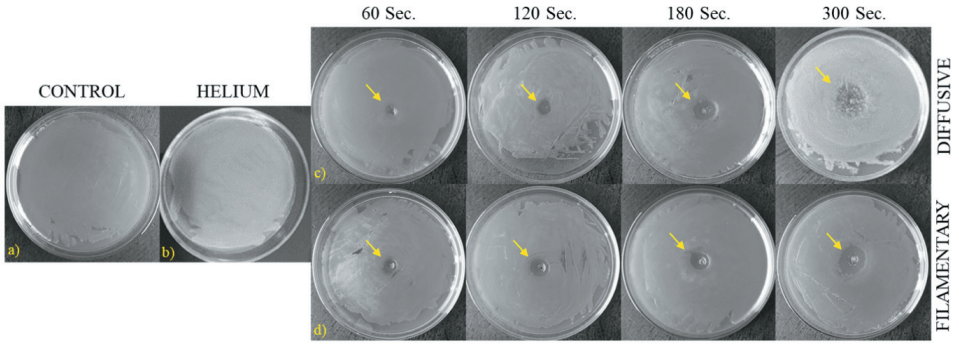

Figure 4. Results of antibacterial direct-contact treatment of *P. aeruginosa* on the agar using the different He-NTAPPJ working modes as well as different treatment times. **a.)** Control plate (no gas and plasma exposure), **b.)** Control plate (Helium gas exposure without plasma ignition), **c.)** and **d.)** the variation of observable inhibition zone diameter with the He diffusive and filamentary mode-plasma exposure times of 60, 120, 180, and 300 sec., respectively. ED was 20 mm.

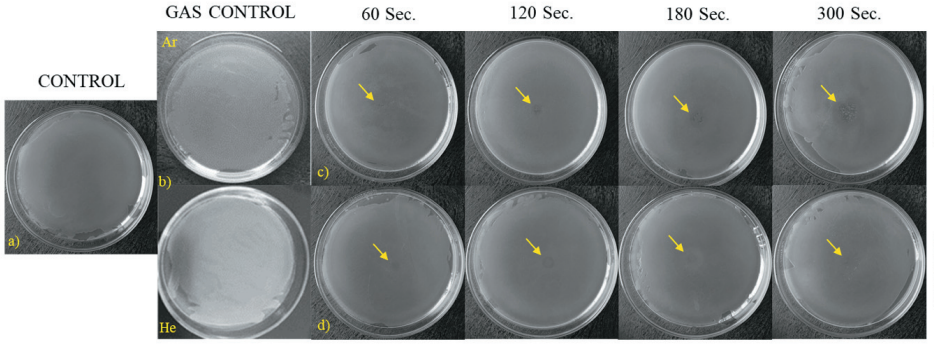

Figure 5. Results of antibacterial contact-free treatment of *P. aeruginosa* on the agar using the Ar and He NTAPPJs at the different treatment times. **a.)** Control plates (no gas and plasma exposure), **b.)** Control plates (Argon and Helium gas exposure without plasma ignition), **c.)** and **d.)** the variation of observable inhibition zone diameter with the Ar and He contact-free NTAPPJ in the diffusive mode exposure times of 60, 120, 180, and 300 sec., respectively. ED was 60 mm.

ing room air, oxygen and nitrogen-based reactive species are produced even if the plasma jet operating gas itself does not contain oxygen or nitrogen. Hydroxyl (OH) is mainly produced by water molecules when struck by high-energy photons and high-speed electrons or molecules. The obtained results of the contact-free NTAPP jet treatment in both Ar and He show that it is less effective, probably due to the absence of charged species in the plasma jet. Bombardment on the cell wall by charged particles, electrons, and ions (positive ions are generally N_2^+, while negative ions are O_2^-) can break chemical bonds, cause erosion through etching, formation of lesions and openings in the membranes, inducing further penetration of plasma toxic compounds inside a bacterial cell (Dobrynin et al., 2009; Bourke et al., 2017)

Fig. 6a and b show typical emission spectrums for the Ar and He NTAPP jet in the air, taken by an Ocean Optics mini-spectrometer USB 2000+XR1-ES as can be shown in Fig. 1.

We can compare the emission spectra between the He and Ar NTAPPJs given in Fig. 6a and b. The emissions of nitrogen second positive band (N_2), atomic oxygen band (O), and OH band were observed in both plasmas, while the emissions of nitric oxide (NO) and the first negative band of nitrogen molecule ions (N_2^+) were observed only in the He-NTAP plasma jet. This is due to the ionization potential of nitrogen molecules, which is 15.5 eV. The metastable levels of Ar are 11.5 and 11.7 eV; the energy provided from Ar metastable atoms is not adequate for the ionization of nitrogen molecules (Shao et al., 2012; Shao et al., 2015). In pure He and Ar, the intensity of O line (777 nm) in the Ar-NTAP plasma jet was slightly smaller than that in the He-NTAP plasma jet, whereas the intensity of OH line in the Ar-NTAP plasma jet was extremely higher than that in the He-NTAP plasma jet. The ionization energy of He is 24.6 eV, and the energies of two kinds of He metastable formed in gas discharge are 19.82 eV and 20.06 eV. Besides, as can

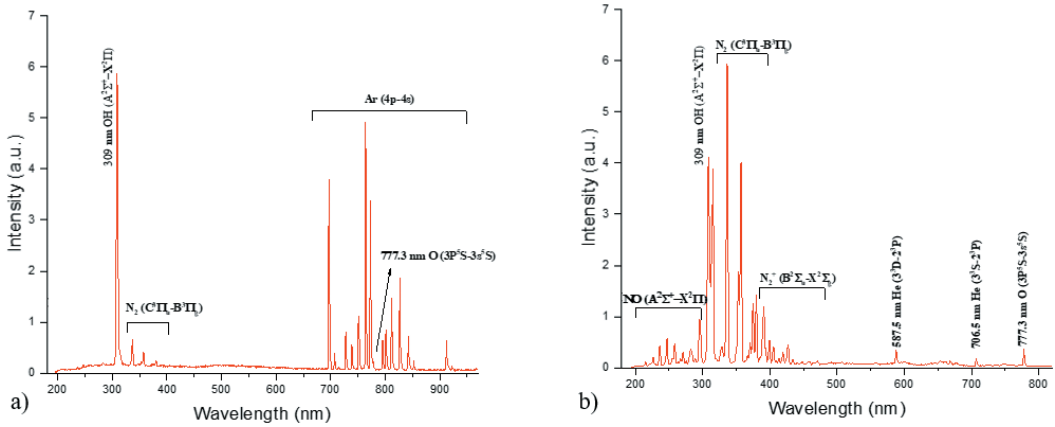

Figure 6. Emission Spectrums of the NTAPP jet (plume) in **a.)** Argon, and **b.)** Helium.

be known that all the upper and lower states related to the He lines have enough energy, so any of the states related to the observed He lines could excite any of the ground states N_2, OH, and N_2^+ to their upper states related to those observed lines through two or three body collisions (Shao et al., 2012; Shao et al., 2015) The Ar-NTAP plasma jet contained a higher concentration of excited OH radicals than that of the He-NTAP plasma jet, which was related to its high-density electrons and more suitable for inactivation.

The results show that the antibacterial efficacy of the Ar-NTAP plasma jet is much better than that of the He-NTAP plasma jet. Because of the lower ionization energy (15.8 eV) of Ar, there are more ions and electrons in the Ar-NTAP plasma jet than that in the He (ionization energy is 24.6 eV) NTAP plasma jet, which will lead to a bigger discharge current. This might be an explanation why the Ar direct-contact plasma jet treatment on the *P. aeruginosa* is more efficient than the He direct-contact NTAP plasma jet treatment.

From the results, it is expected that OH and charges are the most important species for inactivation in treatment between He and Ar NTAP plasma jets. The main agent which induces the difference of antibacterial efficacies between He and Ar NTAP plasma jets is the OH radical and charge activity. The generation of ozone (O_3) can also be checked by the unique smell of ozone in the He and Ar NTAP plasma jets. The Ar-NTAP plasma jet came out to have an intense fishy smell of ozone compared with the He-NTAP plasma jet. Because the lifetime of ozone is longer than other radicals (Jablonowski et al., 2018), ozone might play a crucial role in the inactivation process in the Ar-NTAP plasma jet.

Conclusions

The DBD-like NTAP plasma jet system used in this paper generates the filamentary mode jet at low gas flow rates and the diffuse mode jet at high gas flow rates. The NTAP plasma jets in Ar and He generated in both modes create a spark discharge when they are in contact with the agar containing the *P. aeruginosa* bacteria. While the spark discharges in contact with the agar in filamentary mode cause a visible erosion on the agar, the spark discharges in contact with the agar in diffusive mode do not cause any erosion.

The antibacterial efficacy of the Ar and He NTAPPJs for various treatment times (60, 120, 180, and 300 sec.) were investigated by treatment on the *P. aeruginosa* bacteria without contact and with contact in both filamentary mode and diffuse mode. We compare the effectiveness of direct-contact and contact-free antibacterial treatment by the NTAPPJ generated using the same discharge setup using He and Ar and demonstrate that the direct-contact treatment can achieve antibacterial efficacy much better without any physical or chemical erosion. The *P. aeruginosa* bacteria treatment by direct-contact with the Ar-NTAPPJ showed more antibacterial efficacy than direct-contact with the He-NTAPPJ.

Declaration of interests

The authors declare that they have no known competing financial interests or personal relationships that could have appeared to influence the work reported in this paper.

References

1. Akan, T. and Çabuk, A. (2014). *Indirect plasma inactivation by a low temperature atmospheric pressure plasma (LTAPP) system.* Journal of Electrostatics, 72(3), p. 218-221.
2. Bourke, P., Ziuzina, D., Han, L., Cullen, P. J. and Gilmore, B. F. (2017). *Microbiological interactions with cold plasma.* Journal of applied microbiology, 123(2), 308-324.
3. Bruggeman, P.J., Iza, F. and Brandenburg, R. (2017). *Foundations of atmospheric pressure non-equilibrium plasmas.* Plasma Sources Science and Technology, 26(12), p. 123002.
4. Brun, P., Bernabè, G., Marchiori, C., Scarpa, M., Zuin, M., Cavazzana, R., Zaniol, B. and Martines, E. (2018). *Antibacterial efficacy and mechanisms of action of low power atmospheric pressure cold plasma: membrane permeability, biofilm penetration and antimicrobial sensitization.* Journal of applied microbiology, 125(2), 398-408.
5. Dobrynin, D., Fridman, G., Friedman, G. and Fridman, A., (2009). *Physical and biological mechanisms of direct plasma interaction with living tissue.* New Journal of Physics, 11(11), p. 115020.
6. Dobrynin, D., Friedman G., Fridman, A. and Starikovskiy, A., (2011). *Inactivation of bacteria using dc corona discharge: role of ions and humidity.* New journal of physics, 13(10), p. 103033.
7. Domonkos, M., Ticha, P., Trejbal, J. and Demo, P., (2021). *Applications of cold atmospheric pressure plasma technology in medicine, agriculture, and food industry.* Applied Sciences, 11(11), p. 4809.
8. Gallagher, M.J., Vaze, N., Gangoli, S., Vasilets, V.N., et al., (2007). *Rapid Inactivation of Airborne Bacteria Using Atmospheric Pressure Dielectric Barrier Grating Discharge.* IEEE Transactions on Plasma Science, 35(5), p. 1501-1510.
9. Grill, A., (1994). *Cold plasma in materials fabrication*. Vol. 151. IEEE Press, New York.
10. Ilik, E. and Akan, T. (2016). *Optical properties of the atmospheric pressure helium plasma jet generated by alternative current (ac) power supply.* Physics of Plasmas, 23(5), p. 053501.

11. Ilik, E., Durmus, Ç. and Akan, T. (2020). *Investigation on Optical Properties of Atmospheric Pressure Plasma Jets of N_2 Gas*. Adıyaman University Journal of Science, 10 (1), 326-338.
12. Jablonowski, H., Sousa, J.S., Weltmann, K.D., Wende, K. and Reuter, S. (2018). *Quantification of the ozone and singlet delta oxygen produced in gas and liquid phases by a non-thermal atmospheric plasma with relevance for medical treatment*. Scientific Reports, 8(1), 12195.
13. Khlyustova, A., Labay, C., Machala, Z., Ginebra, M.P. and Canal, C. (2019). *Important parameters in plasma jets for the production of RONS in liquids for plasma medicine: A brief review*. Frontiers of Chemical Science and Engineering, 13(2), 238-252.
14. Laroussi, M. and Akan, T. (2007). *Arc-free atmospheric pressure cold plasma jets: A review.* Plasma Processes and Polymers, 4(9), p. 777-788.
15. Laroussi, M., (2015). *Low-Temperature Plasma Jet for Biomedical Applications: A Review.* IEEE Transactions on Plasma Science, 43(3), p. 703-712.
16. Li, J., Xu, Y., Zhang, T., Tang, J., et al., (2017). *A diffuse plasma jet generated from the preexisting discharge filament at atmospheric pressure.* Journal of Applied Physics, 122(1), p. 013301.
17. Lin, Z.H., Tschang, C.Y.T., Liao, K.C., Su, C.F., Wu, J.S. and Ho, M.T. (2016). *Ar/O2 Argon-Based Round Atmospheric-Pressure Plasma Jet on Sterilizing Bacteria and Endospores.* Ieee Transactions on Plasma Science, 44(12), 3140-3147.
18. Lu, X., Laroussi M. and Puech, V., (2012). *On atmospheric-pressure non-equilibrium plasma jets and plasma bullets.* Plasma Sources Science and Technology, 21(3), p. 034005.
19. Lu, P., Cullen, P. J. and Ostrikov, K., (2016). *Atmospheric pressure nonthermal plasma sources*. In Cold plasma in food and agriculture (pp. 83-116). Academic Press.
20. Mashayekh, S., Rajaee, H., Akhlaghi, M., Shokri, B. and Hassan, Z.M. (2015). *Atmospheric-pressure plasma jet characterization and applications on melanoma cancer treatment (B/16-F10).* Physics of Plasmas, 22(9), 093508.
21. Malyavko, A., Yan, D., Wang, Q., Klein, A.L., Patel, K.C., Sherman, J.H. and Keidar, M. (2020). *Cold atmospheric plasma cancer treatment, direct versus indirect approaches*. Materials Advances, 1(6), 1494-1505.
22. Morris, A., Mccombs, G., Akan, T., Hynes, W.L., et al., (2009). *Cold plasma technology: bactericidal effects on Geobacillus stearothermophilus and Bacillus cereus microorganisms.* American Dental Hygienists' Association, 83(2), p. 55-61.
23. Nicol, M.J., Brubaker, T.R., Honish, B.J., Simmons, A.N., Kazemi, A., Geissel, M.A., Whalen, C.T., Siedlecki, C.A., Bilén, S.G., Knecht, S.D. and Kirimanjeswara, G.S. (2020). *Antibacterial effects of low-temperature plasma generated by atmospheric-pressure plasma jet are mediated by reactive oxygen species*. Scientific Reports, 10(1).
24. Pankaj, S., Wan, Z. and Keener, K., (2018). *Effects of Cold Plasma on Food Quality: A Review.* Foods, 7(1), p. 4.
25. Penkov, O.V., Khadem, M., Lim, W.S., Kim, D.E. (2015). *A review of recent applications of atmospheric pressure plasma jets for materials processing.* Journal of Coatings Technology and Research, 12(2), p. 225-235.
26. Peran, J. and Ercegoviæ Ražiæ, S. (2020). *Application of atmospheric pressure plasma technology for textile surface modification.* Textile Research Journal, 90(9-10), 1174-1197.
27. Raizer, Y.P. and Allen, J.E. (1991). *Gas discharge physics*. Vol. 1. Springer.
28. Saadati, F., Mahdikia, H., Abbaszadeh, H.A., Abdollahifar, M.A., Khoramgah, M.S. and Shokri, B. (2018). *Comparison of Direct and Indirect cold atmospheric-pressure plasma methods in the B16F10 melanoma cancer cells treatment*. Scientific Reports, 8(1).
29. Schmidt, A., Bekeschus, S., Wende, K. and Vollmar, B. (2017). *A cold plasma jet accelerates wound healing in a murine model of full-thickness skin wounds.* Experimental Dermatology, 26(2), p. 156-162.
30. Shao, X.J., Jiang, N., Zhang, G.J. and Cao, Z., (2012). *Comparative study on the atmospheric pressure plasma jets of helium and argon.* Applied Physics Letters, 101(25), p. 253509.
31. Shao, T., Zhang, C., Wang, R, Zhou, Y., et al., (2015). *Comparison of Atmospheric-Pressure He and Ar Plasma Jets Driven by Microsecond Pulses.* IEEE Transactions on Plasma Science, 43(3), p. 726-732.
32. Velichko, I., Gordeev, I., Shelemin, A., Nikitin, D., et al. (2019). *Plasma Jet and Dielectric Barrier Discharge Treatment of Wheat Seeds.* Plasma Chemistry and Plasma Processing, 39(4), p. 913-928.
33. Wu, S., Cao, Y. and Lu, X. (2016). *The State of the Art of Applications of Atmospheric-Pressure Nonequilibrium Plasma Jets in Dentistry.* IEEE Transactions on Plasma Science, 44(2), p. 134-151.
34. Yaopromsiri, C., Yu, L.D., Sarapirom, S., Thopan, Boonyawan, D. (2015). *Effect of cold atmospheric pressure He-plasma jet on DNA change and mutation.* Nuclear Instruments and Methods in Physics Research Section B: Beam Interactions with Materials and Atoms, 365, p. 399-403.

ISSN print: 1224-5984
ISSN online: 2248-3942

Rom Biotechnol Lett. 2022; 27(3): 3507-3516
doi: 10.25083/rbl/27.3/3507.3516

Received for publication: July, 20, 2022
Accepted: August 11, 2022

Original paper

PETase from *Ideonella sakaiensis*: towards facile bacterial expression system

KRISZTINA BOROS[1], ILKA HORVÁTH[1], CĂTĂLINA ROTARU[1], RALUCA BIANCA TOMOIAGĂ[1], DR. MONICA IOANA TOŞA[1], DR. LÁSZLÓ-CSABA BENCZE[1]*

[1]Enzymology and Applied Biocatalysis Research Center, Faculty of Chemistry and Chemical Engineering, Babeș-Bolyai University, Arany János Street 11, RO-400028 Cluj-Napoca, Romania

Abstract

One of the most promising PET-hydrolysing enzyme, *Is*PETase, originates from 'plastic-consuming' bacteria *Ideonella sakaiensis* and operates at moderate temperatures (30-40 °C) in aqueous environment, showing far higher hydrolysing efficiency than several cutinases. Accordingly, the development of proper recombinant expression system providing facile access to the isolated/purified *Is*PETase is also of high interest. In our aim to produce active recombinant *Is*PETase, the unsuccessful expression registered by employing several reported expression systems, directed us towards the optimization/development of a facile/accessible recombinant expression system suitable for *Is*PETase production. Testing several plasmid constructs, providing different N- or C-terminal affinity tags for the expression of full-length or truncated (residues 28-290) *Is*PETase and various *E. coli* expression hosts, revealed several non-reported issues hindering the recombinant expression of *Is*PETase. After optimization of the construct and expression host, the use of N-terminal His-tag and Rosetta-gami B expression host provided recombinant *Is*PETase in high purity and titer-yield. The thermal denaturation profile and PET-hydrolysing activity of the obtained *Is*PETase agree with the reported data, supporting proper folding of the purified protein. The results support that the *in vivo* folding process of *Is*PETase might be differently affected among the different *E. coli* host strains, moreover, underline the importance of the proper selection of the cloning strategy for the successful expression of the *Is*PETase.

Keywords Polyethylene terephthalate (PET), enzymatic PET degradation, *Is*PETase, protein expression

To cite this article: BOROS K, HORVÁTH I, ROTARU R, TOMOIAGĂ RB, TOŞA MI, BENCZE L. PETase from *Ideonella sakaiensis*: towards facile bacterial expression system. *Rom Biotechnol Lett.* 2022; 27(3): 3507-3516 DOI: 10.25083/rbl/27.3/3507.3516

*Corresponding author: Dr. László Csaba Bencze; email: laszlo.bencze@ubbcluj.ro

Introduction

Since several decades, polyethylene terephthalate (PET), the polymerization product of ethylene glycol (EG) and terephthalate (TPA), is one of the most produced and most widely used plastics in the world and thus accumulates in the environment at a staggering rate (W. COURTENE-JONES & al. [1]; L. NIZZETTO & al. [2]; C. E. ENYOH & al. [3]; C. L. WALLER & al. [4]; R. H. WARING & al. [5]; E. S. GRUBER & al. [6]; K. RAGAERTA & al. [7]). Plastic particles can be detected in both marine and terrestrial ecosystems, from surface waters to deep-sea sediments, on the shorelines of every continent, in soils and freshwater, even in the polar regions, but are also present in the air (W. COURTENE-JONES & al. [1]; L. NIZZETTO& al. [2]; C. E. ENYOH & al. [3]; C. L. WALLER & al. [4]). Moreover, plastic particles ingested by animals, enter the food chain and accumulate in the organisms (W. COURTENE-JONES & al. [1]; R. H. WARING & al. [5]), with more recent studies revealing their toxic effects (E. S. GRUBER & al. [6]), however their long-term biological effect mainly remains unexplored.

Recycling PET is one of the solutions for reducing plastic pollution, which is already taking place at various rates worldwide. However, the classic, thermomechanical PET recycling, leads to a loss of the polymer`s mechanical properties, while the chemical degradation/recycling requires harsh conditions, consumes large amount of energy and generates toxic secondary pollutants (K. RAGAERTA & al. [7]). In 2005, the possibility of enzymatic hydrolysis of PET films was firstly reported (R. J. MÜLLER & al. [8]), followed by further significant efforts to provide an industrially feasible and efficient, eco-friendly, biocatalytic PET degradation method (H. F. SON & al. (2020) [9]; H. P. AUSTIN & al. [10]; Y. MA & al. [11]; H. Y. SAGONG & al. [12]; R. WEI & al. [13]; F. KAWAI & al. (2019) [14]). One of the main obstacles remained the inaccessibility of the amorphous domains of the PET polymer for the enzymatic attack, due to the high glass transition temperature (around 75 °C) of PET, thus the biocatalytic degradation efficiency being affected by the different crystallinity degree among the different type of PET pollutants (R. WEI & al. [13]). In this context enzyme variants with improved stability under severe conditions, such as high temperature and presence of swelling agents, are highly desirable (F. KAWAI & al. (2019) [14]), reflecting current research directions in enzymatic PET degradation (F. KAWAI & al. (2020) [15]). Among the enzymes possessing PET-degrading activity, hydrolases such as cutinases (T. BRUECKNER & al. [16a]; E. H. ACERO & al. [16b]; F. KAWAI & al. (2017) [16c]), lipases (M. A. M. E. VERTOMMEN & al. [17]) and PETases (I. TANIGUCHI & al. [18]) have been reported. One of the most promising PET-hydrolysing enzyme, *Is*PETase, derives from 'plastic-consuming' bacteria *Ideonella sakaiensis* (S. YOSHIDA & al. [19]) and operates in aqueous environment with far higher PET-hydrolysing efficiency at moderate temperatures (30-40 °C) than cutinases from *Humicola insolens* (*Hi*C) and from *Thermobifida fusca* (*Tf*Cut1 and *Tf*Cut2), hydrolases from *Thermobifida fusca* (*Tjjf*H) or lipase from *Candida antarctica* (S. JOO & al. [20]; H. F. SON & al. (2019) [21]). Since, in order to carry out the PET-degradation, *Is*PETase needs to be secreted extracellularly or to be used as isolated enzyme biocatalyst, the development of proper recombinant expression system providing facile access to the isolated/purified *Is*PETase is also of high interest.

In our aim to produce active recombinant *Is*PETase and the unsuccessful set-up of several reported expression systems (H. F. SON & al. (2020) [9]; H. P. AUSTIN & al. [10]; S. JOO & al. [20]; H. F. SON & al. (2019) [21]; G. J. PALM & al. [22]; C. LIU & al. [23]; V. TOURNIER & al. [24]; E. Z. L. ZHONG-JOHNSON & al. [25]) directed us towards the optimization and development of facile/accessible recombinant expression system suitable for the production of the PET-degrading enzyme.

Materials and methods

Materials and instrumentation

Tris(hydroxymethyl)aminomethane (TRIS) was purchased from Sigma-Aldrich (USA). The Bradford reagent for protein concentration determinations was purchased from VWR (USA). Technical grade solvents were dried and/or freshly distilled prior to use, while HPLC-grade solvents were purchased from Promochem LGC Standards (Germany). The PET film (product nr. GF25214475-1-EA), bis-(2-hydroxyethyl) terephthalate (BHET) was purchased from Sigma-Aldrich. Terephthalic acid (TPA) was purchased from Alfa Aesar, while mono-(2-hydroxyethyl) terephthalic acid (MHET) was synthesized by previously reported procedure (G. J. PALM & al. [22]). For PCR amplifications Phusion High Fidelity DNA Polymerase (2 U/μL) from Thermo Fisher Scientific was used and a 96-well Eppendorf Mastercycler ProS equipment. Plasmid extraction was performed using GenElute Plasmid Miniprep Kit (Sigma-Aldrich), while the DNA isolation from agarose gel was accomplished using QIAquick Gel Extraction Kit (Qiagen). The T4 DNA Ligase was purchased from Jena Bioscience. Desalting steps from the protein purification procedure were performed using an ÄKTA purifier FPLC (GE Healthcare/Amersham Biosciences) and HiTrap De-

salting columns (Cytiva). UV-Vis measurements were performed on an Agilent 8453 UV-vis spectrophotometer and/or BioTek Epoch 2 microplate reader, using 96-well UV-Microtiter microplates. Enzymatic PET-hydrolysis reactions were carried out in an Eppendorf ThermoMixer C, while HPLC analysis of the reaction samples was conducted on Agilent 1200 instrument. The melting curves of the recombinant proteins were measured using a Bio-Rad CFX 96 Real-Time System and SYPRO Orange Protein Gel Stain (Invitrogen).

Molecular cloning

Cloning the synthetic full-length *ispetase* gene into pET-15b and pET-21a(+) vectors

The codon-optimized synthetic gene encoding the *Is*-PETase, designed with NcoI, NdeI and XhoI restriction sites (**Table S1**), was synthesized by Invitrogen and provided in pMA cloning vector. For subcloning into pET-21a(+) expression vector with a C-terminal His6-tag, the synthetic gene was PCR-amplified without the Stop codon, while for subcloning into pET-15b restriction digestion was employed (the targeted and obtained constructs are presented in **Tables S2**). Accordingly, the amplified gene or the pMA vector harbouring the synthetic gene and empty pET-21a(+) or pET-15b expression vector, respectively, were digested with NdeI and XhoI restriction enzymes for 2 h at 37 °C. The obtained DNA fragments were separated via agarose gel electrophoresis, the DNA bands corresponding to the insert and the recipient plasmid backbone being extracted from the gel and purified. The ligation of the purified DNA fragments was performed for 1 h at 22 °C using T4 DNA ligase, followed by transformation into *E. coli* TOP10 competent cells. The obtained colonies were screened for their insert-content using colony PCR. The plasmid DNA of positive colony/colonies was extracted, and further restriction digestion confirmed the presence of insert gene (**Fig. S1**). The final construct was transformed into different expression hosts (e.g. *E. coli* BL21-Gold (DE3), Rosetta (DE3) pLysS, ArcticExpress (DE3), Rosetta-gami B (DE3)) via heat shock/electroporation for further expression.

Molecular cloning of truncated *Is*PETase (28-290) gene into pET-21a(+) and pET-15b vectors

The first 81 nucleotides corresponding to the signal peptide from the *Is*PETase sequence (residues 1-27) were removed by PCR-amplification using as template DNA the full-length *Is*PETase encoding synthetic gene and the correspondingly designed primers from **Table S3**. The PCR protocol consisted of initial denaturation at 98 °C for 30 s, followed by 30 amplification cycles, each of them involving denaturation at 98 °C for 10 s, annealing at 57 °C for 30 s and extension at 72 °C for 30 s; followed by a final extension step at 72 °C for 10 minutes. The cloning of the truncated *ispetase* gene into pET-21a(+) expression vector was performed using the procedure described for the full-length gene.

For the subcloning of the truncated gene into pET-15b vector the optimized synthetic gene (see *section 2.2.3*) was similarly amplified via PCR using the primers (**Table S6)** allowing Stop codon reinsertion at the 3'-end of the gene. The employed PCR protocol included initial denaturation at 98 °C for 30 s, followed by 30 amplification cycles, each of them consisting of denaturation at 98 °C for 10 s, annealing at 57 °C for 30 s and extension at 72 °C for 30 s; followed by a final extension step at 72 °C for 10 minutes. The cloning of the optimized *ispetase(28-290)* variant into pET-21a(+) expression vector was performed using the procedure described for full-length gene.

Site-directed mutagenesis for sequence optimization

To remove additional ORFs from the codon-optimized synthetic gene encoding *Is*PETase, site-directed mutagenesis was performed using megaprimers (**Table S4**). The PCR protocol consisted of initial denaturation at 98 °C for 30 s, followed by 5 megaprimer amplification cycles (denaturation at 98 °C for 10 s, annealing at 68 °C for 30 s, extension at 72 °C for 2 minutes), followed by 25 cycles for plasmid amplification (denaturation at 98 °C for 30 s and extension at 72 °C for 4 minutes) and a final extension step at 72 °C for 10 minutes. The PCR reaction products were digested with DpnI restriction enzyme at 37 °C for 1 h to remove the DNA template. 5 μL from the digested product was transformed into *E. coli* XL1-Blue chemically competent cells via heat shock. The plasmids isolated from the bacterial colonies were sequenced (Biomi Ltd., Gödöllő) in order to confirm the presence of the mutations.

Transformations into different *E. coli* hosts

The plasmids (pET-21a(+) or pET-15b) harbouring the gene encoding the full-length or truncated *Is*PETase(28-290) were transformed into *E. coli* Rosetta (DE3) pLysS chemically competent cells via heat shock and into *E. coli* BL21-Gold (DE3) electrocompetent cells by electroporation. The plasmids (pET-21a(+) or pET-15b) harbouring the gene encoding the truncated *Is*PETase(28-290) were transformed into *E. coli* ArcticExpress (DE3) host cells via heat shock following the recommendation from the producer. The plasmids (pET-21a(+) or pET-15b) harbouring the improved variant of the gene encoding for truncated *Is*PETase(28-290) were transformed into *E. coli* Rosetta-gami B (DE3) cells via heat shock, following the producer's guidelines.

Protein expression and isolation

Expression and isolation using *E. coli* Rosetta (DE3) pLysS host cells

The recombinant *E. coli* strains harbouring the different *Is*PETase encoding plasmid constructs were grown overnight at 37 °C, in 5 mL Luria-Bertani (LB) medium supplemented with carbenicillin and chloramphenicol. Then, 4 x 0.5 L LB medium was inoculated with 2% (v/v) of the prepared overnight culture and incubated at 37 °C, 220 rpm until OD_{600} = 0.6–0.7 was reached, at which point induction with 0.5 mM (or 1, 1.5 mM) of IPTG was performed, followed by overnight incubation at 20 °C (or, 18, 16 °C), at 180 rpm (or 160 rpm). The cells were harvested by centrifugation at 3000 x *g* for 25 min at 4 °C, followed by resuspension of the cell pellet in lysis buffer (20 mM Tris.HCl, 100 mM NaCl, pH 7.0) and cell disruption by sonication. The cell debris was discarded by centrifugation at 10000 x *g* for 25 min at 4 °C and the *Is*PETase was purified from the cytosolic fraction by gravitational Ni-NTA affinity chromatography. After washing with low salt buffer (50 mM HEPES, 30 mM KCl, pH 7.5) and high salt buffer (50 mM HEPES, 300 mM KCl, pH 7.5), the non-specifically bound proteins were removed with 25 mM imidazole containing buffer (20 mM Tris.HCl, 100 mM NaCl, pH 7.0), followed by the elution of His-tagged proteins with 300 mM imidazole (20 mM Tris.HCl, 100 mM NaCl, pH 7.0). The degree of protein expression and the purity of the obtained fraction was investigated by sodium dodecyl sulphate-polyacrylamide gel electrophoresis (SDS-PAGE) (**Fig. S2, Fig. S3**) and/or Western blot using Mouse anti-His antibody and Rabbit anti-mouse secondary antibody (Invitrogen).

Expression and isolation using *E. coli* BL21 Gold (DE3) host cells

The cell culture preparations for the recombinant *E. coli* BL21-Gold (DE3) strains harbouring the different *Is*PETase encoding plasmid constructs were performed under similar conditions as described in *section 2.4.1*, while the protein isolation protocol via Ni-NTA chromatography followed the previously reported procedures (H. F. SON & al. (2020) [9]; H. F. SON & al. (2019) [21). The eluted protein fraction was subjected to desalting via FPLC, using HiTrap Desalting columns (with Sephadex G-25 resin) and Tris-buffer (20 mM Tris.HCl, 300 mM NaCl, pH 8.0) as mobile phase. The degree of protein expression and the purity of the obtained fraction was investigated by SDS-PAGE (**Fig. S11**), while the protein concentration was determined spectrophotometrically via Bradford method.

Expression and isolation using *E. coli* ArcticExpress (DE3) as host

In case of pET-21a(+) construct containing the improved gene encoding the truncated *Is*PETase, the effect of different cell growth conditions on the protein expression level has been determined in a multi-factorial experiment (**Table S5**). Accordingly, in each case 0.5 L LB medium was inoculated with 2% (v/v) overnight culture and the cells were cultivated at 37 °C, 200 rpm until OD_{600} of 0.6–0.7 followed by induction with different IPTG concentrations (**Table S5**) and overnight incubation at 16 °C or 20 °C and 200 rpm. The cells were harvested by centrifugation at 13000 x *g* for 10 min at 4 °C and suspended in Tris buffer (20 mM Tris.HCl, 100 mM NaCl, pH 7.0), followed by denaturation with SDS-PAGE sample buffer. In case of investigating the autoinduction system ZYM auto inducible medium (F. W. STUDIER [26]) was employed and cell growth was performed by overnight incubation at 16 °C or 20 °C, at 200 rpm. The degree of protein expression, within the samples taken from the different phases of cell growth, was investigated by SDS-PAGE and Western blot techniques.

Expression and isolation using *E. coli* Rosetta-gami B (DE3) host cells

The expression and isolation of the recombinant protein was accomplished as described in the previously reported procedures (H. F. SON & al. (2020) [9]; H. F. SON & al. (2019) [21]). The desalting step was carried out as described above.

In case of the truncated *Is*PETase(28-290) encoding the improved gene/pET-21a(+) construct a similar multi-factorial experiment was carried out as noted above, excepting that the incubation of the cell culture was performed at 20 °C and 25 °C respectively. The degree of protein expression and the purity of the obtained fraction was investigated by SDS-PAGE (**Fig. S10**) and Western blot technique, while the protein concentration was determined using the Bradford method.

PET-hydrolysis reaction

PET-hydrolysis reactions were performed as previously reported (H. F. SON & al. (2020) [9]; S. JOO & al. [20]; H. F. SON & al. (2019) [21]) with slight modifications, using 10 mg of commercial PET film (Sigma-Aldrich) as substrate. The film was soaked in 1 mL of pH 9.0 glycine/NaOH buffer containing 500 nM of isolated *Is*PETase. The reaction mixture was incubated at 45 °C (and/or 30 °C) for 20 h. Samples of 100 µL were removed from the reaction mixture, and in case of UV-activity assay, were analysed directly, while in case of HPLC activity assessments, the reaction samples were quenched by adding an equal volume of acetonitrile,

vortexed and centrifuged (17000 x *g*, 3 minutes), followed by acidification of the supernatant and filtering through a 0.2 μM nylon membrane.

Activity assessment by HPLC

The employed procedure was similar to previously reported methods (H. F. SON & al. (2020) [9]; S. JOO & al. [20]; H. F. SON & al. (2019) [21]; C. LIU & al. [23]), using an Agilent 1200 HPLC system, equipped with DAAD detector. The samples, retrieved from the biocatalytic PET-hydrolysis reactions, were injected onto a Phenomenex Luna C8(2) column (150x4.6 mm; 5 μm), eluted with a flow rate of 1.0 mL/min at 20 °C using a linear gradient elution of the mobile phase consisting of (A) 0.1% formic acid solution and (B) acetonitrile, with varied composition of 15% (B) to 27.5% (B) over 10 minutes elution time, monitoring the product elution at 240 nm. All experiments were performed in triplicate. TPA, MHET, and BHET (the total TPA) content of the reaction samples, and implicitly the enzyme activity, was determined based on calibration curves using the authentic standard of TPA and BHET (Sigma-Aldrich) and synthesized MHET.

Enzyme activity assessment via UV-Vis spectroscopy

The PET-hydrolysis reaction was analysed using the previously described bulk absorbance method (E. Z. L. ZHONG-JOHNSON & al. [25]). UV-absorbance spectra (**Fig. S12**) were determined for all three PET-hydrolysis products (TPA, MHET and BHET) using their 0.1 mM solutions in glycine/NaOH pH 9.0 buffer. Based on this, 235 nm was selected as wavelength for UV-activity measurements (**Fig. 2B**), since at this wavelength the absorbance of the three compounds show the closest magnitude. Further, the extinction coefficients at 235 nm within the glycine/NaOH pH 9.0 buffer were determined for each hydrolysis product separately, the results resembling the reported values (E. Z. L. ZHONG-JOHNSON & al. [25]). Using the average extinction coefficient, the total product (TPA content) of the samples from the PET-hydrolysis reaction could be determined through A_{235} measurements.

Melting temperature (T_M) assessments

The thermostability measurements were performed using differential scanning fluorimetry (DSF). The protein solutions at a concentration of 5-10 μM were mixed with SYPRO Orange dye and glycine/NaOH (pH 9.0) buffer to a final volume of 50 μL. The 5000x stock of the SYPRO Orange dye solution was diluted to 200x with glycine/NaOH (pH 9.0) buffer, then 5 μL of the diluted colorant was added to each sample. The obtained protein samples were loaded into a white-clear-Hard Shell 96-well PCR plate (Bio-Rad), followed by sealing the plate with optically clear Microseal B sealing tape (Bio-Rad). The melting curve of the samples were then measured using the FAM and ROX channels of a Bio-Rad CFX96 system, with 450-490 and 560-590 excitation and 510-530 and 610-650 emission filters, respectively. The samples were heated on a temperature range from 20 °C to 95 °C, while the melting temperature was determined from the peaks of the first derivatives of the melting curve.

Results and discussion

For the production of recombinant *Is*PETase various plasmid constructs, including the full-length *ispetase* gene encoding 290 amino acids with an additional polyhistidine-tag and different types of *E. coli* as expression host cells have been reported (**Table 1**) (H. P. AUSTIN & al. [10]; E. ERICKSON & al. [31]). On the other hand, in several works (H. F. SON & al. (2020) [9]; S. JOO & al. [20]; H. F. SON & al. (2019) [21]; G. J. PALM & al. [22]; C. LIU & al. [23]; V. TOURNIER & al. [24]; E. Z. L. ZHONG-JOHNSON & al. [25]) the expression of *Is*PETase enzyme was performed from the truncated *ispetase* gene (amino acid residues 28-290), lacking the signal sequence (amino acid residues 1-27) (**Table 1**).

Accordingly, we targeted the expression and purification of both the full-length or truncated *ispetase* genes. The nucleotide sequence of *Is*PETase (Genbank: GAP38373.1) was codon optimized and the synthetic gene (**Table S1**) was used for cloning as full-length or truncated version into pET-15b vector (**Fig. S1**), providing an *N*-terminal His-tag. Expression in different *E. coli* host strains, Rosetta (DE3) pLysS, BL21-Gold (DE3), proved to be unsuccessful, no detectable (SDS-PAGE, Western-blot) *Is*PETase levels being registered. The expression of recombinant *Is*PETase with *N*-terminal His-tag (**Fig. S1**) and protein purification by affinity chromatography revealed low protein yields (~1-2 mg from 1 L culture) and no protein band at the expected size of *Is*PETase (~30.1 kDa for full-length version and ~27.7 kDa for truncated *Is*PETase) (**Fig. S2**). Optimization of the expression parameters, such as testing the effect of different incubation temperatures (20 °C, 18 °C and 16 °C) (**Fig. S3**) and the effect of IPTG concentration (0.1, 0.5 and 1 mM) was also performed, however no expression of *Is*PETase had been observed. The Western blot analysis revealed the presence of His-tagged proteins with molecular weights <25 kDa within the induced cells, suggesting possible proteolysis of the targeted protein, while no protein bands were detected within the fractions resulted from protein purification (**Fig. S4**).

Table 1. Reported recombinant expression systems for the production of *Is*PETase.

Entry	*Is*PETase encoding gene	Expression vector	Affinity tag	Expression host	Enzyme activity	Specific activity (mg_{TPAeq}/h/$mg_{IsPETase}$)	Reference
1	truncated	pET-15b	N-terminal His_6-tag	Rosetta gami-B	8.6 µM TPA_{eq} in 24 h	~0.095	H. F. SON & al. [9, 21]
2	full-length	pET-21b(+)	C-terminal (modified) 5xHis-tag	C41(DE3)	[a]	-	H. P. AUSTIN & al. [10]
3	truncated	pET-30a	not mentioned	BL21 (DE3)	[a]	-	X. MENG & al. [27]
4	truncated	pET-15b	N-terminal His_6-tag	Rosetta gami-B	3 mg/L TPA_{eq} in 18 h	~0.027	S. JOO & al. [20]
5	truncated	pET-21b	C-terminal His_6-tag	ArcticExpress (DE3)	[b]	-	C. LIU & al. [23]
6	truncated (*Trx-*Is*PETase)	pET-28b(+) (pET-32b(+))	C-terminal His_6-tag	Rosetta-gami 2	0.7 (0.9) mg_{TPAeq}/h/$mg_{IsPETase}$	0.7 (0.9)	P. WAGNER-EGEA & al. [28]
7	truncated	pET-21b(+)	C-terminal His_6-tag	*Shuffle* T7	[a]	-	G. J. PALM & al. [22]
8	truncated	pET-21a(+)	C-terminal His_6-tag	T7 Express	[b]	-	E. Z. L. ZHONG-JOHNSON & al. [25]
9	$SP_{LamB.}$ *Is*PETase**	pET-22b(+)	C-terminal His_6-tag	-	~2.5 mg/L/24 h 200 nM	~0.017	H. SEO & al. [29]
11	full length	pET32a (pPICZαA)	not mentioned	BL21 trxB (DE3) (*P. pastoris* X33)	[c]	-	C. CHEN & al. [30]
12	full-length	pET-21b(+)	C-terminal His_6-tag	C41(DE3)	1.2 mM aromatic product in 24 h	~0.28	E. ERICKSON & al. [31]
13	truncated	pET-21b(+)	C-terminal His_6-tag	BL21 (DE3)	10^{-2} mg_{TPAeq}/h/$mg_{IsPETase}$	~0.01	V. TOURNIER & al. [24]

[a] The activity of the *Is*PETase not mentioned in conversional units, [b] only kinetic measurements performed towards napthyl ester polymers, [c] reaction volume (for activity deduction) not stated.

* *ispetase* gene with a thioredoxin fusion domain (Trx) at the N-termini.

** leader sequence replaced with *sec*-dependent maltoporin signal peptide in order to produce extracellularly the *Is*PETase.

Further, the truncated version of the *Is*PETase encoding gene was subcloned into pET-21a(+) using restriction sites NdeI and XhoI (**Fig. S5 and Table S3**), providing a C-terminal His-tag to the recombinant protein, however successful expression of *Is*PETase was not achieved, no protein band at the expected size could be observed by SDS-PAGE and Western-blot analysis (**Fig. S6, Fig. S7**). Additionally, to exclude protein folding issues we tested the expression of the truncated gene in *E. coli* ArcticExpress (DE3) host-cells, derived from BL21-Gold (DE3), featuring chaperonins Cpn60 and Cpn10 that facilitate proper folding also at low temperatures, strain previously being reported as successful host for *Is*PETase production (C. LIU & al. [23]). Since again *Is*PETase production was not detectable (**Fig. S8**), the synthetic gene, codon optimized by Invitrogen, was further optimized via the removal of the secondary open reading frame through site-directed mutagenesis (**Fig. S9**, **Table S4**), maintaining the encoded *Is*PETase sequence unaltered. The obtained plasmid harbouring the truncated version of the improved *Is*PETase in pET-21a(+), was transformed into *E. coli* ArcticExpress (DE3) and Rosetta-gami B (DE3) cells, the later also known to enhance the expression of genes with rare codons and also to facilitate proper disulphide bond formation within the protein-folding process (H. F. SON & al. (2020) [9]; S. JOO & al. [20]; H. F. SON & al. (2019) [21]; P. WAGNER-EGEA & al. [28]). Within these two hosts the production of *Is*PETase was attempted, varying the expression conditions (**Table S5**), such as medium type, induction and cell-growth temperature. Despite the multi-factorial experimental set-up, the expression of the desired protein was found to be unsuccessful.

In the final successful attempt, the use of an *N*-terminal His-tag for the truncated, improved gene sequence was considered. Accordingly, we subcloned the truncated, overlapping ORF-lacking *ispetase* gene into the pET-15b vector, then transformed the construct into both *E. coli*

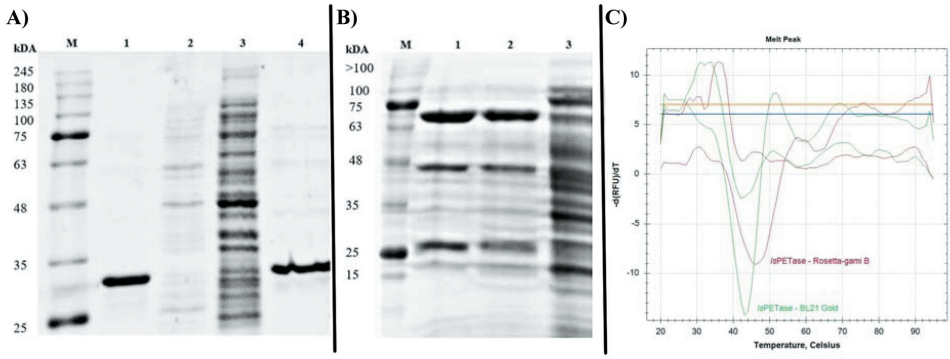

Figure 1. SDS-PAGE analysis of the isolation of mutant *Is*PETase(28-290)-pET-15b using as host *E. coli* **A)** Rosetta-gami B(DE3) cells (M-protein ladder, 1-eluted fraction (300 mM imidazole), 2-washing with 30 mM imidazole, 3-second flow-through, 4-eluted protein after desalting) and **B)** BL21 Gold (DE3) cells (M-protein ladder, 1-eluted protein after desalting, 2- second flow-through, 3-washing with 30 mM imidazole). **C)** Melting temperature measurement of the obtained *Is*PETase enzyme via differential scanning fluorimetry (DSF) (by plotting the negative first derivative of the fluorescence vs the temperature).

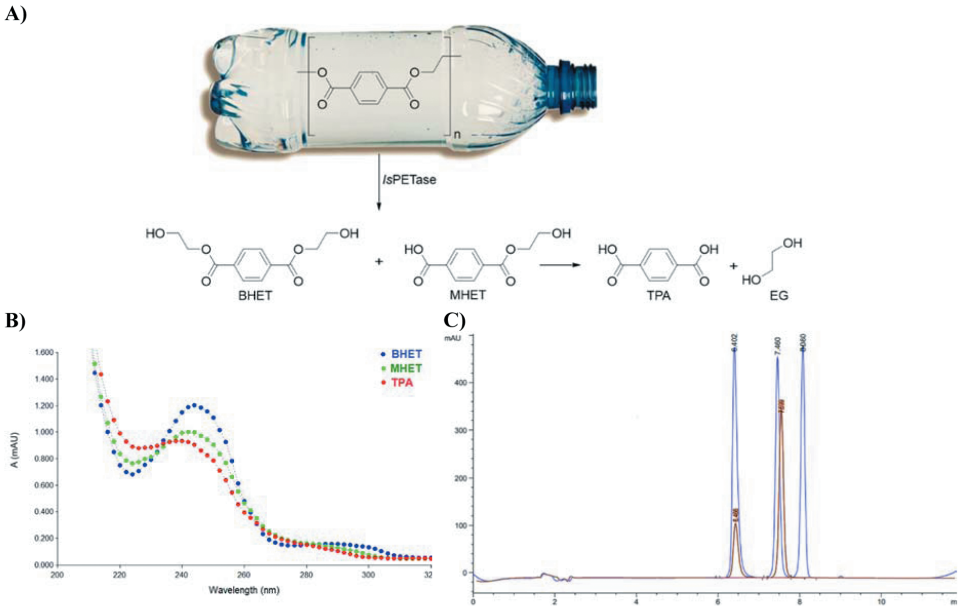

Figure 2. PET degrading activity of the produced recombinant *Is*PETase**. A)** Reaction scheme for the enzymatic PET film degradation. **B)** Overlay UV absorbance spectra of terephthalic acid (TPA), mono-(2-hydroxyethyl) terephthalic acid (MHET) and bis-(2-hydroxyethyl) terephthalate (BHET). **C)** Overlay of the HPLC chromatograms of *i*) the separation of TPA (1st peak), MHET (2nd peak) and BHET (3rd peak) during the measurements within standard curve assessment (blue) and *ii)* of sample from the enzymatic PET hydrolysis reaction (after 24-hour reaction time) (orange).

BL21-Gold (DE3) and Rosetta-gami B (DE3) expression hosts. In both cases, the SDS-PAGE analysis revealed the expression of a ~29 kDa protein, present also within the fraction eluted from the affinity chromatography (**Fig. 1A, Fig. 1B, see also Fig. S10 and Fig. S11**). Interestingly, using Rosetta-gami B as host *Is*PETase have been obtained in high purity (>95% - estimated from SDS-PAGE – **Fig. 1A**) and titer yields of (2.5 mg/L ferment), while in case of expression in *E. coli* BL21-Gold (DE3) host cells significantly lower expression yields (1.5 mg/L ferment)

and lower protein purity have been obtained (**Fig. 1B**). These results strengthen that the formation of the two disulphide-bonds Cys203-Cys239 and Cys289-C273 found within the crystal structures of *Is*PETase monomers (PDB ID: 5XJH) are essential within protein expression in *E. coli* host. Since Rosetta-gami B host cells with mutations in both the thioredoxin reductase (*trxB*) and glutathione reductase (*gor*) genes, enhanced disulphide bond formation in the *E. coli* cytoplasm, it also promoted the proper folding and expression of *Is*PETase. Notable, that in our case the same truncated gene version cloned with a C-terminal His6-tag in the pET-21a(+) vector repeatedly resulted in unsuccessful protein expression even in Rosetta-gami B, despite successful expression of similar C-terminal His6-tagged *Is*PETase encoding truncated genes in pET-21a(+) constructs being reported, *albeit* in other, disulphide bridge formation favouring, T7 Shuffle or T7 express *E. coli* hosts (G. J. PALM & al. [22]; E. Z. L. ZHONG-JOHNSON & al. [25]). The proximity of the C-terminal disulphide-bridge forming C289, and the disulphide bridge forming capability of Rosetta-gami B strains seems of high importance for protein folding/stability, reflected in the more facile expression of *N*-terminal tagged *Is*PETase.

Our results underline the importance of the selection/optimization of the cloning strategy, revealing several non-reported issues hindering the recombinant expression of *Is*-PETase. Apparently, the reported data suggest that PETase activity is not affected by the different N- or C-terminal positioning of the His-tag, however their *in vivo* folding process might be differently affected in the employed *E. coli* hosts, improperly folded *Is*PETase being exposed to protease degradation, as supported by our results.

The thermal stability assessment of the purified *Is*PETase revealed a melting temperature of 46.2°C, (**Fig. 1C**), in agreement with reported values (H. F. SON & al. (2020) [9]; H. P. AUSTIN & al. [10]; S. JOO & al. [20]; H. F. SON & al. (2019) [21]; C. LIU & al. [23]; E. Z. L. ZHONG-JOHNSON & al. [25]). The activity of the obtained *Is*PETase was investigated within the hydrolysis reaction of PET film (**Fig. 2**) using previously reported HPLC (H. F. SON & al. (2020) [9]; S. JOO & al. [20]; H. F. SON & al. (2019) [21]; V. TOURNIER & al. [24]) and UV-spectroscopy (E. Z. L. ZHONG-JOHNSON & al. [25]) methods.

During the analytical scale PET film degradation, we monitored the formation of the three possible products with terephthalic acid (TPA) content, bis-(2-hydroxyethyl) terephthalate (BHET), mono-(2-hydroxyethyl) terephthalate (MHET) and TPA (**Fig. 2A**), from which the global TPA quantity produced upon PET-hydrolysis could be obtained. During the UV-spectroscopy based PETase-activity measurements the molar absorptivity for each reaction product, BHET, MHET, TPA was determined (**Fig. S12**), using, as previously reported (E. Z. L. ZHONG-JOHNSON & al. [25]), the medium molar absorptivity, for products concentration assessments from UV-absorbance measurements at 235 nm. Further, the PETase activity measurements were also performed by employing HPLC procedures (H. F. SON & al. (2020) [9]; S. JOO & al. [20]; H. F. SON & al. (2019) [21]; V. TOURNIER & al. [24]), that upon adaptation provided baseline separation of the three TPA unit containing PET-hydrolysis product, TPA, MHET, BHET (**Fig. 2C**), while calibration using their authentic standard solutions provided quantification of the total TPA content of the samples extracted from enzymatic reactions (**Fig. 2C**).

Accordingly, the PET-hydrolysing activity of the produced *Is*PETase at 45 °C was 0.08 mg TPA produced / mg enzyme / 1 h reaction time with the UV-assay, while HPLC measurements revealed activity of 0.02 mg TPA produced / mg enzyme / 1 h reaction time, both values being in accordance with reported activity values (H. F. SON & al. (2020) [9]; S. JOO & al. [20]; H. F. SON & al. (2019) [21]; V. TOURNIER & al. [24]; H. SEO & al. [29]) and support that the optimized expression system is suitable for the facile production of *Is*PETase.

Conclusions

Within the present study we targeted the recombinant expression of the leading PET-degrading enzyme, *Is*PETase. Employing several reported expression systems, providing different N- or C-terminal affinity tags and various *E. coli* expression hosts, we registered unsuccessful *Is*PETase expressions. Construct and expression host optimizations revealed that the N-terminal His-tag and Rosetta-gami B expression host provided *Is*PETase in high yield and purity. The thermal denaturation profile and PET-hydrolysing activity of the isolated *Is*PETase was in agreement with reported data, supporting its proper fold. The results, while revealing several non-reported issues hindering the recombinant expression of *Is*PETase, suggest that the *in vivo* folding process of *Is*PETase might be differently affected among the different *E. coli* hosts. The revealed issues/solutions underline the importance of the selection/optimization of the cloning strategy for the successful recombinant expression of the *Is*PETase.

Conflicts of interest

The authors declare no conflicts of interest.

Acknowledgements

I. H. thanks the STAR-Institute of the Babeș-Bolyai University for the provided student-research fellowship and K. B. thanks for the support provided by the Collegium Talentum Programme of Hungary.

References

1. W. Courtene-Jones, B. Quinn, S. F Gary, A. O. M. Mogg, B. E Narayanaswamy, Microplastic pollution identified in deep-sea water and ingested by benthic invertebrates in the Rockall Trough, North Atlantic Ocean, Environ. Pollut., 231(1), 271, 280 (2017).
2. L. Nizzetto, M. Futter, S. Langaas, Are Agricultural Soils Dumps for Microplastics of Urban Origin?, Environ. Sci. Technol., 50(20), 10777, 10779 (2016).
3. C. E. Enyoh, A. W. Verla, E. N. Verla, F. C. Ibe, C. E. Amaobi, Airborne microplastics: a review study on method for analysis, occurrence, movement and risks, Environ. Monit. Assess., 191(668), 1, 17 (2019).
4. C. L. Waller, H. J. Griffiths, C. M. Waluda, S. E.Thorpe, I. Loaiza, B. Moreno, C. O.Pacherres, K. A. Hughes, Microplastics in the Antarctic marine system: An emerging area of research, Sci. Total Environ., 598, 220, 227 (2017).
5. R. H. Waring, R. M. Harris, S. C. Mitchell, Plastic contamination of the food chain: A threat to human health?, Maturitas, 115, 64, 68 (2018).
6. E. S. Gruber, V. Stadlbauer, V. Pichler, K. Resch-Fauster, A. Todorovic, T. C. Meisel, S. Trawoeger, O. Hollóczki, S. D. Turner, W. Wadsak, A. D. Vethaak, L. Kenner, To Waste or Not to Waste: Questioning Potential Health Risks of Micro- and Nanoplastics with a Focus on Their Ingestion and Potential Carcinogenicity, Expos. Health (2022).
7. K. Ragaerta, L. Delva, K. Van Geem, Mechanical and chemical recycling of solid plastic waste, Waste Manage., 69, 24, 58 (2017).
8. R. J. Müller, H. Schrader, J. Profe, K. Dresler, W.-D. Deckwer, Enzymatic Degradation of Poly(ethylene terephthalate): Rapid Hydrolyse using a Hydrolase from T. fusca, Macromol. Rapid. Commun., 26(17), 1400, 1405 (2005).
9. H. F. Son, S. Joo, H. Seo, H.-Y. Sagong, S. H. Lee, H. Hong, K.-J. Kim, Structural bioinformatics-based protein engineering of thermo-stable PETase from Ideonella sakaiensis, Enzyme Microb. Tech., 141, 109656 (2020).
10. H. P. Austin, M. D. Allen, B. S. Donohoe, N. A. Rorrer, F. L. Kearns, R. L. Silveira, B. C. Pollard, G. Dominick, R. Duman, K. E. Omari, V. Mykhaylyk, A. Wagner, W. E. Michener, A. Amore, M. S. Skaf, M. F. Crowley, A. W. Thorne, C. W. Johnson, H. L. Woodcock, J. E. McGeehan, G. T. Beckham, Characterization and engineering of a plastic-degrading aromatic polyesterase, PNAS, 115(19), E4350, E4357 (2018).
11. Y. Ma, M. Yao, B. Li, M. Ding, B. He, S. Chen, X. Zhou, Y. Yuan, Enhanced Poly(ethylene terephthalate) Hydrolase Activity by Protein Engineering, Engineering, 4(6), 888, 893 (2018).
12. H. Y. Sagong, H. Seo, T. Kim, H. F. Son, S. Joo, S. H. Lee, S. Kim, J.-S. Woo, S. Y. Hwang, K.-J. Kim, Decomposition of the PET Film by MHETase Using Exo-PETase Function, ACS Catal., 10(8), 4805, 4812 (2020).
13. R. Wei, D. Breite, C. Song, D. Gräsing, T. Ploss, P. Hille, R. Schwerdtfeger, J. Matysik, A. Schulze, W. Zimmermann, Biocatalytic Degradation Efficiency of Postconsumer Polyethylene Terephthalate Packaging Determined by Their Polymer Microstructures, Adv. Sci., 6(14), 1900491 (2019).
14. F. Kawai, T. Kawabata, M. Oda, Current knowledge on enzymatic PET degradation and its possible application to waste stream management and other fields, Appl. Microbiol. Biotechnol., 103, 4253, 4268 (2019).
15. F. Kawai, T. Kawabata, M. Oda, Current State and Perspectives Related to the Polyethylene Terephthalate Hydrolases Available for Biorecycling, ACS Sustain. Chem. Eng., 8(24), 8894, 8908 (2020).
16. a) T. Brueckner, A. Eberl, S. Heumann, M. Rabe, G. M. Guebitz, Enzymatic and chemical hydrolysis of poly(ethylene terephthalate) fabrics, J. Polym. Sci. Pat. A: Polym. Chem., 46(19), 6435, 6443 (2008). b) E. H. Acero, D. Ribitsch, G. Steinkellner, K. Gruber, K. Greimel, I. Eiteljoerg, E. Trotscha, R. Wei, W. Zimmermann, M. Zinn, A. Cavaco-Paulo, G. Freddi, H. Schwab, G. Guebitz, Enzymatic surface hydrolysis of PET: effect of structural diversity on kinetic properties of cutinases from Thermobifida, Macromolecules, 44(12), 4632, 4640 (2011). c) F. Kawai, T. Kawase, T. Shiono, H. Urakawa, S. Sukigara, C. Tu, M. Yamamoto, Enzymatic hydrophilization of polyester fabrics using a recombinant cutinase Cut190 and their surface characterization, J. Fiber. Sci. Technol., 73(1), 8, 18 (2017).
17. M. A. M. E. Vertommen, V. A. Nierstrasz, M. van der Veer, M. M. C. G. Warmoeskerken, Enzymatic surface modification of poly(ethyleneterephthalate), J. Biotechnol., 120(4), 376, 386 (2006).
18. I. Taniguchi, S. Yoshida, K. Hiraga, K. Miyamoto, Y. Kimura, K. Oda, Biodegradation of PET: Current Status and Application Aspects, ACS Catal., 9(5), 4089, 4105 (2019).

19. S. Yoshida, K. Hiraga, T. Takehana, I. Taniguchi, H. Yamaji, Y. Maeda, K. Toyohara, K. Miyamoto, Y. Kimura, K. Oda, A bacterium that degrades and assimilates poly(ethylene terephthalate), Science, 351(6278), 1196, 1199 (2016).
20. S. Joo, I. J. Cho, H. Seo, H. F. Son, H.-Y. Sagong, T. J. Shin, S. Y. Choi, S. Y. Lee, K.-J. Kim, Structural insight into molecular mechanism of poly(ethylene terephthalate) degradation, Nat. Commun., 9, 382 (2018).
21. H. F. Son, I. J. Cho, S. Joo, H. Seo, H.-Y. Sagong, S. Y. Choi, S. Y. Lee, K.-J. Kim, Rational Protein Engineering of Thermo-Stable PETase from Ideonella sakaiensis for Highly Efficient PET Degradation, ACS Catal., 9(4), 3519, 3526 (2019).
22. G. J. Palm, L. Reisky, D. Böttcher, H. Müller, E. A. P. Michels, M. C. Walczak, L. Berndt, M. S. Weiss, U. T. Bornscheuer, G. Weber, Structure of the plastic-degrading Ideonella sakaiensis MHETase bound to a substrate, Nat. Commun., 10, 1717 (2019).
23. C. Liu, C. Shi, S. Zhu, R. Wei, C.-C. Yin, Structural and functional characterization of polyethylene terephthalate hydrolase from Ideonella sakaiensis, Biochem. Bioph. Res. Co., 508(1), 289, 294 (2019).
24. V. Tournier, C. M. Topham, A. Gilles, B. David, C. Folgoas, E. Moya-Leclair, E. Kamionka, M.-L. Desrousseaux, H. Texier, S. Gavalda, M. Cot, E. Guémard, M. Dalibey, J. Nomme, G. Cioci, S. Barbe, M. Chateau, I. André, S. Duquesne, A. Marty, An engineered PET depolymerase to break down and recycle plastic bottles, Nature, 580, 216, 219 (2020).
25. E. Z. L. Zhong-Johnson, C. A. Voigt, A. J. Sinskey, An absorbance method for analysis of enzymatic degradation kinetics of poly(ethylene terephthalate) flms, Sci. Rep., 11, 928 (2021).
26. F. W. Studier, Protein production by auto-induction in high density shaking cultures, Protein Expr. Purif., 41(1), 207, 234 (2005).
27. X. Meng, L. Yang, H. Liu, Q. Li, G. Xu, Y. Zhang, F. Guan, Y. Zhang, W. Zhang, N. Wu, J. Tian, Protein engineering of stable IsPETase for PET plastic degradation by Premuse, Int. J. Biol. Macromol., 180, 667, 676 (2021).
28. P. Wagner-Egea, V. Tosi, P. Wang, C. Grey, B. Zhang, J. A. Linares-Pastén, Assessment of IsPETase-Assisted Depolymerization of Terephthalate Aromatic Polyesters and the Effect of the Thioredoxin Fusion Domain, Appl. Sci., 11(18), 8315 (2021).
29. H. Seo, S. Kim, H. F. Son, H.-Y. Sagong, S. Joo, K.-J. Kim, Production of extracellular PETase from Ideonella sakaiensis using secdependent signal peptides in E. coli, Biochem. Biophys. Res. Commun., 508(1), 250, 255 (2019).
30. C.-C. Chen, X. Han, X. Li, P. Jiang, D. Niu, L. Ma, W. Liu, S. Li, Y. Qu, H. Hu, J. Min, Y. Yang, L. Zhang, W. Zeng, J.-W. Huang, L. Dai, R.-T. Guo, General features to enhance enzymatic activity of poly(ethylene terephthalate) hydrolysis, Nat. Catal., 4, 425, 430 (2021).
31. E. Erickson, T. J. Shakespeare, F. Bratti, B. L. Buss, R. Graham, M. A. Hawkins, G. König, W. E. Michener, J. Miscall, K. J. Ramirez, N. A. Rorrer, M. Zahn, A. R. Pickford, J. E. McGeehan, G. T. Beckham, Comparative Performance of PETase as a Function of Reaction Conditions, Substrate Properties, and Product Accumulation, ChemSusChem., 15(1), e202101932 (2022).

ISSN print: 1224-5984
ISSN online: 2248-3942

Rom Biotechnol Lett. 2022; 27(3): 3517-3526
doi: 10.25083/rbl/27.3/3517.3526

Received for publication: March, 08, 2022
Accepted: April 05, 2022

Original paper

Extraction optimization, characterization and anti-inflammatory activity of functional protein from *Mangifera indica* seeds kernel

BARAKAT AHMED BARAKAT[1,2], SAHAR RAMADAN ABDELHADY[2], ESSAM MOHAMED ELSEBAIE[2]*, MOHAMED ABDELBASET SALAMA[1], MOHAMED ABDIN[1]

[1] Food Technology Research Institute, Agricultural Research Center, Giza, Egypt
[2] Food Technology Department, Faculty of Agriculture, Kafrelsheikh University, Kafrelshiekh, Egypt

Abstract Mango seed kernel (MSK) was observed to be a likely source of bioactive protein. Box-Behnken Design (BBD) was employed to optimize the protein extraction conditions. The optimum extraction conditions for maximum protein yield (68.336%) were corresponding to extraction temperature 54.53 ^{o}C, buffer-to-sample values 41.79 mL/g and extraction time 120 min with desirability value of 0.471%. The results of electrophoresis patterns of MSKP revealed two types of proteins; low molecular weight between 6 to 98 kDa explained the presence of globulin with type (2S) and another principal protein band of 27.6 kDa explained the presence of lectins. The extracted proteins under optimized conditions showed inhibition activity of nitric oxide (NO) release and pro-inflammatory inducers like (IL-6), (IL-1β) and (TNF-α) in lipopolysaccharide (LPS)-induced RAW264.7 macrophages. These findings revealed that MSK could be used as a promising nutraceutical of functional and health-promoting proteins.

Keywords Mango seed kernel; Box-Behnken Design; Optimization; Anti-inflammatory effect

To cite this article: BARAKAT BA, ABDELHADY SR, ELSEBAIE EM, SALAMA MA, ABDIN M. Extraction optimization, characterization and anti-inflammatory activity of functional protein from Mangifera indica seeds kernel. *Rom Biotechnol Lett.* 2022; 27(3): 3517-3526 DOI: 10.25083/rbl/27.3/3517.3526

*Corresponding author: ESSAM MOHAMED ELSEBAIE, Food Technology Department, Faculty of Agriculture, Kafrelsheikh University, Kafrelshiekh, Egypt
E-mail: essam.ahmed@agr.kfs.edu.eg

Introduction

The accumulation of vast quantity of wastes created by food industry produces major environmental issues as well as economical financial losses. These wastes have been discovered to be good sources of potentially important bioactive compounds. Mango by-products, particularly peels and seeds, are thought to be low-cost sources of nutritious foods and nutraceuticals (JAHURUL et al., 2015). Mango (*Mangifera indica*) is a popular tropical fruit cultivated mostly for its pulp. Mango seed (20-60% of the whole fruit) is an abundant waste of the food industry and is increasing due to the development of fruit production (DA SILVA MEIRELES et al., 2010). The seeds represent 30–45% of each mango's weight, contingent on the variety, and remain part which is commonly burned or discarded (ALENCAR et al., 2012). Mango seed kernels (MSK) contain 85-80% of carbohydrates, 6-13% of proteins and 6-16% of fats. Mango seed kernels (MSKP) contain essential amino acids and its oil has a considerable amount of essential fatty acids (DIARRA, 2014). Plant-derived proteins are becoming more popular in the nutraceutical field as parts of functional foods or substitutes of the environmentally costly production of animal protein (LIMA-CABELLO et al., 2018).

Seed proteins may have preventative and protective benefits against a variety of diseases such as obesity, cancer, cardiovascular disease, hypercholesterolemia and diabetes (VILLARINO et al., 2016). Furthermore, the health benefits of uncovered proteins and their hydrolysates derived from natural bioresources have been widely studied.

Various food proteins displayed distinguished anti-inflammatory effect in LPS-stimulated macrophages through regulation the production of iNOS, inflammatory cytokines, and COX-2 (AHN et al., 2012; UDENIGWE et al., 2013), suggesting the possibility of extraction of multifunctional proteins with anti-inflammatory activity.

Inflammation has been defined as a natural physiological reaction to external factors such as physical or chemical stimulation or microbial poisons (KNALL, 2015; LIU et al., 2018). Continued and excessive inflammation promoted by the uncontrolled production of pro-inflammatory cytokines like tumor necrosis factor (TNF-α), interferon gamma (INFγ),interleukin 6 (IL-6), interleukin 1 (IL-1), chemokines (i.e. CCL2, CCL5) ,reactive oxygen species (ROS), adhesion molecules (i.e. ICAM-1, VCAM-1), and the overproduction of nitric oxide (NO) and nitrogen intermediates might elicit a characteristic situation of T2D progression (TURNER et al., 2014).

Most commonly used medications, such as immunosuppressants, have not only been evaluated for efficacy, but also for gastrointestinal side effects and cost, which has limited its use as a medical remedy for a long time (SIEGEL, 2011). Thus, the extraction techniques of natural bioactive compounds as alternatives for industrial remedies are a good choice to avoid their unfavorable side effects.

Response surface methodology (RSM) is an extraction technique used for optimising a process that includes complex calculations. This method creates suitable experimental design that incorporates all of the tested variables and utilizes the data entry from the experiment to produce a set of formulas which can provide outcomes to enhance extraction yields, extraction function and save time (ABDIN et al., 2011; MOTA et al., 2003). In this work, use of MSK as principal material to optimize extraction of functional protein by using response surface technique that might be exploited as potential extract to reduce inflammation effects instead of industrial remedies and to reduce accumulation of wastes in environment.

Materials and methods

Materials

The Murine RAW264.7 cells were procured from Nanjing University of Chinese Medicine (Nanjing, China). The (ELISA) kits for nitric oxide (NO), TNF-α, IL-6, and IL-1β were obtained from Jiancheng Bioengineering Institute (Nanjing, China). Penicillin, LPS and MTT were obtained from Sigma Chemical Co. The Primary and secondary antibodies against anti-inflammatory mediators and β-actin were obtained from Cell Signaling Technology (Danvers, MA, USA). All other chemical reagents utilized were of analytical grade.

Methods

Preparation of Mango seeds kernel

Mango seeds were exposed to tap water for washing twice and air fan was directed to seeds for drying for 10 h on 20 °C. After that, the dried seeds were hammered to facilitate obtaining the kernels by removing the outer cover by hand. Then, an amount of warm sulphited tap water at 50 °C was mixed with resulted kernels for 48 h and dried by tray drier at 23 °C. The dried kernels were milled using a laboratory electronic mill (BRAWN, Model 2001 DL, Germany) to get soft powder. After that, the resulted fine powder was kept in polyethylene bags at 4 °C until further analysis.

Extraction of Mango seeds kernel protein

The extraction process of Mango seeds kernel protein (MSKP) was performed depending on reported method by (SEGURA-CAMPOS et al., 2013) with minor modification. Briefly, an amount of MSKP was suspended in phosphate

buffer solution (pH 8) and subsequently incubated at tested parameters (Time, temperature and buffer – to-sample ratio) to investigate the optimization technique. The resulted solution was centrifuged for 1 h at 3000 rpm and 10°C and the supernatant was obtained. The supernatant pH was adjusted to 4 by using 2N HCl and the solution was mixed for 20 min and the centrifuging step was repeated on the same conditions. Finally, the precipitated was collected and freeze dried on -50°C to afford MSKP.

Determination of protein content

The protein concentration of MSKP was calculated by Bradford method (BRADFORD 1976) using UV/VIS spectrophotometer 722 (Shanghai Jinghua Science & Technology Instruments Co., Ltd, China) at the wavelength of 595 nm and the standard curve was generated by using Bovine Serum Albumin (BSA).

Response surface experimental design

The experimental design of RSM was conducted based on the results of single – factor experiments. The single factor experiments were performed by studying the effects of the following parameters (temperature 30 – 60 °C, buffer-to-sample 20-50 mL/g and time 40 -160 min) on protein yield to generate suitable indicators for the subsequent Box–Behnken design (BBD). The BBD was done with the three independent variables at three levels based on results of single factor experiments. As indicated in (Table 1), the complete BBD was composed of 17 suggested runs carried out randomly, and the experimental design with five central points was conducted to indicate the frequency of the method. The following second order polynomial equation was utilized to investigate the linkage between the independent variables and the responses in BBD.

$$Y=\beta_o+\sum_{i=0}^{n}\beta_i X_i+\sum_{i=o}^{n}\beta_{ii}X_i^2+\sum_{i\neq i=1}^{n}\beta_{ij}X_iX_j \qquad (1)$$

where Y is assessed response, βo indicates the intercept, n belongs to the number of factors investigated, βi, βii and βij showing the linear (main effect), quadratic and cross product model coefficients, respectively; Xi and Xj are the points of the independent parameters.

SDS-PAGE analysis of MSKP

After applying optimized conditions, the resulted MSKP was transferred for electrophoresis technique on a 10% polyacrylamide SDS gel by using Mini-Protean II electrophoresis cell (Bio-Rad, Hercules, CA, USA). After the application of the washing gel, the staining process was performed by using staining solution composed of glacial acetic acid, Coomassie blue, methanol with percentages of 10%, 0.1% and 20%, respectively for 3 h followed by additional distaining using solution of 50% methanol and 10% glacial acetic acid. The migration procedure was done under strength of 20 mA per plate using a generator (PS 500-2 Sigma-Aldrich). The image was taken using a digital camera.

Anti-inflammatory effect of MSKP. Determination the cell viability of MSKP on RAW 264.7 cells

In the current study, MSKP optimized with the highest yield was utilized to test the anti-inflammatory activity in the following experiments. The MTT-colorimetric method was used as indicated by method of LU et al. (2011). Briefly, a density of 1×10^5 cells/mL from murine cells were cultured under modified atmosphere (37°C and 5% CO_2) in DMEM consisted of 1% (v/v) antibiotic solution contained streptomycin (100 IU/mL) and penicillin (100 IU/mL) with 10% (v/v) newborn calf serum. A 96-well culture plate was filled with amount of (100 µL/well) from suspension of murine cells and incubated in incubator for 12 h. A volume of 100 µL of new medium containing various final concentrations of MSKP was added to culture medium. DMEM alone was represented as a blank control. Then, the plates were incubated for extra 24 h and the suspension was replaced by 50 µL of MTT in concentration of 1.0 mg/mL, and the plates were incubated for additional 4 h. After discarding of MTT, an amount of 150 µL from DMSO was pipetted to well. Then, the absorbance was recorded at 570 mm by microplate Reader, and the percentage of the viable cells were determined by the subsequent equation.

$$\text{Cell viability} = \frac{\text{Ab}_{\text{sample}}}{\text{Ab}_{\text{control}}} * 100 \qquad (2)$$

Assay of nitrite oxide

According to our previous procedure (ABDIN et al., 2020), after incubation of RAW 264.7 cells and different concentrations of MSKP in 96-well plate for 150 min, the LPS (1µg/mL) was transferred to each well and the plates were transferred to incubator for further 24 h. The attendance of nitrite (µmol/L) was calculated using the Griess reagent of ELISA kit which recommended by suggested protocols.

Assay of cytokine production

The ELISA kit (Invitrogen) protocol was utilized to determine the amount of tested cytokine (Pg/mL). The preparation method to apply the protocol was done depending on culture of cells into 96-well plate in density of 2×10^5 cells/well and incubation overnight. Then, the cells were mixed with MSKP for 60 min followed by the addition of LPS (1 µg/mL) for one day to induce inflammation. After collecting the supernatant, the assay was performed typically according to guidelines of protocol manufacturing.

Western blot analysis

The western blot method was performed according to (WAN et al., 2019) with suitable modification. Briefly, after treating cells with MSKP for interval times, the cells were centrifuged and the supernatant of each sample with equal protein content was electrophorized with 10% (SDS-PAGE). After finishing running process, the protein on gel was transferred to polyvinylidene difluoride membranes by Semi-Dry Electrophoretic Transfer Cell. Then, the gel membranes were exposed to solution of 5% skim milk in the presence of tris buffered saline Tween 20 (TBST) for 120 min. After that, the blocked membranes were incubated with specific primary antibodies. The next day, the membranes were washed five times with TBST solution and exposed to secondary antibody type (HRP-conjugated goat anti-rabbit secondary antibody (1:50000)) for 120 min. The enhanced chemiluminescence reagents (ECL, Amersham Biosciences, UK) was utilized to visual each band and the Tanon 6000 imaging system was used to investigate the resulted bands.

Statistical analysis

The data of single factors experiment, cell viability and anti-inflammatory activity were statistically analyzed by one-way analysis of variance (ANOVA) by SPSS software. The design expert software was exploited to perform experimental design and analysis the data of RSM.

Results and discussion

Single factor investigation

Effect of temperature on protein yield

The extraction temperature had cleared effect on the protein content of mango seed kernel (MSK) as illustrated from Figure 1A. The percentage of mango seed kernel protein (MSKP) was significantly ($p < 0.05$) increased by heating during the extraction process up to 50 °C. After that, significant ($p < 0.05$) decrease was observed in MSKP. The raising of temperature more than 50 °C could lead to occurrence of denaturation and eventually reduced the protein solubility (YU et al., 2007). Additionally, the raising of temperature could stimulate the interaction between protein and other components inside seeds to form protein complexes in which decreased the solubility of the protein (SIOW & GAN 2014). Hence, the extraction temperature was selected within the ranges of 45 to 55 °C for the subsequent optimization study depending on steepest ascent techniques.

Effect of percentage of buffer-to-sample

As indicated in Figure 1 B, the buffer -to-sample ratios from 20 to 50 mL/g were tested. At ratio of 40 mL/g, the protein yield reached to the maximum value significantly. However, by increasing the ratio to 50 mL/g there was non-significant ($p < 0.05$) differences. The extractability of protein depends on the interactions between protein-protein hydrophobic surface and protein solvent hydrophilic surface (KRISTINSSON & HULTIN 2004). Additionally, with the increase of solvent/solid ratio, the contact area between solute and solvent is also improved to stimulate the solubility of bioactive components within the plants cells (ABDIN et al., 2019).The main objective of the study was to maximize the MSKP yield and as a result the ratios before 35 mL/g were discarded and the ratios in ranges of 35 to 50 mL/g were selected for the subsequent design.

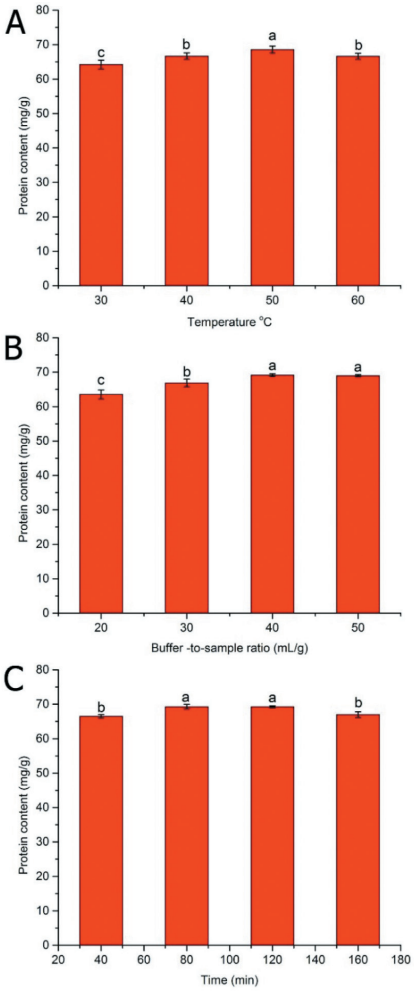

Fig. 1. Effects of temperature (A), buffer -to- sample ratio (B) and time (c) on protein content.

Bars with different letters are significantly different ($P \leq 0.05$).

Effect of time

As shown in Figure 1C, the extracted protein content was significantly ($p < 0.05$) increased from 40 to 80 min. Further extraction to 120 min did not illustrate any significant ($p > 0.05$) changes in yield. Furthermore, the increasing of extraction time more than 120 min caused significant ($P < 0.05$) decrease in MSKP content. The obtained results suggested that extended extraction time did not enhance MSKP extraction efficiency. Thus, the extraction time within the range of 60 to 120 min was selected for further optimization study. The selected extraction time was in the same trend of previously work (SIOW & GAN 2014) who extracted bioactive protein from cumin seed.

Designing BBD and response values

As observed from Table 1, the influences of three extraction parameters: temperature (X_1), buffer – to - sample ratio (X_2) and time (X_3), on the MSKP yield were investigated using a BBD design. The ranges of each factor (maximum and minimum) were selected depending on the previous results of single factor experiment. The design suggested 17 runs with 5 runs in central point at three levels (minimum -1, central 0 and maximum +1). The protein yield seemed to be varied depending on the extraction conditions given. It could be noticed that the maximum protein yield (45.5 mg/g) was obtained under the experimental conditions of X_1 55 °C, X_2 42.5 mL/g and X_3 120 min. The BBD technique was an ideal choice to extract protein from plant seeds with high functionality (KUMAR et al., 2021).

Table 1. BBD and response values for Protein yield

Run	Temperature X1 (°C)	Buffer-to-sample X2 (mLg^{-1})	Time x3 (min)	Protein yield (mg/g)
1	55	42.5	60	65.05
2	50	42.5	90	66.55
3	50	42.5	90	66.67
4	45	42.5	120	63.44
5	50	50	120	65.59
6	55	35	90	64.66
7	50	42.5	90	65.62
8	50	42.5	90	66.17
9	45	50	90	63.96
10	50	35	60	61.42
11	45	35	90	61.65
12	50	50	60	66.49
13	55	42.5	120	68.97
14	55	50	90	65.59
15	45	42.5	60	62.92
16	50	35	120	65.00
17	50	42.5	90	66.99

Analysis of ANOVA and model fitting.

The analysis of ANOVA was performed to investigate the significance of model's coefficient. In the current model, the *F*-value (13.42) of protein content was significant and the *P*-value of the lack of fit (0.1785) was not significant relative to the pure errors. The non-significant values of lack of fit implied that the current model equation was adequate for predicting the extraction yield of MSKP under any combination of temperature, buffer-to-sample and time (WANG et al., 2016). Moreover, the determined variables would be more significant if the absolute *F*-value becomes greater and the *P*-value becomes smaller (ATKINSON & DONEV, 1992) which are in agreement with obtained data in Table (2) .

Table 2. ANOVA for response surface quadratic mode

Source	Sum of Square	Mean square	*F-value*	*P-value*	Signif.
Protein content					
Model	58.04	6.45	13.42	0.0012	Signif.
X_1-Temperature	18.91	18.91	39.35	0.0004	
X_2-Buffer—to sample	9.9	9.9	20.6	0.0027	
X_3-Time	6.34	6.34	13.19	0.0084	
X_1X_2	0.48	0.48	0.99	0.3527	
X_1X_3	2.89	2.89	6.01	0.044	
X_2X_3	5.02	5.02	10.44	0.0144	
Residual	3.36	0.48			
Lack-of-fit	2.26	0.75	0.98	0.1785	Not signif.
Pure error	1.1	0.28			
Adj R-Squared	0.8748				
R-Squared	0.9452				
C.V.	1.06				

p values lower than 0.05 are statistically significant

yield value was obtained by the subsequent euation:

$$\text{Yield} = +66.40 + 1.54\,X_1 + 1.11\,X2 + 0.89\,X3 - 0.35\,X1X2 + 0.85\,X1X3 - 1.12\,X2X3 - 0.98\,X1^2 - 1.45\,X2^2 - 0.32\,X3^2 \quad (3)$$

The fitted quadratic model for MKSP yield in coded variables was generated in Eq. (3). The results of current model emphasize that, the largest effect on MSKP yield was in linear term of temperature X_1, buffer-to-sample X_2, time X_3, quadratic term and collaboration between temperature X_1 & time X_3, buffer-to-sample X_2 & time X_3, X_1^2 and X_2^2. The values of the coefficient of (R^2) and the adjusted coefficient of (adj.R^2) of the predicted model for MSKP yield was convergent, which suggested that there was a high degree of correlation between the observed and predicted values.

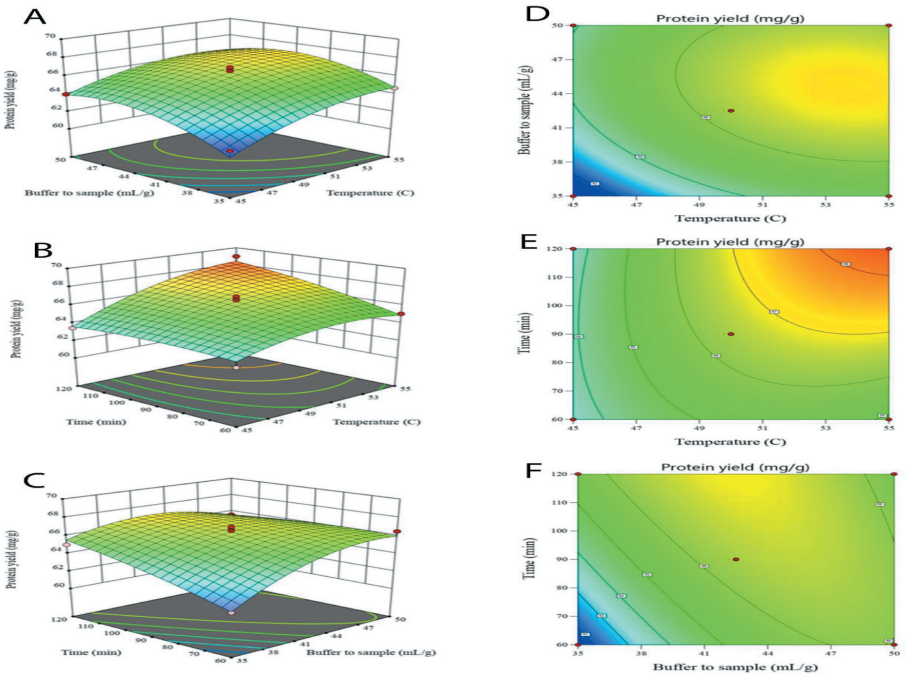

Figure 2. Response surface plots (A-C) and contour plots (D-F) showing effect of extraction variables on protein content.

Analysis of response surfaces

The three-dimensional shape in (Figure 2 A-C) and the two-dimensional contour plots in (Figure 2 D-F) are generated to describe the interaction effects between tested variables and protein content. Circular contour plot expresses that the interactions between the tested variables are non-significant, while the elliptical contour shape suggests that the corresponding variables are significant (MURALIDHAR et al., 2001).

Actually, the elliptical shape in (Figure 2 D-F) suggests that the co-operation between the tested factors is significant. The results are consistent with the results of ANOVA in (Table 2), which indicated that interactions between the variable factors (Temperature, buffer-to-sample and time) were significant and have great effect on MSKP yield.

It was summarized that the optimal settings for the extraction of MSKP while using in range values of tested parameters and maximized value of protein content (68.336%), were extraction temperature 54.53 °C, buffer-to-sample values 41.79 mL/g and extraction time 120 min with desirability value of 0.471%. The additional verification of the practical experiment was conducted based on the optimized predicted values of tested parameters with slight modification in optimized values to facilitate the practical experiment to be temperature 54.5 °C, buffer-to-sample values 42 mL/g and time 120 min. As a result, a practical extraction yield of 68.72 ± 0.52% (n = 3) was attained under the optimal extraction conditions, which is in the same trend with the predict value.

SDS-Page characterization of MSKP

The SDS-page technique was utilized based on protein electrophoretic mobility to notice protein bands as indicated in (Figure 3). The electrophoresis patterns of MSKP revealed that the MW was between 6 to 98 kDa. Depend-

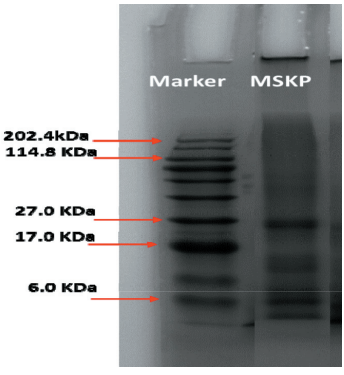

Figure 3. SDS-PAGE profile of MSKP compared to standard protein marker.

ing on the globulin considers the principal storage protein in seeds (ORRUNO & MORGAN, 2007) , the lowest bands in MW may explain attendance of globulin with type (2S). Additionally, another principal protein band of 27.6 kDa explained the presence of lectins , which was detected widely in seeds (NASI et al., 2009). The obtained results were in the same line of Siow et al. 2014 (SIOW & GAN, 2014).

Anti-inflammatory effect of MSKP

The anti-inflammatory effect of MSKP in LPS induced RAW264.7 cells was determined through five determinations; cell viability, production of IL-1β, IL-6, TNF-α and nitrite oxide (NO). Firstly, the cytotoxic concentration of MSKP was observed using MTT assay by calculation of cell viability. As shown in (Figure 4), MSKP showed no cytotoxic influence against RAW264.7 macrophages in all selected concentrations except of 900 µg/mL. Thus, the tested concentrations of 300, 500 and 700 µg/mL were utilized for the subsequent determinations.

As shown in (Figure 5 A – C), the attendance of different concentrations from MSKP in the cultured media caused re-

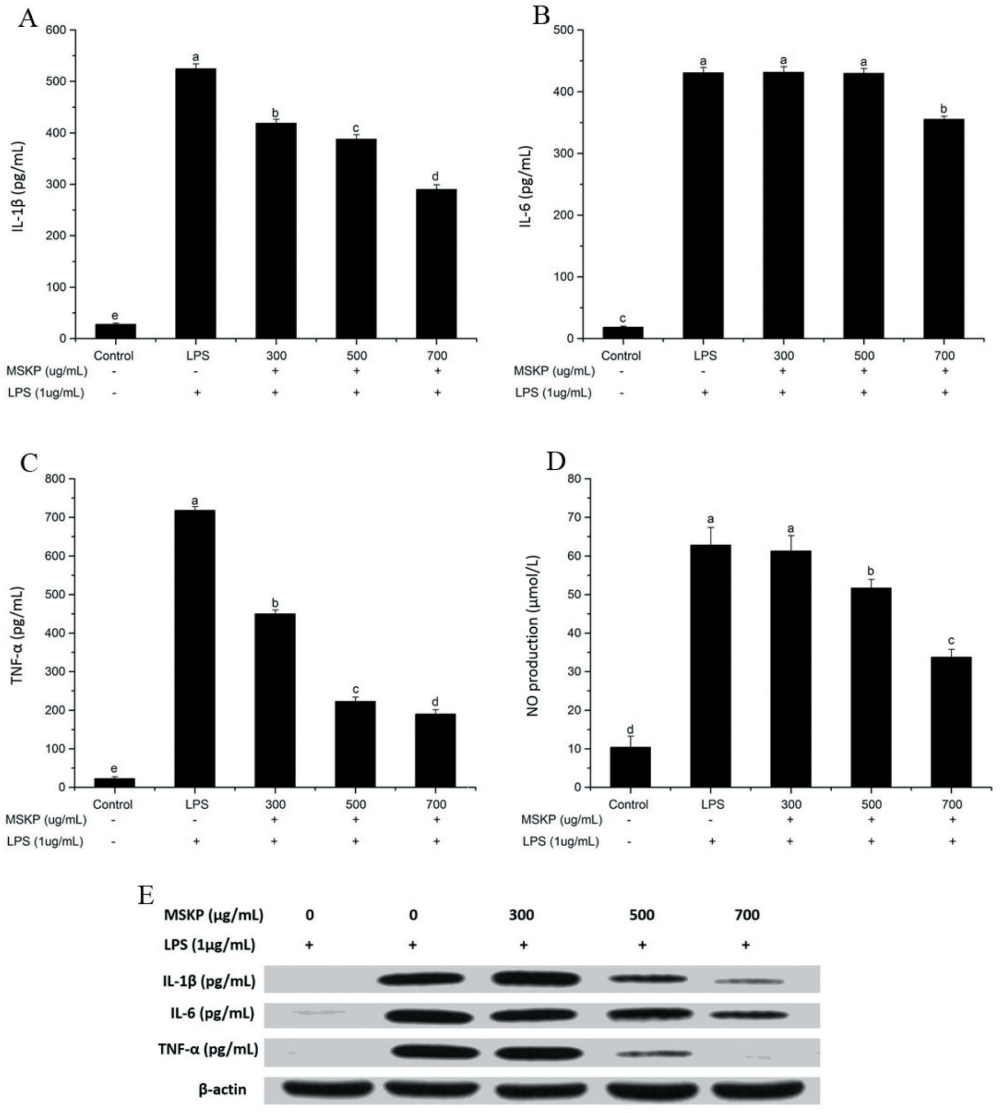

Figure 4. Effects of MSKP concentrations on cell viability of RAW264.7.

duction of proinflammatory mediators activity (IL-1β, IL-6 and TNF-α) in a dose-dependent style compared to those of LPS treatment alone. The current results revealed that MSKP may be beneficial for retarding inflammatory disorder. Similar results by the inhibition of the expression of nuclear factor κB (NF-κB) or another transcription factor, as well as the expression of genes for IL-1β, IL-6, and TNF-α was observed by attendance of *Salvia hispanica* L. seeds proteins inside culture media (CHAN-ZAPATA et al., 2019). Additionally, the extracted protein from seeds of *Myristica fragrans* showed inhibition of the production of interleukin (IL)-6, IL-10, interferon inducible protein-10 and monocyte chemotactic protein (MCP)-1, MCP-3 of RAW 264.7 mouse macrophages (LEE & PARK, 2011).

After treatment with MSKP followed stimulation of LPS, NO concentration in the cultured medium was investigated. As shown in (Figure 5 D), NO concentration by LPS treatment was significantly decreased by pretreatment with MSKP in a dose-dependent manner and it reached to the lowest value by using concentration of 700 µg/mL of MSKP in cell cultured media. NO is one of cellular mediators that is produced at inflammatory spots upon motivation by LPS and the higher concentrations of NO in response to inflammatory inducements is mediated by iNOS, leading to different inflammation and entotoxemia (MORO et al., 2012). Thus, the inhibition of NO is thought to be satisfied technique for retarding of inflammatory reaction. The iNOS and COX-2 might be affected by the extracted proteins from seeds through downregulation of the expressions of mRNA and protein and as a result lead to reduction of NO production (MOON et al., 2019).

Further, Western blot experiment with phosphorylated forms of antibodies following stimulation with LPS was performed to prove the effect of MSKP on protein levels of tested inflammatory cytokines. Electrophoresis and the subsequent western blot analysis are essential to investigate biochemical changes in cells and tissues exposed to tested components (HIRANO, 2012). In line with the results obtained from anti-inflammatory assays, clear decrescent in protein expression levels of TNF-α, IL-1β, and IL-6 were observed and it followed a concentration dependent pattern (Figure 5 E) when cells were treated with MSKP compared to LPS treatment group alone. At the highest concentration of MSKP examined (700 µg/mL) these protein expressions were almost totally inhibited.

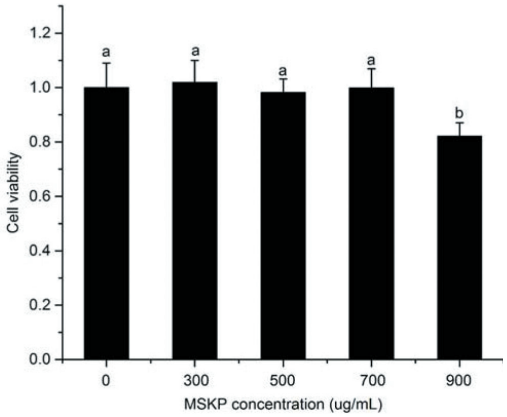

Figure 5. Effects of MSKP concentrations on production of IL-1β (A), IL-6 (B), TNF-α (C), NO (D) and Western blot analysis (E).

Conclusion

In conclusion, the current investigation proved that the single factors experiment had a significant influence on the yield of MSKP. The application of RSM depending on single factors results was successfully verified in the optimization technique of MSKP and expressed on the most efficient extraction conditions corresponding to extraction temperature 54.53 °C, buffer-to-sample values 41.79 mL/g and extraction time 120 min with desirability value of 0.471%. The SDS-PAGE results proved the findings of functional protein. The resulted MSKP showed anti-inflammatory effect against NO and proinflammatory cytokines. Further study of the chemical and biological properties of MSKP is recommended.

Acknowledgments

The study was supported by a project funded by Food Technology Research Institute, Sakha branch, Agricultural Research Center, Egypt and department of food science and technology, Kafrelshiekh university, Egypt.

Conflict of interest

The authors declared that they have no conflict of interest

References

1. Abdin, M., Hamed, Y. S., Akhtar, H. M. S., Chen, D., Chen, G., Wan, P., & Zeng, X. (2020). Antioxidant and anti-inflammatory activities of target anthocyanins diglucosides isolated from Syzygium cumini pulp by high speed counter-current chromatography. *Journal of food biochemistry, 44*(6), 1050-1062.
2. Abdin, M., Hamed, Y. S., Akhtar, H. M. S., Chen, D., Mukhtar, S., Wan, P., Riaz, A., & Zeng, X. (2019). Extraction optimisation, antioxidant activity and inhibition on α-amylase and pancreatic lipase of polyphenols from the seeds of Syzygium cumini. *International journal of food science & technology, 54*(6), 2084-2093.

3. Ahn, C.-B., Je, J.-Y., & Cho, Y.-S. (2012). Antioxidant and anti-inflammatory peptide fraction from salmon by-product protein hydrolysates by peptic hydrolysis. *Food Research International, 49*(1), 92-98.
4. Alencar, W. S., Acayanka, E., Lima, E. C., Royer, B., de Souza, F. E., Lameira, J., & Alves, C. N. (2012). Application of Mangifera indica (mango) seeds as a biosorbent for removal of Victazol Orange 3R dye from aqueous solution and study of the biosorption mechanism. *Chemical Engineering Journal, 209*, 577-588.
5. Atkinson, A. C., & Donev, A. N. (1992). *Optimum experimental designs*.
6. Bradford, M. M. (1976). A rapid and sensitive method for the quantitation of microgram quantities of protein utilizing the principle of protein-dye binding. *Analytical biochemistry, 72*(1-2), 248-254.
7. Chan-Zapata, I., Arana-Argáez, V. E., Torres-Romero, J. C., & Segura-Campos, M. R. (2019). Anti-inflammatory effects of the protein hydrolysate and peptide fractions isolated from Salvia hispanica L. seeds. *Food and Agricultural Immunology, 30*(1), 786-803.
8. da Silva Meireles, C., Rodrigues Filho, G., Ferreira Jr, M. F., Cerqueira, D. A., Assunção, R. M. N., Ribeiro, E. A. M., Poletto, P., & Zeni, M. (2010). Characterization of asymmetric membranes of cellulose acetate from biomass: Newspaper and mango seed. *Carbohydrate polymers, 80*(3), 954-961.
9. Diarra, S. S. (2014). Potential of mango (Mangifera indica L.) seed kernel as a feed ingredient for poultry: a review. *World's Poultry Science Journal, 70*(2), 279-288.
10. Hirano, S. (2012). Western blot analysis. In *Nanotoxicity*, (pp. 87-97): Springer.
11. Jahurul, M., Zaidul, I., Ghafoor, K., Al-Juhaimi, F. Y., Nyam, K.-L., Norulaini, N., Sahena, F., & Omar, A. M. (2015). Mango (Mangifera indica L.) by-products and their valuable components: A review. *Food chemistry, 183*, 173-180.
12. Knall, C. (2015). A review of Parham's 4th edition of the immune system: A clear and clean immunology text. *Journal of Microbiology & Biology Education, 16*(1), 94-94.
13. Kristinsson, H. G., & Hultin, H. O. (2004). Changes in trout hemoglobin conformations and solubility after exposure to acid and alkali pH. *Journal of agricultural and food chemistry, 52*(11), 3633-3643.
14. Kumar, M., Potkule, J., Patil, S., Saxena, S., Patil, P., Mageshwaran, V., Punia, S., Varghese, E., Mahapatra, A., & Ashtaputre, N. (2021). Extraction of ultra-low gossypol protein from cottonseed: Characterization based on antioxidant activity, structural morphology and functional group analysis. *Lwt, 140*, 110692.
15. Lee, J. Y., & Park, W. (2011). Anti-inflammatory effect of myristicin on RAW 264.7 macrophages stimulated with polyinosinic-polycytidylic acid. *Molecules, 16*(8), 7132-7142.
16. Lima-Cabello, E., Morales-Santana, S., Foley, R. C., Melser, S., Alché, V., Siddique, K. H., Singh, K. B., Alché, J. D., & Jimenez-Lopez, J. C. (2018). Ex vivo and in vitro assessment of anti-inflammatory activity of seed β-conglutin proteins from Lupinus angustifolius. *Journal of Functional Foods, 40*, 510-519.
17. Liu, H.-L., Kao, T.-H., Shiau, C.-Y., & Chen, B.-H. (2018). Functional components in Scutellaria barbata D. Don with anti-inflammatory activity on RAW 264.7 cells. *Journal of food and drug analysis, 26*(1), 31-40.
18. Lu, C.-L., Li, Y.-M., Fu, G.-Q., Yang, L., Jiang, J.-G., Zhu, L., Lin, F.-L., Chen, J., & Lin, Q.-S. (2011). Extraction optimisation of daphnoretin from root bark of Wikstroemia indica (L.) CA and its anti-tumour activity tests. *Food chemistry, 124*(4), 1500-1506.
19. Moon, S. W., Ahn, C.-B., Oh, Y., & Je, J.-Y. (2019). Lotus (Nelumbo nucifera) seed protein isolate exerts anti-inflammatory and antioxidant effects in LPS-stimulated RAW264. 7 macrophages via inhibiting NF-κB and MAPK pathways, and upregulating catalase activity. *International journal of biological macromolecules, 134*, 791-797.
20. Moro, C., Palacios, I., Lozano, M., D'Arrigo, M., Guillamón, E., Villares, A., Martínez, J. A., & García-Lafuente, A. (2012). Anti-inflammatory activity of methanolic extracts from edible mushrooms in LPS activated RAW 264.7 macrophages. *Food chemistry, 130*(2), 350-355.
21. Mota, F. J., Ferreira, I. M., Cunha, S. C., Beatriz, M., & Oliveira, P. (2003). Optimisation of extraction procedures for analysis of benzoic and sorbic acids in foodstuffs. *Food chemistry, 82*(3), 469-473.
22. Muralidhar, R. V., Chirumamila, R., Marchant, R., & Nigam, P. (2001). A response surface approach for the comparison of lipase production by Candida cylindracea using two different carbon sources. *Biochemical Engineering Journal, 9*(1), 17-23.
23. Nasi, A., Picariello, G., & Ferranti, P. (2009). Proteomic approaches to study structure, functions and toxicity of legume seeds lectins. Perspectives for the assessment of food quality and safety. *Journal of Proteomics, 72*(3), 527-538.
24. Orruno, E., & Morgan, M. (2007). Purification and characterisation of the 7S globulin storage protein from sesame (Sesamum indicum L.). *Food chemistry, 100*(3), 926-934.
25. Segura-Campos, M. R., Salazar-Vega, I. M., Chel-Guerrero, L. A., & Betancur-Ancona, D. A. (2013). Biologi-

cal potential of chia (Salvia hispanica L.) protein hydrolysates and their incorporation into functional foods. *LWT-Food Science and Technology, 50*(2), 723-731.

26. Siegel, C. (2011). explaining risks of inflammatory bowel disease therapy to patients. *Alimentary pharmacology & therapeutics, 33*(1), 23-32.
27. Siow, H.-L., & Gan, C.-Y. (2014). Functional protein from cumin seed (Cuminum cyminum): optimization and characterization studies. *Food hydrocolloids, 41*, 178-187.
28. Turner, M. D., Nedjai, B., Hurst, T., & Pennington, D. J. (2014). Cytokines and chemokines: At the crossroads of cell signalling and inflammatory disease. *Biochimica et Biophysica Acta (BBA)-Molecular Cell Research, 1843*(11), 2563-2582.
29. Udenigwe, C. C., Je, J.-Y., Cho, Y.-S., & Yada, R. Y. (2013). Almond protein hydrolysate fraction modulates the expression of proinflammatory cytokines and enzymes in activated macrophages. *Food & function, 4*(5), 777-783.
30. Villarino, C., Jayasena, V., Coorey, R., Chakrabarti-Bell, S., & Johnson, S. K. (2016). Nutritional, health, and technological functionality of lupin flour addition to bread and other baked products: Benefits and challenges. *Critical reviews in food science and nutrition, 56*(5), 835-857.
31. Wan, P., Xie, M., Chen, G., Dai, Z., Hu, B., Zeng, X., & Sun, Y. (2019). Anti-inflammatory effects of dicaffeoylquinic acids from Ilex kudingcha on lipopolysaccharide-treated RAW264. 7 macrophages and potential mechanisms. *Food and chemical toxicology, 126*, 332-342.
32. Wang, W., Wang, X., Ye, H., Hu, B., Zhou, L., Jabbar, S., Zeng, X., & Shen, W. (2016). Optimization of extraction, characterization and antioxidant activity of polysaccharides from Brassica rapa L. *International journal of biological macromolecules, 82*, 979-988.
33. Yu, J., Ahmedna, M., & Goktepe, I. (2007). Peanut protein concentrate: Production and functional properties as affected by processing. *Food chemistry, 103*(1), 121-129.E. H. ACERO & al. [16b]; F. KAWAI & al. (2017) [16c]), lipases (M. A. M. E.

ISSN print: 1224-5984
ISSN online: 2248-3942

Rom Biotechnol Lett. 2022; 27(3): 3527-3535
doi: 10.25083/rbl/27.3/3527.3535

Received for publication, August, 8, 2022
Accepted, August 11, 2022

Original paper

Characterization of exopolysaccharide produced by *Ganoderma* sp. TP and its immunomodulatory properties

PRIYA S. VADNERKER[1], TRUPTI K VYAS[1]*, CHINTAN V KAPADIA[2]

[1]Food Quality Testing Laboratory, N M College of Agriculture, Navsari Agricultural University, Navsari – 396450, India,
[2]Department of Plant Molecular Biology and Biotechnology, Aspee College of Horticulture and Forestry, Navsari Agricultural University, Navsari. 396450. Gujarat. India

Abstract

Mushrooms have an excellent nutritional value and are referred to as healthy food. They are a good source of carbohydrates, proteins, vitamins, and minerals while they are low in fat content. Mushrooms are well known as rich sources of nutraceutical molecules also. They produce exopolysaccharides (EPS), having high antioxidant activity. Hence, the present study aims to characterize a mushroom exopolysaccharide for its antioxidant and antitumor activity. A mushroom sample was collected from the Navsari Agricultural University, Navsari campus (20.9302° N, 72.9127° E). The sample was identified by morphological and 18S rRNA as Ganoderma sp TP (Accession No. MF614913). EPS was extracted from the sample, and total carbohydrate 258.3±1.4 µg/ml content was measured. Chemical characterization by FTIR, TLC, HPLC, and NMR analysis revealed that arabinose, lactose, and ribose monomer were present in the structure. TGA analysis revealed 86.34 % weight loss after the second stage. Rheological analysis suggested it is dilatants in nature. Antioxidant activity measured by ABTS and DPPH showed 84.09 % and 86.45% antioxidant activity, respectively. Antitumor activity was examined using the MDA-MB-231 cell line and found 63.49% cell inhibition compared to control. Thus, EPS produced by Ganoderma sp TP is novel from other reported EPS and positively affects tumor cell growth reduction.

Keywords Antioxidant, Antitumor, Breast cancer, Exopolysaccharides, *Ganoderma*

To cite this article: VADNERKER PS, VYAS TK, KAPADIA CV. Characterization of exopolysaccharide produced by *Ganoderma* sp. TP and its immunomodulatory properties. *Rom Biotechnol Lett.* 2022; 27(3): 3527-3535 DOI: 10.25083/rbl/27.3/3527.3535

*Corresponding author: Trupti K Vyas: vyastrupti@hotmail.com, https://orcid.org/0000-0002-1168-7552

Introduction

Medicinal mushrooms are used for their health-promoting properties and nutritional value and as a possible complementary for treating diseases. Many mushrooms are well known for their medicinal properties. India, China, Japan, Korea, and some other South-Eastern countries have used it for 3000 years as a medicinal mushroom in a number of diseases[1]. Molecules, which confer medicinal and or nutritional properties to mushrooms, are called bioactive molecules. Some mushroom metabolites, including polysaccharides, glycoprotein, and proteoglycans, have the potential to modulate immune system response and inhibit tumor growth[2, 3, 4, 5], whereas; other shows potential antiviral, antibacterial, antiparasitic, anti-inflammatory, and anti-diabetic properties[6].

Exopolysaccharides (EPS), high-molecular-weight carbohydrates secreted by an organism into the surrounding environment, are composed of sugar residues. The Biochemical properties of the EPSs depend on the primary structure of the EPS. The kind of glycosidic bonds and monomer types are important in determining their medicinal properties. Many medicinal mushrooms produce exopolysaccharides which have been very well reported for antioxidant activity, superoxide radical scavenging, reducing properties, lipid peroxidation inhibition, suppression of proliferation and oxidative stress, etc. Polysaccharides isolated from different mushrooms like *Agaricus, Calocybe, Ganoderma, Grifola, Inonotus, Lentinus, Phellinus, Pholiota, Pleurotus,* etc., are also capable of providing antitumor activity[7].

Cancer remains one of the significant causes of death worldwide. The most effective treatment strategy for cancer is cytotoxic agent-based chemotherapy, which increases patient survival and has side effects that severely limit its clinical effectiveness, such as the acquisition of drug resistance. Consequently, an alternative option is required to combat the side effect produced by chemotherapy. Hence, the present study aims to characterize EPS for its antioxidant and antitumor activity.

Materials and Methods

Collection and isolation of mushroom sample:

The mushroom sample used in present studies was collected from Navsari Agricultural University, Navsari campus (20.9302° N, 72.9127° E). The isolation of mycelium was carried out on potato dextrose agar (PDA) plates. For the isolation, a small piece of mushroom was inoculated in the PDA plates in aseptic condition and plates were incubated at 25°C for 48-72 hours. Subsequently culture was purified and stored on PDA slant at 4°C until the use.

Identification of mushroom

The morphological characterization was carried out macroscopically by observing growth patterns of fungi and microscopically by wet mounting of fungi in lactophenol. For molecular characterization DNA from mushroom sample was extracted according to the methods described by Graham and coworkers [8]. Amplification of genomic DNA was done by ITS1 and ITS4 primers. PCR conditions were set as described by Kheni and Vyas [2]. Sequence was explored for homology and submitted to GenBank.

Extraction of EPS

For EPS extraction, the sample was dried at 60 °C in a hot air oven to remove water content. Fine powder was prepared from dried samples using a blender for EPS extraction. Three different methods were used for EPS extraction i.e., hot water extraction [9] ethanol extraction and methanol extraction [10]. Among the different methods used, the extraction method which produced higher EPS was used for further work.

Quantification of carbohydrate content

The carbohydrate of crude sample and extracted EPS was measured using the method mentioned by Dubois and coworker [11].

Characterization of EPS

For chemical characterization, sample was partially purified as described by Kheni and Vyas[2]. After partial purification, characterization of EPS was carried out by FTIR, TLC, HPLC, NMR and TGA analysis.

FT-IR

For characterization of EPS, dried EPS powder was ground with KBr and pressed to obtain pellets. Infrared absorption spectra (Nicolet IR200 FT-IR Spectrometer) were recorded on a FT-IR in the 4000-400 cm-1 range. KBr pellet was used as the background reference.

Thin Layer Chromatography [12]

The sugars were detected by spotting the sample on silica gel 60 (F254 Merck, Germany) using ethyl acetate: acetic acid:methanol:distilled water (60:15:15:10) as solvent 12. The TLC plate was sprayed with anisaldehyde-sulfuric acid reagent followed by heating at 100°C for 5-10 minutes for the development of colored spots. Type of sugar present in the sample was identified by comparing the Rf value of standard sugar runs along with the sample.

HPLC (High Performance Liquid Chromatography)

Hydrolyzed EPS sample was analyzed using an analytical HPLC coupled with an RI detector[2]. 0.1% H_2SO_4 in

water was used as a mobile phase and flow rate was 0.5 ml/min. Analysis. The monomers in EPS were detected by an RI detector.

NMR

To confirm the chemical structure, 1H NMR and 13C NMR analysis were carried out. Analysis was carried out at Central Salt & Marine Chemical Research (CSMCRI), Council of Scientific and Industrial Research (CSIR), Bhavnagar, India.

TGA analysis

Thermogravimetric analysis (TGA) of the sample was also carried out in the N2 atmosphere at the heating rate of 10 ºC min. The pyrolysis pattern of the EPS was investigated using a differential scanning calorimeter. The energy level was scanned from 50 to 450 ºC in N atmosphere.

Rheology

One of the important features of EPS is rheological behavior, which has great impact in manufacturing, thickening and stabilization and has potential industrial application. Flow property of EPS solution was determined using Physica MCR 301 (Anton Paar) at shear rate from 0.01 s^{-1} to 196 1000 s^{-1} was applies for 5 mins at 25 °C.

Antioxidant activity

To estimate the antioxidant activity, three different methods viz. Ferric Reducing Antioxidant Power (FRAP) assay, ABTS assay and DPPH assay were used. Antioxidant activity by FRAP assay was measured as a method described by Benzie and Strain[13] and the result was expressed as FeII µmol/gm. ABTS assay was measured as a method of Re and coworker[14] (1999). Antioxidant activity by DPPH assay was measured as mentioned by Garcia and Co-workers [15].

Antitumor Activity

Antitumor activity was measured in vitro by cell growth inhibitory activity against the human breast cancer cell lines (MDA-MB-231) by MTT assay[16]. For the assay, the cells were grown in tissue culture flasks in Leibovitz medium at 37 °C. 105cells/ml was transferred to each well in 96-well microtiter plate. The cells were allowed to grow for 24 hrs and then treated with the sample. 100 µl test sample (concentration range from 100 – 1000 µg/ml) was added to the wells and cells were further incubated for another 24 hrs at 37 °C in an incubator. 20 µl MTT (5 mg/ml in phosphate buffered saline) was added after incubation to each well and cells were further allowed to grow for 4 hrs. Media was removed afterwards and100 µl dimethyl sulfoxide (DMSO) was added to each well. The absorbance was measured on a microplate reader (Multiskan, Thermo Scientific) at 570 nm. Experiment was done in triplicate. Control comprised cell growth without a test sample. The inhibition percentage was calculated using the following formula:

$$\text{Inhibition activity (\%)} = [(\text{Acontrol} - \text{Asample})/\text{Acontrol}] \times 100$$

Where, Acontrol was the absorbance of the control reaction and Asample is the absorbance of the of the sample.

Results and Discussion

Collection and isolation of Mushrooms

A mushroom sample was collected from Navsari Agricultural University, Navsari, Gujarat, India. A portion of the mushroom sample was taken for isolation and purification of mushroom. The rest of the biomass was dried at 60 ºC. Isolation and subsequent purification were done, and pure culture was stored on a PDA slant at 4 ºC until use.

Identification of mushroom

The pure culture was used to study the morphological characteristic of the isolate. The isolate showed secondary mycelia and clam connection when observed under a microscope with lactophenol cotton blue mounting stain. The ITS region of 18S rRNA was amplified with ITS 1 and ITS 4 primers to identify the isolate. It produced a characteristic amplicon of approximately 650bp (Fig 1a). Amplified PCR product was sequenced at Saffron Life Sciences, India, and resulted in sequenced data being aligned using the NCBI blast tool. It showed homology with *Ganoderma* sp. Hence, it is named *Ganoderma* sp TP (Fig 1b). The sequence data was submitted to GenBank with accession number MF614913.

Extraction of EPS

EPS from the mushroom sample was extracted using three different solvents for higher EPS recovery. EPS was extracted by hot water, methanol, and ethanol extraction methods. Maximum EPS was extracted using ethanol ex-

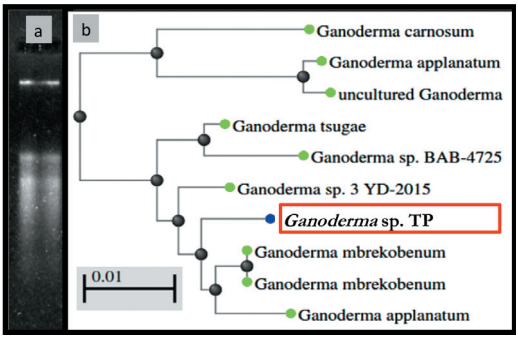

Figure 1. DNA of mushroom (a) phylogenetic tree of *Ganoderma* sp TP (b)

traction (13.47 mg/g) followed by methanol (11.63 mg/g). Hot water extraction extracted the least EPS (8.3 mg/g). Ethanol extraction showed higher EPS production; hence, it was used for further studies.

Quantification of carbohydrate content

To find out the amount of carbohydrate present in the sample, 1 mg/ml of crude mushroom sample and extracted EPS were separately analyzed by phenol sulphuric acid method for carbohydrate content. Carbohydrate content was 48.65±0.07 (µg/ml) and 258.3±1.4 (µg/ml), respectively, in mushroom and EPS samples.

Characterization of EPS

Various analyses like FTIR, TLC, HPLC, NMR TGA were carried out to know the monomers of EPS.

FTIR analysis

The FTIR spectrum of an unhydrolyzed sample of Ganoderma sp. TP EPS (Fig 2) showed the characteristic absorbance of polysaccharides. The absorption between 3426-3000 cm-1 indicates the O-H stretching vibration of the polysaccharide. The absorption band at 2924 cm-1 suggests C–H stretching vibration. The instance absorption between 1150-900 cm-1 is characteristic of carbohydrates and corresponds to stretching vibrations of C–C, C–O–C, and C–O occurring in glucopyranose structure. Thus, IR spectra confirmed the presence of sugar.

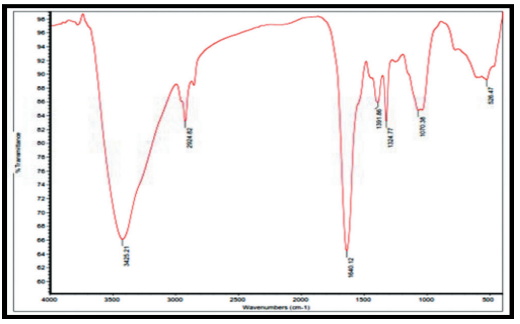

Figure 2. FTIR spectrum of EPS *Ganoderma* sp TP

TLC analysis

To identify monomers of the EPS sample, partial purification of EPS was done using acid hydrolysis. Hydrolysis was monitored using TLC analysis at 1 hr intervals. The product was completely hydrolyzed after 4 hrs of incubation in a boiling water bath. Hydrolyzed product was neutralized with sodium bicarbonate and used further for TLC analysis and HPLC analysis. Three different spots were detected on a thin layer chromatogram and had similar Rf values with standard sugar arabinose, lactose, and ribose.

HPLC analysis

A partially purified sample was analyzed for the presence of monomers in the EPS structure. Samples containing arabinose, lactose, and ribose were detected, matching standard sugars. TLC results also corroborate with HPLC analysis.

NMR

EPS sample was characterized by 1H NMR and 13C NMR analysis. In 1H NMR peak between 3.03 – 3.64 indicates the sugar proton, whereas d 4.83 indicates the anomeric carbon (Fig 3a). In 13C NMR peak at 63.657 indicated the presence of C-6. The peak at 72.577 showed a large amount of terminal C-6 branching at C-2 with β (1®3) linkage. The peak at 106.15 indicates the anomeric carbon, whereas the peak at 51.75 indicates amine and confirms the glycoprotein structure (Fig 3b).

TGA analysis

EPS produced by isolate was characterized by TGA and DSC analysis. Results of TGA analysis showed that EPS from Ganoderma sp. TP takes place in two steps. Initially, 76.84 % weight loss was observed up to 140 ºC with an onset of 91 ºC. After 140 ºC, there is slow degradation observed with continuous exotherm. The second weight loss 9.50 % was it up to 300 ºC and after 300 ºC. In the first step, high % weight loss was due to moisture content and carboxyl group, which increased bond degradation with water molecules. Second stage degradation at 300 ºC corresponds to a pyrolysis temperature. Total weight loss was 86.34 % after the second stage.

Rheology

Shear stress and viscosity of EPS produced by Ganoderma sp. TP was characterized by a rheometer. Results revealed that it is non-Newtonian shear thickening, Dilatant in nature as (n) is greater than one when fitted in the "power-law model". Hence it can also be used as a thickening agent.

Antioxidant activity

Antioxidant activity of EPS was measured using FRAP assay. If molecules have the antioxidant ability, it converts FeIII molecule to FeII. Results revealed that EPS has 15.300 mM/gm antioxidant activities. The second assay used for antioxidant activity was the ABTS assay. EPS showed 84.09 % inhibition of radical ABTS molecules. The third assay used for measuring antioxidant activity was the DPPH assay. In this assay, EPS showed 86.45% antioxidant activity.

Antitumor activity

Antitumor activity was measured by cell viability using an MTT assay. The assay is based on the cleavage of the tetrazolium salt MTT in the presence of an electron-coupling reagent. To examine antitumor activity, MDA-MB-231 cells

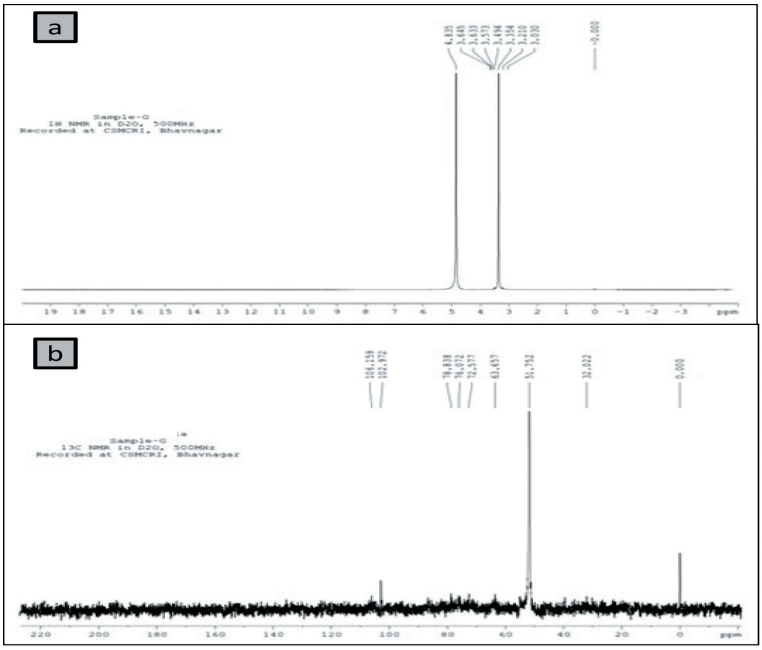

Figure 3. ^{1}H NMR (a) and ^{13}C NMR (b) spectrum of EPS produced by *Ganoderma* sp. TP

were grown in Leibovitz media (Fig 4a). For MTT assay, cells were grown in 96 well ELISA plates for 24 hrs. After 24 hrs of incubation, different concentrations of EPS (0.1 – 1 mg/ml) were added, and cells were further incubated for 24 hrs (Fig 4b). MTT solution was added in 96-well ELISA plates containing pre-grown cells with different EPS concentrations and incubated for 4 hrs. Formazan produced after this incubation period was quantified using a scanning multi-well spectrophotometer ELISA reader. The measured absorbance directly correlates to the number of viable cells. Cells were lysed after 24 hrs of incubation, as shown in Figure 4c. When most of the cells lysed, clumps of EPS were also observed after 24 hours. In control, all wells showed higher formazan production, whereas, in test samples, formazan color production decreased gradually as EPS concentration increased. Cell inhibition was started at a minimum concentration of 0.1 mg/ml of EPS concentration, and maximum cell inhibition of 63.49 % was observed at 0.9 mg/ml concentration.

Human beings are equipped with immune defense systems to neutralize free radicals as free radicals could damage macromolecules, resulting in serious diseases. Many researchers have been done exploring potential natural antioxidants to reduce oxidative damage. Mushrooms are one such source of sustainable bioactive compounds that have been consumed for thousands of years. Polysaccharides are important bioactive components produced by many mushrooms.

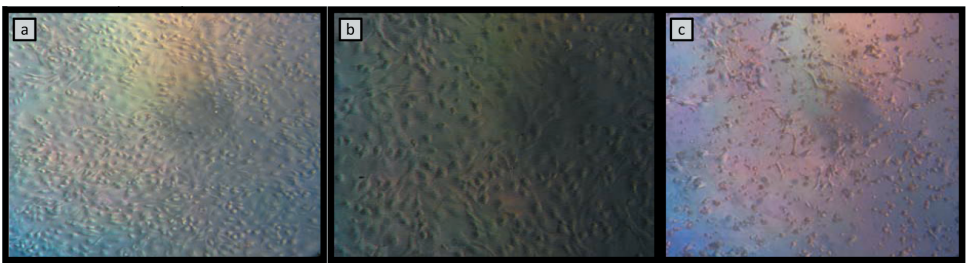

Figure 4. Normal growth of MDA-MB 231 breast cancer cell line (a), cell line with addition of EPS (b) Cell lysis in presence of EPS after 24-hour incubation (c)

In the present study, the mushroom was identified by 18S rDNA as *Ganoderma* sp. TP and submitted to Genbank. Various methods were selected for the extraction of EPS. Among three different methods used, maximum EPS was recovered by ethanol extraction followed by methanol and hot water extraction. Ethanol extraction showed a higher extractive index, and the results are in accordance with many published data [17, 18, 19]. EPS extracted using ethanol extraction method from *Ganoderma* sp. TP showed that it produced 13.47mg/g EPS. EPS contained 258.3±1.4µg/mg of carbohydrate. Sasidhara and Bakki [20] reported 300 mg/g of carbohydrates extracted from *Ganoderma lucidum*, which is higher than our results. EPS production was lower in *Ganoderma* sp. TP compared to *Ganoderma applanatum* (241.8 mg/g) whereas carbohydrate content 303 ± 1.29 mg/g is almost similar as reported by Osinska-Jaroszuk and coworker [21]. Ubaidillah and coworker [22] reported 115.89% total carbohydrate in EPS extracted from *G. neojaponicum*, which is higher than EPS from *Ganoderma* sp.

Polysaccharides are made up of monomeric sugar linked with glycosidic bonds. EPS structure may be homopolymer or heteropolymer, either linear or containing branched side chains linked with β- (1→6) glycosidic bonds [18]. Due to the versatile nature of EPS, it carries much biological information and helps identify structural diversity. These diverse structures provide regulatory mechanisms for cell-cell interactions in higher organisms. FTIR analysis helps in the identification of characteristic bonds present in carbohydrates. Various peaks present in the molecules confirm the carbohydrate structure. Our data are in accordance with the reported EPS structure by FTIR analysis [23, 24, 25].

TLC and HPLC analysis of the exopolysaccharide extracted from *Ganoderma* sp. TP, showed the presence of arabinose, lactose, and ribose monomers. The polysaccharides isolated from *Ganoderma* constitute glucose, mannose, galactose, fucose, xylose, and arabinose, with eight combinations and different types of glycosidic linkages which can be bound to protein or peptide residues [2, 26, 27, 28, 29, 30, 31]. Fraga and coworkers (2014) reported the presence of glucose, galactose, and mannose in the ratio of 69–93%, 4–19%, 2–8%, and 1–5%, respectively, in the EPS extracted from *Ganoderma lucidum* [32]. EPS extracted from *Ganoderma lucidum* contained glucose, galactose, mannose, arabinose, and rhamnose in a ratio of 332:55:32:13:3, respectively [33]. Thus, it showed a different unique structure of EPS.

EPS structure from *Ganoderma sinense* was characterized by NMR spectroscopy and revealed that it contained mannose, glucosamine, glucuronic acid, N-acetyl- ß-D-glucosamine, glucose, and galactose as EPS monomers [25]. Antioxidant activities of different mushrooms were evaluated previously by several researchers using various methods. Methods such as 2,2-diphenyl-1-picrylhydrazyl (DPPH) radical scavenging, 2,2'-azino-bis (3-ethylbenzothiazoline-6-sulfonic acid) (ABTS) radical scavenging, ferric reducing antioxidant power (FRAP), hydroxyl radical scavenging, superoxide radical scavenging, nitric oxide (NO) scavenging, and lipid peroxide inhibition assays were commonly used to determine the antioxidant activities of polysaccharides from various kinds of samples [34, 35, 36, 37(pp. 119 –132)]. The result of antioxidant activity by EPS suggests that it has almost similar activity by ABTS and DPPH assay. Mahendran and coworkers [38] reported lower antioxidant activity 63.75 ± 2.47 % inhibition by ABTS assay from *Ganoderma lucidum*, DPPH radical scavenging ability of crude EPS of *G. lucidum* (82.3 ± 3.27 %) was similar to the DPPH scavenging activity of *Ganoderma* sp. TP (84.58%) [38]. *G. lucidum* showed 50% inhibition by 0.055 mg/ml of ethanolic extracted EPS using the DPPH assay, which is lower than reported here [39].

Here, EPS extracted from *Ganoderma* sp. TP was evaluated on the MDA-MB-231 breast cancer cell line by MTT assay showed 63.49% inhibition of the tumor cell line at 0.9 mg/ml EPS concentration. Polysaccharides extracted from *G. lucidum* showed 80.8% and 77.6% reduction in tumor volume and tumor mass, respectively, of Ehrlich's ascites carcinoma cells [40]. Polysaccharides PG-1 and PG-2 from *G. lucidum* have immunomodulatory properties and showed an inhibitory effect on the growth of a human breast cancer cell line MDA-MB-23141. Their results are in accordance with our findings.

Ganoderma sinense produces a polysaccharide (GSRBPs) effective on the H1299 NSCLC cell line of non-small-cell lung cancer (NSCLC) [41]. Thus, polysaccharide GSRBPs can be effectively used to inhibit H1299 non-small-cell lung cancer. A similar study also revealed that EPS extracted from *Ganoderma* sp. had been reported for its anticancer activity against lung cancer line Murine Lewis lung carcinoma (LLC1) [42]. In one study, the sandwich structured antitumor composite was designed with three layers comprising the first top and bottom layers made from ethyl cellulose-containing triterpenes from *Ganoderma lucidum*; the second layer of polyvinyl alcohol have polysaccharide from G. lucidum [43]. Carcinoma cells, such as SGC-7901, A549, Hela, and Caco-2 were studied in vitro for antitumor activity of the synthesized sandwich drug and found to have IC50 of 51.2, 90.7, 93.0, and 21.7 µg/mL, respectively. Not only antitumor but exopolysaccharide from *Ganoderma* sp. has also been reported for their antioxidant, antiviral, anti-inflammatory, and immunomodulatory effects [44, 45]

Conclusion

Ganoderma sp TP (Accession No. MF614913) contains 258.3±1.4 µg/ml carbohydrate in extracted exopolysaccharide molecules. Chemical characterization of EPS by various analyses revealed that *Ganoderma* sp TP containing novel monomer arabinose, lactose, and ribose monomer were present in the structure. TGA analysis revealed 86.34 % weight loss after the second stage. EPS possesses higher antioxidant activity measured by ABTS and DPPH suggests that it can scavenge free radicals. EPS was able to suppress tumor cell lines, as evidenced by 63.49 % cell inhibition of the MDA-MB-231 cell line. Hence, EPS produced by *Ganoderma* sp TP which is novel than other reported EPS from *Ganoderma* sp., can be used as a potential immunomodulator. However, detailed in vivo studies required for antitumor activity and clinical trials will be further helpful in insight mechanism as an antitumor agent. Thus, EPS extracted from *Ganoderma* sp TP can be used as a food supplement to boost immunity.

Acknowledgments

Authors are thankful to Dr I. H. Kalyani, Department of Microbiology, Vanbandhu College of Veterinary Science & Animal Husbandry, Kamdhenu University for providing laboratory facility to conduct MTT assay.

Conflicts of Interest

The authors declare no conflict of interest.

References

1. G. VENTURELLA, V. FERRARO, F. CIRLINCIONE, M. L GARGANO, Medicinal Mushrooms: Bioactive compounds, use, and clinical trials. Int J Mol Sci, 10, 22(2) ,634 (2021**)**.
2. K. KHENI, T.K. VYAS, Characterization of exopolysaccharide produced by *Ganoderma* sp TV1 and its potential as antioxidant and anticancer agent. J Biol Act Prod from Nat, 7, 72,80 (2017).
3. G. DAS, H.S. SHIN, G. LEYVA-GÓMEZ, M. PRADO-AUDELO, H. CORTES, Y.D. SINGH, M.K. PANDA, A.P. MISHRA, M. NIGAM, M.S. SAKLANI, P.K. CHATURI, M. Martorell, N. CRUZ-MARTINS, V. SHARMA, N. GARG, R. SHARMA, J. K. PATRA, *Cordyceps* spp.: A review on its immune-stimulatory and other biological potentials. Front Pharmacol, 11, 6023 (2021).
4. V. MISHRA, S. TOMAR, P. YADAV, M. P. SINGH, Promising anticancer activity of polysaccharides and other macromolecules derived from oyster mushroom (*Pleurotus* sp.): An updated review. Int J Biol Macromol, 182, 1628, 1637 (2021).
5. H.C. KUO, Y.W. LIU, C.C. LUM, K.D. HSU, S.P. LIN, C.W. HSIEH, H.W. LIN, T.Y. LU, K.C. CHENG, *Ganoderma formosanum* exopolysaccharides inhibit tumor growth via immunomodulation. Int J Mol Sci, 22, 11251 (2021).
6. S. CHUN, J. GOPAL, M. MUTHU, Antioxidant activity of mushroom extracts/polysaccharides-their antiviral properties and plausible antiCOVID-19 properties. Antioxidants, 10(12), 1899 (2021).
7. S. PATEL, A. GOYAL, Recent developments in mushrooms as anti-cancer therapeutics: a review. 3 Biotech, 2, 1,15 (2012).
8. G.C. GRAHAM, P. MAYER, R.J. HENRY, A simplified method for prepration of a fungal genomic DNA for PCR and RAPD analysis. Biotechniques, 16,48,50(1994).
9. L. ZHANG, C. FAN, S. LIU, Z. ZANG, L. JIAO, L. ZHANG, Chemical composition and antitumor activity of polysaccharide from Inonotus obliquus. J Med Plants Res, 5,1251, 1260 (2011).
10. W. XU, F. ZHANG, Y.B. LUO, L. MA, X. KOU, K HUANG, Antioxidant activity of a water-soluble polysaccharide purified from Pteridium aquilinum. *Carbohydr Res*, 344, 217, 222 (2009).
11. M. DUBOIS, K. GILLES, J.K. HAMILTON, P.A. REBERS, F. SMITH, A colorimetric method for the determination of sugars. Nature, 168,167(1951).
12. B.A. LEWIS, F. SMITH, *Sugars and Derivatives In : Thin-Layer Chromatography*, 2nd ed, E. STAHL, eds., Springer and Academic Press: New York and London, 1969, pp. 807 – 837.
13. I.F. BENZIE, J.J STRAIN, The ferric reducing ability of plasma (FRAP) as a measure of "antioxidant power": the FRAP assay. Analyt Biochem, 239, 70, 76 (1996).
14. R. RE, N. PELLEGRINI, A. PROTHEGGENTE, A. PANNALA, M. YANG, C. RICE-EVANS, Antioxidant activity applyi ng an improved ABTS radical cation decolorization assay. Free Radical Biol Med, 26 ,1231, 1237 (1999).
15. E. GARCIA, T. OLDONI, S. ALENCAR, A. REIS, A. LOGUERCIO, R. GRANDE, Antioxidant activity by DPPH assay of potential solutions to be applied on bleached teeth. Braz Dental J, 23, 22, 27 (2012).
16. T. MOSMANN, Rapid colorimetric assay for cellular growth and survival: Application to proliferation and cytotoxicity assays. J Immunol Methods, 65, 55, 63 (1983).
17. J.T. BAE, G.S. SIM, D.H. LEE, B.C. LEE, H.B. PYO, T,B. CHOE, J.W. YUN, Production of exopolysaccharide from mycelial culture of *Grifola frondosa* and its

inhibitory effect on matrix metalloproteinase-1 expression in UV-irradiated human dermal fibroblasts. FEMS Microbiol Lett, 251, 347, 354 (2005).

18. A. ZONG, H. CAO, F. WANG, Anticancer polysaccharides from natural resources: A review of recent research. Carbohydr Polym, 90, 1395, 1410 (2012).
19. C.A. SU, X.Y. XU, D.Y. LIU, M. WU, F.Q. ZENG, M.Y. ZENG, W. WEI, N. JIANG, X. LUO, Isolation and characterization of exopolysaccharide with immunomodulatory activity from fermentation broth of *Morchella conica*. DARU J Pharm Sci, 21(5), 1, 6 (2013).
20. R. SASIDHARA, V. BAKKI, Screening of mushrooms for polysaccharides. Iran J. Biotechnol, 12, 73, 76 (2014).
21. M. OSIŃSKA-JAROSZUK, M. JASZEK, M. MIZERSKA-DUDKA, A. BŁACHOWICZ, T.P. REJCZAK, G. JANUSZ, J. WYDRYCH, J. POLAK, A. JAROSZ-WILKOŁAZKA, M. KANDEFER-SZERSZEŃ, Exopolysaccharide from *Ganoderma applanatum* as a promising bioactive compound with cytostatic and antibacterial properties. Biomed Res Int, 2014(743812) 1, 10 (2014).
22. N.H.N. UBAIDILLAH, N. ABDULLAH, V. SABARATNAMA, Isolation of the intracellular and extracellular polysaccharides of *Ganoderma neojaponicum* (Imazeki) and characterization of their immunomodulatory properties. Electron J Biotechnol, 18, 188, 195 (2015).
23. E.R. CARBONERO, A.H.P. GRACHER, D.L. KOMURA, R. MARCON, C.S. FREITAS, C.H. BAGGIO, A.R.S. SANTOS, G. TORRI, P.A.J. GORIN, M. IACOMINI, *Lentinus edodes* heterogalactan: Antinociceptive and anti-inflammatory effects. Food Chem, 111, 531, 537 (2008).
24. G. SOOD, S. SHARMA, S. KAPOOR, P.K. KHANNA, Optimization of extraction and characterization of polysaccharides from medicinal mushroom *Ganoderma lucidum* using response surface methodology. J Med Plants Res, 7(31), 2323, 2329 (2013).
25. L. PENG, S. QIAO, Z. XU, F. GUAN, Z. DING, Z. GU, L. ZHANG, G. SHI, Effects of culture conditions on monosaccharide composition of *Ganoderma lucidum* exopolysaccharide and on activities of related enzymes. Carbo Pol, 133, 104, 109 (2015).
26. Pk. Md MOYEN UDDIN, R. PERVIN, M. S. BISWAS, M.M. RAHMAN, An antioxidant polysaccharide from *Ganoderma lucidum* induces apoptotic activity in breast cancer cell line. bioRxiv 2022.
27. E. SEWERYN, A. ZIALA, A. GAMIAN, Health-Promoting of Polysaccharides Extracted from *Ganoderma lucidum*. Nutrients, 13(8), 2725, 1, 14 (2021).
28. L. YANG, X. KANG, W. DONG, L. WANG, S. LIU, X. ZHONG, D. LIU, Prebiotic properties of *Ganoderma lucidum* polysaccharides with special enrichment of *Bacteroides ovatus* and *B. uniformis* in vitro. J Funct Foods, 92, 105069, 1, 11 (2022).
29. R. BLEHA, L. TŘEŠŇÁKOVÁ, L. SUSHYTSKYI, P. CAPEK, J. COPÍKOVÁ, P. KLOUČEK, I. JABLONSKÝ, A. SYNYTSYA, Polysaccharides from Basidiocarps of the Polypore Fungus *Ganoderma resinaceum*: Isolation and Structure. Polymers, 14, 255, 1, 18 (2022).
30. G. LIU, J. ZHANG, Q. KAN, M. SONG, T. HOU, S. AN, H. LIN, H. CHEN, L. HU, J. XIAO, Y. CHEN, Y. CAO, Extraction, Structural Characterization, and Immunomodulatory Activity of a High Molecular Weight Polysaccharide From *Ganoderma lucidum*. Front Nutr, 9, 846080,1,12 (2022).
31. YC. LIU, XC. TANG, HP. HU, DL. CHEN, YZ. XIE, XW LIANG, XM LI, C. XIAO, LH. HUANG, QP. WU, Genetic diversity and main functional composition of Lingzhi strains from main producing areas in China. AMB Expr, 11, 119, 1, 13 (2021).
32. I. FRAGA, J. COUTINHO, R.M. BEZERRA, A.A. DIAS, G. MARQUES, F.M. NUNES, Influence of culture medium growth variables on *Ganoderma lucidum* exopolysaccharides structural features. Carbohydr Polym, 111, 936, 946 (2014).
33. H. ZHOU, G. LIU, F. HUANG, X. WU, H. YANG, Improved production, purification and bioactivity of a polysaccharide from submerged cultured *Ganoderma lucidum*. Arch Pharm Res, 37, 1530, 1537 (2014).
34. E. SHARPE, A.P. FARRAGHER-GNADT, M. IGBANUGO, T. HUBER, J.C. MICHELOTTI, A. MILENKOWIC, S. LUDLAM, M. WALKER, D. HANES, R. BRADLEY, F. BOU-ABDALLAH, Comparison of antioxidant activity and extraction techniques for commercially and laboratory prepared extracts from six mushroom species. J Agric Food Res, 4, 100130 ,1, 19 (2021).
35. X.M. Li, X.L. Li, A.G. ZHOU, Evaluation of antioxidant activity of the polysaccharides extracted from *Lycium barbarum* fruits in vitro. Eur Polym J, 43, 488, 497 (2007).
36. S. LI, N.P. SHAH, Characterization, antioxidative and bifidogenic effects of polysaccharides from *Pleurotus eryngii* after heat treatments. Food Chem, 197, 240, 249 (2016).
37. T.K.VYAS, P.S. VADNERKER, R. BHAVSAR, K. KHENI, Mushroom exopolysaccharides: Their antioxidant and antiviral properties to boost immunity against COVID-19. In *Immunity boosting functional foods to*

combat COVID-19. 1st ed., A. GIRI, ed; CRC Press: Abingdon, 2021, pp 119 – 132.

38. S. MAHENDRAN, K.T.K. ANANDAPANDIAN, T. SHANKAR, C. CHELLARAM, P. VIJAYABASKAR, Antioxidant properties of *Ganoderma Lucidum* crude exopolysaccharide. Indian J Innov Dev, 1, 8 (2012).
39. H. YEGENOGLU, B. ASLIM, F. OKE, H. YEGENOGLU, B. ASLIM, F. OKE, Comparison of antioxidant capacities of *Ganoderma lucidum* (Curtis) P. Karst and *Funalia trogii* (Berk.) Bondartsev & Singer by using different in vitro methods. J Med Food, 14, 512, 516 (2011).
40. C.R. CORSO, N. MULINARI TURIN de OLIVEIRA, L. MOURA CORDEIRO, K. SAURUK da SILVA, S. da SILVA SOCZEK, V. FROTA ROSSATO, E.S. FERNANDES, D. MARIA-FERREIRA, Polysaccharides with antitumor effect in breast cancer: A systematic review of non-clinical studies. Nutrients, 13(6), 1, 25 (2021).
41. W. HAN, H. CHEN, L. ZHOU, H. ZOU, X. LUO, B. SUN, X. ZHUANG, Polysaccharides from *Ganoderma Sinense* - rice bran fermentation products and their anti-tumor activities on non-small-cell lung cancer. BMC Complement Med Ther, 21**,** 169 (2021).
42. W.L. QIU, W.H. HSU, S.M. TSAO, A.J. TSENG, Z.H. LIN, W.J. HUA, H. YEH, T.E. LIN, C.C. CHEN, L.S. CHEN, WSG, a glucose-rich polysaccharide from *Ganoderma lucidum*, combined with cisplatin potentiates inhibition of lung cancer In Vitro and In Vivo. Polymers, 13, 4353 (2021).
43. D.G. YU, M. WANG, R. GE, Strategies for sustained drug release from electrospun multi-layer nanostructures. WIRES NANOMED NANOBI, 14(3), (2021).
44. M. CAMPI, C. MANCUELLO, F. FERREIRA, Y. MAUBET, E. CRISTALDO, G. ROBLEDO, Bioactive Compounds and Antioxidant Activity of Four Native Species of the Ganodermataceae Family (Agaricomycetes) from Paraguay. Int J Med Mushrooms, *23*(8), 65, 76 (2021).
45. A. KARUPPUSAMY, S. PUTHANPURA, X. YANG, A concise review of mushrooms antiviral and immunomodulatory properties that may combat against COVID-19. Food Chem Adv, 1, 100023, 1, 16 (2022).

ISSN print: 1224-5984
ISSN online: 2248-3942

Rom Biotechnol Lett. 2022; 27(3): 3536-3543
doi: 10.25083/rbl/27.3/3536.3543

Received for publication: June, 10, 2022
Accepted: July 11, 2022

Original paper

In vitro elicitation supports the enrichment of 2H4MB production in callus suspension cultures of *D. hamiltonii* Wight & Arn

UMASHANKAR KOPPADA, PRADEEP MATAM, GIRIDHAR PARVATAM*

Plant Cell Biotechnology Department, Council of Scientific and Industrial Research – Central Food Technological Research Institute, Mysore – 570 020, Karnataka, India

Abstract

I nfluence of elicitation on *in vitro* production of 2-Hydroxy-4-Methoxy Benzaldehyde (2H4MB), a structural isomer of vanillin from callus suspension cultures of *Decalepis hamiltonii* was investigated. *In vitro* culture conditions were optimized to induce callus, suspension culture and biomass followed by metabolite production. Suspension cultures were established using leaf generated friable callus. Maximum content of 2H4MB production 0.079 ± 0.01 mg $100g^{-1}$ DW and biomass 197.5 ± 1.5 gL^{-1} were observed by 4th week of culturing. Elicitation was induced to suspension cultures by using *m*-topolin (*m*T), sodium nitroprusside (SNP), and pectin individually at different concentrations. *m*-topolin (15 µM), pectin (15 µM) and SNP (10 µM) supported 0.31 mg$100g^{-1}$ DW, 0.27 mg$100g^{-1}$ DW and 0.21 mg$100g^{-1}$ of 2H4MB production respectively by 4th week. This data infers that the elicitation improves 2H4MB content in callus suspension cultures of *D. hamiltonii*.

Keywords

Biomass, Elicitor, Callus cell suspension cultures, *Meta*-topolin (N6-(meta-hydroxybenzyl) adenine), Sodium nitroprusside (SNP), Pectin

To cite this article: KOPPADA U, MATAM P, PARVATAM G. *In vitro* elicitation supports the enrichment of 2H4MB production in callus suspension cultures of *D. hamiltonii* Wight & Arn. *Rom Biotechnol Lett.* 2022; 27(3): 3536-3543 DOI: 10.25083/rbl/27.3/3536.3543

*Corresponding author: GIRIDHAR PARVATAM
Ph :- +91-8212516501; Email address: giridharp@cftri.res.in (P.Giridhar);
Orcid ID: 0000-0001-5555-122X

Introduction

Secondary metabolites produced by the plants have wide range of application as industrial raw materials, in medicines, food products as enzymes, and flavour etc**.** Flavors originate from the natural sources mostly from plants have high commercial value. Vanillin is one such metabolite obtained from plants which has wide application in flavoring industry. *Vanilla planifolia* and *V. tahitensis* are major natural sources for the production of vanillin flavor. Due to its high demand and inadequate availability of natural vanillin, synthetically manufactured vanillin is brought in to application to meet the demand. But this has not been readily accepted in some countries due to regulatory guidelines thereby natural vanillin is having persistent demand (Vaithanomsat P & al [1]**).** 2-Hydroxy-4-methoxybenzaldehyde (2H4MB) is an isomer of vanillin, has sweet fragrance can be readily used as alternative to synthetic vanillin. 2H4MB is reported to synthesized through phenyl propanoid pathway and present in few plant species such as *Decalepis hamiltonii, Hemidesmus indicus* (Mehmood Z & al [2]), *Mondia whytei* and root bark of *Periploca sepium* (Yamashita Shi J &al [3]). Biochemical characterization of key step involved in 2H4MB production in *D. hamiltonii* was reported (Kamireddy K & al [4]. In *Decalepis hamiltonii* tubers 2H4MB constitutes 96% of volatile oil, hence is the major aromatic compound and its flavor extract is recognized as GRAS by United States Food and Drug Authority (Nagarajan S & al [5]. This flavor metabolite 2H4MB along with other bioactives reported to have many bioactive properties like antioxidant antimicrobial, and hepatoprotective etc. (Pradeep M & al [6]. This endemic plant *D. hamiltonii* familiar as swallow root, has been constantly over exploited from ages for various applications for its rich aroma and bioactives and currently in the state of endanger.

Plant tissue culture is a promising technique in which *in vitro* production of secondary metabolites in plant cell suspension cultures has been reported from various food and medicinal plants (Dias MI & al [7]). In *D.hamiltonii,* tissue culture technique is reported to be extensively used for cultivation of plants using nodal explants (Obul Reddy B & al [8]), (Sharma S & al [9]) shoot tips (Giridhar P & al [10]), and *in vitro* rooting of micro shoots (Reddy BO & al [11]). Similar, efforts were made to enhance production of flavor metabolites through precursor feeding in callus cell suspension cultures (Pradeep M & al [12]). Nitric oxide as a bioactive molecule is biosynthesized during plant pathogen interactions and reported to exhibit pro-oxidant as well as antioxidant properties in plants (Delledonne M & al [13]). It induces plant defense genes and accumulation of cyclic acid that leads to expression of systemic acquired resistance (Crawford NM & al [14]). Prior art indicates the presence of NO in the plant kingdom and its connection in growth, development (Beligni MV &al [15]), senescence (Jie TU & al [16]), defense responses (Arun M & al [17]) and *in vitro* regeneration (Tan BC & al [18]). SNP at high concentrations stimulated various secondary metabolites such as catharanthine in *Catharantuse roseus* (Xu J & al [19]), hypericin in *Hypericum perforatum* (Xu MJ & al [20]), phenols and flavonoids in Ginkgo biloba *in vitro* cultures (El-Beltagi HS & al [21]). *Meta*-topolin (N^6-(*meta*-hydroxybenzyl) adenine) is a highly active aromatic, unconventional cytokinin isolated and characterized from poplar leaves (Strnad M & al [22]). *Meta*-t opolin (*m*T) has been shown to promote *in vitro* shoot proliferation and improve quality of shoots in several plant species (Aremu AO & al [23]). The potential of *m*T to induce organogenesis from somatic embryo derived cotyledon explants in Cassava (Chauhan RD & al [24]), *Opuntia stricta* (Souza M & al [25]) and *Corylus colurna* (Gentile A & al [26]) was assessed. It is reported to prevent oxidative stress in sugar cane micropropagation (Souza M & al [27]) and production of flavonoids in *Amburana cearensis* (Vasconcelos JNC & al [28]).

However, there are no reports regarding the influence of elicitation on callus suspension cultures of *D. hamiltonii*. As there is a demand in the market for natural flavor (Giridhar P & al [29]), experiments to obtain flavor metabolites through tissue culture will facilitate effective potentiation. Elicitation is technique which was reported to be most significant approach in enhancement of metabolites (Saini RK& al [30]), (Sridevi V & al [31]). Biotic and abiotic elicitors are reported to increase accumulation of metabolites in plant *in vitro* and *in vivo* (Kim HJ & al [32]), (Perez-Balibrea S & al [33]). Accordingly, in the present study, investigations were carried out to determine potential benefit of *m*-topolin, sodium nitroprusside (SNP) and pectin for efficient augmentation of flavour metabolites, since no such studies on *D. hamiltonii* and its metabolites are available.

Materials and methods

Chemicals

Murashige and Skoog medium, 2, 4-Dichlorophenoxyacetic acid, (2, 4-D), Kinetin (Kn), *m*-topolin and Sodium nitroprusside (SNP) of plant tissue culture grade were purchased from Hi-media (Mumbai, India). 2H4MB standards was supplied by Fluka (Switzerland) and pectin from Sigma-Aldrich India. HPLC grade methanol and acetonitrile obtained from Merck (Mumbai, India)

Plant material and culture conditions

D. hamiltonii Wight & Arn., fruits were collected from 12-year-old plant grown at Departmental Garden in CSIR-Central Food Technological Research Institute, Mysore, India. The seeds were separated from the dried capsule and surface sterilization of seeds was done using 0.1% (w v^{-1}) mercuric chloride (Hi-media, Mumbai) for 5 min followed by washing (4-5 times) with autoclaved distilled water (Saini RK & al [30]). Sterilized seeds were inoculated in the MS media with 0.2 µM gibberellic acid (GA_3), (Murashige T,& Skoog F [34]) containing 3% (wv^{-1}) sucrose (Hi-media, Mumbai) and 0.8% (wv^{-1}) of agar (Hi-media, Mumbai) at 25 ± 2 °C under 45 µmol.m^{-2} s^{-1} light for 16 h photoperiod. The leaves of seedling were used as explant for callus induction.

Callus induction and development of suspension cultures

Leaves from 6 weeks old seedling plant were used as explants for callus induction. Leaves from seedling plant were chopped (leaf 1 sq.cm) and inoculated in MS medium containing 9.06 µM 2,4-D (2,4-D, Hi-media, Mumbai), in combination with 2.32 µM Kinetin (Kin , Hi-media, Mumbai), 3% (w/v) sucrose, and 0.8% (w/v) agar for solid media (not for suspension culture) (Pradeep M & al [12]). The pH of the medium was adjusted to 5.8 and autoclaved at 121 °C for 15 min. Callus cultures were maintained at 25 ± 2 °C in 45 µmol.m^{-2} s^{-1} light for 16 h photoperiod. These calluses were sub-cultured every 4 weeks. The friable callus mass that was obtained after two subcultures was used for preparation of suspension cultures. This callus was transferred to 150 ml conical flasks containing 40 ml liquid medium and grown for 8 weeks on a rotary shaker at 95 rpm at 24 ± 2 °C in 16 h photoperiod.

Elicitor treatment

Preparation of elicitor stock solution

Stock solution of 1M concentration *m*-topolin was prepared by dissolving in 0.5N KOH solution. Similarly, sodium nitroprusside, and pectin stock solutions were prepared in sterile distilled water. These stock solutions were sterilized by filtering through 0.22 µm PVDF membrane filters (Durapore) and were inoculated in known concentration to *in vitro* callus cell suspension cultures of *D. hamiltonii*.

Elicitation in callus suspension cultures

m-topolin, pectin, and SNP were added to callus suspension cultures in different concentrations (10, 15 and 20 µM) for evaluation of callus growth and 2H4MB content. Suspension cultures without elicitor was also maintained in similar conditions as a control. Callus biomass was harvested from the suspension culture medium after every week (1st to 4th week) to record callus biomass accumulation as fresh weight (FW) and content of 2H4MB. All the experiments were performed with three replicates for each concentration treatment and the experiment was conducted twice.

Extraction of metabolites

The 2H4MB content from the callus was extracted as described earlier (Pradeep M & al [12]). Callus from suspension cultures were separated using Whatman no.1 filter paper. The solvent extract thus obtained was evaporated to dryness under vacuum. The cell mass in the filter paper was thoroughly washed with distilled water and dried in an oven at 35^0 C for 12 h, weighed and powdered with mortar and pestle. The powder thus obtained was extracted with 2 volumes of ethyl acetate and centrifuged at 10,000 rpm for 15 min. The supernatant was concentrated and dried under vacuum. The dried residue was dissolved with a known volume of methanol and the flavour attributing compounds such as 2H4MB were analyzed.

Screening of flavour metabolites by HPLC and MS analysis

The major flavour ascribing metabolites quantification and confirmation from the solvent extracts of *D. hamiltonii* callus was done by HPLC (SPD-20AD, Shimadzu, Kyoto, Japan) and MS(QTof Ultima Waters Corporation, Micro Mass UK) as reported earlier but with slight modification (Gururaj HB & al [35]). The isocratic mobile phase contained Methanol: Acetonitrile: Water: Acetic acid (47:10:42:1). C18 column (250 x 4.6 mm and 5-µm diameter) was used (Sunfire column, Waters Corporation, MA, USA) for the sample separation and analysis. The flow rate was maintained at 1 ml min^{-1} throughout analysis and the detection wavelength was 280 nm. The samples were respectively injected and mean area for three replicate analyses were calculated. Quantitative analysis was done based on the area of standard (Fluka, Switzerland) for which known amount was injected. 2H4MB in the samples were identified based on the retention time for the corresponding standard. The mass spectral data were accompanied by a Mass Lynux 4.0 SP4 data acquisition system. The ionization mode was negative(Pradeep M & al [11]).

Statistical analysis

The experiments were conducted in a completely randomized design with three replicates. Data were subjected to an analysis of variance (ANOVA). To determine the significant difference, Duncan's multiple range test (DMRT) was performed using SPSS software (Version 17).

Results and discussion

Culture establishment

Cell suspension cultures were developed on MS medium (without agar) containing 3% sucrose, with the combination of 2 mgL^{-1} 2,4-D and 0.5 mgL^{-1} Kinetin , wherein the biomass and 2H4MB content is observed to be good (Pradeep M & al [12]). The callus cultures biomass was observed at regular interval, which shows that the growth of the callus in suspension cultures had some physical changes that include color and texture. During the first week to second week, the light greenish colored callus cells start changing their color to green, later by 4th week it was friable and dark green with 197.52 ± 1.48 gL^{-1} of biomass and after 8 weeks they turn brown with 184.23 ± 1.84 gL^{-1} of biomass (Fig 2a). Maximum 2H4MB production was recorded by 4th week (0.079 ± 0.01 $mg100g^{-1}$ DW), but showed decline from 6th week (0.003 ± 0.014 $mg100\ g^{-1}$ DW) and 8th week (0.002 ± 0.031 mg 100 g^{-1} DW).

Elicitation with m-topolin (mT)

Callus cultured on MS medium supplemented with different concentration of *m*-topolin gave the highest level of 2H4MB among the treatment when compared to control. The results obtained for *D. hamiltonii* callus cultures suggest that their degree of differentiation had a significant influence on the biochemical synthesis of 2H4MB. However, significant accumulation of all the analyzed flavour metabolites 2H4MB was evident with maximum content at 4 weeks and then a depletion in the metabolites content was observed. There was a gradual increase in levels of flavour metabolites from 1st day to the 4th week. The maximum accumulation of 2H4MB was recorded as 0.31 ± 0.01 mg 100 g^{-1} DW in 4 weeks grown culture that supplemented with 15 µM *mT* as a cytokinin inducer (Fig.4). HPLC analysis of ethyl acetate extract of suspension cultures resulted in the detection of 2H4MB with a retention time of 8.5 min at wavelength of 280 nm in standard HPLC chromatogram. Quantitative HPLC determination (Fig. 3) of respective metabolites in samples showed that the contents of 2H4MB were notably higher in *m*T treated suspension cultures. *m*- topolin is reported to be used as an alternative to cytokinin in tissue culture as it has a great influence on physiological property and in production of quality explant (Aremu AO & al [23]), (Ahmad N & al [35]). It was reported to improve *in vitro* morphogenesis, rhizogenesis and increase biochemical content in differ plants (Chauhan RD & al [23])(Gentile A & al [26], (Ahmad A & al [37]). *Meta*-topolin induced *in vitro* regeneration and enhanced the secondary metabolites in the leaf tissues (Khanam MN & al [38]). (Aremu AO & al [39]) reported higher phenolic production in 'Williams' banana treated with *mT* when compared to the BA-treated and control (PGR-free) plants. It is reported to prevent oxidative stress in sugar cane micro propagation (Souza M & al [24]) and production of flavonoids in *Amburana cearensis* (Vasconcelos JNC& al [28]).

Elicitation with Pectin

In the present study, pectin treatments to cultures resulted in only moderate change in their biomass with progressive increase from 2nd to 4th week (Fig. 5a) in comparison to control. The maximum accumulation of 2H4MB 0.29 ± 0.01 mg $100g^{-1}$ DW was found in 4 weeks of cultured cells supplemented with 15 µM of pectin (Fig. 5b). The addition of pectin has shown a significant influence on cell growth in *Gymnema sylvestre* R. Br (VeerashreeV & al [40]). Pectin involved in activating secondary metabolism in *M. citrifolia* cell suspension cultures (Dornenburg H & al [41]), *Calendula officinalis* (Wiktorowska & al [42]*)*, and *Hypericum adenotrichum* (Yamaner O & al [43]) was known. Pectin's structure is a practically and fundamentally diverse class of galacturonic acid rich polysaccharides which can go through plentiful alteration with an accompanying change in physicochemical properties (Wolf S & al [44]).

Elicitation with Sodium nitroprusside (SNP)

The results obtained for *D. hamiltonii* callus cultures with SNP suggest that their degree of differentiation had a significant influence on the biochemical synthesis of 2H4MB (Fig. 6). The maximum accumulation of 2H4MB 0.21 ± 0.01 $mg100\ g^{-1}$ DW was recorded in 4 weeks of cultured cells supplemented with 10 µM concentration of SNP and it was found to be significant (Fig. 6). In plants, various environmental and hormonal stimuli are transmitted either directly or indirectly by nitric oxide (NO) signalling cascades (Delledonne M & al [13]), (Crawford NM & al [14]). A good number of reports reveal the significance of NO, and the usage of sodium nitroprusside (SNP) that form a transition metal nitroxyl anion (NO-) complexes (Beligni MV & al [15]), (Jie TU &al [16]). SNP in combination with auxin 2,4-D is reported to improve cell division that leads to embryonic cell formation in *Medicago sativa* (Ahmad N & al [36]) and shoot multiplication in vanilla (Tan BC & al [18]).

Conclusion

On the basis of our study augmented production of 2H4MB from callus suspension cultures has been demonstrated. The feeding of m*T* , SNP and pectin to *D. hamil-*

tonii callus suspension culture medium supports the augmented accumulation of 2H4MB, with substantial increase in 4.5 folds under *m*-topolin elicitation, followed by 3.6, 2.4 folds in presence of pectin and sodium nitroprusside, which act as an inducer for the cells to increase the production of 2H4MB. The optimized culture conditions conceivably can be applied for scale-up studies for 2H4MB production.

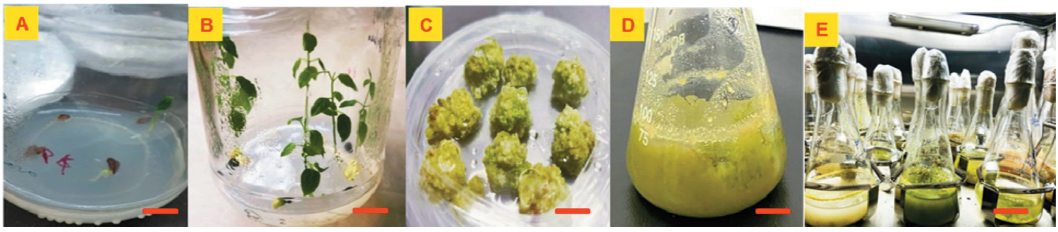

Figure 1. A *In vitro* plants germinated from seeds (bar=10 cm); **B** *In vitro* seedlings of *D. hamiltonii* (bar=10 cm); **C** Callus induction on medium bearing 2,4-D (9.06 µM) & kinetin (2.32 µM) (bar= 5 cm) **D** Callus cell suspension on medium with 9.06 µM 2,4-D and 2.32 µM kinetin after 4 weeks (bar=5 cm); **E** Rotary shaker with suspension cultures (bar=15cm)

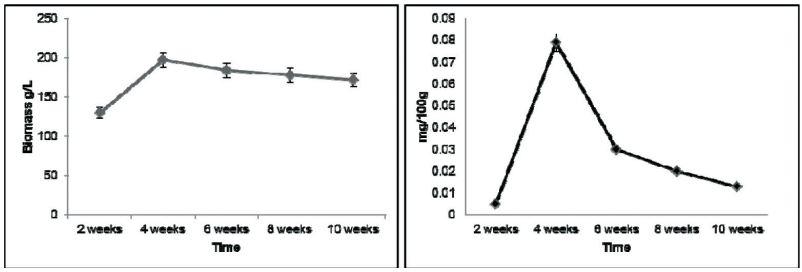

Figure 2. Callus growth and its 2H4MB quantification in suspension cultures. **a)** Callus biomass at different time intervals; **b)** 2H4MB content in callus during its growth.

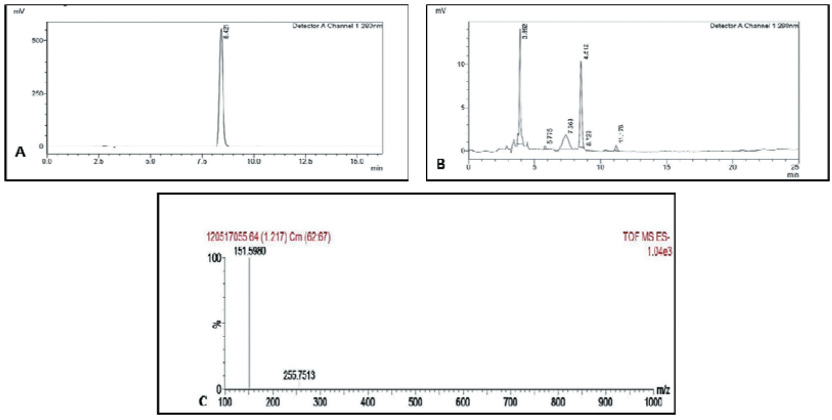

Figure 3. Quantification of 2H4MB using HPLC and confirmation by MS-ESI. **A)** 2H4MB standard; **B)** Chromatogram of Callus elicited with m-topolin ; **C)** MS fragment of 2H4MB Callus elicited with m-topolin

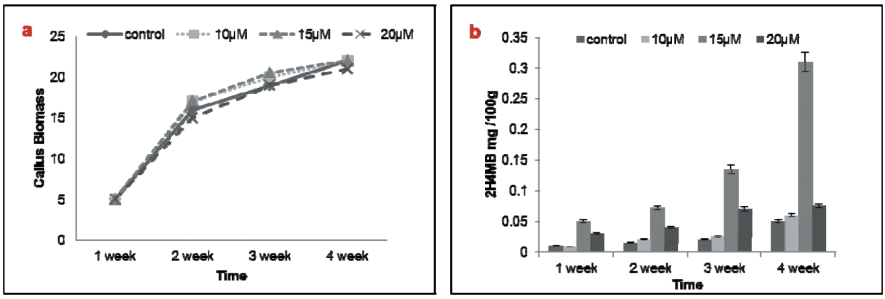

Figure 4. Influence of m-topolin on callus suspension cultures. a) Callus biomass (FW); b) 2H4MB content.

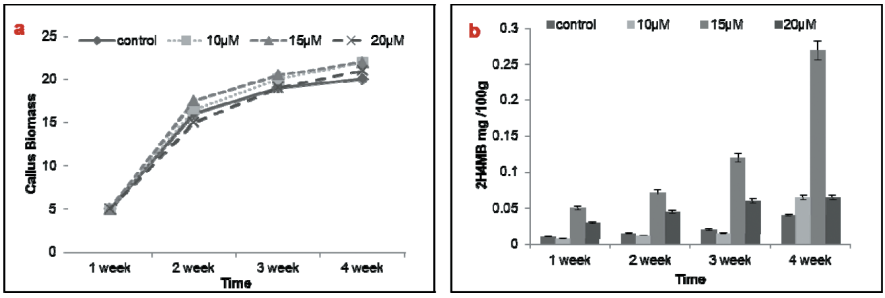

Figure 5. Influence of Pectin on callus suspension cultures. a) Callus biomass (FW); b) 2H4MB content

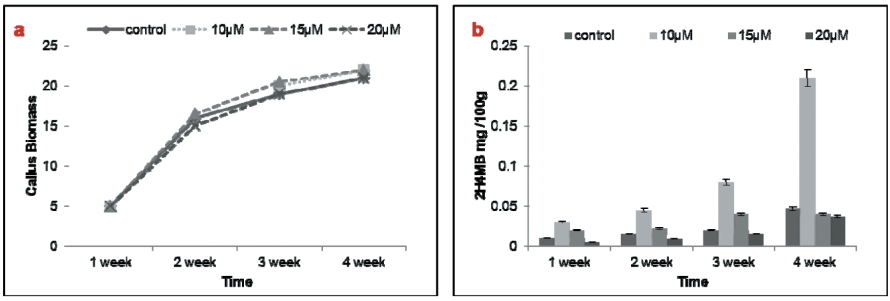

Figure 6. Influence of Sodium nitroprusside on callus suspension cultures. a) Callus biomass (FW); b) 2H4MB content

Conflicts of Interest

The authors declare that there are no conflicts of interest.

Acknowledgements

The authors are thankful to SERB, New Delhi, India for funding the project (SERB/EMR/2016/001049). All the authors are thankful to Director, CSIR-CFTRI, Mysore for providing infrastructure and necessary facilities.

References

1. Vaithanomsat P, Apiwatanapiwat W. Feasibility study on vanillin production from *Jatropha curcas* stem using steam explosion as a pretreatment. *Inter J Chem Biolo Engr.* 2009; 3:839-842
2. Mehmood Z, Dixit AK, Singh A, et al. Indian Herb *Hemidesmus indicus* - A Potential Source of New Antimicrobial Compounds. 2016; 6:734-738. https://doi.org/10.4212/2161-0444.100042
3. Shi J, Yamashita T, Todo A, et al. Repellent from traditional Chinese medicine, *Periploca sepium* Bunge. *Zeitschrift fur Naturforschung Teil* C: *Biochemie, Biophysik, Biologie, Virologie.* 2007; 62:821-825
4. Kamireddy K, Matam P, Giridhar P. Biochemical characterization of a key step involved in 2H4MB production in *Decalepis hamiltonii.* J Plant Physiol. 2017; 214:74-80

5. Nagarajan S, Rao LJM, Gurudutt KN. Chemical composition of the volatiles of *Decalepis hamiltonii* (Wight & Arn). *Flavour Fragance J.* 2001; 16:27–29. https://doi.org/10.1002/1099-1026(200101/02)16:1<27::AID-FFJ937>3.0.CO;2-F
6. Pradeep M, Kiran K, Giridhar P. A Biotechnological Perspective Towards Improvement of *Decalepis hamiltonii*: Potential Applications of Its Tubers and Bioactive Compounds of Nutraceuticals for Value Addition. In: Shahzad A, Sharma S, Siddiqui SA (eds) Biotechnological strategies for the conservation of medicinal and ornamental climbers. *Springer International Publishing, Cham*, 2016; pp 217-238
7. Dias MI, Sousa MJ, Alves RC, Ferreira ICFR. Exploring plant tissue culture to improve the production of phenolic compounds: A review. *Ind. Crops Prod.* 2016; 82:9-22. https://doi.org/10.1016/j.indcrop.2015.12.016
8. Obul Reddy B, Giridhar P, Ravishankar GA. The effect of triacontanol on micropropagation of *Capsicum frutescens* and *Decalepis hamiltonii* W & A. *Plant Cell Tiss Organ Cult.* 2002; 71:253-258. https://doi.org/10.1023/A:1020342127386
9. Sharma S, Shahzad A. Encapsulation technology for short-term storage and conservation of a woody climber, *Decalepis hamiltonii* Wight and Arn. *Plant Cell Tiss Organ Cult* 2012;111 :191-198. https://doi.org/10.1007/s11240-012-0183-0
10. Giridhar P, Gururaj HB, Ravishankar GA. *In vitro* shoot multiplication through shoot tip cultures of *Decalepis hamiltonii* Wight & Arn., a threatened plant endemic to Southern India. *In Vitro Cell. Dev. Biol. Plant.* 2005; 41:77-80. https://doi.org/10.1079/IVP2004600
11. Reddy BO, Giridhar P, Ravishankar GA. *In vitro* rooting of *Decalepis hamiltonii* Wight & Arn., an endangered shrub, by auxins and root-promoting agents. *Curr. Sci*. 2001; 1479-1482
12. Pradeep P, Parvatam G, Shetty NP. Enhanced production of vanillin flavour metabolites by precursor feeding in cell suspension cultures of *Decalepis hamiltonii* Wight & Arn., in shake flask culture. *3 Biotech.* 2017; 7:376. https://doi.org/10.1007/s13205-017-1014-0
13. Delledonne M, Xia Y, Dixon RA, Lamb C. Nitric oxide functions as a signal in plant disease resistance. *Nature*. 1998; 394:585-588. https://doi.org/10.1038/29087
14. Crawford NM, Guo F-Q. New insights into nitric oxide metabolism and regulatory functions. *Trends Plant Sci.* 2005; *10:195-200*
15. Beligni MV, Lamattina L. Nitric oxide counteracts cytotoxic processes mediated by reactive oxygen species in plant tissues. *Planta.* 1999; 208:337-344
16. Jie TU, Wen-Biao S, Lang-Lai XU. Regulation of nitric oxide on the aging process of wheat leaves. *J. Integr. Plant Biol.* 2003; 45:1055-1062
17. Arun M, Naing AH, Jeon SM, et al. Sodium nitroprusside stimulates growth and shoot regeneration in *chrysanthemum*. *Hortic Environ Biotechnol.* 2017; 58:78-84
18. Tan BC, Chin CF, Alderson P. Effects of sodium nitroprusside on shoot multiplication and regeneration of *Vanilla planifolia* Andrews. *In Vitro Cell Dev Biol-Plant.* 2013; 49:626-630. https://doi.org/10.1007/s11627-013-9526-8
19. Xu J, Yin H, Wang W, et al. Effects of sodium nitroprusside on callus induction and shoot regeneration in micropropagated *Dioscorea opposita*. *Plant Growth Regul.* 2009; 59:279-285
20. Xu M-J, Dong J-F, Zhu M-Y. Nitric oxide mediates the fungal elicitor-induced hypericin production of *Hypericum perforatum* cell suspension cultures through a jasmonic-acid-dependent signal pathway. *Plant Physiol.* 2005;139:991-998
21. El-Beltagi HS, Ahmed OK, Hegazy AE. Protective effect of nitric oxide on high temperature induced oxidative stress in wheat (*Triticum aestivum*) callus culture. *Not Sci Biol.* 2016; 8:192–198
22. Strnad M. The aromatic cytokinins. *Physiol. Plant.* 1997; 101:674-688
23. Aremu AO, Bairu MW, Dolezal K, Finnie JF, Van Staden J. Topolins: a panacea to plant tissue culture challenges. *Plant Cell Tiss Organ Cult.* 2012; 108(1):1-6.
24. Chauhan RD, Taylor NJ. Meta-topolin stimulates de novo shoot organogenesis and plant regeneration in cassava. *Plant Cell Tiss Organ Cult.* 2018; 132:219-224. https://doi.org/10.1007/s11240-017-1315-3
25. Souza M, Barbosa M, Zarate-Salazar J, et al. Use of meta-Topolin, an unconventional cytokinin in the *in vitro* multiplication of *Opuntia stricta* Haw. *Biotecnol. Veg.* 19:85–96
26. Gentile A, Frattarelli A, Nota P, et al. The aromatic cytokinin meta-topolin promotes *in vitro* propagation, shoot quality and micrografting in *Corylus colurna* L. *Plant Cell Tiss Organ Cult.* 2017;128:693–703. https://doi.org/10.1007/s11240-016-1150-y
27. Souza M, Barbosa M, Zarate-Salazar J, et al. Use of meta-Topolin, an unconventional cytokinin in the *in vitro* multiplication of *Opuntia stricta* Haw. *Biotecnol. Veg.* 2019;19:85-96
28. Vasconcelos JNC, Brito AL, Pinheiro AL, et al. Stimulation of 6-benzylaminopurine and meta-topolin-induced *in vitro* shoot organogenesis and production of flavonoids of *Amburana cearensis* (Allemao) A.C.

Smith). *Biocatal. Agric. Biotechnol.* 2019; 22:101408. https://doi.org/10.1016/j.bcab.2019.101408

29. Giridhar P, Rajasekaran T, Ravishankar GA. Improvement of growth and root specific flavour compound 2-hydroxy-4-methoxy benzaldehyde of micropropagated plants of *Decalepis hamiltonii* Wight & Arn., under triacontanol treatment. *Sci. Hortic.* 2005; 106:228-236. https://doi.org/10.1016/j.scienta.2005.02.024
30. Saini RK, Harish Prashanth KV, Shetty NP, Giridhar P. Elicitors, SA and MJ enhance carotenoids and tocopherol biosynthesis and expression of antioxidant related genes in *Moringa oleifera* Lam. leaves. *Acta Physiol Plant.* 2014; 36:2695-2704. https://doi.org/10.1007/s11738-014-1640-7
31. Sridevi V, Parvatam G. Impacts of biotic and abiotic stress on major quality attributing metabolites of coffee beans. *J. Environ. Biol.* 2015; 36:377
32. Kim HJ, Chen F, Wang X, Rajapakse NC. Effect of chitosan on the biological properties of sweet basil (*Ocimum basilicum* L.). *J. Agric. Food Chem.* 2005; 53:3696-3701
33. Perez-Balibrea S, Moreno DA, García-Viguera C. Improving the phytochemical composition of broccoli sprouts by elicitation. *Food Chem.* 2011; 129:35-44
34. Murashige T, Skoog F. A Revised Medium for Rapid Growth and Bio Assays with Tobacco Tissue Cultures. *Physiol Plant.* 1962; 15:473-497. https://doi.org/10.1111/j.1399-3054.1962.tb08052.x
35. Gururaj HB, Padma MN, Giridhar P, Ravishankar GA. Functional validation of *Capsicum frutescens* aminotransferase gene involved in vanillylamine biosynthesis using Agrobacterium mediated genetic transformation studies in *Nicotiana tabacum* and *Capsicum frutescens* calli cultures. *Plant Sci.* 2012; 195:96-105.
36. Ahmad N, Strnad M. Meta-topolin: A Growth Regulator for Plant Biotechnology and Agriculture. Springer *Nature*. 2021
37. Ahmad A, Anis M. Meta-topolin Improves *In Vitro* Morphogenesis, Rhizogenesis and Biochemical Analysis in *Pterocarpus marsupium* Roxb.: A Potential Drug-Yielding Tree. *J Plant Growth Regul.* 2019; 38:1007–1016. https://doi.org/10.1007/s00344-018-09910-9
38. Khanam MN, Javed SB, Anis M, Alatar AA. meta-Topolin induced *in vitro* regeneration and metabolic profiling in *Allamanda cathartica* L. *Ind Crops Prod.* 2020; 145:111944. https://doi.org/10.1016/j.indcrop.2019.111944
39. Aremu AO, Bairu MW, Szucova L, et al. Assessment of the role of meta-topolins on *in vitro* produced phenolics and acclimatization competence of micropropagated 'Williams' banana. *Acta Physiol Plant.* 2012; 34:2265-2273. https://doi.org/10.1007/s11738-012-1027-6
40. Veerashree V, Anuradha CM, Kumar V. Elicitor-enhanced production of gymnemic acid in cell suspension cultures of *Gymnema sylvestre* R. Br. *Plant Cell Tiss Organ Cult.* 2012; 108:27-35. https://doi.org/10.1007/s11240-011-0008-6
41. Dornenburg H, Knorr D. Strategies for the improvement of secondary metabolite production in plant cell cultures. *Enzyme Microb. Technol.* 1995; 17:674-684. https://doi.org/10.1016/0141-0229(94)00108-4
42. Wiktorowska E, Długosz M, Janiszowska W. Significant enhancement of oleanolic acid accumulation by biotic elicitors in cell suspension cultures of *Calendula officinalis* L. *Enzyme Microb. Technol.* 2010; 46:14-20. https://doi.org/10.1016/j.enzmictec.2009.09.002
43. Yamaner O, Erdag B, Gokbulut C Stimulation of the production of hypericins in *in vitro* seedlings of *Hypericum adenotrichum* by some biotic elicitors. *Turk J Bot.* 2013; 37:153-159
44. Wolf S, Greiner S. Growth control by cell wall pectins. *Protoplasma*. 2012; 249:169-175. https://doi.org/10.1007/s00709-011-0371-5

ISSN print: 1224-5984
ISSN online: 2248-3942

Rom Biotechnol Lett. 2022; 27(3): 3544-3549
doi: 10.25083/rbl/27.3/3544.3549

Received for publication: July, 20, 2022
Accepted: August 12, 2022

Original paper

Assessment of the antimicrobial activity of some essential oils against multi-resistant bacterial strains

DANIELA-CRISTINA MIHAI (BĂŞA)[1], LIA-MARA DIŢU[1], IRINA GHEORGHE[1], OTILIA BANU[2], GRIGORE MIHĂESCU[1]

[1]University of Bucharest, Faculty of Biology, Bucharest, Romania
[2]Institute of Cardiovascular Diseases Prof. C.C. Iliescu, Bucharest, Romania

Abstract

Volatile oils, also called essential oils, are secreted by plant-specific secretory cells and tissues. These components are a mixture of different substances, primarily mono and sesquiterpenes. Our aim was to assess the antimicrobial activity of different essential oils, i.e. lavender, cloves, eucalyptus, rosemary, thyme and oregano against multidrug resistant bacterial strains belonging to the ESKAPE group.
The most effective oils proved to be the thyme and oregano which induced the occurrence of the largest diameters of the growth inhibition zones against all tested bacterial species. Oregano oil showed the best inhibitory activity against *Pseudomonas aeruginosa*, followed by clove, while thyme oil was the most effevtive against *Staphylococcus aureus* strains.

Keywords essential oils, nosocomial infections, antimicrobial activity, ESKAPE

To cite this article: MIHAI (BĂŞA) DC, LIA-MARA DIŢU LM, GHEORGHE I, BANU O, MIHĂESCU G. Assessment of the antimicrobial activity of some essential oils against multi-resistant bacterial strains. *Rom Biotechnol Lett.* 2022; 27(3): 3544-3549 DOI: 10.25083/rbl/27.3/3544.3549

*Corresponding author: Daniela-Cristina Mihai (Băşa), danielacristina.mihai@gmail.com

Introduction

Volatile oils, also called essential oils, are secreted by plant-specific secretory cells and tissues.These components are a mixture of different substances, primarily mono and sesquiterpenes [1, 2]. More than 5,000 compounds have been identified in the composition of volatile oils, such as mono and sesquiterpenes, aromatic compounds, phenylpropanes and diterpenes. Terpenic compounds are hydrocarbons and oxygenated derivatives such as oxides, ketones, aldehydes, alcohols or their acids, and terpenic alcohols can be esterified [2].

From vegetable products, volatile oils can be obtained by entrainment (distillation) with water vapor, with volatile apolar solvents, by means of fats or by pressing [3].

Volatile oils provide important pharmacological properties, incuding the inhib ition of antibiotic-resistant bacteria growth [4, 5]. Our aim was to assess the antimicrobial activity of different essential oils, i.e. lavender, cloves, eucalyptus, rosemary, thyme and oregano against multidrug resistant bacterial strains belonging to the ESKAPE (*Enterococcus faecium, Staphylococcus aureus, Klebsiella pneumoniae, Acinetobacter baumannii, Pseudomonas aeruginosa,* and *Enterobacter spp*) group. The oils tested in the present study, including lavender, cloves, eucalyptus, rosemary, thyme and oregano were selected for their previously reported antibacterial, bacteriostatic and antiseptic properties [2, 6].

Materials and methods

The study included 30 bacterial strains, both Gram positive and Gram negative, isolated from patients admitted to the Cardiovascular Surgery section of a hospital in Bucharest.

The strains belonged to the *Klebsiella* (12 strains), *Acinetobacter* (8 strains), *Staphylococcus* (5 strains) and *Pseudomonas* (5 strains) genera. The sources of isolation are specified in the tables below (tables 1, 2, 3, 4).

For the study, fresh cultures of 18-20 hours were obtained by seeding the strains studied on solid TSA media (*Tripticase Soy Agar*) and incubation at 37 °C.

The tested essential oils were acheved from commercial producers, i.e. Fares and TrioVerde (Table 5).

Table 1. Bacterial strains belonging to the *Staphylococcus aureus*

Number	Bacterial strains	Source of isolation
1	*Staphylococcus aureus* 882	Blood culture
2	*Staphylococcus aureus* 3118	Nasal exudate
3	*Staphylococcus aureus* 1003/1663	Wound secretion
4	*Staphylococcus aureus* 2971	Nasal exudate
5	*Staphylococcus aureus* 3051	Nasal exudate

Table 2. Bacterial strains belonging to the *Pseudomonas aeruginosa*

Number	Bacterial strains	Source of isolation
1	*Pseudomonas aeruginosa* 5034	Tracheal secretions
2	*Pseudomonas aeruginosa* 914	Central venous catheter
3	*Pseudomonas aeruginosa* 1044	Wound secretion
4	*Pseudomonas aeruginosa* 1441	Urinalysis
5	*Pseudomonas aeruginosa* 845	Blood culture

Table 3. Bacterial strains belonging to the *Acinetobacter baumannii*

Number	Bacterial strains	Source of isolation
1	*Acinetobacter baumannii* 1989	Wound secretions
2	*Acinetobacter baumannii* 1177	Wound secretions
3	*Acinetobacter baumannii* 475	Tracheal secretions
4	*Acinetobacter baumannii* 437	Tracheal secretions
5	*Acinetobacter baumannii* 863	Wound secretions
6	*Acinetobacter baumannii* 693	Wound secretions
7	*Acinetobacter baumannii* 621	Tracheal secretions
8	*Acinetobacter baumannii* 676	Tracheal secretions

Table 4. Bacterial strains belonging to the *Klebsiella pneumoniae*

Number	Bacterial strains	Source of isolation
1	*Klebsiella pneumoniae* 2583	Anal portage
2	*Klebsiella pneumoniae* 1526	Central venous catheter
3	*Klebsiella pneumoniae* 2576	Anal portage
4	*Klebsiella pneumoniae* 2268	Urinalysis
5	*Klebsiella pneumoniae* 5662	Urinalysis
6	*Klebsiella pneumoniae* 5972/8850	Urinalysis
7	*Klebsiella pneumoniae* 6984	Wound secretions
8	*Klebsiella pneumoniae* 5670/8822	Urinalysis
9	*Klebsiella pneumoniae* 6003	Wound secretions
10	*Klebsiella pneumoniae* 6980	Urinalysis
11	*Klebsiella pneumoniae* 2460	Anal portage
12	*Klebsiella pneumoniae* 6982/4091	Urinalysis

Table 5. Bacterial strains belonging to the *Klebsiella pneumoniae*

Code	Name	Provider
1	Lavender	Fares
2	Cloves	Fares
3	Eucalyptus (contains *Eucalyptus globulus* and limonene leaf oil)	TrioVerde
4	Rosemary	Fares
5	Thyme	Fares
6	Oregano (contains essential oil of *Origanum vulgare*, carvacrol, linalol, thymol and limonene)	TrioVerde

Method of qualitative testing of the antimicrobial activity of the essential oils

The testing was performed using the adapted diffusimetric method (according to CLSI recommendations, 2019).

On the surface of the medium Mueller Hinton (without glucose) agarized 2% (pH = 7.2 - 7.4), with the thickness of 4 mm distributed in Petri dishes (Ø = 10 cm) a standardized inoculum (a suspension in physiological water) was seeded "in the canvas" sterile - AFS) from cultures of 18-20 h belonging to the studied bacterial strains, density 1.5 x 108 CFU / ml nephelometrically adjusted with McFarland 0.5 standard.

Subsequently, 10 µl of each essential oil sample was placed in the spot on the surface of the seeded medium. After their free diffusion, the plates were incubated for 16-18 h at 37°C.

The sensitivity was evaluated by measuring the diameters of the growth inhibition zones that appeared around the spot. For some oil samples dilutions were performed in dimethylsulfoxide (DMSO).

Method of the quantitative testing of the antimicrobial activity of the essential oils

The serial microdilution method was performed in liquid medium using the 96-well plates and liquid broth. The intensity of bacterial growth has been appreciated by the absorbance value read spectrophotometrically at 620 nm allowing to establish the minimal inhibitory concentration (MIC) expressed in % of the undiluted essential oil. The MIC was considered as the last concentration at which no microbial growth was observed [7].

Results and Discussions

The results of the qualitative tests to evaluate the antimicrobial activity of the essential oils

The qualitative tests performed by the adapted disc difusion method allowed the evaluation of the degree of sensitivity of all 30 strains to the testes essential oils, by measuring the values of all diameters of inhibition zones and calculating an average value/genus studied (tables 6 - 8). Thus, two suggestive graphs could be drawn to highlight the comparative results of this test (Figures 1, 2).

Analyzing the Figures 1 and 2, it can be seen that the most effective oils proved to be the essential oils of thyme and oregano which exhibited the largest diameters of the growth zones of inhibition against all tested bacterial species (fig. 2).

Oregano oil showed the best inhibitory activity against *P. aeruginosa* strains, while thyme oil induced the largest

Table 6. Diameter values of growth inhibition zones for *S. aureus* strains

***S. aureus*-Diameter of the inhibition zone (mm)**						
Bacterial strain codes	Lavender	Clove	Eucalyptus	Rosemary	Thyme	Oregano
S. aureus 882	11	12	8	10	22*	27*
S. aureus 3118	12	19	15	10	23*	22*
S. aureus 1003/1663	20	15	10	8	22*	31*
S. aureus 2971	9	13	13	14	40*	33*
S. aureus 3051	10	12	16	12	45*	33*
Average diameters	12,42857143	15,1428571	13,285714	10,71428571	28,285714	30,8571429
** oil diluted in DMSO (1/4)*						

Table 7. Diameter values of growth inhibition zones for *P. aeruginosa* strains

***P. aeruginosa* – Diameter of the inhibition zone (mm)**						
Bacterial strain codes	Lavander	Clove	Eucalyptus	Rosemary	Thyme	Oregano
P. aeruginosa 5034	11	14	15	11	23**	32**
P. aeruginosa 914	9	27	12	12	28*	40*
P. aeruginosa 1044	9	11	10	9	19*	36*
P. aeruginosa 1441	10	28	12	11	26**	40**
P. aeruginosa 845	11	20	11	11	22**	34**
Average diameters	10,5	20	11,833333	10,83333333	24,666667	37,6666667
** oil diluted in DMSO (1/4) ; ** oil diluted in DMSO (1/6)*						

Table 8. Diameter values of growth inhibition zones for *A. baumannii* strains

baumannii- Diameter of the inhibition zone (mm)						
Bacterial strain codes	Lavander	Clove	Eucalyptus	Rosemary	Thyme	Oregano
A. baumannii 1989	13	16	20	12	32*	38*
A. baumannii 1177	10	12	9	10	21*	22*
A. baumannii 475	13	16	9	9	25**	15**
A. baumannii 437	11	14	10	10	26*	39*
A. baumannii 863	17	11	19	10	17*	30*
A. baumannii 693	16	20	20	23	40**	39**
A. baumannii 621	15	18	17	10	23**	28**
A. baumannii 676	11	9	10	10	35*	36*
Average diameters	13	13,8947368	12,736842	10,89473684	24,473684	29,8421053
* oil diluted in DMSO (1/4) ; ** oil diluted in DMSO (1/6)						

Table 9. Diameter values of growth inhibition zones for *K. pneumoniae* strains

K. pneumoniae- Diameter of the inhibition zone (mm)						
Bacterial strain codes	Lavander	Clove	Eucalyptus	Rosemary	Thyme	Oregano
K. pneumoniae 2583	12	12	9	11	30*	20*
K. pneumoniae 1526	11	10	9	9	19*	18*
K. pneumoniae 2576	10	12	10	9	15*	13*
K. pneumoniae 2268	11	10	9	10	42*	32*
K. pneumoniae 5662	14	11	10	9	30*	26*
K. pneumoniae 5972/8850	17	11	10	9	15*	16*
K. pneumoniae 6984	8	10	8	10	16*	11*
K. pneumoniae 5670/8822	14	10	9	9	24*	29*
K. pneumoniae 6003	10	12	8	10	23*	30*
K. pneumoniae 6980	8	9	9	9	19*	14*
K. pneumoniae 2460	12	11	10	11	17*	18*
K. pneumoniae 6982/4091	11	16	10	10	25*	38*
Average diameters	11,81481481	11,7037037	9,4814815	9,814814815	22,777778	24,2592593
* oil diluted in DMSO DMSO (1/4)						

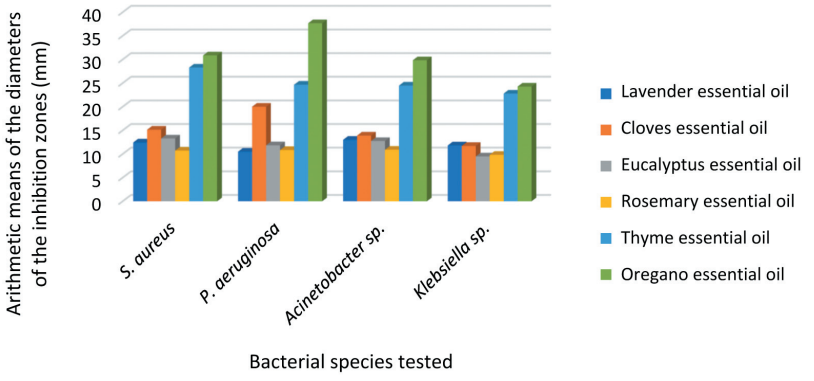

Figure 1. Graphic representation of the values of the arithmetic means of the diameters of the growth inhibition zones.

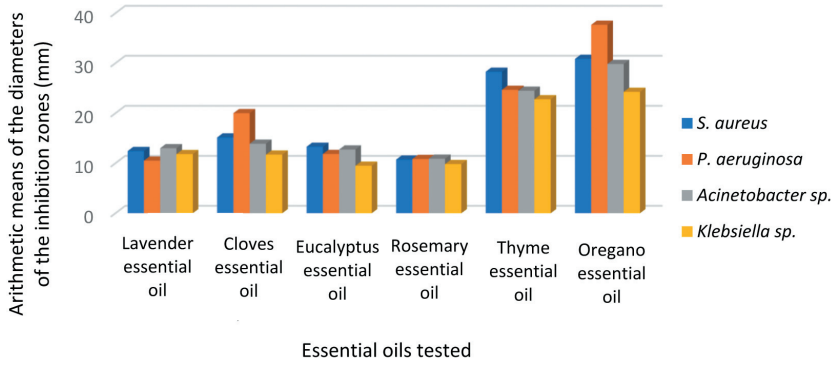

Figure 2. Graphic representation of the values of the arithmetic means of the growth diameters of the inhibition zones.

inhibitory diameter against *S. aureus* strains. Clove essential oil also showed a more pronounced inhibitory effect on the clinical strains of *P. aeruginosa.*

The binary serial dilution method in liquid growth medium allowed the determination of the MIC values for each sample of essential oil separately, at the end also establishing an average CMI value / species tested. Analyzing fig. 3, it can be seen that the lowest CMI values were also recorded for the essential oils of oregano, cloves and thyme, which confirms the qualitative tests on the most effective oils.

Regarding the degree of sensitivity of bacterial strains, it can be seen that the susceptibility profiles of the bacterial strains to the tested essential oils is similar, with a very good activity of oregano, followed by thyme and cloves demonstrated by the low MIC vales, while rosemary, eucaliptus and lavender expressed much higher MIC values (fig. 3).

Among the tested bacterial strains, the most susceptible prove to be the *S. aureus* strains.

Conclusions

Following the interpretation of the results obtained in this study, we can conclude that the most effective oils proved to be the essential oils of thyme, oregano and cloves, which exhibited the largest diameters of the growth zones of inhibition against all tested bacterial strains belonging to the ESKAPE group.

Oregano and clove oil showed the best inhibitory activity against *P. aeruginosa* strains, while thyme oil showed the largest inhibitory diameter against *S. aureus* strains.

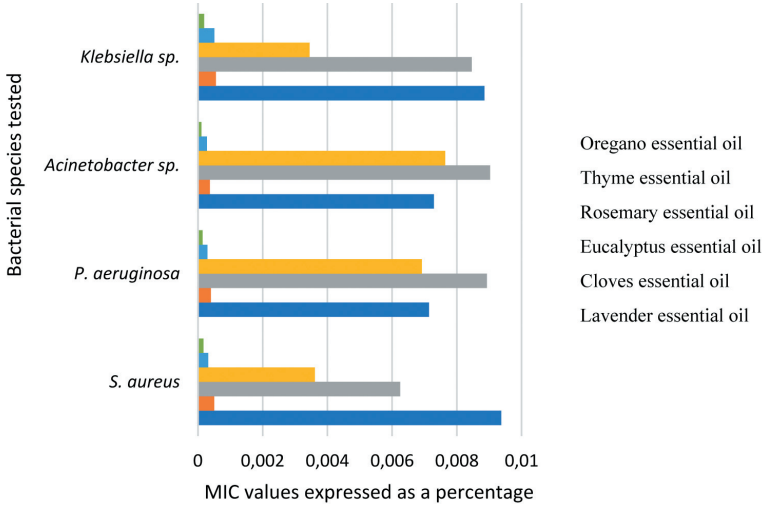

Figure 3. Graphical representation of the degree of sensitivity to the action of different essential oils of clinical bacterial strains.

Regarding the results of the quantitative assay, the susceptibility profiles of the bacterial strains to the tested essential oils was relatively similar, the most active bein, similarly to the qualitative assay results, the oregano, thyme and cloves. This experimental approach may open new perspectives for developing novel strategies to combat the emerging global threat of multiple drug resistance.

References

1. Muntean, L. S., M. Tămaş, S. Muntean, L. Muntean, M. Duda, D. Vârban, & S. Florian, (2007) - Tratat de plante medicinale cultivate şi spontane. Risoprint.
2. Hammer K. A., C. F. Carson, (2011) - Antibacterial and Antifungal Activities of Essential Oils - Lipids and Essential Oils as Antimicrobial Agents, H. THORMAR, ed., John Wiley & Sons, Ltd., pp. 256-293.
3. Ouzzara M. L., W. Louaera, A. Zemanea, A. H. Meniai, (2015) - Comparison of the Performances of Hydrodistillation and Supercritical CO2 Extraction Processes for Essential Oil Extraction from Rosemary (*Rosmarinus officinalis*),Chemical Engineering Transactions, 43: 1129-1134.
4. Zhanel G. G., M. DeCorby, N. Laing, B. Weshnoweski, R. Vashisht, F. Tailor, & P. Lagacé-Wiens, (2008) - Antimicrobial-resistant pathogens in intensive care units in Canada: results of the Canadian National Intensive Care Unit (CAN-ICU) study, 2005-2006. Antimicrobial Agents and Chemotherapy, 52(4), 1430-1437.
5. Rice L. B., (2010) - Progress and Challenges in Implementing the Research on ESKAPE Pathogens, Infect. Control Hosp. Epidemiol., 31 (S1), pp.S7-S10.
6. Chifiriuc M. C., G. Mihăescu, V. Lazăr, (2011) - Medical microbiology and virology, The Bucharest University Press, pp.166-183.
7. Lazar V., Balotescu M.C., Moldovan L., Vasilescu G., Petrache L.M., Bulai D., Cernat R.C. (2005) - Comparative evaluation of qualitative and quantitative methods used in the study of antifungal and antibacterial activity of hydroalcoholic vegetal extracts. Rom. Biotechnol. Lett., 10: 2225–2232
8. Visan D.C., Oprea E. , Radulescu V., Voiculescu I., Biris I.-A., Cotar A.I. , Saviuc C., Chifiriuc M.C., Marinas I.C. (2021) Original Contributions to the Chemical Composition, Microbicidal, Virulence-Arresting and Antibiotic-Enhancing Activity of Essential Oils from Four Coniferous Species. Pharmaceuticals, 2021, 14: 1159.
9. Marinas I.C., Oprea E., Buleandra M., Badea I.A., Tihauan B.M., Marutescu L., Angheloiu M., Matei E., Chifiriuc M.C. (2021)- Chemical Composition, Antipathogenic and Cytotoxic Activity of the Essential Oil Extracted from Amorpha fruticosa Fruits. Molecules, 26:3146.
10. Popa M., Măruțescu L., Oprea E., Bleotu C., Kamerzan C., Chifiriuc M.C., Grădișteanu Pircalabioru, G. (2020) In Vitro Evaluation of the Antimicrobial and Immunomodulatory Activity of Culinary Herb Essential Oils as Potential Perioceutics. Antibiotics, 9: 428.

ISSN print: 1224-5984
ISSN online: 2248-3942

Rom Biotechnol Lett. 2022; 27(3): 3550-3558
doi: 10.25083/rbl/27.3/3550.3558

Received for publication: July, 20, 2022
Accepted: August 12, 2022

Original paper

Effects of prebiotics on acid and bile resistance of *Bifidobacterium lactis* and *Lactobacillus acidophilus* probiotic bacteria

AYLA MUMCU*[,1], AYHAN TEMİZ[2]

[1]Olive Research Institute, Izmir, Turkey
[2]Hacettepe University, Faculty of Engineering, Department of Food Engineering, Ankara, Turkey

Abstract

The effects of prebiotics on acid and bile resistance of probiotics were evaluated. Two commercial strains, *Bifidobacterium lactis* BB-12 and *Lactobacillus acidophilus* LA-5 had higher acid and bile resistance characteristics than the ATCC strains. *B. lactis* BB-12 was the most resistant to acid and bile and showed higher survival capacity. The counts of *B. lactis* BB-12 viable cells in pH 2 medium decreased by 2.7 log unit while the viability of other strains decreased by 4.5-7 log units. The counts of *B. lactis* BB-12 viable cells in the bile medium after 6 and 24 hours of incubation were determined as 6.1 and 2.8 log CFU/ml, respectively, while no viable bacteria could be determined for the other strains after 24 hours of incubation. The acid and bile resistance of probiotic bacteria remarkably varied with the type of prebiotics. Acid and bile resistance properties of *L. acidophilus* LA-5 and *L. acidophilus* ATCC 4356 were found higher when INU was present in the growth medium. Acid and bile resistance properties of *B. bifidum* ATCC 15969 was higher when the medium contained GOS whereas acid and bile resistance of *B. lactis* BB-12 was found to be higher when medium contained XOS.

Keywords Probiotic, prebiotic, acid resistance, bile resistance

To cite this article: MUMCU A, TEMİZ A. Effects of prebiotics on acid and bile resistance of *Bifidobacterium lactis* and *Lactobacillus acidophilus* probiotic bacteria. *Rom Biotechnol Lett.* 2022; 27(3): 3550-3558 DOI: 10.25083/rbl/27.3/3550.3558

*Corresponding author: Ayla Mumcu, ayla.mumcu@tarimorman.gov.tr

Introduction

The effects of probiotics and prebiotics on human health are of great interest to both consumers and food manufacturers and always up to date. Probiotics, derived from the Greek words meaning "for life", are living microorganisms which actively enhance health of consumers by improving the balance of microbiota in the gut when ingested in sufficient numbers (FULLER [1]). The health benefits attributed to probiotic bacteria can be summarized as nutritional benefits, enhancing bio-availability of some minerals, synthesis of vitamins, increase in natural resistance to infectious diseases of the intestinal tract, prevention of diarrhea, reduction of serum cholesterol and lactose intolerance, enhancement of immune system, pre-digestion of proteins, improved absorption, enhancement of bowel motility and maintenance of mucosal integrity (COLLINS and GIBSON [2]; ZIEMER and GIBSON [3]; HOLZAPHEL and SCHILLINGER [4]). The most commonly used probiotics in many functional foods and nutritional supplements are *Bifidobacterium* and *Lactobacillus*, the members of the normal colonic bacterial flora. *Bifidobacterium longum*, *B. bifidum*, *B. breve*, *B. infantis*, *Lactobacillus plantarum*, *L. acidophilus*, *L. helveticus*, *L. rhamnosus*, *L. reuteri* and *L. casei* are the most widely studied probiotic strains and have been shown to exert a wide number of health benefits (GIBSON and ROBERFROID [5]; GIBSON [6]; GISMONDO & al [7]; SHAH [8]; HOLZAPHEL and SCHILLINGER [4]).

Probiotics in the normal intestinal microbiota need some special carbohydrates called "prebiotics" for their survival and growth. Prebiotics, such as fructo-oligosaccharides, gluco-oligosaccharides galacto-oligosaccharides, xylo-oligosaccharides, isomalto-oligosaccharides, gentio-oligosaccharides, lactulose, lactitol, lactosucrose, polydextrose, pyrodextrin, raffinose, resistant starch and inulin are non-digestible substances that provide a beneficial physiological effect on the host by selectively stimulating the favorable growth or activity of a limited number of probiotic bacteria (GIBSON and ROBERFROID [5]; GIBSON [6]; ZIEMER and GIBSON [3]; GIBSON & al [9]; HOLZAPHEL and SCHILLINGER [14; TUOHY & al [10]; SAMINATHAN & al [11]). Prebiotics are short-chain carbohydrates that pass into the large intestine without being digested in the stomach and small intestine. They support the growth and activities of probiotic bacteria such as *Lactobacillus* spp. and *Bifidobacterium* spp. in the large intestine. The synergic combinations of probiotics and prebiotics in nutritional supplements and foods are called synbiotics.

The human gastrointestinal tract is a kinetic micro-ecosystem that enables normal physiological functions of host organism unless harmful and potentially pathogenic bacteria dominate it. It is stated that systematic supplementation of the diet with probiotics, prebiotics or synbiotics may ensure maintaining a proper equilibrium of the microbiota in the gut (GIBSON and ROBERFROID [5]; ZIEMER and GIBSON [3]; HOLZAPHEL and SCHILLINGER [4]; TUOHY & al [10]). Prebiotic compounds are consumed by probiotics as a carbon or energy source in the colon. Increasing in the probiotics count in the gut helps the reduction of gut pathogens. The beneficial effects of probiotics in the gut depend on their viability and metabolic activity. To provide health benefits, probiotics must reach to the large intestine in sufficient numbers. It is recommended to consume about $10^6 - 10^9$ viable probiotic cells per day (LEE and SALMINEN [12]). Therefore, the concentration of probiotic bacteria in a functional food product is suggested to be 10^8 cfu (colony forming unit)/g or over (SHORTT [13]). For sustaining positive effects in humans, the probiotic carrier foods must contain a minimum viable microorganism count of at the time of consumption. However, during the processing, transportation, storage, and marketing of probiotic products, probiotics are harmfully affected by external adverse factors. Furthermore, to fulfill their crucial role, probiotics must survive in the acidic conditions of the stomach and be delivered to the intestines in high numbers. After stomach passage, the probiotic bacteria reach the intestinal tract and meet with bile which also reduce their survival. For this reason, it is extremely important to select the appropriate carrier foods and prebiotics that will increase the resistance of the probiotics and help them to pass adequately into the gastrointestinal tract. Effects of prebiotics on growth and acidifying activity of probiotic bacteria were determined as stated in our previous study (MUMCU and TEMIZ [14]). The results of our previous study indicated that an appropriate prebiotic substance should be selected for each probiotic bacterial strain for its good growth and acidifying performance. In general, as the concentration of the prebiotics increases, the growth and acidifying activity performance of the probiotic strains increases.

Considering the potential influence of prebiotics on the resistance of probiotics to the gastrointestinal conditions, the aim of this study was to investigate the effects of the certain prebiotics on the resistance and viability of probiotic bacteria *in vitro* acid and bile environment (as simulated gastrointestinal conditions).

Materials and methods

Probiotic cultures

Lactobacillus acidophilus ATCC 4356, *L. acidophilus* LA-5 (Chr. Hansen, Denmark), *Bifidobacterium bifidum* ATCC 15969 and *B. animalis* subsp. *lactis* BB-12 (*B. lactis* BB-12; Chr. Hansen, Denmark), purchased in lyophilized form, were used as probiotic test bacteria. *L. acidophilus* cultures were activated in MRS broth (de Man, Rogosa and Sharpe, Merck) at 37 °C for 24 hours. *Bifidobacterium* spp. cultures were activated in RCM broth (Reinforced Clostridial Medium, Fluka) under anaerobic incubation conditions by using anaerobic test kits (GENbox anaer, Biomérieux) at 37 °C for 24 hours.

Prebiotics

As prebiotics, commercial preparations of fructooligosaccharide (FOS; Dora/Orafti, Turkey), inulin (INU; Dora/Orafti, Turkey), galactooligosaccharide (GOS; Oligomate55, Yakult, Japan), soybean oligosaccharide (SOS; Calpis, Japan), and xylo-oligosaccharide (XOS; Suntory, Japan) were used. Stock solutions of 10% prebiotic substances were prepared in distilled water and filter-sterilized by using 0.45 µm pore size membrane filters (Millipore). Considering the results of our previous study (MUMCU and TEMIZ [14]), the prebiotics FOS and INU for *L. acidophilus* ATCC 4356 and *L. acidophilus* LA-5, GOS and SOS for *Bifidobacterium bifidum* ATCC 15969, XOS and SOS for *B. lactis* BB-12 were used in the trials at 2% final concentration.

Basic growth media

MRS broth and RCM without glucose were used as basic growth medium for the growth of *L. acidophilus* LA-5 and *B. lactis* BB-12, respectively.

Saline solution with pH 1, 2 and 3 (similar to gastric juice)

Saline solution (5 g/L NaCl) was adjusted to pH 1, 2 and 3 with 1 N HCl and then sterilized at 121 °C for 15 min.

Bile solution (similar to intestine)

Bile solution containing 0.5% bile (Ox bile, Merck) was prepared in distilled water and then sterilized at 121 °C for 15 min.

Effects of prebiotics to acid tolerance (*in vitro* assay)

For acid tolerance assay, the sterilized saline solutions with pH 1, 2 and 3 were used as gastric juice media. Firstly, the stock solution of the test prebiotic was transferred into the basic growth medium (MRS broth or RCM without glucose) with the final concentration of 2% (w/v). The basic growth medium was used as negative control and glucose (Merck) was used instead of the test prebiotic for comparison. Activated bacterial culture was added into the prebiotic containing media with the final concentration of 1% (v/v) and incubated at 37 °C for 24 h. After the incubation, bacterial cultures were centrifuged at 3000 rpm for 10 min and precipitates were suspended in 4 ml of sterile distilled water. Inoculations of 2% (v/v) were made from the obtained cell suspensions to saline solutions with pH values of 1, 2 and 3. The same amount of cell suspension was transferred directly to 0.5% NaCl solution (pH 5.35) for control. These inoculated solutions were incubated at 37 °C and viable cell counts were assessed after 0, 1/2, 1, 2 and 3 hours of incubation. The effects of prebiotics on the acid-resistance property of probiotic bacteria were evaluated based on the changes in viable cell number levels.

Effects of prebiotics to bile tolerance (*in vitro* assay)

For bile tolerance assay, the sterilized bile solution containing 0.5% bile (similar to intestine) was used. Firstly, the stock solution of the test prebiotic was transferred into the basic growth medium (MRS broth or RCM without glucose) with the final concentration of 2% (w/v).The basic growth medium was used as negative control and glucose (Merck) was used instead of the test prebiotic for comparison. Activated bacterial culture was added into the prebiotic containing media with the final concentration of 1% (v/v) and incubated at 37 °C for 24 h. After the incubation, the cultures were centrifuged at 3000 rpm for 10 min and precipitates were suspended in 4 ml of sterile distilled water. Inoculations of 2% (v/v) were made from the obtained cell suspensions to 25 ml of sterile bile solution. Same amount of cell suspension was transferred directly to 25 ml of sterile distilled water for control. These inoculated solutions were incubated at 37 °C and viable cell counts were assessed after 0, 3, 6 and 24 hours of incubation. The effects of prebiotics on the bile resistance property of probiotic bacteria were evaluated based on the changes in viable cell number levels in bile-containing media.

Statistical analyses

SPSS 15.0 statistical software program was used in the evaluation of the results. The differences in the treatments were established by using the analysis of variance (ANOVA) test at 5% significant level.

Results and Dicussions

Probiotic bacteria should survive during the passage through the stomach and the small intestine and reach enough amount to be effective in the gastrointestinal tract of the host. However, acid secretion in the stomach and bile

secretion in the intestinal tract could significantly affect the probiotic bacterial growth, survival and activities in the gut. On the other hand, it is known that prebiotics can support the growth and activities of probiotic bacteria in the gut. The results of our previous study (MUMCU and TEMIZ [14]) indicated that an appropriate prebiotic substance should be selected for each probiotic bacteria for its maximum growth and acidifying activity. In general, as the concentration of the prebiotics increases, the growth and acidifying activity of the probiotic strains also increases. *Lactobacillus acidophilus* ATCC 4356 and *L. acidophilus* LA-5 exhibited the best growth with FOS and INU, *Bifidobacterium bifidum* ATCC 15696 with GOS and SOS, *B. lactis* BB-12 with XOS and SOS. Considering these results, prebiotics FOS and INU for *L. acidophilus* ATCC 4356 and *L. acidophilus* LA-5, GOS and SOS for *Bifidobacterium bifidum* ATCC 15969, XOS and SOS for *B. lactis* BB-12 were used at the highest concentration (2%) which stimulated the growth of probiotics at maximum level in the trials of the present study. The survival capability of tested bacteria strains varied in terms of prebiotics present in the growth medium. HERNANDEZ & al [15] reported that resistance to gastrointestinal conditions in *Lactobacillus* strains is dependent on the type of carbon source and strain.

Effects of the prebiotics on acid resistance of the probiotic bacteria

The effects of FOS and INU on the acid resistance of *L. acidophilus* ATCC 4356 and *L. acidophilus* LA-5 were evaluated according to the changes in the viable bacterial cell numbers during 3 hours of incubation at pH 1, pH 2 and pH 3 (Figure 1 and Figure 2). Both *L. acidophilus* strains were found to be sensitive to pH 1 medium. No viable bacterial cell was determined at pH 1 after 30 min of incubation. Since the results obtained by pH 3 trials were very close to each other, the effects of FOS and INU on the acid resistance property of both *L. acidophilus* strains were evaluated according to the results obtained at pH 2 trials. As it can be seen in Figure 1 and 2, there were important decreases in the levels of viable bacterial cell especially after the first hour of incubation at pH 2 medium. Both *L. acidophilus* strains showed more acid-resistance when INU was included in the growth medium. The initial viable bacterial cell levels of both *L. acidophilus* strains were approximately 7 log CFU/ml. The initial viable cell numbers of *L. acidophilus* ATCC 4356 and *L. acidophilus* LA-5 decreased to 4 log and 4.9 log CFU/ml with INU, 2.9 log and 3.5 log CFU/ml with FOS, and 2.4 log and 2.3 log CFU/ml with GLU, respectively after 3 hours of incubation at pH 2. Compared to GLU, it was observed that FOS also increased the acid resistance property of these bacterial strains. Although *L. acidophilus* ATCC 4356 displayed the best growth with FOS (MUMCU and TEMIZ [14]), it is noteworthy that INU caused more acid resistance in this bacterial strain than FOS. It was found that the differences between the prebiotic substances and the incubation period were significant in terms of the acid resistance of both *L. acidophilus* strains ($p<0.05$). According to the results of KOCER and UNAL's study [16], it was also found that supplementation with INU may increase the viability of *L. acidophilus* La-5 during the simulation of GI conditions. At pH 3, the decreasing in the level of live bacteria was much less than in pH 2. The changes in the bacterial levels of *L. acidophilus* strains, grown in environments with INU and FOS, during the incubation period in pH 3 were found to be statistically insignificant ($p<0.05$), the changes were very low decrease and almost close to the control. When the results are evaluated in general, it is possible to say that the acid resistance property of *L. acidophilus* LA-5 is higher than that of *L. acidophilus* ATCC 4356.

The effects of GOS and SOS on the acid resistance property of *B. bifidum* ATCC 15696, and XOS and SOS on the acid resistance property of *B. lactis* BB-12 were evaluated

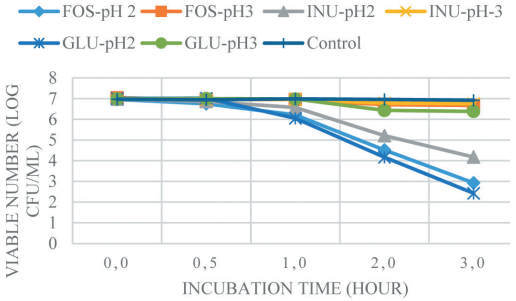

Figure 1. Effects of prebiotics on acid resistance of *L. acidophilus* ATCC 4356 (viable cell count as log CFU/mL at pH 1, 2 and 3)

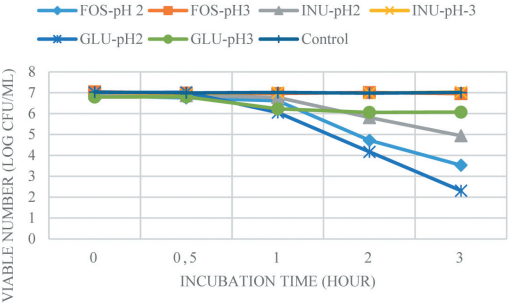

Figure 2. Effects of prebiotics on acid resistance of *L. acidophilus* LA-5 (viable cell count as log CFU/mL at pH 1, 2 and 3)

according to the changes in the viable bacterial cell numbers during 3 h of incubation at pH 1, pH 2 and pH 3 (Figure 3 and Figure 4). Both *Bifidobacterium* spp. strains were found to be sensitive to pH 1 medium, as similarly *L. acidophilus* strains. No viable bacterial cell was determined at pH 1 after 30 min of incubation. *B. bifidum* ATCC 15696 strain showed much more acid sensitivity than *B. lactis* BB-12. No viable *B. bifidum* ATCC 15696 cell was determined at pH 2 after the first hour of incubation (Figure 3). In addition, the viable cell count results of *B. bifidum* ATCC 15696 obtained by pH 2 trials were very close to each other and the difference was statistically insignificant. For this reason, the effects of GOS and SOS on the acid resistance properties of *B. bifidum* ATCC 15696 were compared according to the results obtained by pH 3 trials. It was found that the differences between the prebiotic substances and the incubation period were significant in terms of the the acid resistance of *B. bifidum* ATCC 15696 strain ($p<0.05$). The initial viable cell level (approximatelly 7 log (CFU/ml) of *B. bifidum* ATCC 15696 decreased to 5.1, 3.8 and 4.5 log (CFU/ml) with GOS, SOS and GLU, respectively after 3 hours of incubation at pH 3. The acid resistance property of *B. bifidum*

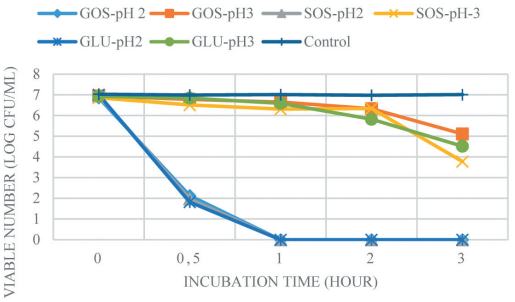

Figure 3. Effects of prebiotics on acid resistance of *B.bifidum* ATCC 15696 (viable cell count as log CFU/mL at pH 1, 2 and 3)

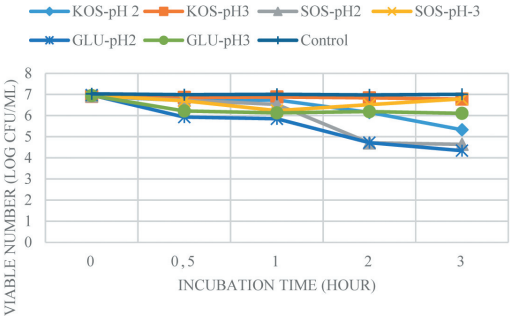

Figure 4. Effects of prebiotics on acid resistance of *B.animalis* subsp. *lactis* BB-12 (viable cell count as log CFU/mL at pH 1, 2 and 3)

ATCC 15696 was higher at pH 3 when GOS was included in the growth medium. The fact that the number of viable bacteria could not be determined at the end of 30 minutes of incubation in pH 1 and after the first hour of incubation in pH 2, it can be said that *B. bifidum* ATCC 15696 was highly sensitive to pH 1 and 2 and the test prebiotics could not be effective on the acid resistance property of this strain at those pH values.

Contrary to the results from *B. bifidum* ATCC 15696 trials, the viable cell count results of *B. lactis* BB-12 obtained by pH 3 trials were very close to each other and the difference was statistically insignificant. For this reason, the effects of XOS and SOS on the acid resistance properties of *B. lactis* BB-12 were compared according to the results obtained by pH 2 trials. It was found that the differences between the prebiotic substances and the incubation period were significant in terms of the the acid resistance of *B. animalis* subsp. *lactis* BB-12 strain ($p<0.05$). The initial viable cell level (approximatelly 7 log (CFU/ml) of this strain decreased to 5.3, 4.5 and 4.3 log (CFU/ml) with XOS, SOS and GLU, respectively after 3 hours of incubation at pH 2. XOS was more effective on the acid resistance property of this strain than SOS. The common prebiotic examined for both *Bifidobacterium* spp. strains was SOS. According to the results obtained by SOS trials, it can be said that *B. lactis* BB-12 is more acid resistant strain than *B. bifidum* ATCC 15696.

Effects of the prebiotics on bile resistance of the probiotic bacteria

The effects of FOS and INU on the bile resistance property of *L. acidophilus* ATCC 4356 and *L. acidophilus* LA-5 were evaluated according to the changes in the viable bacterial cell numbers during 24 hours of incubation at 0.5% bile solution (Figure 5 and Figure 6). The initial viable bacterial cell levels of both *L. acidophilus* strains were approximately 7 log CFU/ml. The effects of the test prebiotics on the bile resistance property of both *L. acidophilus* strains can be easily observed with the results obtained at the third hour of incubation. The viable cell counts of *L. acidophilus* ATCC 4356 and *L. acidophilus* LA-5 detected at the third hour of incubation were 6.3 and 6.9 log CFU/ml with INU, 5.5 and 5.5 log CFU/ml with FOS, and 4.7 and 5.3 log CFU/ml with GLU containing media, respectively. At the sixth hour of the incubation, the viable cell levels of *L. acidophilus* ATCC 4356 were found to be very close to each other, and at the end of the 24-hour incubation, the viable cells could not be determined in any of the samples. In contrast, the viable cell levels of *L. acidophilus* LA-5 at the third and sixth hour of the incubation was significantly higher when

the growth medium was included INU. It was found that the differences between the prebiotic substances and the incubation period were significant in terms of the the bile resistance of *L. acidophilus* strains ($p<0.05$). In the control samples, sharp decreases in the number of viable bacteria were observed in the transition from the sixth hour of incubation to the 24-hour incubation of both test strains. The viable cell level of *L. acidophilus* LA-5 was 4.1 log CFU/ml at the end of the 24-hour incubation period in the medium containing INU whereas no viable *L. acidophilus* ATCC 4356 cell was determined at the end of 24-hour incubation. According to these results, it is possible to say that bile resistance of *L. acidophilus* LA-5 is much more higher than *L. acidophilus* ATCC 4356. The prebiotic INU increased the bile resistance properties of both *L. acidophilus* strains. However, INU had a significantly more positive effect on the bile resistance of *L. acidophilus* LA-5 during the incubation period compared to *L. acidophilus* ATCC 4356.

The prebiotics GOS and SOS were used for the evaluation of the bile resistance of *B. bifidum* ATCC 15696, whereas XOS and SOS for *B. lactis* BB-12 (Figure 7 and Figure 8). *B. bifidum* ATCC 15696 exhibited the highest bile resistance property when the growth medium containing GOS. It was found that the differences between prebiotic substances and the incubation period were important in terms of their effects on the bile resistance ($p<0.05$). *B. bifidum* ATCC 15696 was found to be seriously sensitive to 0.5% bile culture medium. No viable bacterial cell was detected at the third hour of incubation of the bile culture medium containing SOS, and at the sixth hour of incubation when GOS and GLU were included in the bile culture media. After three hours of the incubation, the viable cell counts of *B. bifidum* ATCC 15696 decreased to 4.2 and 3.1 log CFU/ml with GOS and GLU containing media, respectively. At the end of the 24 hour incubation, the presence of viable cells could not be detected in the control sample either. *B. lactis* BB-12 was found to be greatly resistance to 0.5% bile culture medium. In all prebiotic trials, there was very little reduction in the number of viable bacteria during the incubation period. After 24 hours of incubation in bile solutions, viable bacterial cell levels of *B. lactis* BB-12 were determined as 4.8, 4.1 and 2.8 log CFU/ml with XOS, SOS and GLU containing bile culture media, respectively. When the results obtained are evaluated comparatively, it is possible to say that the bile resistance of *B. lactis* BB-12 is much higher than that of *B. bifidum* ATCC 15696. While the prebiotic XOS significantly increased the bile resistance of the *B. lactis* BB-12 strain during the 24-hour incubation period, GOS was able to increase the bile resistance of *B. bifidum* ATCC 15696 strain only to a certain level until the third hour of incubation (Figure 7 and Figure 8).

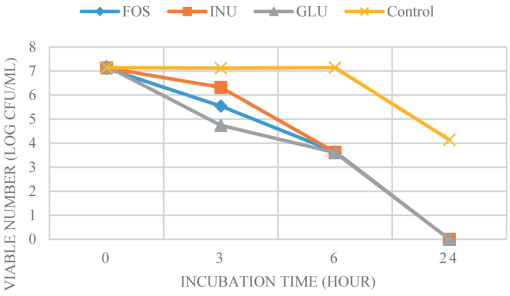

Figure 5. Effects of prebiotics on bile resistance of *L. acidophilus* ATCC 4356 (viable cell count as log CFU/mL)

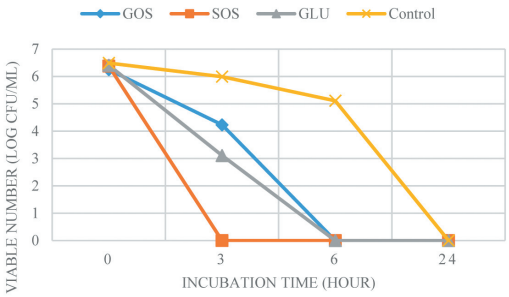

Figure 7. Effects of prebiotics on bile resistance of *B.bifidum* ATCC 15696 (viable cell count as log CFU/mL)

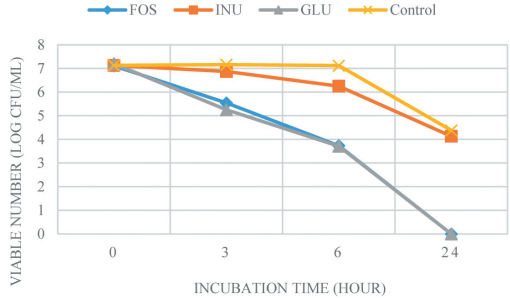

Figure 6. Effects of prebiotics on bile resistance of *L. acidophilus* LA-5 (viable cell count as log CFU/mL)

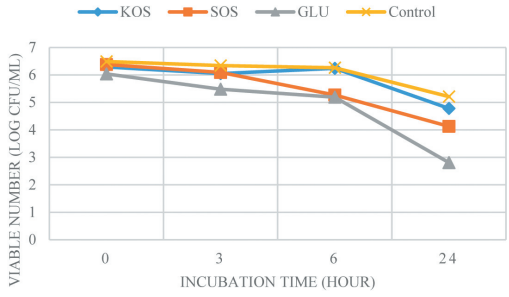

Figure 8. Effects of prebiotics on bile resistance of *B.animalis* subsp. *lactis* BB-12 (viable cell count as log CFU/mL)

The overall results of the present study indicated that commercial probiotic strains, *L. acidophilus* LA-5 and *B. lactis* BB-12 exhibited higher acid and bile resistance characteristics than the other two test probiotic strains. It is possible to compare the acid and bile resistance property of the tested probiotic bacterial strains by looking at the viable cell count results of the strains grown in the medium containing GLU (Figure 1-8). In this sense, it was found that *B. lactis* BB-12 was the most resistance strain to acid and bile. *B. lactis* BB-12 showed higher survival rates compared to other tested bacteria strains. While the viability of the other probiotic strains in the acid medium decreased 4.5-7 log units, the viable bacterial cell level of *B. lactis* BB-12 decreased around 2.7 log unit only. After 24 hours of incubation, the viable cell level of *B. lactis* BB-12 in the bile medium was determined as 2.8 log CFU/ml, whereas the presence of viable cells could not be determined in the other probiotic strains. Although *B. lactis* BB-12 showed more resistance to acid and bile than the other strains, in fact a noteworthy decrease in the viable cell level occurred. KOCER and UNAL [16] studied the effects of inulin, polydextrose and resistant starch (Hi-maize) on viability of *L. acidophilus* La-5, *B. animalis* subsp. *lactis* BB-12, and *Streptococcus thermophilus* under simulated gastrointestinal conditions. They found that *B. animalis* subsp. *lactis* BB--12 presented higher survival rates under gastrointestinal stress than *L. acidophilus* La-5. The higher survivability of *B. animalis* subsp. *lactis* BB-12 compared to that of *L. acidophilus* La-5 during *in vitro* simulated gastrointestinal conditions has also been reported by some other researchers (BEDANI & al [17]; BEDANI & al [18]; CASAROTTI & al [19]; CASAROTTI and PENNA [20]). CRITTENDEN & al [21] demonstrated that B. *animalis* subsp. *lactis* BB-12 was both acid and protease tolerant among commercial strains. In a study of AMBALAM & al [22], the high resistance property of *B. animalis* subsp. *lactis* strains to the bile environment was also verified. VERNAZZA & al [23] found that most bifidobacteria were poorly resistant to strongly acidic conditions with the exception of *B. lactis* BB-12. It was stated that bile tolerances of five *Bifidobacterium* strains were widely variable. *B. lactis* BB-12 and *B. infantis* 20088 were able to grow in the bile-containing medium as demonstrated by the high viable counts. MADUREIRA & al [24] pointed out that resistance property of a *B. animalis* strain to the simulated gastrointestinal conditions (acid and bile environment) was higher than those of *L. casei* and *L. acidophilus* strains.

Another essential result in the present study was the positive effects of the tested prebiotics on improving acid and bile resistance properties of the tested probiotic bacteria. Certain prebiotics added to the growth media enhanced the acid and bile resistance properties of the test probiotic strains. Acid and bile resistant characteristics of *L. acidophilus* ATCC 4356 and *L. acidophilus* LA-5 strains were higher when INU was included in the growth medium. Acid and bile resistance characteristics of *B. bifidum* ATCC 15969 and *B. lactis* BB-12 were higher with GOS and XOS, respectively. As a result, INU in the growth medium increased the acid and bile resistance properties of LA-5 to a higher level whereas acid and bile resistance properties of B. *lactis* BB-12 were further enhanced when XOS was included in the growth medium. These results emphasize the importance of prebiotic selections to be added to the growth medium for increasing the acid and bile resistance of the probiotic strains.

The effect of the prebiotic preparations on the resistance property of the probiotic strains in the simulated gastrointestinal conditions has been investigated by some researchers. KOCER and UNAL [24] showed that the acid and bile resistance property of *L. acidophilus* La-5 was improved by INU among three prebiotics, while the use of Hi-maize resistant starch improved the acid and bile resistance property of *B. animalis* BB-12. Nevertheless, there are also some studies reported that the prebiotics, such as INU, had no effect on the survival of some commercial probiotics under gastrointestinal conditions. The study of BEDANI & al [17] showed that the addition of inulin and/or okara flour (a byproduct of the soymilk industry) into the fermented soy product (FSP) matrix did not affect the survival of *L. acidophilus* La-5 and *B. animalis* BB-12 under *in vitro* simulated gastrointestinal conditions. VERNAZZA & al [23] found that GOS and IMO (isomaltooligosaccharide) among the other substrates were generally well utilized by the tested bifidobacteria strains. It was demonstrated that the prebiotic GOS gave higher growth rates than XOS and was fermented by all of the tested bifidobacteria.

On the other hand, it was stated that probiotic survival in the simulated gastrointestinal conditions was dependent upon the type of matrix (CASAROTTI & al [19]). CASAROTTI & al [19] used MRS, milk and milk supplemented with INU as the matrix and demonstrated that milk and INU protected the probiotic strains from the deleterious conditions of the gastrointestinal conditions. These results suggest that it is critical to formulate the food matrix to be used as probiotic carrier. To exert its beneficial effects on the host, probiotic bacteria should be viable in the product upon consumption (SHAH [8]). Like prebiotics, the components of the food can have a protective effect on probiotics in the stomach and bile environment. WANG & al [25] demonstrated that the delivery of *L. casei* Zhang through fermented soymilk and bovine milk significantly enhanced the viability

of the strain in simulated gastric transit when compared to the pure culture suspended in sterile saline solution. For this reason, it can be said that the use of foods as a carrier in the intake of probiotics would be more appropriate. In addition, it was shown that the fermented milk with the fruit flours (apple, banana and grape) improved *L. acidophilus* tolerance to the simulated gastrointestinal conditions, specifically at days 14 and 28 of storage. Only banana flour had a protective effect on *B. animalis* subsp. *lactis* after 28 days of storage (CASAROTTI and PENNA [20]). The results of the present study indicate that the type of prebiotic exhibit a selective influence on the acid and bile resistance properties of probiotics under simulated gastrointestinal conditions.

Conclusions

The beneficial effects of probiotics depend on their viability and metabolic activity in the gastrointestinal environment. To provide health benefits, probiotics must reach to the large intestine in sufficient viable numbers. The resistance to low pH and bile salts are important for the growth and survival of probiotics in the gastrointestinal tract, thus the appropriate carrier foods and prebiotics should be selected for assuring their adequate passing into the gut. The *in vitro* analysis used in this study provided information about the survival rate of probiotic bacteria under gastrointestinal conditions and the effect of test prebiotics on improving the acid and bile resistance of the test probiotics. There were important differences in the resistance characteristics of probiotics to gastrointestinal conditions. As a result of this study, it is possible to say that *L. acidophilus* LA-5 and *B. animalis* subsp. *lactis* BB-12 were the most resistant strains against acid and bile exposure than the other strains, indicating that these strains would have an increased chance of reaching to the large intestine in sufficient viable numbers. Prebiotics increased the resistance properties of probiotic organisms to gastrointestinal conditions. However, the ability of prebiotics to increase the acid and bile resistance properties of probiotics could vary depending on the prebiotic type in the growth environment. The results of this study indicated that the selection of appropriate probiotics and their appropriate prebiotics to be added to functional products is very important. The results suggest that it is critical to formulate the food matrix to be used as probiotic and prebiotic carrier. Therefore, choosing an appropriate prebiotic and the supplementation with prebiotics for the manufacture of functional products can contribute to maintain the viability of probiotic bacteria during the shelf-life of the product and in the gut. On the other hand, the *in vivo* conditions are difficult to simulate in the laboratory and the conditions of stomach and bile in the gastrointestinal system may vary by individual hosts. Thus, *in vivo* studies should be performed to confirm the *in vitro* studies.

References

1. R. FULLER. History and development of probiotics. *In Probiotics: the Scientific Basis*, Fuller R. (ed), Chapman and Hall, London; pp.1-7 (1992).
2. M.D. COLLINS, G.R. GIBSON. Probiotics, prebiotics, and synbiotics: approaches for modulating the microbial ecology of the gut. *American J Clin Nutr*.; 69 (5): 1052–1057 (1999).
3. C.J. ZIEMER, G.R. GIBSON. An Overview of probiotics, prebiotics and synbiotics in the functional food concept: perspectives and future strategies. *International Dairy Journal*; 8: 473-479 (1998).
4. W.H. HOLZAPHEL, U. SCHILLINGER. Introduction to pre- and probiotics. *Food Research International*; 35: 109-116 (2002).
5. G.R. GIBSON, M.B. ROBERFROID. Dietary modulation of the human colonic microbiota: introducing the concept of prebiotics. *J Nutri*.; 125: 1401–1412 (1995).
6. G. R. GIBSON. Dietary modulation of the human gut microflora using prebiotics. *British J Nutr*.; 80 (2): S209-S212 (1998).
7. M.R. GISMONDO, L. DRAGO, A. LOMBARDI. Review of probiotics available to modify gastrointestinal flora. *Int J Antimicrob Ag*.; 12: 287-292 (1999).
8. N.P. SHAH. Functional foods from probiotics and prebiotics. *Food Technol*; 55 (11): 46-53 (2001).
9. G.R. GIBSON, R.A. RASTALL, M.B. ROBERFROID. *Prebiotics. In Colonic microbiota, nutrition and health*, Gibson GR, Roberfroid MB (ed.), Kluwer Academic Press. Dordrecht, The Netherlands, pp. 101-124 (1999).
10. K.M. TUOHY, G.C.M. ROUZAUD, W.M. BRÜCK, G.R. GIBSON. Modulation of the human gut microflora towards improved health using prebioticsAssessment of efficacy. *Curr Pharm Des*: 11: 75-90 (2005).
11. M. SAMINATHAN, C.C. SIEO, R. KALAVATHY, N. ABDULLAH, Y.W. HO. Effect of prebiotic oligosaccharides on growth of Lactobacillus strains used as a probiotic for chickens. *African J Microbiol Res*; 5 (1): 57-64 (2011).
12. Y. LEE, S. SALMINEN. The coming of age of probiotics. *Trends in Food Science & Technology*; 6 (7): 241-245 (1995).
13. C. SHORTT. The probiotic century: historical and current perspective. *Trends Food Sci Technol*; 10: 411-417 (1999).

14. A.S. MUMCU, A. TEMIZ. Effects of prebiotics on growth and acidifying activity of probiotic bacteria. *Gıda*; 39 (2): 71-77 (2014).
15. O. HERNANDEZ-HERNANDEZ, A. MUTHAIYAN, F.J. MORENO, A. MONTILLA, M.L. SANZ, S.C. RICKE. Effect of prebiotic carbohydrates on the growth and tolerance of *Lactobacillus*. *Food Microbiology*; 30 (2): 355-361 (2012).
16. E. KOCER, G. UNAL. Effects of different prebiotics on viability under *in vitro* gastrointestinal conditions and sensory properties of fermented milk. *Italian Journal of Food Science*; 30: 568-582 (2018).
17. R. BEDANI, E.A. ROSSI, S.M.I. SAAD. Impact of inulin and okara on Lactobacillus acidophilus La-5 and Bifidobacterium animalis Bb-12 viability in a fermented soy product and probiotic survival under in vitro simulated gastrointestinal conditions. *Food Microbiology*; 34: 382-389 (2013).
18. R. BEDANI, M.M.S. CAMPO, I.A. CASTRO, E.A. ROSSI, S.M.I. SAAD. Incorporation of soybean by-product okara and inulin in a probiotic soy yoghurt: texture profile and sensory acceptance. *Journal of the Science of Food and Agriculture*; 94 (1): 119-125 (2014).
19. S.N. CASAROTTI, S.D. TODOROV, A.L.B. PENNA. Effect of different matrices on probiotic resistance to *in vitro* simulated gastrointestinal conditions. *International Journal of Dairy Technology*; 68(4): 595-601 (2015).
20. S.N. CASAROTTI, A.L.B. PENNA. Acidification profile, probiotic in vitro gastrointestinal tolerance and viability in fermented milk with fruit flours. *International Dairy Journal*; 41: 1-6 (2015).
21. R.G. CRITTENDEN, L.F. MORRIS, M.L. HARVEY, L.T. TRAN, H.L. MITCHELL, M.J. PLAYNE. Selection of a *Bifidobacterium* strain to complement resistant starch in a symbiotic yoghurt. *Jornal of Applied Microbiology*; 90: 268-278 (2001).
22. P. AMBALAM, K.K. KONDEPUDI, I. NILSON, T. WADSTRÖM, A. LJUNGH. Bile enhances cell surface hydrophobicity and Biofilm Formation of Bifidobacteria. *Applied Biochemistry and Biotechnology*; 172: 1970-1981 (2014).
23. C.L. VERNAZZA, G.R. GIBSON, R.A. RASTALL. Carbohydrate preference, acid tolerance and bile tolerance in five strains of *Bifidobacterium*. *Journal of Applied Microbiology*,; 100: 846-853 (2006).
24. A.R. MADUREIRA, C.I. PEREIRA, K. TRUSZKOWSKA, A.M. GOMES, M.E. PINTADO, F.X. MALCATA. Survival of probiotic bacteria in a whey cheese vector submitted to environmental conditions prevailing in the gastrointestinal tract. *International Dairy Journal*; 15 (6-9): 921-927 (2005).
25. J. WANG, Z. GUO, Q. ZHANG, L. YAN, W. CHEN, X-M. LIU, H-P. ZHANG. Fermentation characteristics and transit tolerance of probiotic *Lactobacillus casei* Zhang in soymilk and bovine milk during storage. *Journal of Dairy Science*; 92 (6): 2468-2476 (2009).

ISSN print: 1224-5984
ISSN online: 2248-3942

Rom Biotechnol Lett. 2022; 27(3): 3559-3569
doi: 10.25083/rbl/27.3/3559.3569

Received for publication, April, 17, 2021
Accepted, August 12, 2022

Original paper

Impact of ligustrazine on chondrocyte apoptosis in knee osteoarthritis through FAK/PI3K/Akt pathway

GUANYUN SHENG[1,3], JING YANG[2,3], PENG RONG[3], XUEYI YANG[1,3]*

[1]Department of Orthopaedics, Liuzhou Traditional Chinese Medical Hospital, Liuzhou City, Guangxi Province, 545001, China
[2]Department of Intensive Care Unit, Liuzhou Traditional Chinese Medical Hospital, Liuzhou City, Guangxi Province, 545001, China
[3]Guangxi University of Chinese Medicine, graduate school, Nanning City, Guangxi Province, 530000, China

Abstract

Objective: To probe into the impact of ligustrazine on chondrocyte apoptosis in knee osteoarthritis (OA) and its possible mechanism.

Methods: Our team extracted the human primary chondrocytes to construct the IL-1β-induced chondrocyte damage model, detected the impact of ligustrazine on chondrocyte apoptosis through TUNEL and Western blot, applied Western blot to detect the impact of ligustrazine on matrix-degrading enzymes, matrix-associated proteins, as well as FAK/PI3K/Akt pathway, using ELISA detected the impact of ligustrazine on MCP-1, IL8, PEG2 and NO levels, applied FAK/PI3K/Akt pathway inhibitor PF573228 to inhibit FAK/PI3K/Akt pathway to detect whether the chondroprotective impact of ligustrazine was inhibited, constructed a New Zealand rabbit osteoarthritis model, applied HE staining to evaluate the impacts of ligustrazine and ligustrazine+PF573228 on cartilage histomorphology, and applied Western blot to detect the impacts of ligustrazine and ligustrazine+PF573228 on apoptotic proteins, matrix-degrading enzymes and matrix-related proteins in cartilage tissue.

Results: Ligustrazine signally inhibited IL-1β-induced chondrocyte apoptosis, reduced Bax, caspase-9, caspase-3, caspase-7, MMP3, MMP13, collagen X protein expression levels, and reduced MCP-1, IL8, PEG2, and MCP-1. NO contents, promoted collagen II and aggrecan protein expression. Additionally, ligustrazine activated the FAK/PI3K/Akt pathway, and applying PF573228 to inhibit the FAK/PI3K/Akt pathway abolished the chondroprotective impact of ligustrazine. At the in vivo level, ligustrazine activated the FAK/PI3K/Akt pathway to inhibit Bax, caspase-9, caspase-3, caspase-7, MMP3, MMP13, collagen X protein expression levels, promoted collagen II and aggrecan protein expression, and improved cartilage histomorphology.

Conclusion: Ligustrazine exerts chondroprotective impact through FAK/PI3K/Akt pathway

Keywords

Ligustrazine, FAK/PI3K/Akt pathway, knee osteoarthritis, chondrocyte apoptosis

To cite this article: SHENG G, YANG J, RONG P, YANG X. Impact of ligustrazine on chondrocyte apoptosis in knee osteoarthritis through FAK/PI3K/Akt pathway. *Rom Biotechnol Lett.* 2022; 27(3): 3559-3569 DOI: 10.25083/rbl/27.3/3559.3569

*Corresponding author: Xueyi Yang, Department of Orthopaedics, Liuzhou Traditional Chinese Medical Hospital, Guangxi University of Chinese Medicine, 32 North Jiefang Road, Liuzhou City, Guangxi Province, 545001, China, Email: yang_xy11@outlook.com

Introduction

Knee osteoarthritis (OA) is a universal clinical disease in orthopedics, also known as proliferative arthritis in the knee. It is a kind of osteoarthritis, which refers to the primary or secondary degeneration and structural disorder of the articular cartilage of the knee joint. Accompanied by subchondral hyperosteogeny and cartilage exfoliation, the joints are gradually destroyed and deformed, and finally a degenerative disease of knee joint dysfunction [1]. The main clinical manifestations are slow onset and development of joint pain, stiffness, tenderness, crepitus, swelling with limited functional activities. In severe cases, it is the key reason for joint dysfunction, even pain and disability in the elderly [2]. Every epidemiological survey implies that 240 people out of 100,000 suffer from this disease every year. The incidence of knee osteoarthritis is visually related to gender, age, BMI, occupation and other factors. Among them, the incidence of women is signally higher. For men, the elderly is at high risk of knee osteoarthritis. The prevalence rate can reach about 50% for people over 65, and about 80% for those over 75 [3].

At present, joint replacement clinically is still the main therapy for treating end-stage knee osteoarthritis, and there is still a lack of effective methods to prevent knee osteoarthritis from entering end-stage [4]. OA pathogenesis has not been fully studied. Among them, a large amount of evidence reveals that chondrocyte apoptosis acts pivotally in OA occurrence and development, and the number of chondrocyte apoptosis links closely with the severity of arthritis [5]. Chondrocytes are key in the structure of cartilage tissue. Mature chondrocytes are extremely weak in proliferation. Once chondrocytes enter the apoptotic process, they are almost impossible to regenerate. This will eventually result in declined extracellular matrix synthesis and enhanced degradation, thereby accelerating OA progression [6]. At present, it is generally believed that inhibiting chondrocyte apoptosis is available to delay OA progression.

Ligustrazine is the main active ingredient in the traditional Chinese medicine *Ligusticum chuanxiong Hort*. Ligustrazine injection has long been applied to treat ischemic stroke, coronary heart disease, diabetic nephropathy, and knee arthritis [7]. In the past few decades, a large number of research findings pointed out that ligustrazine has anti-inflammatory, -oxidant, -platelet, and -apoptotic as well as other pharmacological activities. In treating OA, ligustrazine has presented good clinical effect. First of all, studies have pointed out that ligustrazine is available to signally inhibit osteoarthritis-induced articular cartilage degradation. For example, the research by Liang [8] et al. pointed out that ligustrazine is available to reduce GAG degradation and MMP-3, MMP-13, COX-2, iNOS, type X collagen expressions, while increase TIMP-1 and type II collagen expressions. Additionally, other research findings indicate that ligustrazine can significantly inhibit OA-induced increase in oxidative stress, inhibit chondrocyte apoptosis, and reduce mitochondrial membrane potential [9]. But at present, the main mechanism of ligustrazine inhibiting chondrocyte apoptosis is still not clear. In this work, our team intend to probe into the main mechanism of ligustrazine inhibiting chondrocyte apoptosis, thus providing a basis for the clinical application of ligustrazine.

Methods

Primary chondrocyte culture

The isolation and culture of human-derived chondrocytes are as described above [10]. Here is a brief description in the following. In accordance with the approved guidelines, our team processed normal human articular cartilage tissues, and later prepared the digested chondrocytes with 0.2% collagenase II (Sigma) in Dulbecco's modified Eagle's medium (DMEM, Invitrogen, USA). After filtration and centrifugation, our team washed them with sterile phosphate buffer saline (PBS), and the cultured the extracted chondrocytes in DMEM containing 10% fetal bovine serum (FBS, Invitrogen) at 37°C, 5% CO2 humidified incubator. We changed the medium every two days, and obtained the first generation of human-derived primary chondrocytes after two weeks.

Western blot

Our team lysed the cartilage or chondrocyte tissue was with RIPA lysis buffer containing protease inhibitors, and then centrifuged it in a low-temperature high-speed centrifuge at 14000×g for 30 min at 4°C, and taken the supernate. We applied the BCA experiment to determine the protein content of the sample and adjusted it to the same concentration with RIPA lysis buffer. After protein denaturation, our team 20μg sample loading each, electrophoresed in 8-12% SDS-polyacrylamide gel (Bio-Rad, USA), and later transferred to PVDF membrane. After blocking with 5% skim milk for 1 hour, our team incubated the primary antibody overnight at 4°C, later incubated the PVSF membrane with the peroxidase-bound secondary antibody for 2 hours, performed the color reaction through ECL, and quantified the protein through Image J software.

TUNEL

In this work, our team applied the TUNEL to detect chondrocyte apoptosis in situ, spread the primary chondrocytes in a 6-well plate, washed with PBS, fixed with 4% paraformaldehyde for 20 minutes, blocked with 5% BSA for 1 hour,

and then treated with the TUNEL reaction mixture for 1 hour (Roche), finally examined the apoptotic cells under microscopes (LSM 510; Zeiss: Jena, Germany), and calculated the percentage of TUENL-positive cells (apoptosis).

ELISA to detect IL8 and MCP-1 level

After the drug treatment, our team collected the supernate in cell culture solution, and detected IL-8 and MCP-1 contents in cell supernate via ELISA, collected the cells and applied BCA to detect the total cell protein contents, and expressed IL-8 and MCP-1 content as the ratio of protein content (ng/g).

Detection of NO and PGE2 contents in cell supernate

After the drug treatment, our team collected the supernate in cell culture solution, and detected NO and PGE2 contents in cell supernate via ELISA, and applied nitrate reductase to determine the NO content at 550nm.

Animal feeding

In this work, our team purchased 80 male SD clean-grade New Zealand rabbits from Beijing Weitong Lihua Experimental Animal Technology Co., Ltd. (production license number: SCXK (Beijing) 2018-004, animal qualification number: No.1100112011035947), kept all experimental animals in a clean-grade animal room, with breeding temperature at 20-26°C (daily temperature difference ≤ 4°C), and 40-70% relative humidity, artificial lighting, alternating light and shade for 12 hours.

Osteoarthritis model [11]

In total 80 clean-grade New Zealand rabbits qualified for quarantine, our team selected 20 at random as normal control group, and the remaining animals were modeled. After fasting overnight before surgery and weighing, our team injected intraperitoneally 2% sodium pentobarbital (60 mg/kg) into rabbits for anesthesia. After anesthesia, made rabbits lie supine and fixed them, performed skin preparation skin on the right knee joint, and measured it. Later our team routinely disinfected the scope of surgery, spread surgical towels, applied a scalpel to make a longitudinal incision on the inside of the knee, separated the subcutaneous tissue to find the white patellar tendon, and cut the joint capsule along the inner side, dislocated the lateral patella (toward the outside of the knee), bent the knee joint to find the anterior cruciate ligament, cut and exposed the inner meniscus with ophthalmic scissors, put the meniscus back into the joint cavity, straightened the knee joint, reset the patella, and finally closed the wound with suture layer by layer. Through the anterior drawer test our team verified the operation findings. Each animal was injected intramuscularly with 80,000 units of penicillin for 3 consecutive days. If an infected animal was found, the number of injections could be elevated. They were returned to the cage after surgery. Treadmill exercise (20 m/min) was started on the second day after the operation, for 6 consecutive days per week, one day off, each time 30 min for 3 consecutive weeks. Our team screened the successful animals molding, and after random grouping, administered the animals in each group in accordance with the dosage, concentration and volume in the following table. The specific dosage was in the following(Table 1)

Table 1. Test design for dosage

	Groups	Dosage (mg/kg)	Volume (ml/each)	The number of animals
1	Normal control group	0	2	20
2	Model control group	0	2	20
3	Ligustrazine group	20mg/kg	2	20
4	PF573228+ ligustrazine group	10mg/kg + 20mg/kg	2	20

HE staining

Our team sacrificed the rabbits to be tested, separated cartilage tissues, fixed with them 4% paraformaldehyde/PBS (pH 7.4) for 24 hours, later embedded in paraffin to prepare 20 μm paraffin sections, applied HE staining kit (Biyuntian Biological Technology Co., Ltd.) for staining in strict accordance with the instructions.

Statistical experiment method

Our team applied descriptive analysis for general status and other information, quantified indicators, and calculated by group mean ± standard deviation ($\bar{X} \pm SD$). We performed the comparison between the two groups through t test, and $p<0.05$ was considered statistically significant. In the comparison between multiple groups, our team analyzed the data of various indicators based on the following procedures:

Our team applied Levene's to test the homogeneity of variance. If there was no statistical significance ($P>0.05$), applied one-way analysis of variance (ANOVA) for statistical analysis. If ANOVA was statistically significant ($P\leq0.05$), applied LSD for a comprehensive comparison. If the variance was not uniform ($P\leq0.05$), our team performed Dunnett's T3 test for statistical analysis and applied SPSS 23.0 for the above statistical operations.

Results

IL-1β induced chondrocyte apoptosis and increased metabolic activity in a dose-dependent manner

The pathological process of osteoarthritis is manifested as chondrocyte apoptosis, increased matrix degrading-enzyme expression, enhanced extracellular matrix (ECM) degradation, and increased inflammatory factor expression in articular cartilage tissue. A large number of studies have revealed that exposure of chondrocytes to the pro-inflammatory cytokine IL-1β is available to induce pathological phenotypes similar to that in the articular chondrocytes during OA progression, including cell apoptosis and increased decomposition activity. Therefore, our team applied 0, 3, 10, 15 μg/ml IL-1β to treat chondrocytes. Consistent with literature reports, IL-1β increased apoptosis-related proteins expression levels, including caspase-9, caspase-3, and caspase-7 in a dose-dependent manner (P<0.05) (Figure 1A).

Additionally, IL-1β was up-regulated in a dose-dependent manner by which it promoted matrix degrading-enzyme expression levels, like MMP3, MMP13, and collagen X (P<0.05), while down-regulated collagen II, and aggrecan protein expression levels (P<0.05) (Figure 1B). Our subsequent research findings pointed out that IL-1β increased MCP-1, IL-8, NO and PGE2 contents in a dose-dependent manner (P<0.05) (Figure 1C), which indicates that IL-1β induces chondrocyte apoptosis and catabolism activity in a dose-dependent manner.

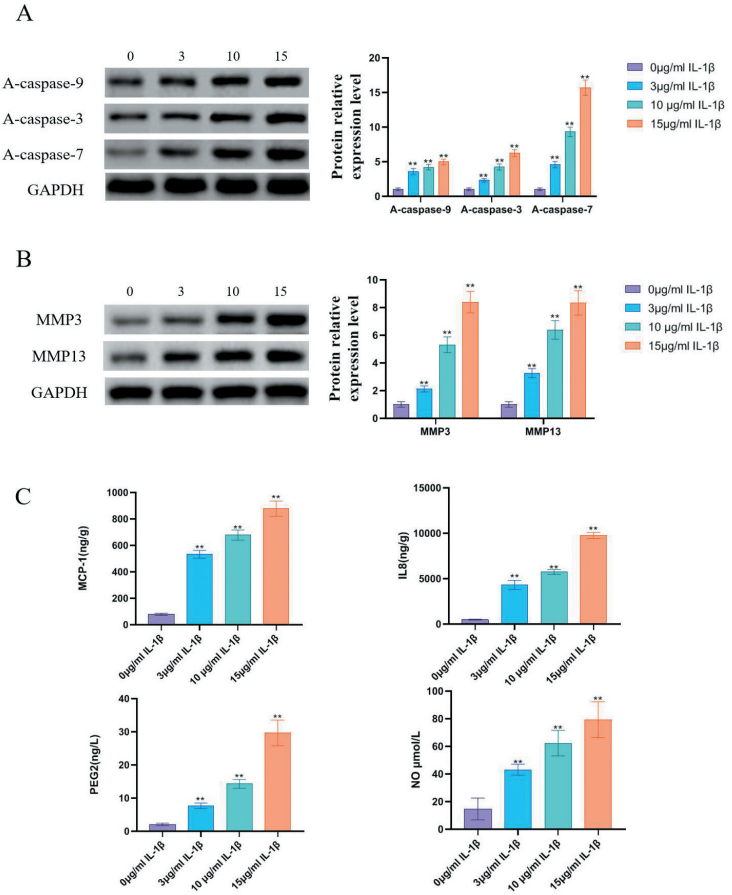

Figure 1. IL-1β induced chondrocyte apoptosis and enhanced its metabolic activity in a dose-dependent manner. Figure 1A Western blot to detect the impact of IL-1β on apoptotic protein content such as caspase-9, caspase-3, and caspase-7 in chondrocytes (n=3). Figure 1B Western blot to detect the impact of IL-1β on chondrocyte matrix degrading enzymes like MMP3, MMP13 as well as extracellular matrix collagen II, aggrecan and collagen X expression levels (n=3). Figure 1C Impact of IL-1β on inflammation-related factor content like MCP-1, IL-8, NO and PGE2. ** represented the control group V.S. IL-1β model group P<0.05;

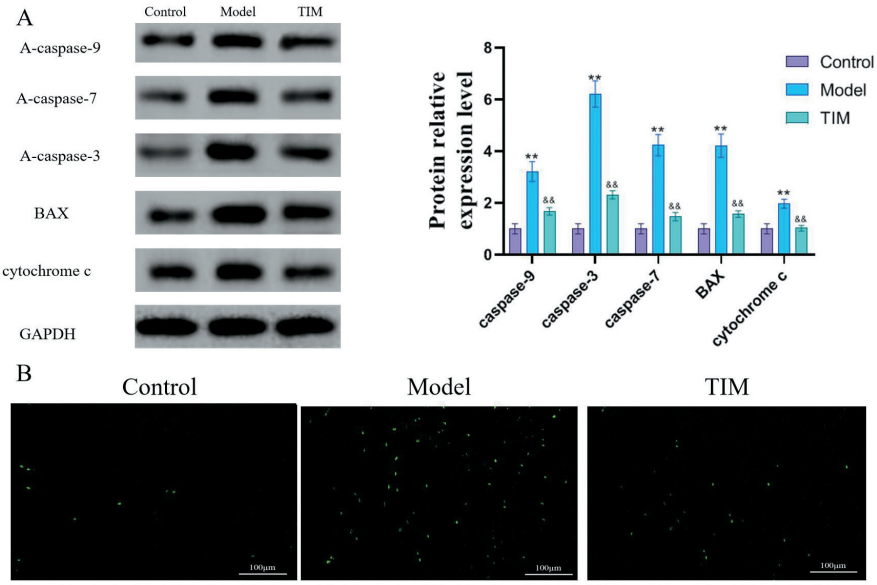

Figure 2. Ligustrazine inhibited IL-1β-induced chondrocytes apoptosis. Figure 2A Western blot test to detect the impact of ligustrazine on caspase-9, caspase-3, caspase -7, Bax, cytochrome c protein and other apoptotic protein levels (n=3). Figure 2B TUNEL to detect the impact of ligustrazine on chondrocyte apoptosis level induced by IL-1β (n=3). ** represented the control group V.S. IL-1β model group $P<0.05$; && represented the IL-1β model group V.S. Ligustrazine group $P<0.05$.

Ligustrazine inhibited IL-1β-induced chondrocyte apoptosis

Since articular cartilage completely relies on chondrocyte to maintain the extracellular matrix, damage to chondrocyte function and viability will result in articular cartilage failure. The degree of cartilage damage is certainly related to chondrocyte apoptosis. Chondrocyte apoptosis and matrix loss may form a positive feedback loop that promotes each other.

In this work, our team applied TUNEL and Western blot to probe into the impact of ligustrazine on IL-1β-induced chondrocyte apoptosis level. Our research pointed out that in comparison with those in the IL-1β model group, ligustrazine could signally inhibit IL-1β-induced increase in caspase-9, caspase-3, caspase-7, Bax, cytochrome c protein expressions ($P<0.05$) (Figure 2A). TUNEL findings pointed out that in comparison with those in the IL-1β model group, ligustrazine could visually inhibit the IL-1β-induced increase in the number of apoptotic cells ($P<0.05$) (Figure 2B). Our research findings indicate that ligustrazine is available to visually inhibit IL-1β-induced chondrocyte apoptosis.

Ligustrazine inhibited IL-1β-induced increase in inflammation-related factors and metabolic activity

Aiming to further detect the impact of ligustrazine on IL-1β-induced increase in inflammation-related factor levels and enhanced metabolic activity, our team applied Western blot to detect the impact of ligustrazine on MMP3 and MMP13, as well as collagen II, aggrecan, and collagen X protein expression levels. The experimental findings pointed out that in comparison with those in the IL-1β model group, ligustrazine could signally inhibit IL-1β-induced increase in MMP3, MMP13, collagen X protein expressions ($P<0.05$). Additionally, in comparison with those in the IL-1β model group, ligustrazine could visually increase collagen II and aggrecan protein expressions inhibited by IL-1β (Figure 3A).

Our subsequent research findings pointed out that ligustrazine could signally inhibit the IL-1β-induced increase in MCP-1, IL-8, NO and PGE2 levels ($P<0.05$) (Figure 3B). The research findings indicate that ligustrazine inhibited IL-1β-induced increase in inflammation-related factor level and the metabolic activity.

Ligustrazine activated FAK/PI3K/Akt pathways

Aiming to probe into the relative mechanism of ligustrazine inhibiting chondrocyte apoptosis, increase in matrix decomposition protein expression, and inflammation-related factor expression. In this research, our team probed into the influence of ligustrazine on the FAK/PI3K/Akt pathway. Focal adhesion kinase (FAK) is a non-receptor tyrosine kinase that accelerates cytoskeleton dynamics to regulate cell

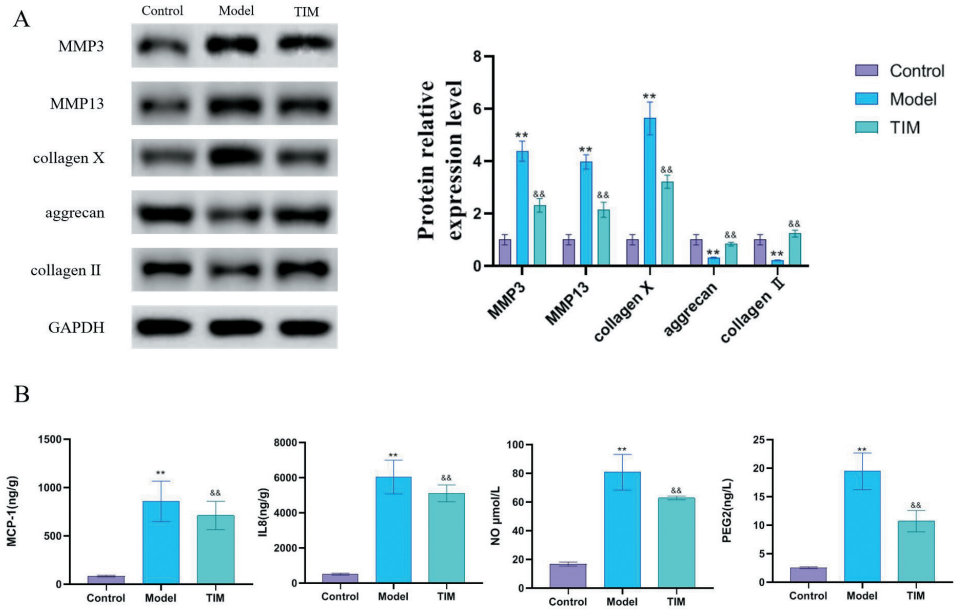

Figure 3. Ligustrazine inhibited IL-1β-induced increase in inflammation-related factor levels and enhanced metabolic activity. Figure 3A Western blot to detect the impact of ligustrazine on IL-1β-induced MMP3, MMP13, collagen II, aggrecan, and collagen X protein expression levels (n=3). Figure 3B Impact of ligustrazine on inflammation-related factor level including MCP-1, IL-8, NO and PGE2. **represented the control group V.S. IL-1β model group $P<0.05$; && represented the IL-1β model group V.S. Ligustrazine group $P<0.05$.

movement. A large number of studies have pointed out that the FAK/PI3K/Akt pathway acts pivotally in the pathological process of osteoarthritis. In this work, our experimental findings pointed out that in comparison with the IL-1β model group, ligustrazine could signally promote p-FAK/FAK, p-PI3K/PI3K and p-Akt/Akt protein expression levels ($P<0.05$) (Figure 4). Our findings pointed out that ligustrazine could activate the FAK/PI3K/Akt pathway, and its protective effect on chondrocytes may be related to the activation of the FAK/PI3K/Akt pathway.

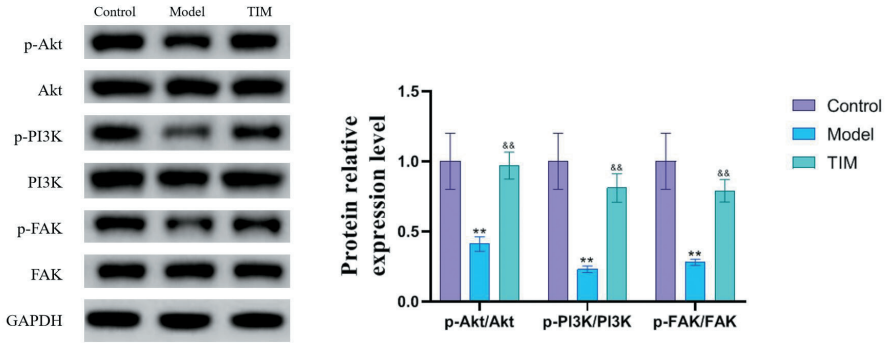

Figure 4. Ligustrazine activated the FAK/PI3K/Akt pathway. Western blot to detect the impact of ligustrazine on p-Akt/Akt, p-PI3K/PI3K and p-FAK/FAK expression levels in chondrocytes (n=3). ** represented the control group V.S. IL-1β model group $P<0.05$; && represented the IL-1β model group V.S. Ligustrazine group $P<0.05$.

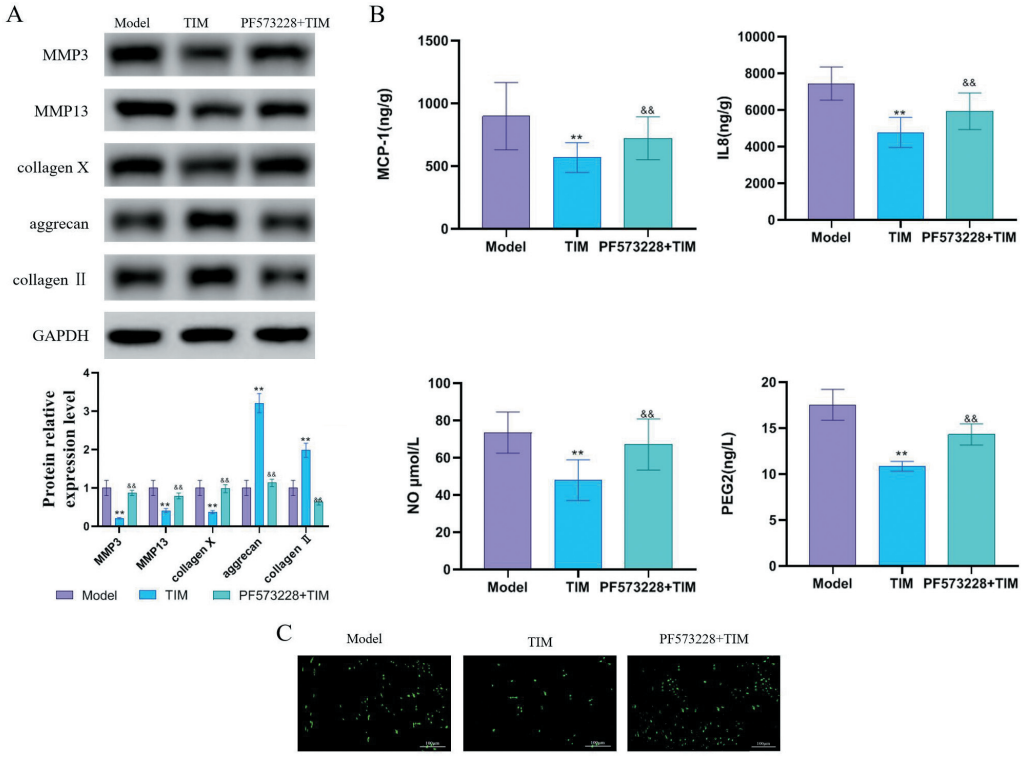

Figure 5. Inhibiting FAK/PI3K/Akt pathway abolished the chondroprotective effect of ligustrazine. Figure 5A Western blot to detect the impact of inhibiting FAK/PI3K/Akt signaling pathway on the ability of ligustrazine to inhibit matrix degradation (n=3). Figure 5B TUNEL to detect the impact of inhibiting FAK/PI3K/Akt signaling pathway on the anti-apoptotic effect of ligustrazine (n=3). Figure 5C Impact of inhibiting FAK/PI3K/Akt signaling pathway on the anti-inflammatory effect of ligustrazine (n=3). ** represented the ligustrazine group V.S. IL-1β model group $P<0.05$; && represented the ligustrazine group V.S.PF573228 + ligustrazine group $P<0.05$.

Inhibiting FAK/PI3K/Akt pathway abolished the chondroprotective effect of ligustrazine

In this work, with aim to further probe into whether the protective effect of ligustrazine on chondrocytes was achieved by activating the FAK/PI3K/Akt pathway, our team applied PF573228 to inhibit the FAK/PI3K/Akt signaling pathway in chondrocytes. PF573228 is a widely used FAK signaling pathway inhibitor.

The TUNEL findings indicated that in comparison with the ligustrazine group, the amount of apoptosis in the PF573228+ligustrazine group elevated signally ($P<0.05$) (Figure 5A). As shown in Figure 5B, in comparison with the ligustrazine group, MMP3, MMP13, and collagen X expression levels in the PF573228+ligustrazine group elevated ($P<0.05$), while collagen II and aggrecan expression levels decreased signally ($P<0.05$). As shown in Figure 5C, in comparison with the ligustrazine group, MCP-1, IL-8, NO and PGE2 contents in the cells in the PF573228+ligustrazine group elevated significantly ($P<0.05$). Our findings revealed that ligustrazine could activate the FAK/PI3K/Akt pathway to inhibit IL-1β-induced chondrocyte apoptosis, elevate matrix degradation activity, as well as inflammatory factor expression.

Ligustrazine improved OA-induced cartilage damage through activating FAK/PI3K/Akt pathway

Based on Western blot findings, ligustrazine could activate the FAK/PI3K/Akt pathway. In comparison with the model group, the p-Akt/Akt, p-PI3K/PI3K and p-FAK/FAK protein expression levels elevated signally in the cartilage tissue in the ligustrazine treatment group ($P<0.05$), while those in the PF573228+ligustrazine group were visually decreased ($P<0.05$) (Figure 6A).

Aiming to further probe into the protective mechanism of ligustrazine on rabbit cartilage tissue damage at the *in vivo* level, our team constructed a knee osteoarthritis model with

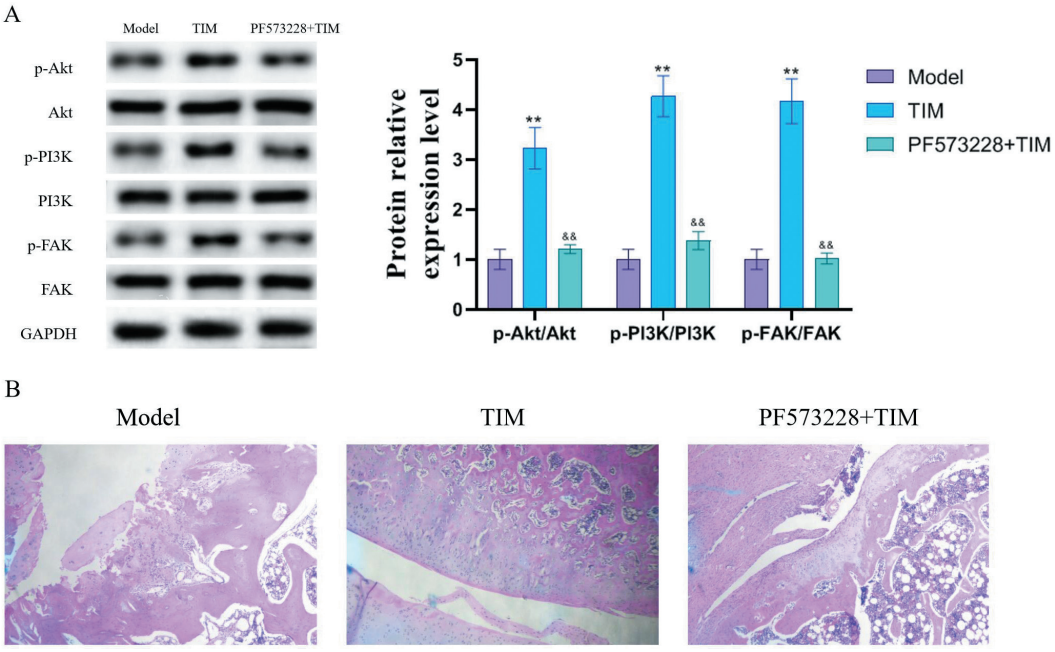

Figure 6. Ligustrazine improved cartilage damage induced by osteoarthritis through activating FAK/PI3K/Akt pathway. Figure 6A Western blot to detect the impacts of PF573228+Ligustrazine and Ligustrazine on FAK/PI3K/Akt signaling pathway (n=3). Figure 6B HE staining to detect the impact of inhibiting FAK/PI3K/Akt signaling pathway on the protective effect of ligustrazine on cartilage tissue morphology (n=3). ** represented the ligustrazine group V.S. PF573228+ligustrazine group $P<0.05$; && represented the ligustrazine group V.S. model group $P<0.05$.

meniscus tear of the right knee joint to investigate the protection mechanism of ligustrazine on rabbit cartilage tissue damage. The HE staining findings were shown in Figure 6B. The experimental findings implied that the cartilage surface of the model group had fallen off, the boundaries of each layer disappeared, and chondrocytes decreased. The morphology of articular cartilage in the ligustrazine group was signally improved, while that in the PF573228+ligustrazine group was visually worse.

Ligustrazine inhibited apoptosis induced by osteoarthritis model and enhanced metabolic activity

In this work, our team applied Western blot to determine the impact of ligustrazine and PF573228+ligustrazine on apoptotic protein level in cartilage tissue. Our work pointed out that in comparison with the model group, ligustrazine could visually inhibit the increase in caspase-9, caspase-3, caspase-7, Bax, and cytochrome c protein expression levels ($P<0.05$). Compared with the ligustrazine group, PF573228+Ligustrazine signally elevated caspase-9, caspase-3, caspase-7, Bax, and cytochrome c protein expression levels (Figure 7A).

Subsequently, Western blot findings pointed out that in comparison with the model group, ligustrazine could signally inhibit MMP3, MMP13, and collagen X expression levels ($P<0.05$), and up-regulate collagen II and aggrecan expression levels ($P<0.05$). In comparison with the ligustrazine group, PF573228+ligustrazine observably elevated MMP3, MMP13, and collagen X expression levels ($P<0.05$), while inhibited collagen II and aggrecan expression levels ($P<0.05$) (Figure 7B).

Discussion

Knee osteoarthritis, among the most universal chronic joint diseases, features a high incidence among the elderly worldwide and is the main cause of disability. Knee osteoarthritis affects approximately 60% men and 70% women over 65. Due to aging population, the rising rate of obesity, and the lack of clear treatments to prevent the progression of this disease, its harm is still increasing [12]. In the past few decades, treatment strategies for knee osteoarthritis have been greatly enriched, like non-drug, drug and surgical treatments [13]. However, none of these treatments is available to completely reverse the cartilage destruction in OA progression.

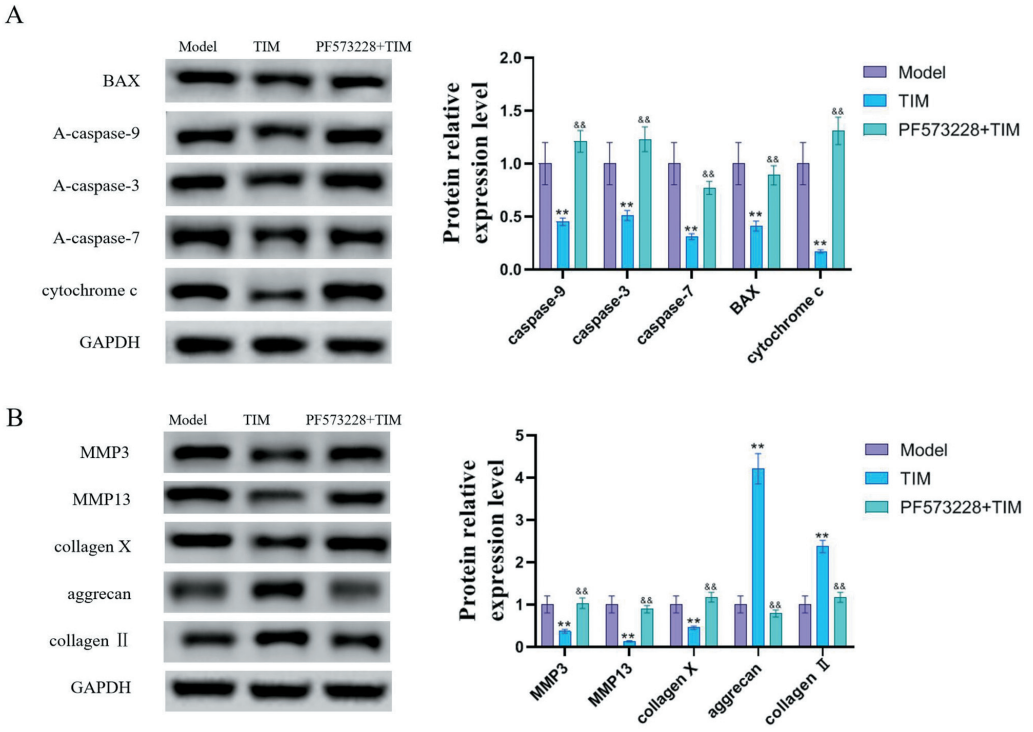

Figure 7. Ligustrazine inhibited cell apoptosis induced by osteoarthritis model and enhanced metabolic activity. Figure 7A Western blot to detect the impact of PF573228+ligustrazine on apoptosis-related protein expression (n=3). Figure 7B Western blot to detect the impact of PF573228+ligustrazine on MMP3, MMP13, collagen X, collagen II, and aggrecan expression levels (n=3). ** represented the ligustrazine group V.S. PF573228+ligustrazine group $P<0.05$; && represented the ligustrazine group V.S. the model group $P<0.05$.

Therefore, there is still an urgent need for new drugs for knee osteoarthritis. Ligustrazine is the main active ingredient in the traditional Chinese medicine *Ligusticum chuanxiong Hort*. Recently, ligustrazine has also been confirmed as a potential drug candidate for treating knee osteoarthritis [14]. Although clinical evidence reveals that ligustrazine is available to signally improve knee osteoarthritis, the relevant molecular mechanism is still not clear.

In this work, our team studied the impact of ligustrazine on knee osteoarthritis and IL-1β-induced chondrocyte damage *in vitro* and *in vivo*. Our research findings indicate that ligustrazine could reduce IL-1β-induced chondrocyte apoptosis through activating the FAK/PI3K/Akt pathway *in vitro* and *in vivo*, inhibit the apoptotic proteins Bax, caspase-9, caspase-3, caspase-7 protein expression level, as well as matrix-degrading enzymes MMP3 and MMP13 expression levels, and reduce collagen X (index of chondrocyte hypertrophy) protein expression level, and promote matrix proteins collagen II and aggrecan expressions. Additionally, ligustrazine could inhibit inflammatory factors MCP-1 and IL8 contents in the supernate of primary chondrocytes and reduce PEG2 and NO contents through activating the FAK/PI3K/Akt pathway *in vivo*. In the pathological mechanism of knee osteoarthritis, NO and PGE2 had the impact of inhibiting matrix synthesis [15]. In conclusion, our research results implied that ligustrazine could inhibit chondrocyte apoptosis, inhibit cartilage mechanism degradation, promote cartilage matrix synthesis, and inhibit inflammatory factor expression through activating the FAK/PI3K/Akt pathway.

In vitro and *in vivo*, ligustrazine can inhibit chondrocyte apoptosis, cartilage mechanism degradation, and promote cartilage matrix synthesis, which is in line with our research findings. Studies by Ju and Xu [16] pointed out that, ligustrazine inhibits chondrocyte apoptosis *ex vivo* and *in vivo*, protects cartilage tissue morphology, and inhibits cartilage mechanism degradation. As the only resident cells in cartilage tissue, chondrocytes adhere to the adjacent extracellular matrix to survive. This phenomenon is called anchorage dependence [17]. A large number of research findings pointed out that the destruction of proteoglycan and col-

lagen network in the cartilage matrix in knee osteoarthritis is the main pathological feature of cartilage degeneration. Therefore, the possible reason for chondrocyte apoptosis is under that pathological environment of knee osteoarthritis, the anchorage of chondrocytes to the extracellular matrix is destroyed [18]. For example, the research findings by Pulai [19] et al. pointed out that α5β1 integrin provides the binding between the extracellular matrix and the chondrocyte skeleton, and blockingα5β1 integrin knockout *in vitro* is available to signally promote chondrocyte apoptosis. Since articular cartilage completely relies on chondrocyte to maintain the extracellular matrix, damage to chondrocyte function and viability will result in articular cartilage failure. Therefore, chondrocyte apoptosis will further promote cartilage degeneration. Our research results thus pointed out that one of the mechanisms of ligustrazine in OA treatment may be that ligustrazine is available to inhibit matrix degradation and chondrocyte apoptosis induced by OA pathological conditions.

Subsequently, our work also pointed out that ligustrazine activates the FAK/PI3K/Akt pathway to inhibit chondrocyte apoptosis, cartilage mechanism degradation, while promote cartilage matrix synthesis. FAK is a key molecule in the signal transduction pathway mediated by integrin, and FAK phosphorylation is available to further activate the downstream PI3K/Akt pathway [20]. PI3K/Akt acts pivotally in the pathological process of OA, and is closely related to chondrocyte growth, differentiation, apoptosis and matrix remodeling [21]. For example, Tao [22] et al. pointed out that miR-34a can promote articular chondrocyte proliferation and inhibit its apoptosis through activating the PI3K/Akt pathway. Additionally, Fan [23] et al. pointed out that miR-155 is available to inhibit cartilage matrix degradation and promote cartilage matrix synthesis through activating PI3K/Akt. Consistent with our findings, Yang [24] et al. pointed out that ligustrazine can protect against myocardial injury induced by acute myocardial ischemia through activating the PI3K/Akt pathway. In summary, *in vitro* and *in vivo* ligustrazine is available to reduce IL-1β-induced chondrocyte apoptosis, inhibit cartilage mechanism degradation, and promote cartilage matrix synthesis through activating the FAK/PI3K/Akt pathway.

Venue of the research

Department of Orthopaedics, Liuzhou Traditional Chinese Medical Hospital, Guangxi University of Chinese Medicine, 32 North Jiefang Road, Liuzhou City, Guangxi Province, 545001, China

Funding

Not applicable

Declaration of Conflicting Interests

The authors declare that they have no competing interests.

Authors' contributions

GS designed the research study. JY performed the research. PR provided help and advice on the experiments. JY and XY analyzed the data. GS and XY wrote the manuscript. All authors contributed to editorial changes in the manuscript. All authors read and approved the final manuscript.

References

1. Driban JB, Harkey MS, Barbe MF, Ward RJ, MacKay JW, Davis JE, Lu B, Price LL, Eaton CB, Lo GH and McAlindon TE. Risk factors and the natural history of accelerated knee osteoarthritis: a narrative review. *BMC Musculoskelet Disord.* May 29 2020;21(1):332. doi: 10.1186/s12891-020-03367-2.
2. van Tunen JAC, Dell'Isola A, Juhl C, Dekker J, Steultjens M, Thorlund JB and Lund H. Association of malalignment, muscular dysfunction, proprioception, laxity and abnormal joint loading with tibiofemoral knee osteoarthritis - a systematic review and meta-analysis. *BMC Musculoskelet Disord.* Jul 28 2018;19(1):273. doi: 10.1186/s12891-018-2202-8.
3. Fernandes GS, Parekh SM, Moses J, Fuller C, Scammell B, Batt ME, Zhang W and Doherty M. Prevalence of knee pain, radiographic osteoarthritis and arthroplasty in retired professional footballers compared with men in the general population: a cross-sectional study. *Br J Sports Med.* May 2018;52(10):678-683. doi: 10.1136/bjsports-2017-097503.
4. Mahmoudian A, Van Assche D, Herzog W, Luyten FP. Towards secondary prevention of early knee osteoarthritis. *RMD Open.* 2018;4(2):e000468. doi: 10.1136/rmdopen-2017-000468.
5. Zamli Z, Adams MA, Tarlton JF, Sharif M. Increased chondrocyte apoptosis is associated with progression of osteoarthritis in spontaneous Guinea pig models of the disease. *Int J Mol Sci.* Aug 29 2013;14(9):17729-17743. doi: 10.3390/ijms140917729.
6. Charlier E, Relic B, Deroyer C, Malaise O, Neuville S, Collée J, Malaise MG and De Seny D. Insights on Molecular Mechanisms of Chondrocytes Death in Osteoarthritis. *Int J Mol Sci.* Dec 20 2016;17(12). doi: 10.3390/ijms17122146.
7. Guo M, Liu Y, Shi D. Cardiovascular Actions and Therapeutic Potential of Tetramethylpyrazine (Active Component Isolated from Rhizoma Chuanxiong): Roles and Mechanisms. *Biomed Res Int.* 2016;2016:2430329. doi: 10.1155/2016/2430329.

8. Li L, Liu H, Shi W, Liu H, Yang J, Xu D, Huang H and Wu L. Insights into the Action Mechanisms of Traditional Chinese Medicine in Osteoarthritis. *Evid Based Complement Alternat Med.* 2017;2017:5190986. doi: 10.1155/2017/5190986.
9. Wei Z, Dong C, Guan L, Wang Y, Huang J, Wen X. A metabolic exploration of the protective effect of Ligusticum wallichii on IL-1β-injured mouse chondrocytes. *Chin Med.* 2020;15:12. doi: 10.1186/s13020-020-0295-0.
10. Khan NM, Ahmad I, Haqqi TM. Nrf2/ARE pathway attenuates oxidative and apoptotic response in human osteoarthritis chondrocytes by activating ERK1/2/ELK1-P70S6K-P90RSK signaling axis. *Free Radic Biol Med.* Feb 20 2018;116:159-171. doi: 10.1016/j.freeradbiomed.2018.01.013.
11. Kuyinu EL, Narayanan G, Nair LS, Laurencin CT. Animal models of osteoarthritis: classification, update, and measurement of outcomes. *J Orthop Surg Res.* Feb 2 2016;11:19. doi: 10.1186/s13018-016-0346-5.
12. Vincent TL. Of mice and men: converging on a common molecular understanding of osteoarthritis. *Lancet Rheumatol.* Oct 2020;2(10):e633-e645. doi: 10.1016/s2665-9913(20)30279-4.
13. Cooper C, Adachi JD, Bardin T, Berenbaum F, Flamion B, Jonsson H, Kanis JA, Pelousse F, Lems WF, Pelletier JP, Martel-Pelletier J, Reiter S, Reginster JY, Rizzoli R and Bruyère O. How to define responders in osteoarthritis. *Curr Med Res Opin.* Jun 2013;29(6):719-729. doi: 10.1185/03007995.2013.792793.
14. Gao B, Lin X, Jing H, Fan J, Ji C, Jie Q, Zheng C, Wang D, Xu X, Hu Y, Lu W, Luo Z and Yang L. Local delivery of tetramethylpyrazine eliminates the senescent phenotype of bone marrow mesenchymal stromal cells and creates an anti-inflammatory and angiogenic environment in aging mice. *Aging Cell.* Jun 2018;17(3):e12741. doi: 10.1111/acel.12741.
15. Zhang J, Wang JH. Prostaglandin E2 (PGE2) exerts biphasic effects on human tendon stem cells. *PLoS One.* 2014;9(2):e87706. doi: 10.1371/journal.pone.0087706.
16. Ju XD, Deng M, Ao YF, Yu CL, Wang JQ, Yu JK, Cui GQ and Hu YL. The protective effect of tetramethylpyrazine on cartilage explants and chondrocytes. *J Ethnopharmacol.* Nov 11 2010;132(2):414-420. doi: 10.1016/j.jep.2010.08.020.
17. Pulai JI, Del Carlo M, Jr., Loeser RF. The alpha5beta1 integrin provides matrix survival signals for normal and osteoarthritic human articular chondrocytes in vitro. *Arthritis Rheum.* Jun 2002;46(6):1528-1535. doi: 10.1002/art.10334.
18. Zeng YF, Wang R, Bian Y, Chen WS, Peng L. Catalpol Attenuates IL-1β Induced Matrix Catabolism, Apoptosis and Inflammation in Rat Chondrocytes and Inhibits Cartilage Degeneration. *Med Sci Monit.* Sep 5 2019;25:6649-6659. doi: 10.12659/msm.916209.
19. Loeser RF. Integrins and chondrocyte-matrix interactions in articular cartilage. *Matrix Biol.* Oct 2014;39:11-16. doi: 10.1016/j.matbio.2014.08.007.
20. Fan S, Zhang D, Liu F, Yang Y, Xu H. Artesunate alleviates myocardial ischemia/reperfusion-induced myocardial necrosis in rats and hypoxia/reoxygenation-induced apoptosis in H9C2 cells via regulating the FAK/PI3K/Akt pathway. *Ann Transl Med.* Oct 2020;8(20):1291. doi: 10.21037/atm-20-5182.
21. Li H, Xie S, Qi Y, Li H, Zhang R, Lian Y. TNF-α increases the expression of inflammatory factors in synovial fibroblasts by inhibiting the PI3K/AKT pathway in a rat model of monosodium iodoacetate-induced osteoarthritis. *Exp Ther Med.* Dec 2018;16(6):4737-4744. doi: 10.3892/etm.2018.6770.
22. Tao H, Cheng L, Yang R. Downregulation of miR-34a Promotes Proliferation and Inhibits Apoptosis of Rat Osteoarthritic Cartilage Cells by Activating PI3K/Akt Pathway. *Clin Interv Aging.* 2020;15:373-385. doi: 10.1111/jcmm.15388.
23. Fan Z, Liu Y, Shi Z, Deng K, Zhang H, Li Q, Cao S, Li S and Zhang H. MiR-155 promotes interleukin-1β-induced chondrocyte apoptosis and catabolic activity by targeting PIK3R1-mediated PI3K/Akt pathway. *J Cell Mol Med.* Aug 2020;24(15):8441-8451.
24. Yang Q, Huang DD, Li DG, Chen B, Zhang LM, Yuan CL and Huang HH. Tetramethylpyrazine exerts a protective effect against injury from acute myocardial ischemia by regulating the PI3K/Akt/GSK-3β signaling pathway. *Cell Mol Biol Lett.* 2019;24:17. doi: 10.1186/s11658-019-0141-5.

ISSN print: 1224-5984
ISSN online: 2248-3942

Rom Biotechnol Lett. 2022; 27(3): 3570-3573
doi: 10.25083/rbl/27.3/3570.3573

Received for publication, July 27, 2022
Accepted, August 24, 2022

Review

Monkeypox Virus review

HASSINA GUETARNI*

University Bounaama Djilali of Khemis Miliana, Faculty of Natural Sciences, Life Sciences and and Earth, Biology Department, Laboratory of Natural Substances Valorization, 44225, Ain Defla, Algeria

Abstract

In 1958, the first case human infected by Poxivirus was detected in Democratic Republic of the Congo. This virus can produce after an incubation period of 5 to 21 a large spectrum of symptoms which can be severe, and, in many cases, medical care is necessary. The research of Monkeypox requires special laboratory conditions. Different tests can help to identify this virus in human specimens, like PCR and ELISA. Vaccinia vaccines prepared from viral variants can offer protection against monkeypox.

Keywords Monkeypox Virus, Poxivirus, Democratic Republic of the Congo, ELISA, PCR,Vaccinia Virus Smallpox

To cite this article: GUETARNI H. Monkeypox Virus review. *Rom Biotechnol Lett.* 2022; 27(3): 3570-3573 DOI: 10.25083/rbl/27.3/3570.3573

*Corresponding author: kmhg2009@yahoo.fr

Introduction

The Monkeypox Virus was discovered in 1958 during an outbreak in an animal facility in Copenhagen, Denmark (AABB, 1). The first human case was diagnosed in 1970 in a 9-month-old baby boy in Zaire (now the Democratic Republic of the Congo, DRC), and the infection has since then been reported in a number of central and western African countries(WHO, 2). The first monkeypox cases outside of Africa were reported in 2003 in the US when an outbreak occurred following importation of rodents from Africa, with all people infected becoming ill after contact with pet prairie dogs. Over the past 5 decades, monkeypox outbreaks have been reported in 10 African countries and 4 countries outside Africa. In total, 219 confirmed cases have been reported world wide from countries where the disease is not considered to be endemic (BENVENUTO et al. 3).

Surveillance for human monkeypox infections in endemic areas is a real challenge. Poor infrastructure, scarce resources, inappropriate diagnostic specimens and/or lack of specimen collection, and clinical difficulties in recognizing monkeypox illness are some of the many problems encountered by surveillance systems. As more information is gained from contemporary monkeypox cases, together with the data from past efforts, it will be important to re-assess the characteristics of the disease that help differentiate monkeypox from other rash illnesses (MCCOLLUM & DAMON, 4).

In 2022, 6027 laboratory confirmed cases of monkeypox and three deaths have been reported from 59 countries/territories/areas in five WHO Regions (African, Americas, Eastern Mediterranean, European, Western Pacific) (WHO, 5).

Characteristics of Poxvirus

The family Poxviridae consists of complex double stranded DNA viruses that are distinguished by their replication in the cytoplasm of vertebrate or invertebrate cells (SHCHELKUNOV et al. 6). Eight genera of Poxvirus are discovered in vertebrate: *Orthopoxvirus*, *Parapoxvirus*, *Avipoxvirus*, *Capripoxvirus*, *Leporipoxvirus*, *Suipoxvirus*, *Molluscipoxvirus* and *Yatapoxvirus*. They all share a similar DNA sequence with very similar antigens that have cross-reactivity. Poxviruses include human smallpox virus (Variola)(PHLN, 7), which was declared eradicated by the WHO in 1980. Other poxviruses that can affect humans include Cowpox, the virus used in the smallpox vaccine preparation , Akhmeta virus and monkeypox virus (MPVX), as well as other zoonotic species with epidemic potential (MARTÍN-DELGADO et al. 8). The reference Monkeypox virus, available on NCBI with accession code NC_003010.1 and derived from the sample Zaire-96-I-16, carries a 196,858 nucleotide-long double-stranded DNA linear genome, containing 191 non-overlapping genes, and is a representative of the CentralAfrican clade (GIORGI et al. 9).

Transmission of Monkeypox Virus

Aerosol transmission has been demonstrated in animals and may explain a nosocomial outbreak in the Central African Republic (PETERSEN et al. 10). Indirect or direct contact with live or dead animals is assumed to be the driver of human monkeypox infections in humans (LI et al. 11). Poverty and continued civil unrest force people to hunt small mammals (bushmeat) to obtain protein-richfood, thus increasing exposure to wild rodents, which may carry monkeypox (PETERSEN et al. 10).

Clinical characteristics

The incubation period for monkeypoxcan range from 5-21 days but usually falls within 7-14 days. Clinical presentation of monkeypox infection can be similar to chickenpox, caused by varicella-zoster virus. Symptoms usually begin within 5 days of infection with fever and chills, headache, muscle aches, back pain, fatigue, and swollen lymph nodes, the latter symptom differentiating monkeypox from smallpox (CCFSPH.IASTATE, 12). About 1-3 days, sometimes later, after the initial onset of symptoms, a rash or lesions can appear, usually beginning on the face and spreading throughout the body, often to the extremities rather than the trunk (Fig. 2) (LABORATORY GUIDELINES FOR THE DETECTION OF MONKEYPOX VIRUS, 13). Notably, monkeypox lesions can appear on the palms of the hands and soles of the feet (75% of cases). Most individuals with monkeypox experience rash with 1 to >100 skin lesions, but there are cases when no rush occurs. In most patients, symptoms of monkeypox are usually self-limiting and spontaneously resolve within 14-21 days. However, symptoms can be severe and require medical care (POTTER et al. 14).

Diagnosis

WHO and CDC have put forth case definitions for monkeypox during the 2022 outbreak that combine clinical, epidemiologic, and laboratory data. Diagnostic assays include virus isolation, electronmicroscopy, PCR, ELISA, and immunofluorescent antibody assay. Characteristic brick-shaped poxvirus virions are found on electronmicroscopy. Histopathologic analysis may demonstrate ballooning degeneration of keratinocytes, prominent spongiosis, dermal edema, and acute inflammation. CDC developed an IgM-capture and IgG ELISA that demonstrated recent monkeypox virus infection. Serum IgM and IgG were detected five and eight days after

Figure 1. Images of individual monkeypox lesions (Photo credit: UK Health Security Agency)(LABORATORY GUIDELINES FOR THE DETECTION OF MONKEYPOX VIRUS, 13).

onset of rash, respectively. If the diagnosis of monkeypox is being considered, local and state public health officials, along with the CDC, should be notified so that the samples are quickly processed (Fig. 2)(ISAACS, 15).

Treatment

There is no specific treatment for human monkeypox infection. Nor is there a specific vaccine fully protective against monkeypox virus. Cross-reactivity with vaccinia virus smallpox vaccine can provide cross immunity with partial protection against infection and reduction in disease severity, but with waning vaccine-derived immunity, the strength of this protective effect is decreasing. Earlier vaccinia vaccines have suboptimal safety profiles, but later vaccines derived from viral variants that do not replicate within cells, have been approved for use with human monkeypox infection (HSE, 17).

Conflict of interest

No

Funding Ressources

No

References

1. AABB, APPENDIX 2. MonkeypoxVirus. Transfusion, 49, 132S (2009).

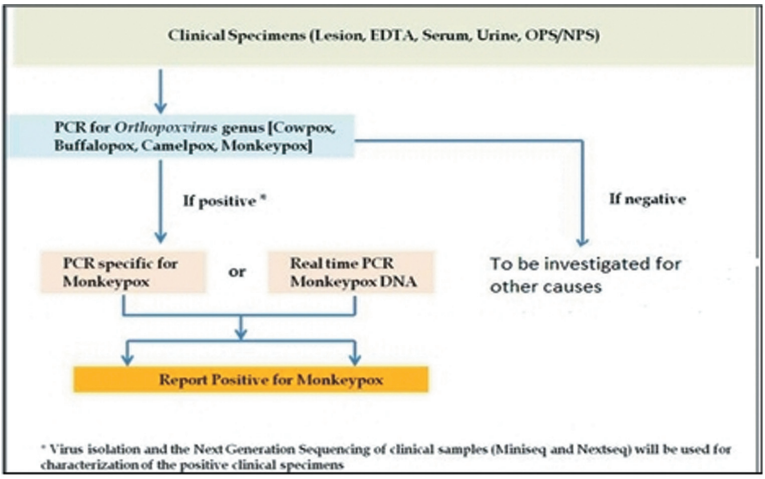

Figure 2. Steps of diagnosis of Monkeypox Virus (MHFWGI, 16).

2. WHO, Multi-country outbreak of monkeypox. External Situation Report 1(2022).https://cdn.who.int/media/docs/default-source/2021-dha-docs/20220706_monkeypox_external_sitrep_final.pdf?sfvrsn=1b580b3d_4.
3. D. BENVENUTO, S. VITA, S. PASCARELLA, M. BIANCHI, M. GIOVANETTI, R. CAUDA , E. NICASTRI, A. CASSONE, M. CICCOZZI, The evolution of Monkeypox virus: a genetic and structural analysis reveals mutations in proteins involved in host-pathogen interaction.bioRxiv(2022).https://doi.org/10.1101/2022.06.22.497195.
4. M. ANDREA, A.M. MCCCOLLUM, I.K. DAMOND, Human Monkeypox. *Clinical Infectious Diseases*.58(2), 260, 7(2014).
5. WHO, Monkeypox Current status in West and Central Africa(2018). https://apps.who.int/iris/bitstream/handle/10665/272620/WHO-WHE-IHM-2018.3-eng.pdf.
6. S.N. SHCHELKUNOV, A.V. TOTMENIN, P.F. SAFRONOV, M.V. MIKHEEV, V.V. GUTORO, O.I. RYAZANKINA, N.A. PETROV, I.V. BABKI, E.A. UVAROVA, L.S. SANDAKHCHIEV, J.R. SISLER, J.J. ESPOSITO, I.K. DAMON, P.B. JAHRLING, B. MOSS, Analysis of the Monkeypox Virus Genome. *Virology*, 297, 172,194(2002).
7. PHLN(Public Health Laboratory Network) Monkeypox (Monkeypox Virus) Laboratory case definition (2022).https://www.health.gov.au/sites/default/files/documents/2022/07/monkeypox-laboratory-case-definition.pdf
8. M.C. MARTÍN-DELGADO, F.J. MARTÍN-SANCHEZ, M. MARTINEZ-SELLES, J.M. MOLERO GARCIA, S.M. GUILLÉN, F. RODRÍGUEZ-ARTALEJO, J. RUIZ-GALIANA, R. CANTÓN, P. DE LUCAS RAMOS, A. GARCÍA-BOTELLA, A. GARCÍA-LLEDÓ, T. HERNÁNDEZ-SAMPELAYOT, J. GÓMEZ-PAVÓN, J. GONZÁLEZ DEL CASTILLO, P. MUÑOZ, M. VALERIO , P. CATALÁN, A. BURILLO, A. COBO, A. ALCAMÍ, E. BOUZA, Monkeypox in humans: a new outbreak. *Revista Española de Quimioterapia*(2022). doi:10.37201/req/059.
9. F.M. GIORGI, D. POZZOBON, A. DI MEGLIO, D. MERCATELLI, Genomic analysis of the recent monkeypox outbreak(2022). https://www.researchgate.net/publication/11291150_Analysis_of_the_Monkeypox_Virus_Genome.
10. E. PETERSEN, A. KANTELE, M. KOOPMANS, D. ASOGUN, A. YINKA-OGUNLEYE, C. IHEKWEAZU, A. ZUMLA, Human Monkeypox Epidemiologic and Clinical Characteristics, Diagnosis, and Prevention. *Infect Dis Clin Nam* (2019).https://doi.org/10.1016/j.idc.2019.03.001.
11. D. LI, k. WILKINS, A.M. MCCCOLLUM, L. OSADEBE, J. KABAMBA, B. NGUETE, T. LIKAFI, M. PIE BALILO, R. SHONGO LUSHIMA , J. MALEKANI, I.K. DAMOND, M.C.L. VICKERY, E. PUKUTA, F. NKAWA, S. KARHEMERE, J.J. MUYEMBE TAMFUM, E. WEMAKOY OKITOLONDA, Y. LI, M.G. REYNOLDS, Evaluation of the GeneXpert for Human Monkeypox Diagnosis. *Am. J. Trop. Med. Hyg*., 96(2), 405, 410(2017).
12. CFSPH.IASTATE, Monkeypox(2020). www.cfsph.iastate.edu.
13. LABORATORY GUIDELINES FOR THE DETECTION OF MONKEYPOX VIRUS(2022). https://www.nih.org.pk/wp-content/uploads/2022/06/1-Laboratory-Testing-Guidelines-for-Diagnosis-of-Monkeypox-Virus-Final.pdf.
14. C. POTTER, L. WARMBROD, R.A.VAHEY, A. BROWETT, Monkeypox. Factsheet. The Johns Hopkins University. centerforhealthsecurity.org (2022).
15. S.N. ISAACS, Monkeypox(2022). https://www.binasss.sa.cr/mono/1.pdf.
16. MHFWGI(Ministry of Health and Family Welfare Government of India), Guidelines of Monkeypox For Management Disease(2022). https://main.mohfw.gov.in/sites/default/files/Guidelines%20for%20Management%20of%20Monkeypox%20Disease.pdf.
17. HSE (Health Protection Surveillance Centre), Human Monkeypox Infection, *Guidance for Clinicians and Public* Health, 1, 7 (2022).www.hpsc.ie.